Journal of Experimental Biology And Agricultural Sciences

Assistant Editors

Dr. Senthilkumar Natesan

Associate Professor

Department of Infectious Diseases, Indian Institute of Public Health

Gandhinagar, Opp to Airforce station HQ, Lekawada, Gandhinagar, Gujarat - 382042, India

Email: snatesan@iiphg.org

Mr. Ram Bahadur Khadka (Microbiologist)

Assistant Professor (Pokhara University)

Crimson College of Technology (CCT)

Butwal-13, Rupandehi, Lumbini Province, Nepal

Email: rambahadurkhadka00@gmail.com

Prof. A. VIJAYA ANAND

Professor

Department of Human Genetics and Molecular Biology

Bharathiar University

Coimbatore – 641 046

Dr. Phetole Mangena

Department of Biodiversity, School of Molecular and Life Sciences,

Faculty of Science and Agriculture, University of Limpopo, Republic of South Africa

Private Bag X1106, Sovenga, 0727

Email: Phetole.Mangena@ul.ac.za ; mangena.phetole@gmail.com

Table of contents

Immune-Cell-Mediated Cancer Treatment: Advantages, Drawbacks And Future Direction

Ohn Mar Lwin[1], Atif Amin Baig[2], Nurul Akmal Jamaludin[1], Thin Thin Aung[1], Haziq Hazman Norman[1], Aung Myo Oo[1,3*]

[1]Faculty of Medicine, International Medical School, Management and Science University, Selangor, Malaysia
[2]University Institute of Public Health, Faculty of Allied Health Sciences & Institute of Molecular Biology and Biotechnology, The University of Lahore, Pakistan
[3]Faculty of Medicine, Universiti Sultan Zainal Abidin (UniSZA), Terengganu, Malaysia, and International Medical School, Management and Science University, Selangor, Malaysia

ABSTRACT

Cancer ranks as the most lethal and prevalent non-communicable disease in clinical settings. Therapeutic options for cancer comprise chemotherapy, radiotherapy, surgery, and combined treatment. Cancer remission and relapse cases are widespread despite having various advanced medications and sophisticated dissection techniques. A new approach involving immune-cell-mediated cancer therapy has been adopted extensively for cancer treatments by utilizing immune cells. Immunotherapy has gained much attention to prevent and treat various types of cancer. Immunotherapy treatments operate in multiple contexts. Several immunotherapy therapeutic interventions assist the immune function in halting or reducing the advancement of cancer cells. Many also facilitate the immune cells in destroying cancerous cells or safeguarding against cancer from disseminating to certain other regions of the human body. Among other methods, genetic manipulation of immune cells offers hope for innovative anticancer treatment. T lymphocytes and natural killer cells have become the most extensively documented immune cells for immunotherapy. Chimeric antigen receptor T-cell therapy exhibits the most promising blood cancer treatment. However, adoptive NK cell transfer therapy displays potential anticancer treatment options, although more research is needed to be carried out. In addition, cytokine-induced immunomodulation is also plausible for cancer immunotherapy. This review will highlight the most comprehensive information, observations, and consequences associated with different cancer immunotherapy initiatives.

* Corresponding author

E-mail: aungmo@unisza.edu.my, dr.agmyooo@gmail.com (Aung Myo Oo)

Peer review under responsibility of Journal of Experimental Biology and Agricultural Sciences.

1 Introduction

Cancer is one of the fastest-growing causes of fatalities across the globe, accounting for substantially 10 million mortalities in 2020 (WHO 2022). This horrifying disease presents an unacceptable health risk to all communities, regardless of economic or social status. Also, it is the fundamental cause of roughly 30 percent of all non-communicable (NCD) related deaths in people aged 30-69. Female breast carcinoma is the most widespread cancer after pulmonary, colorectal, and prostate tumours (Sung et al. 2021). Prevention strategies, such as monitoring, early recognition, multidisciplinary therapeutic interventions, longevity, and rehabilitation, are all part of the cancer management spectrum. Nowadays, surgical intervention, medical therapy (chemotherapy, immunotherapy, endocrine therapy), radiation therapy, or a combination of these treatments are used for cancer treatment (Figure 1). Cancer is a growing global public health concern and contributes to one out of every six deaths worldwide. The strain on individuals, societies, healthcare, and financial systems grows daily. The psychosocial impact of cancer ranges from profound physical devastating effects to financial crises within the family and suicidal attempts (WHO 2020).

After two famous research experts were awarded Nobel Prizes in Medicine or Physiology in 2018 for their pioneering work on cancer immunotherapy, interest in the treatment skyrocketed. These two researchers uncover the activation mechanism of the immune system's cells to fight against cancer, an advance in developing new cancer treatments. Their incredible discoveries have guided the development of several potential chemotherapeutic agents that mete effective cancer immunotherapy's routine use. Nowadays, immunotherapy stands apace with chemotherapy, radiotherapy, and surgery as a new way of cancer management. To date, immune-mediated cancer treatment is currently merely impactful in a few forms of cancer. The subsequent step for researchers is crucial to expand the percentage of patient populations who could benefit from this strategy (Simon and Uslu 2018).

For the past decade, the scientific community has gained a greater awareness of the connections between innate immune lymphocytes and tumour cells and the underlying biochemical pathways by which disease can avoid the immune system. The immunity is monitored by the active link of two distinct categories of cells, particularly lymphoid cell lines, i.e. T and B lymphocytes (natural killer "NK" cells), and myeloid cell lines (neutrophils, macrophages) and the by-products of their synthesis, for instance, cytokines and antibodies. In cancer, the immune system is dwindled primarily due to the effects of radiotherapy and chemotherapy, so research has been carried out in recent years to boost immune cell activity, and immunotherapy is explored to treat cancer (Grigore 2017). This new treatment seems to be a broader range of therapeutic approaches that induce immune-cell-mediated malignant cell breakdown (Mostafa and Morris 2014). As a result, this modern concept of cancer immunotherapy policies and procedures emerges that overrides the restrictions imposed by traditional treatment modalities (Gleichmann 2020). This article will provide information about the most comprehensive data, observations, and consequences related to various cancer immunotherapy initiatives.
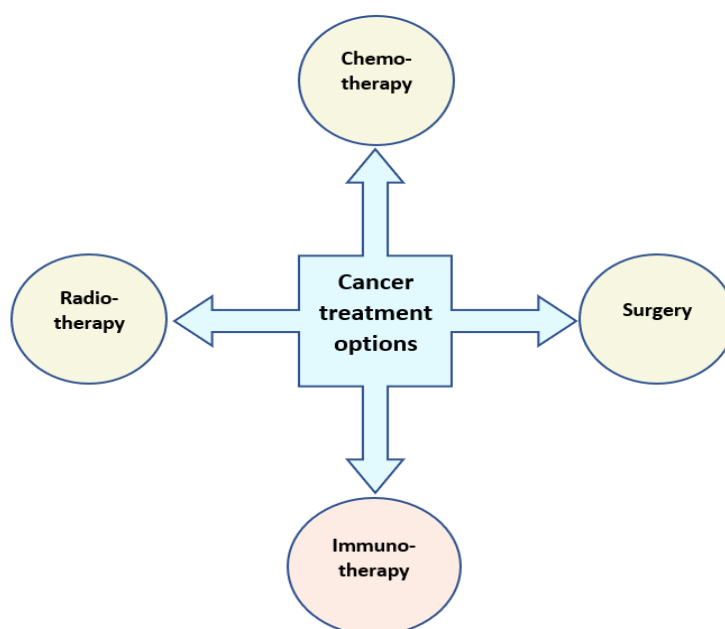
Figure 1 Types of cancer treatment.

2 Types of Immunotherapies

A few types of immunotherapies operate in an array of aspects. Several immunotherapeutic treatment methods assist the immune function in stopping or slowing cancer cell development. Some even aid the immune lymphocytes in destroying tumour cells or preventing cancer from extending toward other tissues throughout the body. Immunotherapy is effective in itself or conjunction with several other anticancer agents. Monoclonal antibodies, immune checkpoint blockers, oncolytic virus treatment, T-cell and NK-cell-mediated therapy, and cancer vaccines are presently offered as immunotherapeutic remedies (Chhabra and Kennedy 2021; Saxena et al. 2021).

Monoclonal antibodies are manufactured in sophisticated laboratories, and these proteins boost the body's natural immunities. Antibody production occurs when the immune cells identify potentially hazardous microbes or abnormally transformed cells during an early phase of the immune response. Then, these antibodies fight against invading organisms and cancerous cells by binding to specific antigens. Later, these proteins could restrict the function of unusual specific proteins in tumour tissue. Also, monoclonal antibodies boost the activity of the cells' immune system by modulating immune checkpoints (Zahavi and Weiner 2020).

Immune checkpoint blockers enhance the body's immune cell's ability to eradicate unnaturally dividing tumours. These blockers commonly target the programmed-cell-death-1 or its ligand (PD-1)/PD-L1 and cytotoxic-T-lymphocyte-associated antigen-4 (CTLA-4) processes. United States Food and Drug Administration (US-FDA) recently certified many immune checkpoint blockers to be used clinically for specific types of cancer. The most commonly used immune checkpoint blockers include ipilimumab, nivolumab, atezolizumab, avelumab, and durvalumab (Robert 2020).

Oncolytic virus treatment employs laboratory-modified viruses to suppress malignant cells. Firstly, the virus that has been genetically manipulated is administered into the tumour. Then, the virus invades tumour cells and replicates itself. As an outcome of this, the cancerous cells erupt and start dying. While the cells perish, viral proteins are released, which induce the immune function to identify any irregular cells throughout the body that contain similar protein molecules as the dying tumour cells. In 2015, the FDA granted the first oncolytic virus treatment to cure extensive melanoma that could not be managed surgically. The virus used in the therapy is designated as talimogene laherparepvec (T-VEC). However, various untoward effects of this treatment were reported, such as fatigue, flu-like illness, and discomfort at the injection site. Numerous viral vectors for various types of cancers are being studied in clinical studies (Lawler et al. 2017). Furthermore, the co-administration

of T-VEC and immune checkpoint inhibitors appears to be a favourable melanoma therapeutic modality (Zhang et al. 2023).

T cells are the primary lymphocytes that fight against infection and abnormal cells. In T-cell-mediated cancer treatment, they are isolated from peripheral blood and then transformed by introducing particularly associated receptor proteins to the cells. These receptor proteins enable T cells to identify abnormally transformed cell populations. The modified T cells are then reinstated into the human organism. After entering one's body, they locate and eliminate tumour cells. This is widely recognized as chimeric antigen receptor (CAR) T-cell therapy. CAR T-cell treatment is successful in curing certain kinds of blood-related cancer. In exceptional cases, febrile reactions, disorientation, hypotension, and epileptic episodes are among the complications. Research teams nowadays are looking into avenues for enhancing this kind of treatment and certain other methods of changing T-cells to combat malignancy (Cerrano et al. 2020; Fischer and Bhattarai 2021; Martino et al. 2021).

Cancer vaccines can improve the body's ability to fight diseases. Vaccine uncovers the body's immune lymphocytes to an antigen, a foreign protein. This activates the immune system, causing it to detect and dismantle the antigen or associated compounds. There are two kinds of cancer vaccines presently offered: a vaccine for preventive measures and a vaccine for therapeutic options; nevertheless, their utilization remains relatively small (Saxena et al. 2021).

NK cells are lymphocytes with cytotoxic capabilities that are essential for natural immunity. NK cell adoptive transfer treatment is the latest area of interest in immunotherapy due to T cell therapy's severe unwanted side effects. NK cell immunotherapy is extensively developing, and many clinical trials have been going on and reaching phase II clinical trials. Several research investigations have taken place to assess the risks and benefits of adoptive NK therapeutic strategies to treat haematological malignancies (Veluchamy et al. 2017). But then again, as a result of inadequate NK cell relocation and incursion into the tumour, implementing the application of NK cells to cure solid tumours poses significant obstacles. Animal studies are now aimed at enhancing these NK cell processes for adoptive transfer. Contemporary NK cell treatment methods focus on autologous, allogeneic, or CAR-NK cells (Franks et al. 2020; van Vliet et al. 2021). Among all the available treatment options for cancer immunotherapy, CAR-T and adoptive NK cell transfer treatment are the most promising, although various side effects are still a significant problem. This article will address the positive and negative aspects of the two common types of immunotherapies. In addition, the possible ways for future developments in the area of immune-cell-mediated cancer treatment will also be highlighted.
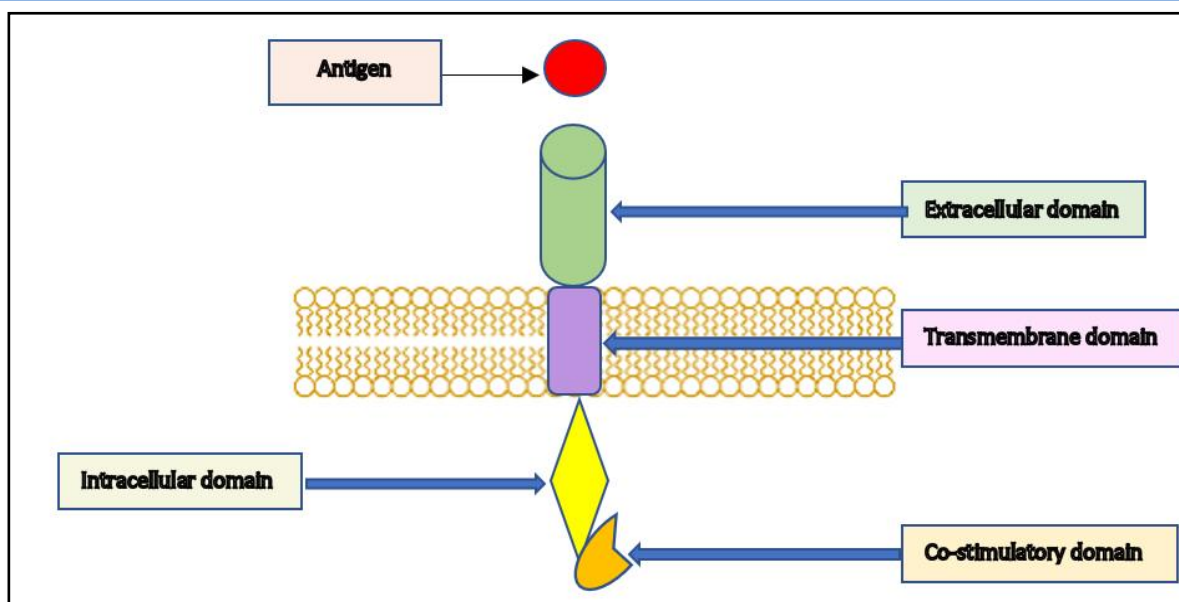
Figure 2 Schematic diagram of the domains of the chimeric antigen receptor.

2.1 Chimeric Antigen Receptor or CAR-T Therapy

The most popular adoptive cell transfer therapy nowadays is chimeric antigen receptor T cell or CAR-T cells that identify and destroy tumours independently of major histocompatibility complex (MHC) protein; thus, downregulation of MHC molecules overcomes immune escape of tumour cells (Zhang et al., 2020). CAR-T cells are genetically modified and manufactured to recognize tumour-associated antigen (TAA) and subsequent stimulation of T lymphocytes and lysis of cancer. As displayed in Figure 2, CARs are designed with several distinct regions: an extracellular domain, a transmembrane portion, and intracellular and costimulatory domains. Each domain possesses a specific operation, and the ideal biological configuration of the CAR can be attained through many modifications of the component amino acid sequences (Rafiq et al. 2020).

The external antigen binding region of CAR is in charge of antigen specificity. At first, antigen-binding regions were extracted from monoclonal antibodies and linked with a flexible linker to form a single-chain variable fragment (scFv). The scFv binds to the exterior protein of the cancer antigen, culminating in MHC-independent T-cell induction (Zhang et al. 2014). Essentially, the fundamental determinant of CAR function depends on the binding affinity of scFv to the target cell antigen. This binding must be precise enough to recognize cancer cells and subsequent induction of CAR signal transduction and T-cell stimulation; nevertheless, extremely high affinity could also result in activation-induced cell death (AICD) of the CAR-expressing cell and, plausibly, lead to toxic effects (Dholaria et al. 2019). The transmembrane domain links the antigen-binding region and the intracellular signal transduction domain. The transmembrane domain primarily stabilizes the CAR to the T-cell lipid bilayer (Guedan et al., 2018). It is extracted mainly from type-I protein molecules such as clusters of differentiation-3 (CD3, CD4, or CD28 (Alabanza et al. 2017). The intracellular signal transduction domain is the most critical component of CAR and primarily consists of an activation domain and one or more costimulatory sites. Most CARs invoke CAR-T cell lines via immunoreceptor tyrosine-based activation motifs sourced from CD3. Nevertheless, stimulation mediated through these motifs was ineffective and could lead to restricted *in vivo* T-cell longevity and interaction (Rafiq et al. 2020).

A costimulatory domain is crucial for effective T-cell activation, operation, proper metabolic activity, and consistency. The addition of the costimulatory domain not only improves cytokine production but also favours proliferation upon repeated antigen exposure (Tariq et al. 2018).

2.2 Eureka moment of CAR-T treatment

The breakthrough of CAR-T approval was determined after successful trials were done between 2015 and 2020. Firstly, Maude and co-researchers conducted the very first global CAR-T-cell therapy enrolment cohort study, which resulted in the FDA's recommendation of tisagenlecleucel (tisacel) for paediatric and teenage patients with relapsed/refractory B-cell-acute lymphoblastic leukaemia (R/R B-ALL). In that phase-II experiment, 75 patients were injected with tisacel, with a mean average follow-up of 13.1 months. The ideal overall response rate (ORR) was 81%, with 60% complete remission (CR), and all were measurable residual disease (MRD) negative (0.01% by flow

cytometry). Tisacel was found in the patient's blood for 20 months, even after injection. At twelve months, the event-free survival (EFS) and overall survival (OS) rates were 50% and 76%, respectively. However, 73% of the infused patients experienced severe adverse effects, and intensive care unit (ICU) treatment was needed in 47% of these patients for cytokine-related toxicity management. Neurotoxicity was also witnessed in 40% of the cases after eight weeks of such injection, with 13% severe scenarios, but none of the patients required ICU treatment (Maude et al., 2018).

Similarly, the product's registration resulted in another multicenter phase-II clinical experiment using axicabtagene ciloleucel (axicel) in advanced B-cell-non-Hodgkin lymphoma (B-NHL). In this phase II trial, 108 cancer patients were administered axicel, and 101 were evaluated for clinical response. The enrolled in-patients began receiving CAR-T cells at a 2×10^6 cells/kg target dose following lymphodepletion chemotherapy. According to Locke and colleagues' updated experiment evaluation, the best ORR and CR rates were 83% and 58%, respectively. However, 93% of patients reported cytokine-released syndrome (CRS), with 13% severe symptoms. Neurotoxicity was also observed in 64% of patients, 28% severe and very severe (Neelapu et al. 2017; Bouchkouj et al. 2019; Locke et al. 2019).

Following the second multicenter clinical phase II trial, the FDA approved Tisacel for adult patients with R/R diffuse large B-cell lymphoma (DLBCL). Overall, 111 enrolled patients were infused with tisacel, and clinical response was assessed in 93 patients. The highest ORR was 52%, with a CR of 40% and a partial response (PR) of 12%. Severe and very severe CRS rate was observed in 22% and 24% of the patients, respectively, and they were referred to the ICU for CRS treatment. Neurotoxicity occurred in 21% of patients, with severe complications experienced in 12% of cases, with no fatalities(Schuster et al. 2019).

The US FDA and the European Medicine Agency (EMA) have both granted two distinct CAR-T cell products, namely tisacel and axicel, for the treatment of R/R B-ALL in patients under the age of 25 and adult patients with different types of lymphoma in late 2017. However, more improvements are required to improve CAR-T efficacy to widen the spectrum of target cancer cells and lessen unwanted complications. Furthermore, more research is needed to translate innovations in early-stage clinical research into the clinical setting (Cerrano et al. 2020).

2.3 CAR-T cell toxic effects and potential solutions

Despite being a ground-breaking cancer therapy weapon, high numbers of systemic toxicity and fatal accidents have prevented CAR-T immunotherapy from becoming a mainstream cancer therapeutic option. The severity of complications during CAR-T cell treatment becomes a significant disturbance in developing effective CAR-T. Developing a more significant breakthrough will be challenging if these hindrances are not solved. There are some serious adverse side effects reported on CAR-T therapy, and Cytokine Release Syndrome (CRS) is the most frequent negative impact, followed by neuronal toxicities, off-tumour toxicity, and additional side effects (Zhang et al., 2020).

2.3.1 Cytokine Release Syndrome (CRS)

Cytokine Release Syndrome is a severe and, in some cases, deadly consequence. In many clinical trials, the elevation of systemic cytokine production was endorsed in patients administered with CAR-T cells. In substantial clinical studies, CRS is prominently featured in 50-90% of the clients and most commonly occurs within the following day after the infusion of CAR-T cells (Schuster et al. 2019; Neelapu et al. 2017). CRS can vary from self-contained influenza-like symptoms to potentially fatal multi-organ impairment requiring urgent attention and rigorous life-sustaining therapeutic interventions. Hypotensive shock, decreased blood supply to the kidneys, and pulmonary congestion can result from CRS-associated capillary leak syndrome (Giavridis et al. 2018; Norelli et al. 2018). For severe CRS, supplemental Tocilizumab or corticosteroids alone would be required for intensive care. Conversely, there remain incidents where clinical manifestations could not improve or worsen following aggressive therapy (Brudno and Kochenderfer 2016).

To tackle this problem, the American Society for Transplantation and Cellular Therapy strongly advocated a principle scoring system for CRS and neurotoxic effects linked to the immune impacts of cell therapies (Lee et al. 2019). In addition to intense therapeutic interventions and ICU monitoring, severe CRS management requires cytokine inhibitors. Tocilizumab, an IL-6 receptor blocker, has been granted FDA approval as a first-line intervention for CRS and is also being studied as a preventive initiative. Systemic corticosteroids are used as a second-line drug for clients with a dissatisfying effect. In this context, current stats demonstrated that earlier stage therapeutic approach during the initial signs and symptoms of CRS, which includes administering glucocorticoids, can preclude severe conditions without affecting outcomes, dispelling concerns that these drugs could impair the efficacy of CAR-T therapy (Gardner et al., 2019; Liu et al., 2020).

CRS is a widespread inflammatory process triggered by T cells' immediate activation and propagation following interaction with target tissues, releasing unnecessarily high cytokines. Furthermore, activated monocytes are mainly accountable for interleukin-6 (IL-6) and IL-1 secretion, a significant occasion in the advancement of CRS. Although the detailed pathophysiology has yet to be understood, the latest evidence has shed light on the potential molecular pathways of CAR-T cell-induced CRS (Bouchkouj et al.

2019). CAR-T cells proliferate after the scFv attaches to the target cell antigens, become activated, and secrete many proinflammatory cytokines as an acute response (Hay et al. 2017; Neelapu et al. 2017). The secreted cytokines stimulate lymphocytes, particularly T cells and non-immune cells like epithelial cells, to emit more cytokines of different forms and amounts (Shimabukuro-Vornhagen et al. 2018). According to study results, interferon-gamma (IFN-γ) activates macrophages and provokes the discharge of tumour necrosis factor (TNF), IL-6, IL-15, IL-1, and IL-12, thereby sustaining or improving following immune responses, and IL-6 is one of the crucial cytokines amongst these. The amount of IL-6 released by immune cells coincides with the amount of CD40L displayed on the outer layer of CAR-T cells. Two other research investigations have revealed that extreme CRS is coupled with vascular endothelial stimulation or impairment (Giavridis et al. 2018; Obstfeld et al. 2017). In clinical trials, Tocilizumab, siltuximab, kinase inhibitors, and corticosteroids that block IL-6 can quickly reverse fever, hypotension, and hypoxia (Zhang et al. 2020).

2.3.2 Neurotoxicity

Neurotoxicity, also known as immune effector cell-associated neurotoxicity syndrome (ICANS), is CAR-T therapy's next-most prevalent detrimental impact. ICANS is characterized by an interruption of the blood-brain-barrier (BBB) and elevated cerebrospinal fluid (CSF) inflammatory cytokines, which may manifest as dysarthria, altered psychological condition, involuntary movements, convulsions, headache, and life-threatening brain oedema, frequently concomitantly or continuing to follow CRS (Santomasso et al. 2018; Rafiq et al. 2020). As a result, central nervous system perivascular stress and over-expression of endothelium-activating proinflammatory cytokine increased BBB permeability in an endless cycle (Gust et al. 2017). Furthermore, in an animal study, CAR and non-CAR-T cells were found to accumulate in the CSF and nervous system tissue, implying a central role in neurotoxicity development (Taraseviciute et al. 2018). The most current neurotoxicity scoring method incorporates

a 10-point grading scale based on the Immune Effector Cell-Associated Encephalopathy (ICE) evaluation system and considers five significant neurological aspects (Lee et al. 2019).

Individuals with serious ICANS must always be performed assertively, and a comprehensive strategy, including neurologic collaboration, is frequently required. An electroencephalography, brain magnetic resonance imaging, and CSF examination are all necessary in the practice of a presumed ICANS to sort out other causal factors of neuronal damage (Dholaria et al. 2018). Levetiracetam, an anti-epileptic, could be a preventive remedy for avoiding convulsions, starting immediately following CAR-T cell administration or at the first sign of Neurotoxicity. The first-line intervention for neuronal damage has now become dexamethasone or high-dose methylprednisolone (Neelapu 2019). Recently conducted studies have found that granulocyte-macrophage colony-stimulating factor (GM-CSF) played an essential player in the aetiopathogenesis of Neurotoxicity. In preclinical studies, lenzilumab, an anti-GM-CSF monoclonal antibody, successfully blocked CD19-CAR-mediated Neurotoxicity and CRS (Sterner et al. 2019). Although life-threatening complications were encountered, ICANS, like CRS, is manageable in some instances, including a few fatal reports, and most sick people even have self-limited courses (Gust et al. 2017; Cerrano et al. 2020). There is no specific treatment guideline to prevent the above toxicities. Therefore, optimization of CAR genetic manipulation and employing other approaches to reducing CAR-induced toxicity are essential (Sterner and Sterner 2021).

2.3.3 On-target-off-tumour

On-target-off-tumour is an additional common complication of CAR-T treatment. T-cell antigen receptors, upon genetically engineered, recognize tumour cells by identifying specific antigenic proteins on the tumour cells' membrane (Leyfman 2018). Meanwhile, these antigens could also be depicted in healthy cells. Thus, administering the CAR-T cell line could attack healthy cells,
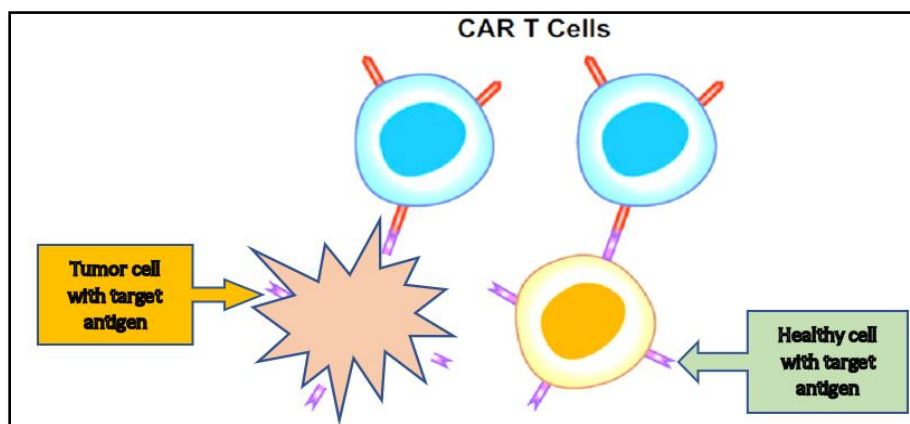
Figure 3 Schematic presentation of On-target Off-tumour side effects.

leading to tissue and organ damage, the on-target/- off-tumour effect (Morgan et al. 2010). The TAA identified by CAR-T treatment is not only specific to these abnormal cells, and when CAR-T cells attach non-tumour target proteins, it generates an off-target effect, as illustrated in Figure 3. CAR-T cells that observe two antigens have evolved to avert off-target adverse effects. Initially, CAR-T cells recognize malignant cell antigenic protein and invoke the transcription of CAR embedding codons within the cell. The single-chain immunoglobulin identifies antigen B after CAR translation, restricting CAR-T cells from attempting to kill healthy tissue (Zhang et al. 2020).

However, the problem remains a challenge in recognizing antigens expressed by solid tumours. The solid tumour antigens are frequently expressed at different levels of complexity in healthy tissue. Hence, antigen selection is essential in the CAR construct to secure curative potency and reduce the "on-target off-tumour" toxic effect. Designed to target tumour-restricted post-translational alteration, it could help overcome the attacking of antigens on solid tumours likewise found in normally functioning tissues. To broaden the medical usage of available CAR-T cell therapies in haematological malignancies and solid tumours, more groundbreaking methods to minimize antigen escape and then choose antigens that can generate adequate antitumor activity whilst also lessening toxicity issues will be required (Du et al. 2019; Sterner and Sterner 2021).

2.3.4 Additional Negative Impacts

Additional negative impacts of CAR-T treatment include tumour lysis syndrome, prolonged B-cell aplasia, hypogammaglobulinemia, and severe pancytopenia, which is prevalent and persists a few months following CAR-T cell injection (Fried et al. 2019; Neelapu 2019). Numerous biochemical markers, including lactate dehydrogenase, ferritin, C-reactive protein, inflammatory cytokines, GM-CSF, von Willebrand factor, and angiopoietin-2 (representing endothelial stimulation), and relatively low platelet count, were also linked to CRS and neurotoxicity complications, and yet a convincing developed model remains missing (Santomasso et al. 2018; Karschnia et al. 2019).

2.4 Improving CAR-T cell Efficacy

CAR-T cell treatments are considered particularly effective for the curative purposes of haematological cancers. Immunological and molecular biology innovations have enabled the development of the forthcoming generations of CAR-T cells endowed with various biological functions. Some include extra costimulatory motifs, safety switches, immune-checkpoint regulation, cytokine production, or deletion of therapy-interfering proteins. Deployment of contemporary CAR T-cells might enable circumventing present constraints on CAR-T therapy, reducing undesirable adverse

reactions, and addressing other haematological cancers (Tomasik et al. 2022; Hu et al. 2022). Immune checkpoint protein molecules, such as PD-L1, commonly expressed in tumour cells, can inhibit CAR-T cell function. Experimental results indicate that incorporating CAR-T cells into established systemic checkpoint blockade antibodies significantly improves tumour destruction (Cherkassky et al. 2016; Moon et al. 2016). As a result, the administration of immune checkpoint inhibitors in conjunction with CAR-T cells is being investigated. The pairing of axicel and atezolizumab has been started testing in the ZUMA-6 experiment, with promising initial findings, and lisocel in pairing with some other anti-PD-L1 antibody, durvalumab, is now being examined in clients with R/R B-NHL (Jacobson et al. 2018; Hirayama et al. 2018; Siddiqi et al. 2019). Aside from the potential dangers regarding CAR-T cell-based therapy, it's also widely documented that cancer cells frequently establish methods to circumvent T-cell identification. T cells are activated and proliferated when antigens are presented to them in a human leucocytic antigen (HLA)-restricted manner. By decreasing the expression of HLA class-I compounds, malignant cells dissuade T-cell attention and killing (Chhabra and Kennedy 2021; van Vliet et al. 2021). NK cells, another prominent innate immune cell, have become an alternative possible target of CAR carriers for off-the-shelf product lines. Thus, there is a pressing need to develop efficient and safe targeted immunotherapies to treat advanced cancer. Unlike T cells, NK cells are a constituent of the innate immune system and could strike cancerous cells without previous sensitization; their operation relies upon the equilibrium of activating and inhibiting receptors located on cell surfaces (Karre 2002).

3 NK cell Adoptive transfer therapy

NK cells are cytotoxic lymphocytes that are essential for natural immunity. NK cells, which account for about 10% of blood leukocytes, are effective immune effectors linked to the control of tumorigenesis (Rey et al. 2009). Immune cells recognize MHC complexes represented on infective or unnaturally altered cell surface membranes to elicit cytokine production, resulting in immune system response and apoptotic cell death or lysis of target cells (Glienke et al. 2015). NK cells represent the sole immune system cells that can distinguish cancer cells without MHC and antibodies, resulting in an immediate immune system response. Thus, these cells have been referred to as "natural killers" because they can operate without being activated to dismantle cells lacking 'self' MHC class-I chemical biomarkers (Klingemann 2014). NK cells produce several cytokines, interleukins, and interferons, which act as immune suppressors (Jiang et al. 2014). Contrary to T lymphocytes, non-hematopoietic cells are not targeted by NK cells, implying that NK cell-mediated anticancer activity can be powered up in the non-appearance of graft-vs-host disease (GvHD) (Tang et al. 2018).

Transduced NK cells can identify malignant cells using their innate membrane proteins and CAR-specific target detection, lowering the risk of tumour expulsion (Quintarelli et al. 2019). Allogeneic cell lines could not induce GvHD as they do not imply HLA matching to identify targets. Furthermore, the relatively short lifetime of NK cells mitigates the likelihood of long-term adverse effects. In a murine model, NK cells designed and implemented to assert a CD19-directed CAR, release IL-15 to sustain ectopic proliferation and longevity, and evoke a suicide gene (i.e., inducible caspase-9) demonstrated destruction capacity (Liu et al. 2018). The preclinical trial outcomes recently explore the findings on the security and success of CD19-iCasp9-IL15 transduced umbilical cord-derived NK cells in individuals with R/R CD19-positive B-lymphoid leukaemias. Following lymphodepletion chemotherapeutics, 11 patients were given one CAR-NK injection. Eight of the eleven treated groups reacted immediately (within 30 days), with seven achieving CR, and no substantial complications, such as CRS,

neurotoxic effects, or GvHD, were observed (Liu et al. 2020). In animal and *in vitro* studies, the CD19-CAR concept could be efficaciously expressed on the NK-92 cultured cells, imparting cytolytic functionality against initially impervious CD19-positive malignant cells (Romanski et al. 2016). Regrettably, before *in-vivo* activity, cells must be irradiated to prevent unnecessary cancer cell adhesion and proliferation, which may reduce their effectiveness.

Numerous investigations have been performed to assess the risks and benefits of adoptive NK cell treatment to cure haematological malignancies. But even so, since there is inadequate NK cell attachment and incursion into the tumour, applying NK cells to remediate solid tumours poses shortcomings. New therapeutic research is dedicated to enhancing NK cellular activities for adoptive transfer. Figure 4 depicts Contemporary NK cell therapy strategies that depend on autologous, allogeneic, or CAR-NK cells (Veluchamy et al. 2017).
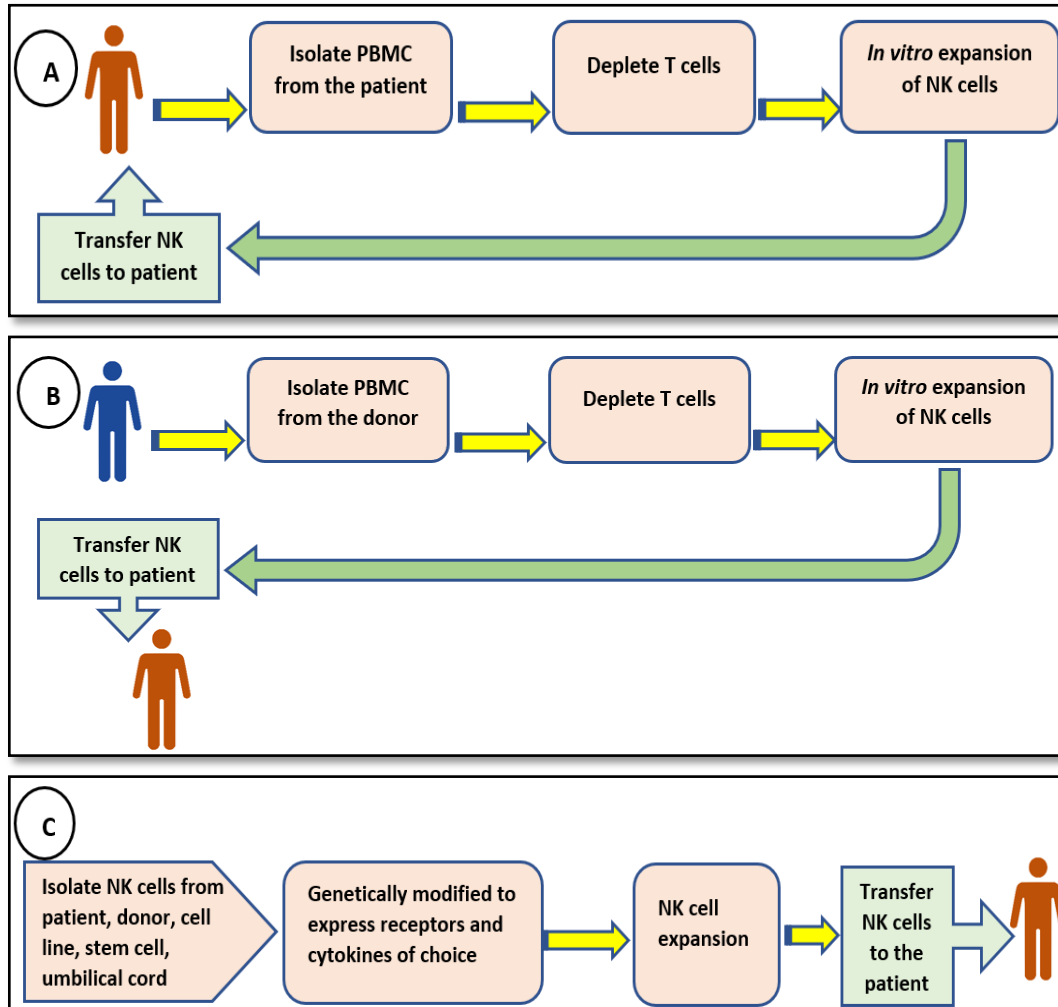

Figure 4 Schematic diagram for NK cell therapy (A) Autologous NK cell therapy, (B) Allogeneic NK cell therapy, and (C) CAR-NK therapy.

3.1 In autologous NK cell therapy

In autologous NK cell therapy, the patient's NK cells are collected, cultured, expanded outside the body, and reintroduced. The earlier experiments in NK adoptive transfer were designed to boost autologous NK cell antineoplastic actions by strengthening NK cell activity and multiplication with cytokines. When NK cells are prompted with cytokines like IL-2, IL-12, IL-15, and IL-18, they become powerful, with the elevated synthesis of adhesion molecules, activating receptors (NKp44), cytolytic protein perforin, granzymes, FasL, and TNF-related apoptosis-inducing ligand (TRAIL), along with improved cytokine release and cell multiplication (Smyth et al. 2004; Becknell and Caligiuri 2005; Davis et al. 2015). Some advantages of autologous NK cell therapy include minimizing the likelihood of system-wide immunogenicity, bio-incompatibility, and disease development affiliated with grafts or cell lines not fostered by the patient. Individuals who underwent adoptive transfer of autologous lymphokine-activated killer cells or more abundant NK cells augmented *ex vivo* in combined application with IL-2 execution had equivalent clinical outcomes (Parkhurst et al. 2011; Jiang et al. 2016). Furthermore, cytokine-induced autologous NK immune function advancement could be hampered by inhibitory activity via tumour-expressed self-MHC or prolonged immunodeficiency by the host tumour cells (Verneris 2013). With these considerations, the usefulness of allogeneic NK cells from relevant donors in the adoptive transfer was studied.

3.2 In an allogeneic NK cell immunotherapy

In an allogeneic NK cell immunotherapy, NK cells are extracted from a donor with a matching HLA-type and reintroduced into the patient to suppress the cancer cells and restore the patient's immune cell activity. An allogeneic NK cell therapy differs from an autologous one, where the latter uses NK cells from the patient's body. After several stem cell transplantation and allogeneic infusions of isolated NK cells, allogeneic NK cell studies have revealed beneficial outcomes for many types of cancer, notably acute myeloid leukaemia (AML)(Geller and Miller 2011; Davis et al. 2015). Allogeneic NK cells can be obtained from the peripheral circulation, umbilical cord, or bone marrow; meanwhile, peripheral blood remains the most frequently employed type of cell line for stem cell transplantation (Shah et al. 2013). Another NK cell contributor, including NK cell lines, provides the advantage of being free of containing T and B cells, thereby lessening any alloreactive consequences and GvHD connected with blood-derived NK cells. Then again, NK cell lines, in addition, consistently show promise to be employed in adoptive transfer contexts, with several medical studies currently in progress. Consequently, difficulties in procuring and extracting those certain cells confine their pervasive clinical application in interventional NK cell therapies (Lupo and Matosevic 2019). NK cells derived from healthy and blood-related donors gain benefit from being guided in a non-immunosuppressive atmosphere and are, hence, completely operational. NK cells' contribution to GvHD progression after adoptive transfer into receivers has been hotly debated (Simonetta et al. 2017). Several research studies have indicated that in allogeneic adoptive transfer contexts, NK cells mitigate GvHD by restricting alloreactive T lymphocytes (Bachanova et al. 2014). The difficulties in obtaining NK cell supplementation exempt from alloreactive T cells, which are operationally developed and cannot facilitate GvHD, are apparent. Though some new clinical studies have revealed that NK cell adoptive transfer therapies are reliable and successful in treating cancer, the responsibility of NK cells in linking to GvHD must not be underestimated. Achievement in establishing NK cell therapeutic strategies will depend heavily on improvements in diverse cell sources, such as NK cell cultures and stem cell-derived NK cells, as well as understanding NK cell operational physiology (Lupo and Matosevic 2019).

3.3 CAR-NK cells

CAR-NK cells have been gaining popularity due to the advancement of CAR-engineered NK cells for cancer immunotherapy. The tumour microenvironment (TME) is complex, and immune escape is needed for cancerous cells to advance and invade nearby tissues. According to an article, T-cell immunotherapy's limited success considers the notoriety of burgeoning numerous revolutionary immunotherapeutics, particularly NK-cell-based treatment options. Biological NK cells have become the most important innate immune specialized cells against cancerous cells, and they are extremely diverse inside this TME (Basar et al. 2020). CAR-NK cell lines outperform CAR-T cells in safety parameters (e.g., total lack or relatively limited CRS and GvHD, activation of diverse measures for strengthening cytolytic activity, and greater achievability for 'off-the-shelf' large-scale production). All those adaptive immune cells might be adjusted to detect specific antigens, maximize *in vivo* expansion and intensity, increase infiltration into tumour tissues, and subdue impervious TME, culminating in the preferred antineoplastic reaction. More pertinently, CAR-NK responses are considered antigen receptors for TAAs, rerouting immunoregulatory NK cells and assisting with tumour-related immunotherapy (Marofi et al. 2021).

Many animal model experiments have examined the effectiveness of CAR-NK cells against a wide range of targeted antigens for leukaemia and lymphoma along with solid tumours, constructed on the insights obtained with CAR-Tcells. To improve malignant cell identification, NK cells could be phenotypically manipulated to produce a CAR that acknowledges TAAs (Zhao et al. 2015; Chen

et al. 2016; Park et al. 2017). CAR-T's new treatment is steeply advancing. Meanwhile, CAR-NK cell advancement is struggling to keep up due to being generally restricted to early clinical trials (Mehta and Rezvani 2018). Even with their potential benefits, NK cells have downsides that might constrain their usefulness. These involve a limited lifetime of between a week and two in the case of lack of cytokine intervention, limited cell quantities that frequently necessitate *ex vivo* growth and stimulation, and high susceptibility to the immunosuppressive TME, which could hinder their tumour invasion and effective killing (Basar et al. 2020).

3.4 Future Directions in NK Cell Therapy

CAR-NK therapy could be improved by investigating the significance of optimizing the immunochemical characteristics of the CAR model, comprehending variables that contribute to cell product persistence, improving transporting of transferred cells to the tumour, facilitating metabolic wellness of the newly delivered product category, and finding ways for minimizing tumour escape via antigen destruction as well as trogocytosis (Kilgour et al. 2023; Raftery et al. 2023). NK cell therapy can be improved further by implementing different approaches, as shown in Figure 5. By initiating transformation using the C-X-C motif chemokine receptor (CXCR1), NK cells can be channelled to the tumour site. TME immunosuppressive influence could be thwarted at the cancer tissue by antagonists designed to target immunosuppressive features such as transforming growth factor-beta (TGF-β). Combined treatment could potentiate cytotoxic effects, such as hindering checkpoint blockers (i.e., NKG2A) or employing killer engagement proteins, such as bi/tri-specific antibodies. One further

method for increasing immune cell cytotoxic activity is to modify NK cells to over-express NK receptors like NKG2D genetically or to modify NK cells with CARs that target TAAs (van Vliet et al. 2021; Laskowski et al. 2022).

4 Conclusion and Future Prospects

Immunotherapy has gained much attention nowadays due to its promising results in clinical trials. CAR-T treatment is promising; however, the adverse effects are the primary concerns and must be overcome. CAR-T immunotherapy has progressed from a novel concept at the turn of the century to an immensely successful treatment with effective therapeutic prospects in B-cell neoplasms. Then again, CAR-T immunotherapy is still in its early stages, along with its numerous obvious benefits above other kinds of anticancer medications, such as in vivo expansion and long-term intensity. The prevailing deficiencies under these therapeutic interventions are already being addressed by implementing new operating systems for CAR construction, such as CAR-NK cells. Although NK cell adoptive transfer therapy showed lesser toxicity than CAR-T, the clinical trials are still ongoing and have yet to be approved by the FDA. Elaborating on the pivotal variables that influence NK cell effectiveness and consistency would be critical as the realm moves towards emerging strategies for dealing with unique challenges on every disease evidence. Eventually, creating and incorporating optimal NK proliferation, differentiation, and cryopreservation methods will be vital to maintaining high production efficiency. More scrutiny and innovations on CAR-NK cells' origin, modification of gene transfer strategies, and manufacturing for clinical use should also be considered.
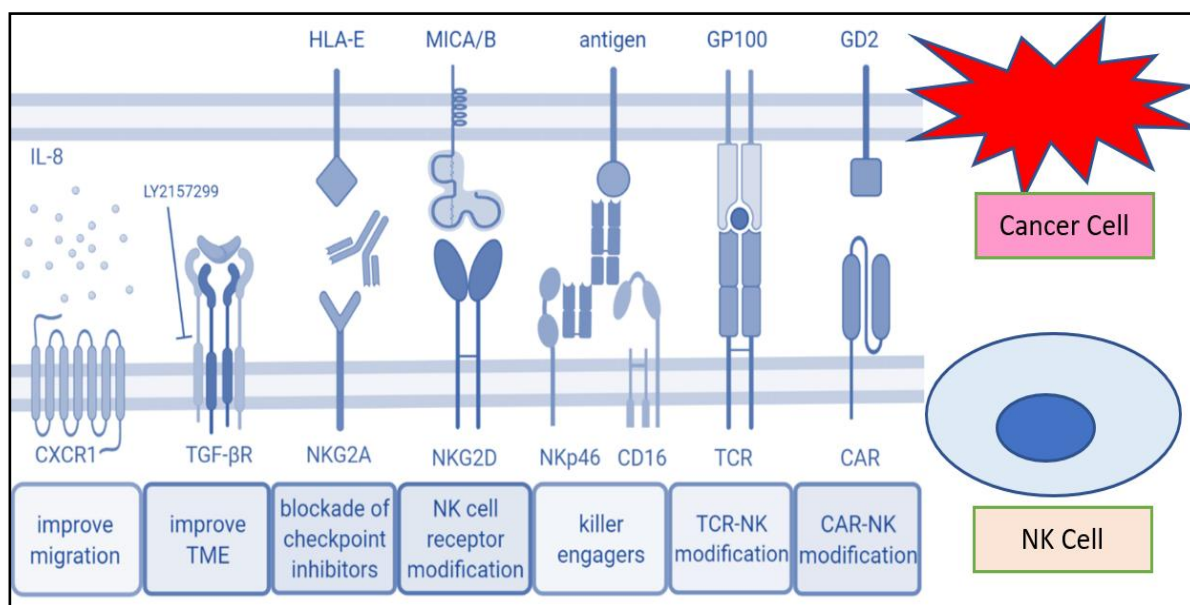
Figure 5 The schematic diagram for the strategies to improve NK cell therapy (Adapted from van Vliet et al., 2021). MICA/B =MHC class I chain-related protein A/B, GP= Glycoprotein, GD= disialoganglioside, TCR= T cell receptor, NKG2A/2D= NK cell receptor group-2A/2D

Advanced techniques, which include clustered, regularly interspaced short palindromic repeats (CRISPR) gene processing and editing, should be assessed to help combat tumour-initiated immunosuppressive strategies. When such gene-editing techniques are likely to succeed, immune-cell-mediated cancer treatment will become a standard therapy instead of a secondary choice. Operationally, for evolving NK immunotherapy implementation to be successful, interdisciplinary team systems comprised of research scientists, physicians, and regulatory bodies will be required to depict a multifaceted direction to therapeutic applications cooperatively. Combined therapy seemed promising, but more experiments are necessary to achieve the most reliable result and appropriate combination. Since tumour cells downregulate MHC-I to eschew being recognized from T lymphocytes, MHC-I negative cells are readily identified and killed by NK cells. Thus, trials comprising the alternate use of CAR-T and allogenic NK cell therapy should be considered to achieve better outcomes, especially in preventing remission and relapse of various cancers.

Conflict of Interest

All authors claim that they have no competing interests.

Acknowledgement

References

Alabanza, L., Pegues, M., Geldres, C., Shi, V., et al. (2017). Function of novel Anti-CD19 chimeric antigen receptors with human variable regions is affected by hinge and transmembrane domains. *Molecular Ther*apeutics, *25*(11), 2452–65.

Bachanova, V., Cooley, S., Defor, T.E., Verneris, M.R., et al. (2014). Clearance of acute myeloid leukemia by haploidentical natural killer cells is improved using IL-2 diphtheria toxin fusion protein. *Blood, 123*(25), 3855-63. doi: 10.1182/blood-2013-10-532531.

Basar, R., Daher, M., & Rezvani, K. (2020). Next-generation cell therapies: the emerging role of CAR-NK cells. *Blood Advances*, *4*(22), 5868–76.

Becknell, B., & Caligiuri, M.A. (2005). Interleukin-2, interleukin-15, and their roles in human natural killer cells. *Advance inImmunol*ogy, *86*, 209–39.

Bouchkouj, N., Kasamon, Y.L., de Claro, R.A., George, B., et al. (2019). FDA Approval Summary: Axicabtagene Ciloleucel for Relapsed or Refractory Large B-cell Lymphoma. *Clinical Cancer Research*, *25*(6),1702-1708. doi: 10.1158/1078-0432.CCR-18-2743.

Brudno, J.N., & Kochenderfer, J.N. (2016). Toxicities of chimeric antigen receptor T cells: recognition and management. *Blood, 127*(26), 3321–30.

Cerrano, M., Ruella, M., Perales, M. A., Vitale, C., Faraci, D. G., et al. (2020). The Advent of CAR T-Cell Therapy for Lymphoproliferative Neoplasms: Integrating Research Into Clinical Practice. *Frontiers in immunology*, *11*, 888. https://doi.org/10.3389/fimmu.2020.00888

Chen, K.H., Wada, M., Firor, A.E., Pinz, K.G., et al. (2016). Novel anti-CD3 chimeric antigen receptor targeting of aggressive T cell malignancies. *Oncotarget, 7*(35), 56219–32.

Cherkassky, L., Morello, A., Villena-Vargas, J., Feng, Y., et al. (2016). Human CAR T cells with cell-intrinsic PD-1 checkpoint blockade resist tumor-mediated inhibition. *Journal of Clinical Investigation,126*(8), 3130-44. doi: 10.1172/JCI83092.

Chhabra, N., & Kennedy, J. (2021). A Review of Cancer Immunotherapy Toxicity II: Adoptive cellular therapies, kinase inhibitors, monoclonal antibodies, and oncolytic viruses. *Journal of Medical Toxicology, 18*(1), 43-55. doi: 10.1007/s13181-021-00835-6

Davis, Z.B., Felices, M., Verneris, M.R., & Miller, J.S. (2015). Natural Killer Cell Adoptive Transfer Therapy. *The Cancer Journal*, *21*(6), 486–91.

Dholaria, B.R., Bachmeier, C.A., & Locke, F. (2018). Mechanisms and Management of Chimeric Antigen Receptor T-Cell Therapy-Related Toxicities. *BioDrugs, 33*(1), 45–60.

Dholaria, B.R., Bachmeier, C.A., & Locke, F. (2019). Mechanisms and Management of Chimeric Antigen Receptor T-Cell Therapy-Related Toxicities. *BioDrugs, 33*(1), 45-60. doi: 10.1007/s40259-018-0324-z.

Du, H., Hirabayashi, K., Ahn, S., Kren, N.P., et al. (2019). Antitumor Responses in the Absence of Toxicity in Solid Tumors by Targeting B7-H3 via Chimeric Antigen Receptor T Cells. *Cancer Cell, 11, 35*(2), 221-237.e8. doi: 10.1016/j.ccell.2019.01.002.

Fischer, J. W., & Bhattarai, N. (2021). CAR-T Cell Therapy: Mechanism, Management, and Mitigation of Inflammatory Toxicities. *Frontiers in immunology*, *12*, 693016. https://doi.org/10.3389/fimmu.2021.693016

Franks, S. E., Wolfson, B., & Hodge, J. W. (2020). Natural Born Killers: NK Cells in Cancer Therapy. *Cancers*, *12*(8), 2131. https://doi.org/10.3390/cancers12082131

Fried, S., Avigdor, A., Bielorai, B., Meir, A., et al.(2019). Early and late hematologic toxicity following CD19 CAR-T cells. *Bone Marrow Transplant*, *54*(10), 1643-1650. doi: 10.1038/s41409-019-0487-3.

Gardner, R. A., Ceppi, F., Rivers, J., Annesley, C., Summers, C., et al. (2019). Preemptive mitigation of CD19 CAR T-cell cytokine release syndrome without attenuation of antileukemic efficacy. *Blood*, *134*(24), 2149–2158. https://doi.org/10.1182/blood.2019001463.

Geller, M.A., & Miller, J.S. (2011). Use of allogeneic NK cells for cancer immunotherapy. *Immunotherapy, 3*(12), 1445–59.

Giavridis, T., van der Stegen, S.J.C., Eyquem, J., Hamieh, M., et al. (2018). CAR T cell-induced cytokine release syndrome is mediated by macrophages and abated by IL-1 blockade. *Nature Medicine, 24*(6), 731-738. doi: 10.1038/s41591-018-0041-7.

Gleichmann, N. (2020). Innate Vs Adaptive Immunity. From Technology Networks. Retrieved from: https://www.technologynetworks.com/immunology/articles/innate-vs-adaptive-immunity-335116

Glienke, W., Esser, R., Priesner, C., Suerth, J. D., Schambach, A., et al. (2015). Advantages and applications of CAR-expressing natural killer cells. *Frontiers in pharmacology*, *6*, 21. https://doi.org/10.3389/fphar.2015.00021

Grigore, A. (2017). Plant Phenolic Compounds as Immunomodulatory Agents. In M., Soto-Hernandez, M., Palma-Tenango, & M. R., Garcia-Mateos (Eds.) *Phenolic Compounds - Biological Activity*. IntechOpen. http://dx.doi.org/10.5772/66112.

Guedan, S., Posey, A.D. Jr., Shaw, C., Wing, A., et al. (2018). Enhancing CAR T cell persistence through ICOS and 4-1BB costimulation. *JCI Insight*, *3*(1), e96976. doi: 10.1172/jci.insight.96976.

Gust, J., Hay, K.A., Hanafi, L.A., Li, D., et al.(2017). Endothelial Activation and Blood-Brain Barrier Disruption in Neurotoxicity after Adoptive Immunotherapy with CD19 CAR-T Cells. *Cancer Discovery,7*(12), 1404-1419. doi: 10.1158/2159-8290.

Hay, K. A., Hanafi, L. A., Li, D., Gust, J., Liles, W. C., Wurfel, M. M., et al. (2017). Kinetics and biomarkers of severe cytokine release syndrome after CD19 chimeric antigen receptor-modified T-cell therapy. *Blood*, *130*(21), 2295–2306. https://doi.org/10.1182/blood-2017-06-793141.

Hirayama, A.V., Gauthier, J., Hay, K.A., Sheih, A., et al. (2018). Efficacy and Toxicity of JCAR014 in Combination with Durvalumab for the Treatment of Patients with Relapsed/Refractory Aggressive B-Cell Non-Hodgkin Lymphoma. *Blood*,*132*(Supplement 1), 1680–0.

Hu, Y., Feng, J., Gu, T., Wang, L., et al. (2022). CAR T-cell therapies in China: rapid evolution and a bright future. *The Lancet Haematology*, *9*(12), e930–e941. https://doi.org/10.1016/S2352-3026(22)00291-5

Jacobson, C.A., Locke, F.L., Miklos, D.B., Zheng, L., et al. (2018). End of phase 1 results from Zuma-6: Axicabtagene Ciloleucel (Axi-Cel) in combination with atezolizumab for the treatment of patients with refractory diffuse large B Cell Lymphoma. *Blood, 132*(Supplement 1), 4192–2.

Jiang, H., Zhang, W., Shang, P., Zhang, H., Fu, W., et al. (2014). Transfection of chimeric anti-CD138 gene enhances natural killer cell activation and killing of multiple myeloma cells. *Molecular oncology*, *8*(2), 297–310. https://doi.org/10.1016/j.molonc.2013.12.001

Jiang, T., Zhou, C., & Ren, S. (2016). Role of IL-2 in cancer immunotherapy. *Oncoimmunology*, *5*(6), e1163462. https://doi.org/10.1080/2162402X.2016.1163462.

Karre, K. (2002). NK Cells, MHC Class I Molecules and the Missing Self. *Scandinavian Journal of Immunology, 55*(3), 221–8.

Karschnia, P., Jordan, J. T., Forst, D. A., Arrillaga-Romany, I. C., Batchelor, T. T., et al. (2019). Clinical presentation, management, and biomarkers of neurotoxicity after adoptive immunotherapy with CAR T cells. *Blood*, *133*(20), 2212–2221. https://doi.org/10.1182/blood-2018-12-893396.

Kilgour, M. K., Bastin, D. J., Lee, S. H., Ardolino, M., McComb, S., & Visram, A. (2023). Advancements in CAR-NK therapy: lessons to be learned from CAR-T therapy. *Frontiers in immunology*, *14*, 1166038. https://doi.org/10.3389/fimmu.2023.1166038.

Klingemann, H. (2014). Are natural killer cells superior CAR drivers?. *Oncoimmunology*, *3*, e28147. https://doi.org/10.4161/onci.28147

Laskowski, T. J., Biederstädt, A., & Rezvani, K. (2022). Natural killer cells in antitumour adoptive cell immunotherapy. *Nature reviews. Cancer*, *22*(10), 557–575. https://doi.org/10.1038/s41568-022-00491-0

Lawler, S. E., Speranza, M. C., Cho, C. F., & Chiocca, E. A. (2017). Oncolytic Viruses in Cancer Treatment: A Review. *JAMA oncology*, *3*(6), 841–849. https://doi.org/10.1001/jamaoncol.2016.2064

Lee, D.W., Santomasso, B.D., Locke, F.L., Ghobadi, A., et al. (2019). ASTCT Consensus Grading for Cytokine Release Syndrome and Neurologic Toxicity Associated with Immune Effector Cells. *Biology of Blood Marrow Transplant,25*(4), 625-638. doi: 10.1016/j.bbmt.2018.12.758

Leyfman, Y.(2018). Chimeric antigen receptors: unleashing a new age of anticancer therapy. *Cancer Cell International, 18,* 182. doi: 10.1186/s12935-018-0685-x.

Liu, E., Tong, Y., Dotti, G., Shaim, H., et al. (2018). Cord blood NK cells engineered to express IL-15 and a CD19-targeted CAR show long-term persistence and potent antitumor activity. *Leukemia, 32*(2), 520-531. doi: 10.1038/leu.2017.226.

Liu, S., Deng, B., Yin, Z., Pan, J., et al. (2020). Corticosteroids do not influence the efficacy and kinetics of CAR-T cells for B-cell acute lymphoblastic leukemia. *Blood Cancer Journal,10*(2), 15. doi: 10.1038/s41408-020-0280-y.

Locke, F.L., Ghobadi, A., Jacobson, C.A., Miklos, D.B., et al. (2019). Long-term safety and activity of axicabtagene ciloleucel in refractory large B-cell lymphoma (ZUMA-1): a single-arm, multicentre, phase 1-2 trial. *Lancet Oncology, 20*(1), 31-42. doi: 10.1016/S1470-2045(18)30864-7

Lupo, K.B., & Matosevic, S.(2019). Natural Killer Cells as Allogeneic Effectors in Adoptive Cancer Immunotherapy. *Cancers, 11*(6), 769.

Marofi, F., Al-Awad, A.S., Sulaiman, H.R., Markov, A., et al. (2021). CAR-NK Cell: A New Paradigm in Tumor Immunotherapy. *Frontiers in Oncology,11,* 673276. doi: 10.3389/fonc.2021.673276.

Martino, M., Alati, C., Canale, F. A., Musuraca, G., Martinelli, G., & Cerchione, C. (2021). A Review of Clinical Outcomes of CAR T-Cell Therapies for B-Acute Lymphoblastic Leukemia. *International journal of molecular sciences*, *22*(4), 2150. https://doi.org/10.3390/ijms22042150.

Maude, S. L., Laetsch, T. W., Buechner, J., Rives, S., Boyer, M., et al. (2018). Tisagenlecleucel in Children and Young Adults with B-Cell Lymphoblastic Leukemia. *The New England journal of medicine*, *378*(5), 439–448. https://doi.org/10.1056/NEJMoa1709866.

Mehta, R. S., & Rezvani, K. (2018). Chimeric Antigen Receptor Expressing Natural Killer Cells for the Immunotherapy of Cancer. *Frontiers in immunology*, *9*, 283. https://doi.org/10.3389/fimmu.2018.00283.

Moon, E. K., Ranganathan, R., Eruslanov, E., Kim, S., Newick, K., et al. (2016). Blockade of Programmed Death 1 Augments the Ability of Human T Cells Engineered to Target NY-ESO-1 to Control Tumor Growth after Adoptive Transfer. *Clinical cancer research : an official journal of the American Association for Cancer Research*, *22*(2), 436–447. https://doi.org/10.1158/1078-0432.CCR-15-1070.

Morgan, R.A., Yang, J.C., Kitano, M., Dudley, M.E., Laurencot, C.M., & Rosenberg, S.A.(2010). Case report of a serious adverse event following the administration of T cells transduced with a chimeric antigen receptor recognizing ERBB2. *Molecular Therapeutics,18*(4), 843–51.

Mostafa, A. A., & Morris, D. G. (2014). Immunotherapy for Lung Cancer: Has it Finally Arrived?. *Frontiers in oncology*, *4*, 288. https://doi.org/10.3389/fonc.2014.00288

Neelapu, S.S., Locke, F.L., Bartlett, N.L., Lekakis, L.J., et al. (2017). Axicabtagene Ciloleucel CAR T-Cell Therapy in Refractory Large B-Cell Lymphoma. *New England Journal Medicine*, *377*(26), 2531-2544. doi: 10.1056/NEJMoa1707447

Neelapu, S.S. (2019). Managing the toxicities of CAR T-cell therapy. *Haematological Oncology,* 37(S1):48–52.

Norelli, M., Camisa, B., Barbiera, G., Falcone, L., et al. (2018). Monocyte-derived IL-1 and IL-6 are differentially required for cytokine-release syndrome and Neurotoxicity due to CAR T cells. *Nature Medicine, 24*(6), 739-748. doi: 10.1038/s41591-018-0036-4.

Obstfeld, A.E., Frey, N.V., Mansfield, K., Lacey, S.F., et al .(2017). Cytokine release syndrome associated with chimeric-antigen receptor T-cell therapy: clinicopathological insights. *Blood, 130*(23), 2569-2572. doi: 10.1182/blood-2017-08-802413.

Park, H., Awasthi, A., Ayello, J., Chu, Y., et al.(2017). ROR1-Specific chimeric antigen receptor (CAR) NK cell immunotherapy for high-risk neuroblastomas and sarcomas. *Biology of Blood and Marrow Transplant, 23*(3), S136–7.

Parkhurst, M.R., Riley, J.P., Dudley, M.E., & Rosenberg, S.A. (2011). Adoptive Transfer of Autologous Natural Killer Cells Leads to High Levels of Circulating Natural Killer Cells but Does Not Mediate Tumor Regression. *Clinical Cancer Research, 17*(19), 6287–97.

Quintarelli, C., Sivori, S., Caruso, S., Carlomagno, S., et al. (2019). Efficacy of third-party chimeric antigen receptor modified peripheral blood natural killer cells for adoptive cell therapy of B-cell precursor acute lymphoblastic leukemia. *Leukemia, 34*(4), 1102-1115. doi: 10.1038/s41375-019-0613-7.

Rafiq, S., Hackett, C.S., & Brentjens, R.J. (2020). Engineering strategies to overcome the current roadblocks in CAR T cell therapy. *Nature Review Clinical Oncology, 17*(3), 147–67.

Raftery, M. J., Franzén, A. S., & Pecher, G. (2023). CAR NK Cells: The Future is Now. *Annual Reviews of Cancer Biology*, *7*(1). https://doi.org/10.1146/annurev-cancerbio-061521-082320

Rey, J., Veuillen, C., Vey, N., Bouabdallah, R., & Olive, D. (2009). Natural killer and γδ-T cells in haematological malignancies: enhancing the immune effectors. *Trends in Molecular Medicine, 15*(6), 275–84.

Robert C. (2020). A decade of immune-checkpoint inhibitors in cancer therapy. *Nature communications*, *11*(1), 3801. https://doi.org/10.1038/s41467-020-17670-y

Romanski, A., Uherek, C., Bug, G., Seifried, E., et al. (2016). CD19-CAR engineered NK-92 cells are sufficient to overcome NK cell resistance in B-cell malignancies. *Journal of Cellular and Molecular Medicine, 20*(7), 1287-94. doi: 10.1111/jcmm.12810.

Santomasso, B.D., Park, J.H., Salloum, D., Riviere, I., et al. (2018). Clinical and Biological Correlates of Neurotoxicity Associated with CAR T-cell Therapy in Patients with B-cell Acute Lymphoblastic Leukemia. *Cancer Discovery, 8*(8), 958-971. doi: 10.1158/2159-8290.CD-17-1319.

Saxena, M., van der Burg, S.H., Melief, C.J.M., & Bhardwaj, N. (2021). Therapeutic cancer vaccines., *Nature Review Cancer, 21*(6), 360–78.

Schuster, S.J., Bishop, M.R., Tam, C.S., Waller, E.K., et al. (2019). Tisagenlecleucel in Adult Relapsed or Refractory Diffuse Large B-Cell Lymphoma. *New England Journal Medicine*, *380*(1), 45-56. doi: 10.1056/NEJMoa1804980.

Shah, N., Martin-Antonio, B., Yang, H., Ku, S., et al. (2013). Antigen presenting cell-mediated expansion of human umbilical cord blood yields log-scale expansion of natural killer cells with anti-myeloma activity. *PLoS One, 8*(10), e76781. doi: 10.1371/journal.pone.0076781.

Shimabukuro-Vornhagen, A., Gödel, P., Subklewe, M., Stemmler, H.J., et al. (2018). Cytokine release syndrome. *Journal of Immunotherapy and Cancer, 6*(1), 56. doi: 10.1186/s40425-018-0343-9.

Siddiqi, T., Abramson, J.S., Lee, H.J., Schuster, S., Hasskarl J.,et al. (2019). Safety of lisocabtagene maraleucel given with durvalumab in patients with relapsed/refractory aggressive b-cell non-Hodgkin lymphoma: first results from the platform study. *Haematological Oncology, 37,* 171–2.

Simon, B., & Uslu,U. (2018). CAR-T cell therapy in melanoma: A future success story? *Experimental Dermatology, 27*(12), 1315–21.

Simonetta, F., Alvarez, M., & Negrin, R. S. (2017). Natural Killer Cells in Graft-versus-Host-Disease after Allogeneic Hematopoietic Cell Transplantation. *Frontiers in immunology*, *8*, 465. https://doi.org/10.3389/fimmu.2017.00465

Smyth, M.J., Cretney, E., Kershaw, M.H.,& Hayakawa, Y. (2004). Cytokines in cancer immunity and immunotherapy. *Immunological Reviews, 202,* 275–93.

Sterner, R.C., & Sterner, R.M. (2021). CAR-T cell therapy: current limitations and potential strategies. *Blood Cancer Journal,11*(4), 1–11.

Sterner, R.M., Sakemura, R., Cox, M.J., Yang, N., et al. (2019). GM-CSF inhibition reduces cytokine release syndrome and neuroinflammation but enhances CAR-T cell function in xenografts. *Blood, 133*(7), 697-709. doi: 10.1182/blood-2018-10-881722.

Sung, H., Ferlay, J., Siegel, R.L., Laversanne, M., Soerjomataram, I., Jemal, A., & Bray, F. (2021). Global Cancer Statistics 2020: GLOBOCAN Estimates of Incidence and Mortality Worldwide for 36 Cancers in 185 Countries. *CA Cancer Journal of Clinician, 71*(3), 209-249. doi: 10.3322/caac.21660

Tang, X., Yang, L., Li, Z., Nalin, A. P., Dai, H., et al. (2018). First-in-man clinical trial of CAR NK-92 cells: safety test of CD33-CAR NK-92 cells in patients with relapsed and refractory acute myeloid leukemia. *American journal of cancer research*, *8*(6), 1083–1089.

Taraseviciute, A., Tkachev, V., Ponce, R., Turtle, C.J., et al. (2018). Chimeric Antigen Receptor T Cell-Mediated Neurotoxicity in Nonhuman Primates. *Cancer Discovery, 8*(6), 750-763. doi: 10.1158/2159-8290.

Tariq, S.M., Haider, S.A., Hasan, M., Tahir, A., Khan, M., Rehan, A., & Kamal, A. (2018). Chimeric Antigen Receptor T-Cell Therapy: A Beacon of Hope in the Fight Against Cancer. *Cureus,10*(10), e3486. doi: 10.7759/cureus.3486.

Tomasik, J., Jasiński, M., & Basak, G. W. (2022). Next generations of CAR-T cells - new therapeutic opportunities in hematology? Frontiers in Immunology, *13*, 1034707. https://doi.org/10.3389/fimmu.2022.1034707

van Vliet, A.A., Georgoudaki, A-M., Raimo, M., de Gruijl, T.D., & Spanholtz, J. (2021). Adoptive NK cell therapy: A promising treatment prospect for metastatic melanoma. *Cancers, 13*(18), 4722.

Veluchamy, J. P., Kok, N., van der Vliet, H. J., Verheul, H. M. W., de Gruijl, T. D., & Spanholtz, J. (2017). The Rise of Allogeneic

Natural Killer Cells As a Platform for Cancer Immunotherapy: Recent Innovations and Future Developments. *Frontiers in immunology*, *8*, 631. https://doi.org/10.3389/fimmu.2017.00631

Verneris M. R. (2013). Natural killer cells and regulatory T cells: how to manipulate a graft for optimal GVL. *Hematology. American Society of Hematology. Education Program*, *2013*, 335–341. https://doi.org/10.1182/asheducation-2013.1.335

World Health Organization (2020). Palliative Care. Available from: https://www.who.int/news-room/fact-sheets/detail/palliative-care

World Health Organization (2022). Cancer. Available from: https://www.who.int/news-room/fact-sheets/detail/cancer

Zahavi, D., & Weiner, L. (2020). Monoclonal antibodies in cancer therapy. *Antibodies, 9*(3), 34.

Zhang, G., Wang, L., Cui, H., Wang, X., Zhang, G., et al. (2014). Anti-melanoma activity of T cells redirected with a TCR-like chimeric antigen receptor. *Scientific reports*, *4*, 3571. https://doi.org/10.1038/srep03571

Zhang, Q., Ping, J., Huang, Z., Zhang, X., Zhou, J., Wang, G., Liu, S., & Ma, J. (2020). CAR-T Cell Therapy in Cancer: Tribulations and Road Ahead. *Journal of immunology research*, *2020*, 1924379. https://doi.org/10.1155/2020/1924379

Zhang, T., Jou, T.H., Hsin, J., Wang, Z., et al. (2023). Talimogene Laherparepvec (T-VEC): A Review of the Recent Advances in Cancer Therapy. *Journal of Clinical Medicine,12*(3):1098. doi: 10.3390/jcm12031098.

Zhao, Q., Ahmed, M., Tassev, D.V., Hasan, A., et al. (2015). Affinity maturation of T-cell receptor-like antibodies for Wilms tumour 1 peptide greatly enhances therapeutic potential. *Leukaemia*, *29*(11), 2238–47.

CrossMark
click for updates

Journal of Experimental Biology and Agricultural Sciences

Assessment of bacterial diversity in the chicken litter:
A potent risk to environmental health

Sunil Kumar[1, 2*] iD, Razique Anwer[3] iD, Neera Mehra[4] iD, Tamanna Devi[2] iD,
Mukesh Yadav[2] iD, Nirmala Sehrawat[2] iD, Anil Kumar Sharma[2] iD

[1]Department of Microbiology, Kampala International University, Western Campus, Ishaka City, UGANDA
[2]Department of Biotechnology, Maharishi Markandeshwar (Deemed to be) University, Mullana (Ambala City), Haryana, INDIA
[3]Department of Pathology, College of Medicine, Imam Mohammad Ibn Saud Islamic University (IMSIU), Riyadh, SAUDI ARABIA
[4]Department of Zoology, Swami Shraddhanand College, University of Delhi, Alipur, Delhi, INDIA

ABSTRACT

Using chicken litter as an organic fertilizer on land is the most common, cheapest and environmentally safest way to manage the latter generated swiftly from the poultry industry. Raw chicken litter has been applied to field soils where various vegetables are cropped to increase yield or productivity. However, the chicken litter frequently come in contact with different environments, such as water, soil, microbes and vegetation. When chickens defecate, their litters, in a few countries, are particularly reused for the next flock, potentially causing cross-contamination. Due to various contact points in the environment, a high probability of bacterial transmission is predicted, which could lead to infection spread in animals and humans. Consumption of contaminated water, food, and meat could lead to the transmission of deadly infections. Microbes in the chicken litter also affect the grazing animals while feeding on fields duly applied with chicken litter as manure. The maximum permissible limits (MPLs) in the chicken litter for land application should not exceed 10^6-10^8 CFU/g for Coliform bacteria. Antibiotics are regularly mixed in the diet or drinking water of chicken grown in marketable poultry farms for treating bacterial diseases. Rampant usage of antimicrobials also results in resistant bacteria's survival in animal excreta. Herein, we surveyed the literature to identify the major bacterial genus harboured in the fields applied with chicken manure to increase soil fertility. Our detailed survey identified different bacterial pathogens from chicken litter samples from different investigations. Most studies showed the prevalence of *Campylobacter, Salmonella, Enterococcus*, *E. coli*, *Bacillus, Comamonas, Proteus* and *Citrobacter*,

* Corresponding author

E-mail: sunilhr10h@gmail.com, kumar.sunil@kiu.ac.ug (Sunil Kumar)

including many other bacterial species in the chicken litter samples. This article suggested that chicken litter does not meet the standard parameters for direct application as organic fertilizer in the fields. Before being applied to the ground, chicken litter should be treated to lessen the danger of polluting crops or water supplies by reducing the prevalence of harmful bacteria carrying antibiotic-resistance genes.

1 Introduction

Poultry litter may have various environmental health issues when applied to agricultural land. Despite its role in improving soil fertility, it serves as a pipeline for transmitting bacterial species to the environment carrying different antibiotic resistance genes (ARGs) (Gurmessa et al. 2020; Kubasova et al. 2022). Antibiotics are used in chicken farming for treating infections caused by various microbes, including bacteria, fungi and protozoans and as growth promoters (Amarsy et al. 2021; Muhammad et al. 2022). Bacterial pathogens also carry ARGs and multidrug-resistant (MDR) genes in the digestive tract (food pipe to the gut) of farm animals and afterwards in their waste (IFT 2006; Subirats et al. 2020). Livestock manure/litter is the major origin of ARGs in the soil ecosystem in agricultural fields (Peng et al. 2017). Chander et al. (2007) stated that antibiotic resistance is one of the leading human health challenges, and it seems that the world is worryingly close to going back to the time before antibiotics. Due to the growing demand for meat products and eggs, poultry is one of the top-growing agro-based industries worldwide (Bolan et al. 2010; Kim et al. 2022).

Chicken excreta or litter is the waste created in huge amounts all over the globe (Aires 2009; Dornelas et al. 2023). Poultry litter remains a serious concern, and it is comprised of excrement, feathers, stray feed, dietary products and support matrix, which can differ as per the national and local conditions, like sawdust, shavings, nut shell, rice husk and others (Sanchuki et al. 2011). The chicken litter contains different pathogenic or non-pathogenic microorganisms, including bacteria, fungi, pathogenic protozoa, helminthes, and viruses (Figure 1). Besides carrying pathogenic microoranisms harboring antimicrobials resistance genes, chicken litter also possesses growth hormones, sex hormones like estrogen, testosterone and polycyclic aromatic hydrocarbons, heavy metals and pesticides (Deng et al. 2020). Traditionally, Antibiotics are used in broiler feed on typical or conventional farms to assist in rejuvenating growth and upgrade feed efficiency (Threlfall et al. 2000). Castanon noted that, as a result of recent developments in the study of MDR microbes, the U.S. government has stopped using antibiotics as a preventive measure, whilst the E.U. has banned their usage in poultry feed and as the growth promoters (Castanon 2007). Recently, microbial energy generation systems, i.e., bioelectrochemical systems (BESs), have been used as
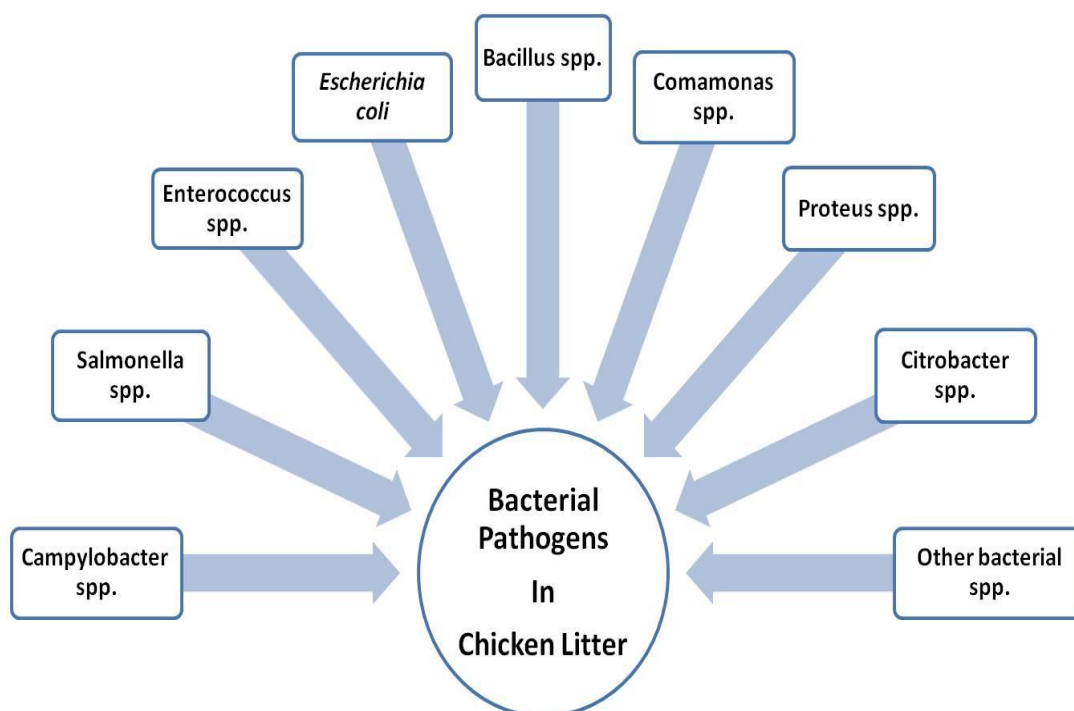
Figure 1 Different types of pathogenic or non-pathogenic microorganisms in the chicken litter

emerging sustainable technology with wide applications like wastewater treatment, heavy metal removal and biofuel production (Apollon et al. 2022). Such BESs systems can be proven helpful for managing chicken litter samples.

Antibiotic-resistant microbes spread into human and animal populations through a variety of routes like irrigation water, natural water, portable water and various eatables such as fruits, vegetables and other items (Kumar et al. 2021a; Kumar et al. 2021b; Kumar et al. 2021c; Kumar et al. 2021d; Kumar et al. 2022). Such resistant bacteria are passed in faeces, which can invade other organisms and share extrachromosomal genetic material called plasmids with neighbouring bacteria (Castanon 2007; Dhanarani et al. 2009; Olofinsae et al. 2022). Nsofor et al. (2021) gave systematic data that antibiotic use approaches are hardly followed in Nigeria, and antimicrobials are broadly utilized in the poultry industry without any check. Another study demonstrated that over 83% of poultry ranchers use tetracyclines, 50% use tylosin, 40% use gentamicin and under 30% use enrofloxacin, furazolidone, chloramphenicol, ciprofloxacin, penicillin, ampicillin and streptomycin (Dhanarani et al. 2009). Okonko et al. (2010) demonstrated that tetracycline is generally utilized in African poultry feeds, amongst other accessible antimicrobials. A recent study showed that poultry are of specific interest given their revealed linkage to vancomycin-resistant Enterococci diseases in humans (Fatoba et al. 2022). Antibiotic ratio is a significant element affecting ARGs (Bucher et al. 2020). After applying excrement or chicken litter as manure to fields, bacteria transmit from the animal's digestive tract to the environment carrying ARGs, influencing the environment and health of grazing animals in such areas (Subirats et al. 2020). To address the growing demand without a veterinarian's prescription, the U.S. Food and Drug Administration approved the use of antimicrobial agents as livestock feed supplements in 1951 (Rothrock et al. 2016). The present study aimed to survey the detailed literature for identifying the major bacterial genera that harboured in the chicken litter before being applied to the fields without treatment to increase soil fertility.

2 Bacterial Pathogens Found in Poultry Waste

Bolan et al. (2010) reported that microbial population density in poultry excreta or waste could outstrip 10^{10} cells per g of litter, and gram-positive bacteria composed almost 90% of the microbial diversity. According to the available research, *Salmonella spp* and *Campylobacter spp* are those poultry bacteria that mainly cause human foodborne illnesses (Hafez 2005).

2.1 *Campylobacter* spp.

Campylobacter spp plays a vital role in foodborne diseases and is the leading cause of zoonotic enteric infections across the globe (Li

et al. 2022). Diseases caused by *Campylobacter* in humans are primarily transmitted through the food chain (Giaouris 2023). In the case of a known poultry house infection, there is no confirmation of horizontal or vertical transfer from one flock to another. Microorganisms, on the other hand, can be found in the guts of dead birds. As a result, environmental horizontal transmission appears to be the primary mode of *Campylobacter* infection in chickens (Dawson et al. 2023). Various slaughter techniques, such as shipping, de-feathering, and evisceration, increase the external *Campylobacter* load per bird (Hafez et al. 2014). Recently, the role of chicken litter in the ecology of Campylobacter has been revealed by Valeris-Chacin et al. (2022). They examined the association between litter microbiome and Campylobacter throughout the broiler production cycle. Another study suggested that management practices and environmental factors affected Campylobacter in the litter, which was linked with the number of flocks grown over broiler houses, litter, and pH (Oladeinde et al. 2023). The rampant rise of antibiotic-resistant Campylobacter demands advancing antibiotic-alternative methods to curb infections in humans and poultry. Recently, the ability of *E. coli* Nissle 1917 (EcN) was assessed to reduce *C. jejuni* colonization in chickens (Helmy et al. 2022). The effect of EcN on the intestinal morphology, immune responses, and gut microbes of chickens was measured. Another study was performed to address the existence of *Campylobacter* in chicken litter, which was reused for consecutive flocks (Rauber Wurfel et al. 2019). *C. jejuni* strain was traced as the leading one in the sentinel broilers and in the other environmental samples, suggesting a common and constant source of contamination within the flocks.

2.2 *Salmonella* spp.

Salmonella is found in a diversified range of foods but is most commonly found in animal products, particularly pig and poultry (Hugas and Beloeil 2014; Wojcicki et al. 2022). *S. typhimurium* is spread by infected meat, eggs, and dung, among other things (Asefa Kebede and Duga 2022; Igbinosa et al. 2023). When applied to croplands via animal manure, this bacterium, particularly those with antibiotic resistance, poses a major environmental and human health hazard that should be monitored closely (Jeamsripong et al. 2023; Malik et al. 2021). Australia's study showed contamination of 100% of broiler litter samples with *Salmonella* when reused as Organic Fertilizer on land (Kyakuwaire et al. 2019). Chicken litter is also found contaminated with a vast array of heavy metals and antibiotics in this study. Competitive exclusion factors are temperature and pH, which are crucial in influencing the level of pathogens in chicken litter. *Salmonella enterica* serovar Heidelberg (S.H.) has shown a high bacterial fitness over others, which survived for 14 days in the reused litter. The microcosm, incubation duration, and microcosm plus Heidelberg strain combination significantly affected the β diversity of the litter microbiome, including *Salmonella* (Bucher et

al. 2020). Little is known about how the horizontal gene transfer is affected by commensal microbes for antimicrobial resistance. Recently, a study showed that commensal bacteria contribute to reducing the horizontal gene transfer of antibiotic resistance to *Salmonella* (Oladeinde et al. 2022). Authors in this study used shotgun metagenomics and 16S rRNA gene sequencing to demonstrate that chicks were not at a high risk of being colonized by *Salmonella* Heidelberg strains when grown on reused litter.

2.3 *Enterococcus* spp.

Multi-drug-resistant bacteria such as vancomycin-resistant enterococci (VRE) have enhanced nosocomial infections in humans (Rafey et al. 2022; Simonetti et al. 2018). *Enterococci* are Gram-positive bacteria that are natural habitats of humans and animals' gastrointestinal tracts with a broad range of species such as *E. casseliflavus*, *E. faecalis*, *E. faecium*, *E. gallinarum*, *E. durans*, *E. munditi*, *E. avium* and *E. hirae* (Zhou et al. 2020). Due to their frequent occurrence in human and animal faeces and prolonged environmental survival, *Enterococcus* spp. has developed into a widespread indicator of faecal contamination in the environment (WHO 2018; Dzelalija et al. 2023). Despite being regarded as commensal in humans, several *Enterococcus* species have been found as high-ranking (second only to staphylococci) agents responsible for nosocomial infections in humans (Haslam and St. Geme 2018). The presence of Enterococci is the marker of faecal contamination. A comparative examination of genome sequences revealed that *E. faecium* was found in fertilized soil, which is up to seven weeks older after manure application, as well as in exhaled dust (Rajendiran et al. 2022). Previously, comparable enterococci retention in manure-fertilized soil has been described. Genome sequencing of bacterial species had not been used before to track down the source of faecal contamination (Hodgson et al. 2016). A study from South Africa showed novel enterococci strains of antibiotic-resistant *Enterococcus* spp. by genomic analysis, which witnessed the transmission of plasmid-borne three AMR genes from chicken litter to agricultural land in South Africa (Fatoba et al. 2022). As per Pubmed search only seven studies has reported the incidence of *Enterococcus* spp. in the last five years, which suggested the need of more investigation for this bacteria in the chicken litter.

2.4 *Escherichia coli*

E. coli is a Gram-negative rod-shaped, not spore-forming bacteria. It is found in chicken litter samples harbouring multiple antimicrobial resistance genes (Khong et al. 2022). It could be mobile, i.e. through flagella or some other means, while others may be non-motile or non-flagellated. The bacterial species is a facultative anaerobe that can ferment simple carbohydrates like glucose to end products like produce lactic, acetic, and formic acids; the favourable pH for development is 6.0 to 8.0, but growth

can be observed at pH 4.3 and as high as pH 9 to 10 (Mitscherlich and Marth 1984). *E. coli* is an extensive and diversified bacterial group. Most E. coli strains are innocuous, but some strains have developed features, such as the ability to produce toxins, that render them hazardous to humans (Garcia et al. 2010; Woyda et al. 2023).

E. coli may survive in the environment for long periods and multiply in vegetables and other foods. According to the pathogenic mechanism, pathogenic *E. coli* has been divided into six types: (i) Enteropathogenic *E. coli* (EPEC), (ii) Enterohemorrhagic *E. coli* (EHEC), (iii) Enterotoxigenic *E. coli* (ETEC), (iv) Enteroaggregative *E. coli* (EAggEC), (v) Enteroinvasive *E. coli* (EIEC) and (vi) Attaching and Effacing *E. coli* (A/EEC) (Croxen et al. 2013; WHO 2015).

When chicken litter was used as manure, *E. coli* that were resilient to carbapenems and extended range beta-lactams might have gotten into the ecosystem, and the improper utilization of antibiotics as growth boosters in chicken and poultry diet may be the cause of this (Sebastian et al. 2021). A recent study investigated the antimicrobial resistance profile of *E. coli* isolates of chicken litter samples from pens in a broiler chicken experiment (Khong et al. 2022). This study showed high resistance to tetracycline, cephalothin, streptomycin, ampicillin, sulphonamides, colistin, and imipenem antimicrobials and 22% of *E. coli* isolates were observed with multidrug resistance (MDR) to at least three antimicrobials.

2.5 *Bacillus* spp.

Bacillus subtilis, *B. pumilus,* and *B. megaterium* are the bacteria generally found in fresh chicken litter but can also be a part of reused or old litter. Typically, these are used as prebiotic-based cleaning products. The results of this study show that treatment with P.B. can accelerate the naturally occurring process of diminishing populations of Enterobacteriaceae, which mainly contain the genus *Escherichia*, hence improving animal health and preventing poultry diseases (De Cesare et al. 2019).

2.6 *Comamonas* spp.

Four significant species of the genus Comamonas, *C. aquatica*, *C. kerstersii*, *C. terrigena*, and *C. testosteroni, are* found in poultry litter. These are the areas where the low-virulence diseases that occasionally affect humans and animals are caused by the cascade cage layers houses' nipple drinking mechanism (Chen et al. 2021).

2.7 *Proteus* spp.

Proteus species comes under the family Enterobacteriaceae of Gram-negative bacilli. According to reports, the bacterium Proteus mirabilis is one of the major causes of human pneumonia (Lysy et

al. 1985) and other infection conditions related to lungs (Wu et al. 2006). Further, 90% of Proteus infections are caused by *P. mirabilis*, typically in individuals with weakened immune systems (Cordoba et al. 2005). This infection can potentially progress endotoxin-induced sepsis, which causes systematic inflammatory response syndrome and has a 50% fatality risk. Additionally, it has been demonstrated that *P. mirabilis* can infect the CNS (Central Nervous System) (Kassim et al. 2003). The urea hydrolysis mediated by the enzyme urease produced by this bacterium leads to the development of urolithiasis. The hydrolysis causes an increase in pH that results in the precipitation of crystals of Calcium Phosphate (apatite) and magnesium ammonium phosphate (struvite), which obstructs the urinary system (Mobley and Warren 1987). *P. mirailis* also contributes to the inability of some avian species to reproduce (Cabassi et al. 2004). Additionally, *P. mirabilis* has been linked to animal kidney and urinary tract infections in earlier studies (Greenberg et al. 2004).

Research on the biochemical responses of human *P. mirabilis* isolates, and the degree of variation in their traits has been extensively published in the literature (Bergey and Holt 1993). Unfortunately, very scant information is available about *P. mirabilis,* which is of animal origin. Finding biochemical similarities between organisms causing illnesses in humans and animals is crucial, mainly when the biochemical trait is also a virulence factor, like the urease enzyme in *P. mirabilis*, which contributes to the development of kidney stones (Li et al. 2002).

2.8 *Citrobacter* spp.

Citrobacter genus bacteria and *Salmonella* share similarities in their cell surface antigens and biochemical characteristics because of their close kinship. Pillar et al. (2020) confirmed the close association of *Citrobacter* and *Salmonella* by demonstrating that they share 33% common core genes at the genome level. Their shared evolutionary history and genetic exchange can account for this unusually high genotypic resemblance. *Citrobacter* spp could be mistaken for *Salmonella* due to the characteristics mentioned above. It is also crucial to note that it takes an additional day or two to confirm ambiguous identifications, delaying the results and driving up the cost of analysis (Retchless and Lawrence 2010). *Citrobacter* spp was the second most prevalent bacteria to be retrieved and recognized from chicken litter during research, following *E. coli*, out of 149 isolates (Meshref et al. 2021).

2.9 Other bacterial species

Culture-based bacterial identification indicated *Enterococcus* spp. and *Coliforms*, but culture-independent approaches revealed additional bacteria such as *Globicatella sulfidofaciens, Corynebacterium ammoniagenes, C. urealyticum, Clostridium aminovalericum*, *Arthrobacter* spp and *Denitrobacter*

permanens. When chicken litter DNA samples were utilized as templates for microbial diversity evaluation, other harmful bacterial species such as *Clostridia, Staphylococci, and Bordetella* spp were also discovered (Meshref et al. 2021). A study from the USA reported the microbial diversity associated with offensive odour modification for the production of fertilizers from chicken litter in the USA (Enticknap et al. 2006). Bacterial strains such as *Atopostipessuicloacalis*, *Aerococcus viridians*, *C. ammoniagenes*, *Facklamia sourekii*, *Brevibacterium avium*, *Jeotgalicoccus* spp, *Salinicoccus halodurans, Virgibacillus marismortui, Staphylococcus arlettae, Staphylococcus cohnii* and *Bacilli hackensackii* were found to be prominent in both wet and dry poultry litter samples, out of which *Staphylococcus*, *Salinicoccus*, *Virgibacillus*, *Jeotgalicoccus*, *Facklamia*, *Brevibacterium* and *Bacilli* were found to be dominant (Wadud et al. 2012).

The impact of fresh or used excrement on the maturation of broiler chicken's immune systems has recently been described, in addition to the relationship between the kind of litter and gut microbiota, demonstrating the intricate relationship between the development of immune cells and the type of litter used for chicken growth (Lee et al. 2011; Torok et al. 2009).

3 Conclusions and Future Prospects

This study showed that multiple bacterial species have been identified from poultry litter because the gut of animals acts like their habitat. Various bacterial species have previously been isolated from chicken litter in many investigations where Enterococcus faecium, Proteus mirabilis, and *Campylobacter jejuni* have been identified as the most common ones. These pathogenic bacteria transmitted to the environment cause several diseases in animals and humans after coming in contact with infected chicken litter. Studies have also proved that some are responsible for transmitting antimicrobial resistance genes in the environment when they come in contact through any means. There is a dire need to periodically perform environmental safety surveys to trace harmful bacteria in the region where chicken litter is regularly applied in the agricultural fields.

This study highlighted the presence of different bacteria in the chicken litter in the other geographical regions. An economically viable solution is highly suggested for waste disposal from chicken houses to produce a natural fertilizer by a suitable treatment procedure, which can be commercially marketed for garden and commercial use. Treatment or modification of chicken litter includes enzymatic treatment and addition of Streptomyces sp. spores during composting, which may lead to achieving maximum benefits. The future directions underscore the efforts towards effectively converting chicken litter into a valuable fertilizer to alleviate the negative environmental effects.

Conflict of interest disclosure

Authors declare no conflict of interest.

Availability of data and material

Data is transparent and will be available when required.

Code availability

Custom codes.

Author contributions

Sunil Kumar planned the study. Mukesh Yadav, Nirmala Sehrawat & Tamanna Devi drafted the manuscript. Razique Anwer monitored the content and arranged the references. Razique Anwer, Anil Kumar Sharma & Neera Mehra reviewed the grammar and English check manuscript.

Ethics approval

Not required.

References

Aires, A. (2009). Biodigestão anaeróbica da cama da cama de frangos de corte com ou sem separação das frações sólida e líquida. Master's thesis, Faculdade de Ciências Agrárias e Veterinárias-UNESP Jaboticabal, Brazil.

Amarsy, R., Jacquier, H., Munier, A.L., et al. (2021). Outbreak of NDM-1-producing Klebsiella pneumoniae in the intensive care unit during the COVID-19 pandemic: Another nightmare. *American Journal of Infection Control*, *49*, 1324-1326. doi:10.1016/j.ajic.2021.07.004

Apollon, W., Iryna, R., Nancy, G.G., et al. (2022). Improvement of zero waste sustainable recovery using microbial energy generation systems: A comprehensive review. *Science of The Total Environment,* 817. doi:10.1016/j.scitotenv.2022.153055.

Asefa Kebede, I., & Duga, T. (2022). Prevalence and Antimicrobial Resistance of Salmonella in Poultry Products in Central Ethiopia. *Veterinary Medicine International, 2022,* 8625636. doi:10.1155/2022/8625636

Bergey, D., & Holt, J. (1993). *Bergey's manual of determinative bacteriology*. Williams & Wilkins, Baltimore 9th edition.

Bolan, N.S., Szogi, A.A., Chuasavathi, T., et al. (2010). Uses and management of poultry litter. *World's Poultry Science Journal, 66,* 673-698. doi:10.1017/S0043933910000656

Bucher, M.G., Zwirzitz, B., Oladeinde, A., et al. (2020). Reused poultry litter microbiome with competitive exclusion potential against Salmonella Heidelberg. *Journal of Environmental Quality, 49,* 869-881. doi:10.1002/jeq2.20081

Cabassi, C.S., Taddei, S., Predari, G., et al. (2004). Bacteriologic findings in ostrich (Struthio camelus) eggs from farms with reproductive failures. *Avian Diseases, 48,* 716-722. doi:10.1637/7142

Castanon, J.I. (2007). History of the use of antibiotic as growth promoters in European poultry feeds. *Poultry Science, 86,* 2466-2471. doi:10.3382/ps.2007-00249

Chander, Y., Gupta, S.C., Goyal, S.M., et al. (2007). Antibiotics: Has the magic gone? *Journal of the Science of Food and Agriculture, 87,* 739-742.

Chen, C.M., Wang, M., Li, X.P., et al. (2021). Homology analysis between clinically isolated extraintestinal and enteral *Klebsiella pneumoniae* among neonates. *BMC Microbiology, 21*, 25. doi:10.1186/s12866-020-02073-2

Cordoba, A., Monterrubio, J., Bueno, I., et al. (2005). [Severe community-acquired pneumonia due to Proteus mirabilis]. *Enfermedades Infecciosas y Microbiología Clínica*, *23,* 249-250. doi:10.1157/13073156

Croxen, M.A., Law, R.J., Scholz, R., et al. (2013). Recent advances in understanding enteric pathogenic *Escherichia coli*. *Clinical Microbiology Reviews, 26,* 822-880. doi:10.1128/CMR.00022-13

Dawson, P., Buyukyavuz, A., Ionita, C., et al. (2023). Effects of DNA extraction methods on the real time PCR quantification of *Campylobacter jejuni*, *Campylobacter coli*, and *Campylobacter lari* in chicken feces and ceca contents. *Poultry Science, 102,* 102369. doi:10.1016/j.psj.2022.102369

De Cesare, A., Caselli, E., Lucchi, A., et al. (2019). Impact of a probiotic-based cleaning product on the microbiological profile of broiler litters and chicken caeca microbiota. *Poultry Science, 98.* doi:10.3382/ps/pez148

Deng, W., Zhang, A., Chen, S., et al. (2020). Heavy metals, antibiotics and nutrients affect the bacterial community and resistance genes in chicken manure composting and fertilized soil.

Journal of Environmental Management, 257, 109980. doi:10.1016/j.jenvman.2019.109980

Dhanarani, T.S., Shankar, C., Park, J., et al. (2009). Study on acquisition of bacterial antibiotic resistance determinants in poultry litter. *Poultry Science, 88,* 1381-1387. doi:10.3382/ps.2008-00327

Dornelas, K.C., Mascarenhas, N.M.H., Dos Santos da Rocha, P.A., et al. (2023). Chicken bed reuse. *Environmental Science Pollution Research International, 30,* 39537-39545. doi:10.1007/s11356-023-25850-8.

Dzelalija, M., Kvesic, M., Novak, A., et al. (2023). Microbiome profiling and characterization of virulent and vancomycin-resistant *Enterococcus faecium* from treated and untreated wastewater, beach water and clinical sources. *Science of Total Environment, 858,* 159720. doi:10.1016/j.scitotenv.2022.159720

Enticknap, J.J., Nonogaki, H., Place, A.R., et al. (2006). Microbial diversity associated with odor modification for production of fertilizers from chicken litter. *Applied Environmental Microbiology, 72,* 4105-4114. doi:10.1128/AEM.02694-05

Fatoba, D.O., Amoako, D.G., Akebe, A.L.K., et al. (2022). Genomic analysis of antibiotic-resistant Enterococcus spp. reveals novel enterococci strains and the spread of plasmid-borne Tet(M), Tet(L) and Erm(B) genes from chicken litter to agricultural soil in South Africa. *Journal of Environmental Management, 302,* 114101. doi:10.1016/j.jenvman.2021.114101

Garcia, A., Fox, J.G., & Besser, T.E. (2010). Zoonotic enterohemorrhagic Escherichia coli: A One Health perspective. *ILAR Journal, 51,* 221-232. doi:10.1093/ilar.51.3.221

Giaouris, E. (2023). Relevance and Importance of Biofilms in the Resistance and Spreading of *Campylobacter spp*. within the Food Chain. *Advanced Experimental Medicine and Biology, 1370,* 77-89. doi:10.1007/5584_2022_749

Greenberg, C.B., Davidson, E.B., Bellmer, D.D., et al. (2004). Evaluation of the tensile strengths of four monofilament absorbable suture materials after immersion in canine urine with or without bacteria. *American Journal of Veterinary Research, 65,* 847-853. doi:10.2460/ajvr.2004.65.847

Gurmessa, B., Pedretti, E.F., Cocco, S., et al. (2020). Manure anaerobic digestion effects and the role of pre- and post-treatments on veterinary antibiotics and antibiotic resistance genes removal efficiency. *Science of Total Environment*, *721*, 137532. doi:10.1016/j.scitotenv.2020.137532

Hafez, H. (2005). Governmental regulations and concept behind eradication and control of some important poultry diseases. *World's Poultry Science Journal, 61,* 569-582 doi:10.1079/WPS200571

Hafez, H., Schroth, S., Stadler, A., et al. (2014). Detection of Campylobacter, Salmonella and *E. coli* that produce verotoxin during the growing and processing of turkey flocks. *Archiv für Geflügelkunde*, *65,* 130-136.

Haslam, D., & St. Geme, J.W. (2018). Enterococcus Species: Principles and Practice of Pediatric Infectious Diseases. Elsevier Inc; Amsterdam, The Netherlands: pp. 729–732. https://doi.org/10.1016/B978-0-323-40181-4.00120-1.

Helmy, Y.A., Closs, G., Jr., Jung, K., et al. (2022). Effect of Probiotic *E. coli* Nissle 1917 Supplementation on the Growth Performance, Immune Responses, Intestinal Morphology, and Gut Microbes of *Campylobacter jejuni* Infected Chickens. *Infection and Immunity, 90,* e0033722. doi:10.1128/iai.00337-22

Hodgson, C.J., Oliver, D.M., Fish, R.D., et al. (2016). Seasonal persistence of faecal indicator organisms in soil following dairy slurry application to land by surface broadcasting and shallow injection. *Journal of Environmental Management*, *183,* 325-332. doi:10.1016/j.jenvman.2016.08.047

Hugas, M., & Beloeil, P. (2014). Controlling *Salmonella* along the food chain in the European Union - progress over the last ten years. *Euro Surveillance*, *19,* doi:10.2807/1560-7917.es2014.19.19.20804

IFT ERP. (2006). Antimicrobial Resistance: Implications for the Food System: An Expert Report, Funded by the IFT Foundation. *Comprehensive Reviews In Food Science and Food Safety, 5,* 71-137. doi:10.1111/j.1541-4337.2006.00004.x

Igbinosa, I.H., Amolo, C.N., Beshiru, A., et al. (2023). Identification and characterization of MDR virulent Salmonella spp isolated from smallholder poultry production environment in Edo and Delta States, Nigeria. *PLoS One, 18*, e0281329. doi:10.1371/journal.pone.0281329

Jeamsripong, S., Kuldee, M., Thaotumpitak, V., et al. (2023) Antimicrobial resistance, Extended-Spectrum beta-Lactamase production and virulence genes in Salmonella enterica and Escherichia coli isolates from estuarine environment. *PLoS One*, *18,* e0283359. doi:10.1371/journal.pone.0283359

Kassim, Z., Aziz, A.A., Haque, Q.M., et al. (2003). Isolation of Proteus mirabilis from severe neonatal sepsis and central nervous system infection with extensive pneumocephalus. *European Journal of Pediatrics*, *162,* 644-645. doi:10.1007/s00431-003-1240-9

Khong, M.J., Snyder, A.M., Magnaterra, A.K., et al. (2022). Antimicrobial resistance profile of Escherichia coli isolated from poultry litter. *Poultry Science, 102,* 102305. doi:10.1016/j.psj.2022.102305

Kim, E., Morgan, N.K., Moss, A.F., et al. (2022). Characterization of undigested components throughout the gastrointestinal tract of broiler chickens fed either a wheat- or maize-based diet. *Animal Nutrition, 8,* 153-159. doi:10.1016/j.aninu.2021.09.011

Kubasova, T., Faldynova, M., Crhanova, M., et al. (2022). Succession, Replacement, and Modification of Chicken Litter Microbiota. *Applied and Environmental Microbiology, 88,* e0180922. doi:10.1128/aem.01809-22

Kumar, S., Anwer, R., Yadav, M., Sehrawat, N., et al. (2021a). Molecular Typing and Global Epidemiology of *Staphylococcus aureus*. *Current Pharmacology Reports, 7,* 179–186 doi:10.1007/s40495-021-00264-7

Kumar, S., Anwer, R., Yadav, M., et al. (2021b). Isolation and characterization of acinetobacter baumannii from chicken meat samples in north India. *Asian Journal of Biological and Life Sciences, 10,* 462-468. doi:10.5530/ajbls.2021.10.61

Kumar, S., Anwer, R., Sehrawat, A., et al. (2021c). Assessment of Bacterial Pathogens in Drinking Water: a Serious Safety Concern. *Current Pharmacology Reports, 7,* 206-212. doi:10.1007/s40495-021-00263-8

Kumar, S., Anwer, R., Sehrawat, A., et al. (2021d). Isolation and characterization of pathogenic bacteria from drinking water in North India. *International Journal of Environmental Science and Technology, 19,* 12605–12610. doi:10.1007/s13762-021-03774-5

Kumar, S., Yadav, M., Devi, A., et al. (2022). Assessment of Pathogenic Microorganisms Associated with Vegetable Salads. *Asian Journal of Biological and Life Sciences, 11,* 1-7 doi:10.5530/ajbls.2022.11.1

Kyakuwaire, M., Olupot, G., Amoding, A., et al. (2019). How Safe is Chicken Litter for Land Application as an Organic Fertilizer? A Review. *International Journal of Environmental Research and Public Health, 16,* doi:10.3390/ijerph16193521

Lee, K.W., Lillehoj, H.S., Lee, S.H., et al. (2011). Impact of fresh or used litter on the posthatch immune system of commercial broilers. *Avian Diseases, 55,* 539-544. doi:10.1637/9695-022511-Reg.1

Li, X., Tang, H., Xu, Z., et al. (2022). Prevalence and characteristics of Campylobacter from the genital tract of primates and ruminants in Eastern China. *Transboundary and Emerging Diseases*, 69, e1892-e1898. doi:10.1111/tbed.14524

Li, X., Zhao, H., Lockatell, C.V., et al. (2002). Visualization of Proteus mirabilis within the matrix of urease-induced bladder stones during experimental urinary tract infection. *Infection and Immunity, 70,* 389-394 doi:10.1128/IAI.70.1.389-394.2002

Lysy, J., Werczberger, A., Globus, M., et al. (1985). Pneumatocele formation in a patient with Proteus mirabilis pneumonia. *Postgraduate Medical Journal, 61,* 255-257 doi:10.1136/pgmj.61.713.255

Malik, Y., Arun, A., Milton, P., Ghatak, S., & Ghosh, S. (2021). Role of Birds in Transmitting Zoonotic Pathogens. Livestock Diseases and Management. Singapore Springer Nature. https://doi.org/10.1007/978-981-16-4554-9.

Meshref, A.E., Eldesoukey, I.E., Alouffi, A.S., et al. (2021). Molecular Analysis of Antimicrobial Resistance among Enterobacteriaceae Isolated from Diarrhoeic Calves in Egypt. *Animals* (Basel), 11, doi:10.3390/ani11061712

Mitscherlich, E., & Marth, E. (1984). *Microbial Survival in the Environment: Bacteria and Rickettsiae Important in Human and Animal Health*. Springer-Verlag. doi:10.1002/jobm.3620251017

Mobley, H.L., & Warren, J.W. (1987). Urease-positive bacteriuria and obstruction of long-term urinary catheters. *Journal of Clinical Microbiology*, 25, 2216-2217. doi:10.1128/jcm.25.11.2216-2217.1987

Muhammad, B., Diarra, M.S., Islam, M.R., et al. (2022). Effects of litter from antimicrobial-fed broiler chickens on soil bacterial community structure and diversity. *Canadian Journal of Microbiology, 68,* 643-653 doi:10.1139/cjm-2022-0086

Nsofor, C.M., Tattfeng, M.Y., Nsofor, C.A. (2021). High prevalence of qnrA and qnrB genes among fluoroquinolone-resistant *Escherichia coli* isolates from a tertiary hospital in Southern Nigeria. *Bulletin of The National Research Centre, 45,* doi:10.1186/s42269-020-00475-w

Okonko, I., Nkang, A., Fajobi, E., et al. (2010). Incidence of multidrug resistant (mdr) organisms in some poultry feeds sold in calabar metropolis, Nigeria. *Electronic Journal of Environmental, Agricultural and Food Chemistry*, 9(3), 514-532.

Oladeinde, A., Abdo, Z., Zwirzitz, B., et al. (2022). Litter Commensal Bacteria Can Limit the Horizontal Gene Transfer of Antimicrobial Resistance to Salmonella in Chickens. *Applied and Environmental Microbiology, 88,* e0251721. doi:10.1128/aem.02517-21

Oladeinde, A., Awosile, B., Woyda, R., et al. (2023). Management and environmental factors influence the prevalence and abundance

of foodborne pathogens and commensal bacteria in peanut hull-based broiler litter. *Poultry Science, 102,* 102313 doi:10.1016/j.psj.2022.102313

Olofinsae, S.A., Adeleke, O.E., & Ibeh, B.O. (2022). Occurrence of *Pseudomonas lactis* and *Pseudomonas paralactis* Amongst Non-Lactose-Fermenting Bacterial Isolates in Chickens and Their Antimicrobial Resistance Patterns. *Microbiology Insights, 15,* 11786361221130313. doi:10.1177/11786361221130313

Peng, S., Feng, Y., Wang, Y., et al. (2017). Prevalence of antibiotic resistance genes in soils after continually applied with different manure for 30 years. *Journal of Hazardous Materials, 340,* 16-25. doi:10.1016/j.jhazmat.2017.06.059

Pilar, A.V.C., Petronella, N., Dussault, F.M., et al. (2020). Similar yet different: phylogenomic analysis to delineate Salmonella and Citrobacter species boundaries. *BMC Genomics*, *21, 377.* doi:10.1186/s12864-020-06780-y.

Rafey, A., Nizamuddin, S., Qureshi, W., et al. (2022). Trends of Vancomycin-Resistant Enterococcus Infections in Cancer Patients. *Cureus, 14,* e31335 doi:10.7759/cureus.31335

Rajendiran, S., Veloo, Y., Thahir, S.S.A., et al. (2022). Resistance towards Critically Important Antimicrobials among *Enterococcus faecalis* and *E. faecium* in Poultry Farm Environments in Selangor, Malaysia. *Antibiotics* (Basel), *11* doi:10.3390/antibiotics11081118

Rauber Wurfel, S.F., Voss-Rech, D., Dos Santos Pozza, J., et al. (2019). Population Dynamics of Thermotolerant Campylobacter in Broilers Reared on Reused Litter. *Foodborne Pathogens and Disease, 16,* 738-743. doi:10.1089/fpd.2019.2645

Retchless, A.C., & Lawrence, J.G. (2010). Phylogenetic incongruence arising from fragmented speciation in enteric bacteria. *Proceedings of the National Academy of Sciences. U S A*, *107,* 11453-11458. doi:10.1073/pnas.1001291107

Rothrock, M.J., Hiett, K.L., Guard, J.Y. et al. (2016). Antibiotic Resistance Patterns of Major Zoonotic Pathogens from All-Natural, Antibiotic-Free, Pasture-Raised Broiler Flocks in the Southeastern United States. *Journal of Environmental Quality, 45,* 593-603. doi:10.2134/jeq2015.07.0366

Sanchuki, C., Soccol, C., Carvalho, J., et al. (2011). Evaluation of poultry litter traditional composting process. *Brazilian Archives of Biology and Technology*, *54,* 1053-1058. doi:10.1590/S1516-89132011000500024

Sebastian, S., Tom, A.A., Babu, J.A., et al. (2021). Antibiotic resistance in *Escherichia coli* isolates from poultry environment and UTI patients in Kerala, India: A comparison study.

Comparative Immunology, Microbiology & Infectious Disease, 75, 101614. doi:10.1016/j.cimid.2021.101614

Simonetti, O., Morroni, G., Ghiselli, R., et al. (2018). In vitro and in vivo activity of fosfomycin alone and in combination with rifampin and tigecycline against Gram-positive cocci isolated from surgical wound infections. *Journal of Medical Microbiology, 67,* 139-143 doi:10.1099/jmm.0.000649

Subirats, J., Murray, R., Scott, A., et al. (2020). Composting of chicken litter from commercial broiler farms reduces the abundance of viable enteric bacteria, Firmicutes, and selected antibiotic resistance genes. *Science of Total Environment, 746,* 141113. doi:10.1016/j.scitotenv.2020.141113

Threlfall, E.J., Ward, L.R., Frost, J.A., et al. (2000). The emergence and spread of antibiotic resistance in foodborne bacteria. *International Journal of Food Microbiology, 62,* 1-5. doi:10.1016/s0168-1605(00)00351-2

Torok, V.A., Hughes, R.J., Ophel-Keller, K., et al. (2009). Influence of different litter materials on cecal microbiota colonization in broiler chickens. *Poultry Science, 88,* 2474-2481. doi:10.3382/ps.2008-00381

Valeris-Chacin, R., Weber, B., Johnson, T.J., et al. (2022). Longitudinal Changes in Campylobacter and the Litter Microbiome throughout the Broiler Production Cycle. *Applied and Environmental Microbiology, 88,* e0066722. doi:10.1128/aem.00667-22

Wadud, S., Michaelsen, A., Gallagher, E., et al. (2012). Bacterial and fungal community composition over time in chicken litter with high or low moisture content. *Brazilian Journal of Poultry Science, 53,* 561-569. doi:10.1080/00071668.2012.723802

WHO. (2015). WHO estimates of the global burden of foodborne diseases: foodborne disease burden epidemiology reference group 2007-2015. World Health Organization; Geneva, Switzerland

WHO. (2018). A Global Overview of National Regulations and Standards for Drinking-Water Quality. World Health Organization; Geneva, Switzerland

Wojcicki, M., Chmielarczyk, A., Swider, O., et al. (2022). Bacterial Pathogens in the Food Industry: Antibiotic Resistance and Virulence Factors of *Salmonella enterica* Strains Isolated from Food Chain Links. *Pathogens, 11,* doi:10.3390/pathogens11111323

Woyda, R., Oladeinde, A., & Abdo, Z. (2023). Chicken Production and Human Clinical Escherichia coli Isolates Differ in Their Carriage of Antimicrobial Resistance and Virulence Factors. *Applied and Environmental Microbiology, 89,* e0116722. doi:10.1128/aem.01167-22

Wu, L.T., Wu, H.J., Chung, J.G., et al. (2006). Dissemination of Proteus mirabilis isolates harboring CTX-M-14 and CTX-M-3 beta-lactamases at 2 hospitals in Taiwan. *Diagnostic Microbiology and Infectious Disease, 54,* 89-94. doi:10.1016/ j.diagmicrobio.2005.09.005

Zhou, X., Willems, R.J.L., Friedrich, A.W., et al. (2020). Enterococcus faecium: from microbiological insights to practical recommendations for infection control and diagnostics. *Antimicrobial Resistance & Infection Control, 9,* 130. doi:10.1186/s13756-020-00770-1

Argania spinosa Leaves and Branches: Antiaggregant, Anticoagulant, Antioxidant Activities and Bioactive Compounds Quantification

Fatima Zahra LAFDIL[1] iD, Asmae AMIROU[1] iD, Mohamed BNOUHAM[1] iD,
Abdelkhaleq LEGSSYER[1] iD, Abderrahim ZIYYAT[1] iD, Rachid SEDDIK[2,3] iD,
Fahd KANDSI[1] iD, Nadia GSEYRA[1] iD, Hassane MEKHFI[1*] iD

[1]Laboratory of Bio-resources, Biotechnology, Ethnopharmacology and Health, Mohammed the First University, Faculty of Sciences, Oujda, Morocco
[2]Faculty of Medicine and Pharmacy, Mohammed the First University, Oujda, Morocco
[3]Laboratory of Hematology, Mohammed VI University Hospital Center, Oujda, Morocco

ABSTRACT

Thrombocytes, also known as platelets, are crucial in maintaining the balance between blood clotting. Platelet hyperactivity and oxidative stress are the primary factors contributing to cardiovascular complications. Antithrombotic therapy remains one of the most effective treatments, but various potential side effects hinder its effectiveness, including the risk of haemorrhage. Intense research has been conducted on medicinal plants to discover the natural antithrombotic compounds. *Argania spinosa*, commonly known as the argan tree or argan oil tree, is a native species of southwestern Morocco. This study evaluated the primary and secondary hemostasis and antioxidant activity of leaf and branch aqueous extracts of *A. spinosa* and also assessed the phytochemical composition of these extracts. Platelet aggregation assay was performed using washed platelets stimulated with thrombin. For plasmatic coagulation, activated partial thromboplastin time and prothrombin time were measured using the poor plasma method. Bleeding time was evaluated by inducing bleeding at the tip of a mouse tail. The antioxidant activity of the extracts was determined through the DPPH, β-carotene, and FRAP methods. The presence or absence of the secondary metabolites was carried out with the help of specific reagents, and the quantitative analysis was carried out using spectrophotometric and colorimetric methods. The study results revealed the presence of phenols, total flavonoids, cardiac glycosides, tannins, and coumarins type of secondary metabolites in both types of aqueous extracts and a higher concentration of

these was recorded in the leaves extracts. Both aqueous extracts significantly reduced *in vitro* thrombin-induced platelet aggregation, extended tail bleeding time, prolonged activated partial thromboplastin and prothrombin time and exhibited remarkable antioxidant activity. The leaf extract of *A. spinosa* exerts significant effects against thrombotic manifestations and could be a promising source of new antithrombotic compounds.

1 Introduction

Thrombotic complications related to cardiovascular diseases consist of the abnormal formation of a blood clot (thrombosis) at the level of the vessel, and its constitute is the same, which involves mechanisms as in normal hemostasis. This phenomenon causes ten million deaths yearly despite several effective antithrombotic remedies (Rosendaal and Raskob 2014). This led the researchers to put more effort into developing new natural remedies rich in bioactive compounds with fewer side effects. Ethnobotanical studies conducted in Morocco have demonstrated the antithrombotic, antiplatelet and anticoagulant potentials of various herbal extracts such as *Ageratum conyzoides*, *Brownea grandiceps Jacq* and *Lamiophlomis rotata* (Ebrahimi et al. 2020). In addition, various previous laboratory studies have shown the antiaggregating activity of *Juglans regia* (Amirou et al. 2018)*, Arbutus unedo, Cistus ladaniferus* and *Urtica dioïca* (El Haouari and Mekhfi 2017; Mekhfi et al. 2004)*, and *Petroselinum crispum* (Gadi et al. 2009).

"Argane" is the vernacular name of *Argania spinosa,* belonging to the family Sapotaceae, also known as the "tree of life". The 10th May of each year is declared International Day of *Argania spinosa* by the United Nations. *A. spinosa* is a tree native to the Souss-Massa Region of Morocco and is found across approximately 800,000 hectares in this area. Other trees of the same species have also been discovered in the Orientale Region of Morocco. It is a drought and heat resistance tree characterized by a height of 8 to 10 meters and a life period of 150 to 200 years (Rammal et al. 2009). The local population widely uses this tree for therapeutic, food and cosmetic purposes (Moukal 2004). Several studies have shown that Argan oil may have remedies for diseases such as diabetes (Bnouham et al. 2008) and cardiovascular diseases (Cherki et al. 2006). Another experimental study also showed that argane oil could benefit by exercising an antiplatelet and antithrombotic effects (Mekhfi et al. 2012).

Besides the oil's intense phytotherapeutic and nutritional values, the other parts of *A. spinosa* remained unexploited. Hence, this study was focused on the leaves and branches of *A. spinosa* in the Oriental Region of Morocco. According to available research, no studies have been conducted on these parts to test their effects on platelet aggregation and plasmatic coagulation. Therefore, this study aimed to assess the *in vitro* effects of aqueous extracts of leaves and branches of *A. spinosa* on platelet aggregation, bleeding time and plasmatic coagulation in rats. Studies of *in vitro* antioxidant activity of both aqueous extracts were also evaluated to elucidate their mechanism of action, and the qualitative and quantitative phytochemical compositions were also determined.

2 Materials and Methods

2.1 Preparation of crude aqueous extracts of *Argania spinosa*

The preparation of *A. spinosa* crude aqueous extracts (CAE) was carried out from the leaves and branches of the tree. After washing and drying in the oven at 40°C, the leaves of *A. spinosa* are crushed in a blender to make leaves powder. After this, 300 mL of boiled distilled water was mixed with the 30 g of leaves powder. The mixture was left for 30 minutes and then filtered with filter paper. The obtained filtrate was concentrated under vacuum with a rotary evaporator (Instruments Heidolph, Germany) at 45°C and then dried overnight in the oven at 40°C.

For the branches, the CAE was prepared by decoction. After washing and drying, 40 g of small branches were heated in 400 mL of distilled water until boiling. Then, the solution was filtered, concentrated with the rotary evaporator at 45°C and dried in the oven overnight at 40°C. The yield Y of each extract was calculated using the following formula:

$$Y\ (\%) = X/Z \times 100$$

Y: Yield expressed as a percentage.

X: Final weight of dry extract in grams.

Z: Initial weight of dry plant part (leaves or branches) in grams.

All extracts were aliquoted and stored at -4°C until use.

2.2 Qualitative determination of phytochemical compounds

The qualitative screening study for various extracts was conducted to determine the presence or absence of some secondary metabolites such as alkaloids, flavonoids, tannins, cardiac glycosides and coumarins.

2.2.1 Tests for alkaloids

For evaluating the presence of alkaloids in CAE, the Dragendorff test was used, for this, addition of Dragendorff reagent to particular extracts results in the formation of a dark precipitate, which shows the presence of alkaloids (Raal et al. 2020).

2.2.2 Tests for flavonoids

Aluminium chloride ($AlCl_3$) reagent test was used for recording the presence of flavonoids in all extracts of *A. spinosa*. These extracts were treated with a few drops of the $AlCl_3$ reagent solution, and the formation of green colour indicates the presence of flavonoids and colour detection was performed using fluorescence at 370 nm (Jesus et al. 2018).

2.2.3 Tests for tannins

A Ferric chloride ($FeCl_3$) test was used to evaluate the presence of tannins. For this, 1 % $FeCl_3$ is added to the sample. The development of a blue-green colour indicates the presence of tannins (Jesus et al. 2018).

2.2.4 Tests for cardiotonic heterosides

Cardiotonic heterosides were identified using the Liebermann-Buchard reaction, which involves mixing acetic anhydride and sulfuric acid with a portion of aqueous extract. The formation of a green coloring indicates the presence of the steroidal nucleus characteristic of cardiotonic compounds (Jesus et al. 2018).

2.2.5 Tests for coumarins

The extracts were treated with a few drops of 10% NaOH solution (Alkaline reagent test). The formation of yellow color indicates the presence of coumarins (Buvaneswari et al. 2011).

2.3 Determination of total phenolic content

Total phenolic (TP) was determined according to the method of Folin-Ciocalteu (Hagerman 1988), with minor modifications. 0.25 mL of Folin-Ciocalteu reagent and 0.5 mL of (2%) Na_2CO_3 solution were mixed with 0.5 mL of each CAE. After adjusting the volume with 3.5 mL of distilled water, the mixture was stirred carefully and incubated at room temperature in the dark for 90 minutes. The absorbance of the mixture was then measured by a spectrophotometer (Beijing Rayleigh Analytical Instrument, China) at 750 nm. The standard curve was prepared by using gallic acid as a standard at 0, 25, 50, 75, 125, 250, 500 µg/mL. The content of TP was expressed as "g gallic acid equivalent per 100 g dry extract". All experiments were repeated three times.

2.4 Determination of total flavonoid content

Total flavonoid contents (TF) were determined using a colorimetric method (Mu et al. 2010). 1 mL of $AlCl_3$, dissolved in 2% methanol, was added to 1 mL of each extract. After 30 min of incubation at room temperature, the absorbance of the mixture was determined by a spectrophotometer at 415 nm. A standard curve was performed using rutin as a standard at 10, 20, 30, 40, 50, 60, 70, 80, 90, and 100 µg/mL. The concentration of the TF amount was expressed in "g rutin equivalent per 100 g dry extract. Each treatment has been repeated three times.

2.5 Antioxidant assays of *A. spinosa* extracts

2.5.1 DPPH Free Radical Scavenging Activity

This test aimed to evaluate the antiradical potential of *A. spinosa* leaves and branches CAE against a stable free radical of 1, 1-diphenyl-2- picrylhydrazyl (DPPH). This assay followed the method given by de la Rosa et al. (2011) with few modifications. 1 mL of the DPPH solution was added to a final concentration range for each CAE. The samples were incubated for 30 minutes in darkness at room temperature. The absorbance was measured with a spectrophotometer at 517 nm. Ascorbic acid (AA) was used as a standard antioxidant at 25, 50, 100, 200, 400, 800, and 1000 µg/mL. All measurements were performed in triplicate. The scavenging effect is calculated according to the following equation:

$$\text{Radical Scavenging Activity (\%)} = [(A_o - A_t) / A_o] \times 100$$

A_o represents the absorbance of DPPH solution without extract; A_t represents the absorbance of the test extract mixed with DPPH solution.

2.5.2 β-Carotene Bleaching Test

This study aimed to evaluate the protective potential of leaves and branches CAE against the bleaching of β-carotene by linoleic acid degradation products. A solution of β-carotene was prepared by dissolving 2 mg in chloroform and then mixed with 20 mg of linoleic acid and 200 mg of Tween-80. The chloroform was removed by rotary evaporator at 40°C. The dry β-carotene/linoleic acid emulsion was reconstituted by adding 100 mL of distilled water with vigorous stirring. From this emulsion, 0.2 mL was transferred into different test tubes containing the sample solution. The first absorbance of the samples (t_0) was immediately read at 470 nm. Then, all samples were incubated in a water bath at 50^oC with continuous stirring. Two hours later, a second absorbance was recorded. Butylated hydroxyanisole(BHA) was used as standard at 25, 50, 100, 200, 400, 800, 1000 µg/mL, and all the measurements were performed three times. The percentage of residual color is calculated according to the following formula:

$$\text{Residual color (\%)} = 100 - [((\text{initial OD - sample OD}) / \text{initial OD}) \times 100]$$

Where initial OD represents the absorbance before incubation, sample OD represents the absorbance after 2 hours of incubation.

2.5.3 Ferric Reducing Antioxidant Power (FRAP) of extracts

The iron-reducing activity reduces Fe^{3+} present in the potassium ferricyanide ($K_3 Fe(CN)_6$) complex in Fe^{2+}. Ferric ion-reducing

power from extracts was determined by following the protocol of Bekkouch et al. (2019). Various concentrations of extracts have been prepared (25, 50, 100, 200, 400, 800, 1000 µg/mL). 1.25 mL phosphate buffer (pH=6.6) and 1.25 mL of 1 % potassium ferricyanide were added to 0.5 mL of each extract. The mixture was incubated at 50°C for 20 minutes. Then, 1.25 mL of 10% trichloroacetic acid was added to the test sample, and subsequently, the mixture was centrifuged at 3000 rpm for 10 minutes. After raising the supernatant, it is mixed with 1.25 mL of distilled water and 0.25 mL of ferric chloride solution (0.1%); the absorbance of the solution was read at 700 nm. AA was used as a standard control (25, 50, 100, 200, 400, 800, 1000 µg/mL), all measurements were carried out in triplicate.

2.6 Experimental Animals

Male and female Wistar rats and Albinos mice used in the studies were raised in the Department of Biology at the Faculty of Sciences animal house (Mohammed the First University, Oujda, Morocco) at a temperature of $22\pm2^{\circ}$C, 12 hours light/dark cycle and with free access to water and food. All animals in these experiments comply with the Guide for the Care and Use of Laboratory Animals published by the US National Institutes of Health (2012, Guide for the Care and Use of Laboratory Animals), where a minimal statistically valid number of rats and mice was respected.

2.7 *In vitro* platelet study

2.7.1 Washed Platelet Preparation

Washed platelets (WP) were prepared as described by Mekhfi et al. (2008). After light ether anaesthesia, rat blood was collected by catheterization of the abdominal aorta in a plastic tube containing (9:1, v/v) an anticoagulant solution (170 mM of trisodium citric acid, 130 mM of citric acid, and 4% dextrose). Centrifugations separated the platelet-rich plasma (PRP) from other blood cells. After noting its volume, the PRP was centrifuged again to obtain a pellet of platelets. The supernatant, known as platelet-poor plasma (PPP), was discarded, and the platelet pellet was resuspended in a washing buffer equal to the initial PRP volume. A last centrifugation was conducted, and the platelet pellet was then suspended in a calculated volume of a final buffer (NaCl 137 mM, KCl 2.6 mM, $MgCl_2$ 0.9 mM, Glucose 5.5 mM, $CaCl_2$ 1.3 mM, Gelatin 0.25%, Hepes 5 mM, pH of 7.4) to achieve a constant concentration of 5×10^5 washed platelets/mm^3.

2.7.2 *In vitro* Platelet Aggregation Study

In vitro measurement of platelet aggregation was performed using a semi-automatic aggregometer (Helena, USA) under a constant temperature (37°C) and at a stirring speed (1000 rpm), and AggroLink Software piloted the results. To study the effect of *A.*

spinosa, 250 µL of the washed platelets were incubated for one minute in an aggrometer tube with CAE (1 g/L). The control tube contained only WP suspension without plant extract. Then, platelet aggregation was triggered by adding an aggregant agonist, the thrombin at 0.5 U/mL, and the aggregation signal was recorded for at least 5 minutes. Two parameters were deducted from the original traces of platelet aggregation. The computer software automatically calculated the amount of aggregation (%) in the absence and presence of plant extracts. The following formula calculates the amount of inhibition of aggregation (%):

$$\text{Inhibition (\%)} = (A-B/A) \times 100$$

A: Maximum aggregation in the absence of the extract (control)

B: Maximum aggregation in the presence of the extract

2.8 Bleeding time determination

Bleeding time (BT) overall reflects the primary hemostasis process. Male and female Albino mice (18-22 g) were divided into six groups, with 5 mice per group. A single oral administration was performed as follows: the control group received distilled water (1 mL/100 g), the four test groups received branches and leaves CAE from the two regions (1 g/Kg), and the positive control group received acetylsalicylic acid (ASA) (30 mg/Kg). Intraperitoneal anaesthesia with sodium pentobarbital (50 mg/kg) was applied one hour after the treatment. The animals were then placed on a heating plate at 37°C. Afterwards, the mouse's tail was disinfected with alcohol and sectioned 1.5 cm from its tip with a scalpel. The stopwatch was started as soon as the first drop of blood appeared. When no drops came out, the stopwatch was stopped, and the BT (seconds) was noted.

2.9 *In vitro* anticoagulant activity

2.9.1 Platelet Poor Plasma Preparation

The blood sample was taken using the abdominal aorta catheterization method in anaesthetized rats (250-300 g). The blood was placed in a plastic tube containing the anticoagulant (3.8% trisodium citrate, 1/9, v/v), and centrifuged immediately at 3000 rpm for 20 minutes to recover platelet-poor plasma (PPP) (Amirou et al. 2022).

2.9.2 Determination of coagulation times

Coagulation tests are performed on the PPP using an automatic coagulometer "CS-2100i-sysmex". 100 µL of PPP and 50 µL of different *A. spinosa* extracts (1 g/L) or 50 µL of distilled water were incubated at 37°C for 5 minutes. A 50 µL aliquot of the mixture is taken and re-incubated for 2 min at 37°C. The coagulation process is triggered by adding 100 µL of the reagent

Table 1 Yields of the extraction of *A. spinosa* leaves and branches

Plant site	Part used	Yield (%)
Chwihia	Leaves	26.06
	Branches	4.32
Oujda city	Leaves	14.52
	Branches	1.07

Table 2 Qualitative phytochemical screening of the different *A. spinosa* crude extracts

Collected sample	Alkaloids	Flavonoids	Tannins	Coumarins	Cardiac glycosides
ASLC	-	+++	++	++	+++
ASBC	-	+	-	-	-
ASLO	-	+++	++	++	++
ASBO	-	++	+	-	+

ASLC - *A. spinosa* leaves from Chwihia site; ASBC - *A. spinosa* branches from Chwihia site; ASLO - *A. spinosa* leaves from Oujda site; ASBO - *A. spinosa* branches from Oujda site; "+++" Heavily present; "++" Moderately present; "+" Slightly present; "-" Not present.

Thromborel S to determine the prothrombin time (PT). To determine the activated partial thromboplastin time (APTT), 50 μL of the reagent CK PREST is added, and the mixture is incubated for 3 minutes. Then, the reaction is triggered by adding 50 μL of calcium. Heparin, an anticoagulant molecule, was used as a reference positive control for clotting tests.

2.10 Statistical analysis

The obtained data was analyzed using GraphPad Software (version 5.01, GraphPad Software, Inc.). For all studies, the results were expressed as mean ± SEM. Differences between values were analyzed using two-way and analysis of variance (ANOVA) followed by Bonferroni's post-test (*: $p < 0.05$, **: $p<0.01$, ***: $p<0.001$, NS: $p> 0.05$, vs control group).

3 Results

3.1 Yields of aqueous extractions

To prepare the *A. spinosa* leaves and branches, CAE samples were collected from the Chwihia and Oujda sites. The yields of leaves and branches CAE were determined with the weight of dry plant material. As per the results presented in Table 1, the highest yields

were obtained from the leaves rather than the branches. In addition, *A. spinosa* samples collected from the Chwihia's site showed higher yields than the Oujda site.

3.2 Qualitative phytochemical screening of the crude extracts

The presence of the secondary phytochemical compounds was evaluated by using specific reagents. From the qualitative phytochemical screening, it was reported that the flavonoids are the most represented secondary metabolites, followed by cardiac glycosides, tannins and coumarins, while the presence of the alkaloids wasn't detected in any CAE (Table 2). In addition, leaves of *A. spinosa* seem richer than branches, especially in *A. spinosa* branches of the Chwihia, where nearly all compounds don't exist.

3.3 Quantitative phytochemical evaluation of polyphenolic and flavonoid compounds

Total polyphenols and flavonoids compounds were quantified in all CAE of *A. spinosa* and expressed in equivalent milligrams of gallic acid and rutin per 1 g of dry extract weight, respectively. As presented in Table 3, total polyphenols were more concentrated in our extracts than flavonoids, and in general, *A.spinosa* branches CAE were poorer than the leaves, regardless of the collection site.

Table 3 Total polyphenols and flavonoids of *A. spinosa* crude aqueous extracts.

Extracts	Polyphenols compounds (mg eq Gallic acid/g dry ext)	Flavonoids compounds (mg eq Rutin/g dry ext)
ASLC	162.5±1.8	49.6±0.8
ASBC	59.3±1.3	33.8±0.9
ASLO	160.3±5.4	34.2±0.8
ASBO	150.4±1.1	22.0±2.1

ASLC - *A. spinosa* leaves from Chwihia; ASBC - *A. spinosa* branches from Chwihia; ASLO - *A. spinosa* leaves from Oujda, and ASBO - *A. spinosa* branches from Oujda; All data are represented by mean ± SEM (n = 3).

3.4 Antioxidant activities of the crude extracts

Three methods used for the antioxidant measurement were DPPH, β-carotene and FRAP. Table 4 presents the IC_{50} values for the four types of CAE. They ranged between 294 and 2500 µg/mL, obtained with the FRAP method. Depending on the plant part, leaves seem to have the most robust antioxidant activity, with IC_{50} values smaller than in branches, except for ASLO and ASBO extracts in the β-carotene test. On the other hand, all extracts' values are higher than those of the antioxidant references, AA and BHA.

Table 4 Half inhibition concentration (IC_{50}; µg/mL) values for leaves and branches of *A. spinosa* obtained with three antioxidant methods

Extracts	IC_{50} (µg/mL)		
	DPPH	β-carotene	FRAP
ASLC	434.4 ± 2.8	380.5 ± 1.5	357.1 ± 0.01
ASBC	735.2 ± 15.2	433.6 ± 6.7	2500 ± 0.3
ASLO	419.8 ± 5.6	425.8 ± 16.2	294.1 ± 0.1
ASBO	454.5 ± 10.5	406.5 ± 6.1	555.5 ± 0.1
AA	137.6 ± 0.1	-	33.6 ± 0.1
BHA	-	144.7 ± 1.1	-

ASLC - *A. spinosa* leaves from Chwihia; ASBC - *A. spinosa* branches from Chwihia; ASLO - *A. spinosa* leaves from Oujda, and ASBO - *A. spinosa* branches from Oujda; AA - ascorbic acid; BHA - Butylated Hydroxyl Anisole; Data are presented as mean ± SEM; Number of independent experiments = 3.

Figure 1 Original plots (A, C) and histograms (B, D) representing the effect of the crude aqueous extracts of *A. spinosa* leaves and branches (1 g/L) on *in vitro* thrombin-induced platelet aggregation; the values given are means ± SEM; Number of independent experiments 6-8; ASLC - *A. spinosa* leaves from Chwihia; ASBC - *A. spinosa* branches from Chwihia; *** (*p*<0.001) vs control

3.5 *In vitro* effect of aqueous extracts of *A. spinosa* on platelet aggregation

This study evaluates the *in vitro* effect of the *A. spinosa* leaves and branches CAE from the two regions on rat platelet aggregation. One minute after preincubation with extract (1 g/l), the WP aggregation was evoked by thrombin (0.5 U/mL). As shown in Figure 1, the aggregation control was around 90%. While *A. spinosa* leaves (ASLC) and branches (ASBC) extracts collected from the Chwihia region caused a significant reduction in aggregation amount as compared to the control ($p<0.001$). The calculated amounts of inhibition were 76.1 ± 1.6 and 17.97 ± 1.4 for ASLC and ASBC, respectively. The comparison of these values showed that ASLC was statistically more effective ($p<0.001$) on aggregation inhibition than ASBC.

Figure 2 shows the *in vitro* effect of *A. spinosa* leaves (ASLO) and branches (ASBO) CAE collected from the Oujda site on thrombin-induced platelet aggregation compared to the control (without extract) ($\approx 95\%$). The two extracts reduced the platelet aggregation significantly ($p<0.001$). The amount of inhibition was similar in both extracts, 66.1 ± 8.3 % and 68.7 ± 4.0 % for ASLO and ASBO, respectively.

3.6 Effect of aqueous extracts of *A. spinosa* on tail bleeding time

In control, the BT is about 150 seconds (n=5) and after treatment with the *A. spinosa* leaves CAE from Chwihia and Oujda sites (1 g/kg), significantly extended ($p<0.001$, and $p<0.01$ respectively) the BT (Figure 3). Among the tested extracts, the ASLC effect is

(A)

(B)

(C)

(D)
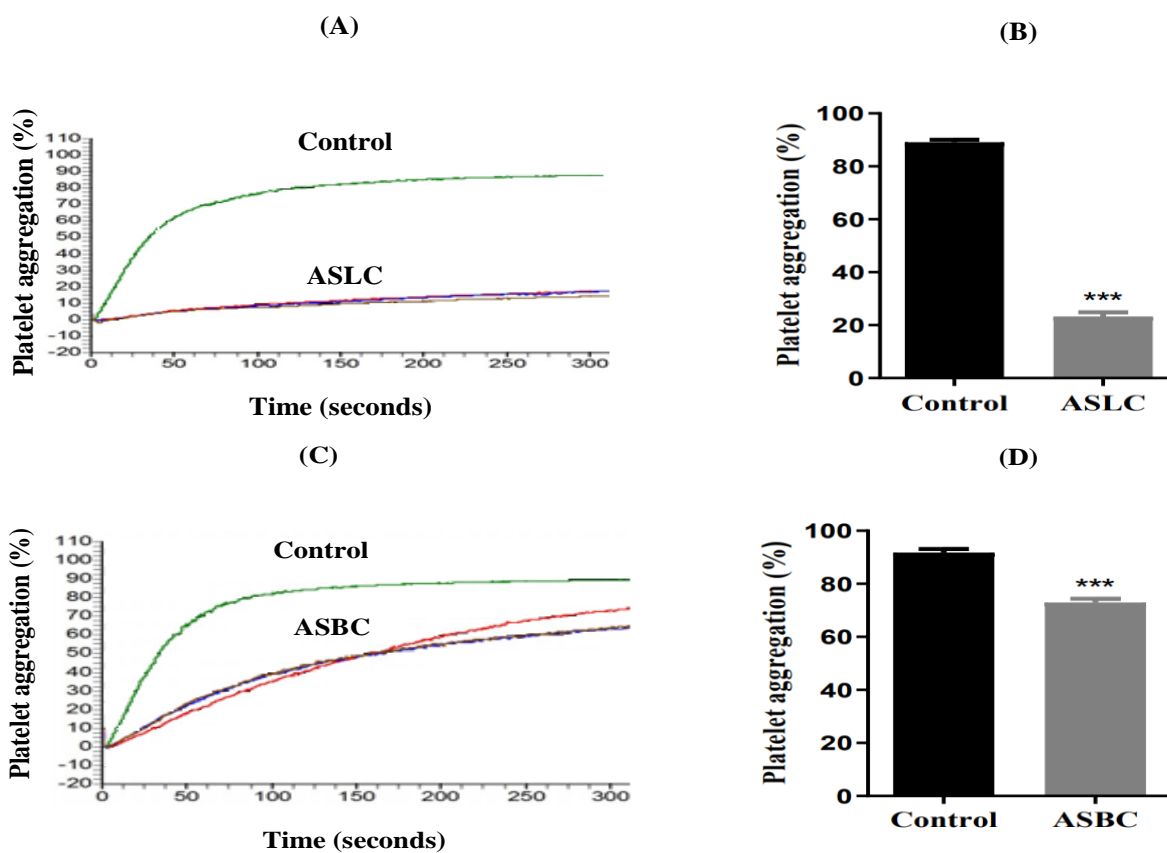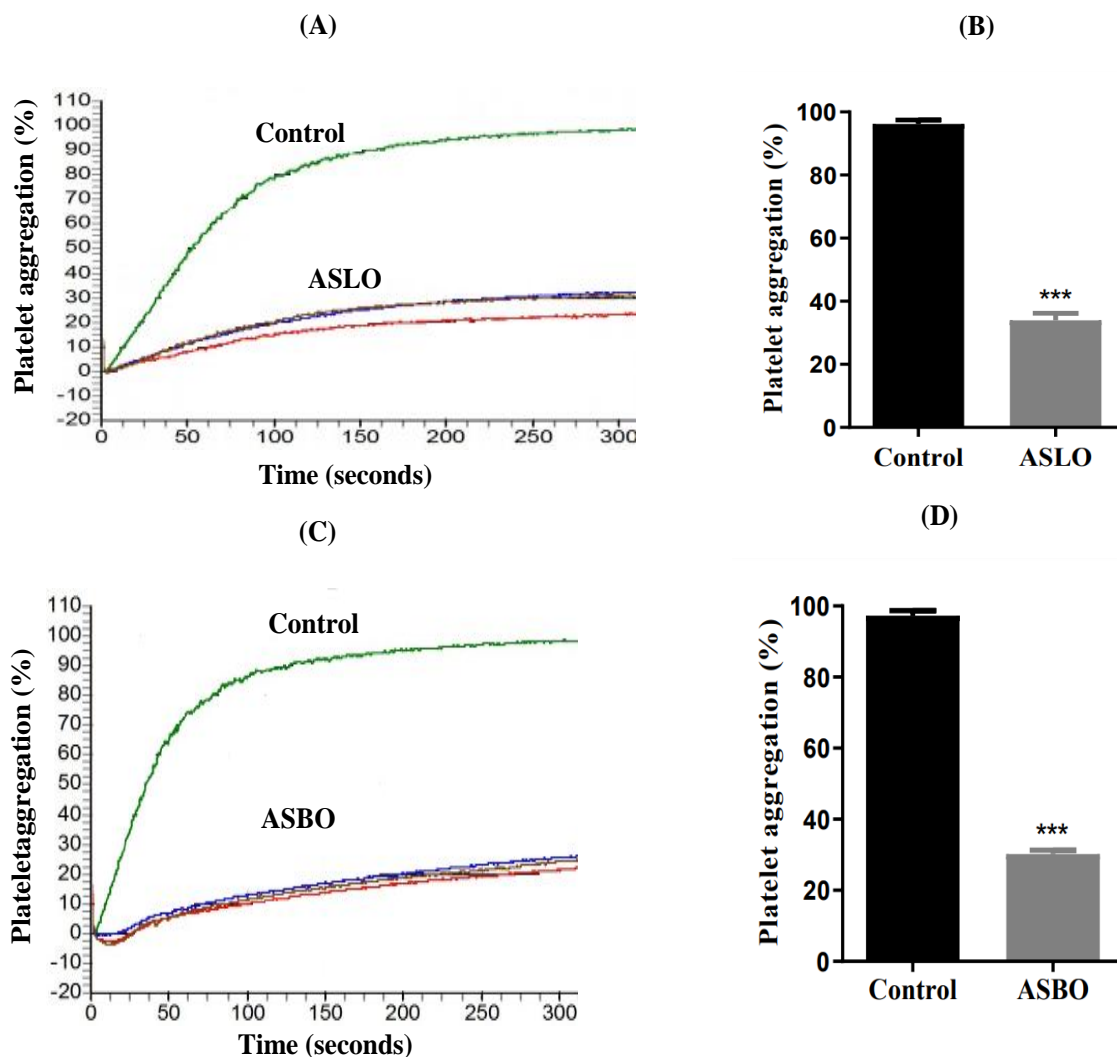

Figure 2 Original plots (A, C) and histograms (B, D) representing the effect of the crude aqueous extract of *A. spinosa* leaves and branches (1 g/L) on *in vitro* thrombin-induced platelet aggregation in rats; the number of independent experiments 6-8, ASLO: *A. spinosa* leaves from Oujda and ASBO: *A. spinosa* branches from Oujda, significance level at *** $p<0.001$ vs control.
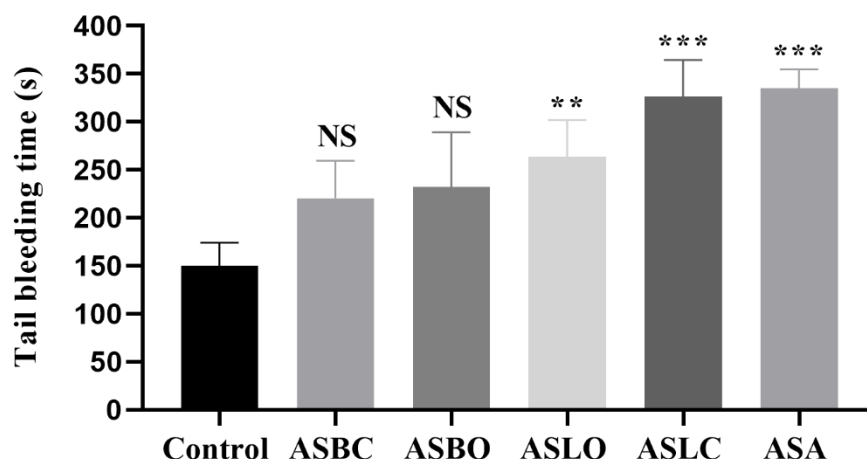
Figure 3 Effect of crude aqueous extracts of leaves and branches of *A. spinosa* (1 g/kg) on tail bleeding time in mice; Number of independent experiments 5; ASLC - *A. spinosa* leaves from Chwihia; ASBC - *A. spinosa* branches from Chwihia; ASLO - *A. spinosa* leaves from Oujda and ASBO - *A. spinosa* branches from Oujda; ASA - acetylsalicylic acid; **$p<0.01$, ***$p<0.001$ compared to control.

Table 5 *In vitro* effect of aqueous extracts of leaves and branches of *A. spinosa* on coagulation times

Sample	PT (s)	APTT (s)
Control	10.3±0.3	37.0±1.4
ASLC	17.9±0.8[***]	51.4±3.5[***]
ASBC	9.6±0.2[NS]	39.6±3.5[NS]
ASLO	26.7±2.6[***]	60.4±2.7[***]
ASBO	9.9±0.2[NS]	48.4±0.1[*]
Heparin (0.4U/ml)	10.7±0.2[NS]	77.6±1.4[***]

ASLC - *A. spinosa* leaves from Chwihia; ASBC - *A. spinosa* branches from Chwihia; ASLO - *A. spinosa* leaves from Oujda and ASBO - *A. spinosa* branches from Oujda; PT - Prothrombin time; APTT - Activated partial thromboplastin time; *$p<0.05$, ***$p<0.001$ compared to control; Number of independent experiments = 5-6.

comparable to the ASA. While, in the case of branches, the results show an increase in BT, these differences did not reach significance.

3.7 *In vitro* effect of aqueous extracts of *A. spinosa* on plasmatic coagulation

As presented in Table 5, the two leaf extracts (1 g/l) significantly ($p<0.001$) prolonged the PT and APTT compared to the control. However, the branch extracts didn't change these coagulation times, except for the ASBO action on the APTT ($p<0.05$).

4 Discussion

Blood platelets or thrombocytes play a key role in the hemostasis process, specifically in primary hemostasis. In case of a vascular lesion, their mission is to prevent bleeding and plug the vascular injury by forming a platelet thrombus. Thus, several sequential mechanisms involving these cells are triggered: sub-endothelium adhesion, activation, shape change, granular secretion, and finally, platelet aggregation. On the other hand, abnormal platelet hyperactivity linked to many diseases (arterial hypertension, diabetes) is widely described in literature (El Haouari and Rosado 2016), which contribute to the development of thrombotic complication, ischemic stroke, coronary heart disease, myocardial infarction, and cerebral vascular accident (Morel et al. 2010). Several antithrombotic drugs have been developed to treat or prevent these adverse effects. Unfortunately, they cause severe side effects, including hemorrhagic disorder, ulcers, allergies, and hepatic and renal toxicities (Li et al. 2020). So, intense research and efforts are deployed to develop new antiplatelet or antithrombotic molecules with less or no side effects.

In this context, this study focused on *A. spinosa*, an endemic tree of Morocco. The choice of this plant is mainly based on ethnobotanical studies that have shown its wider use in various traditional medicines for treating several diseases by the Moroccan population. The tree is widely known for its oil and therapeutic virtues. Many experimental investigations have already proven that *A. spinosa* oil exert several beneficial actions against

cardiovascular (Cherki et al. 2006) and metabolic disorders, such as hypocholesterolemic (Berrougui et al. 2003), antioxidant and antidiabetic (Ben Mansour et al. 2018), antiplatelet aggregation and antithrombotic (Mekhfi et al. 2012).

In the present study, to explore additional information, leaves and branches of *A. spinosa* were collected from two different localities of the Oriental Region of Morocco (Chwihia and Oujda sites). After exploring their phytochemical composition, the CAE of leaves and branches of *A. spinosa* were tested on platelet aggregation, bleeding time, and plasmatic coagulation and evaluated their antioxidant power. Results of the phytochemical analytical study revealed that alkaloids are absent in both types of aqueous extract. However, flavonoids are present in all extracts with different concentrations. Tannins, phenols, and cardiac glycosides have been identified only in three extracts, i.e. ASLC, ASLO and ASBO. While the coumarins are present in the same amount in *A. spinosa* leaves collected from both sites. These phytochemicals are known for their therapeutic importance because they have many biological roles. Indeed, flavonoids exert antibacterial activity, phenols are antioxidants, and tannins have antiviral and healing effects (Rai et al. 2013).

The quantification of polyphenols and flavonoids is commonly done through spectrophotometric methods (Folin-Ciocalteu test and aluminium trichloride test). The study results revealed a high content of polyphenols in the leaves aqueous extracts of both regions, although a remarkable amount of flavonoids was observed in the CAE of the leaves of Chwihia. These results are consistent with the previous scientific works on the same plant (Charrouf and Guillaume 1999; Mercolini et al. 2016). Indeed, some flavonoids, quercetin and myricetin, have been isolated from the leaves of *A. spinosa* (Charrouf and Guillaume 1999). Other phytochemical studies have shown that *A. spinosa* leaves are rich in various phenolic compounds such as epicatechina, catechin, myricetin, quercetin, rutin, myricetin 3-O-galactoside and melatonin (Mercolini et al. 2016).

The literature has reported that flavonoids have exceptional antioxidant potential and act by their anti-inflammatory and anti-thrombogenic effects that would be potentially effective against chronic diseases (Nijveldt et al. 2001). For this reason, this study tested the effect of polyphenolic and flavonoid compounds rich *A. spinosa* extracts against platelet aggregation, bleeding time, plasmatic coagulation and antioxidant activity.

Further, antioxidant activity should not be decided based on a single antioxidant test model. Several *in vitro* test procedures are performed to evaluate antioxidant activities with samples of interest (Alam et al. 2013). Therefore, we used three tests with different antioxidant principles in this study. The ability of the extracts to give a hydrogen atom or an electron has been assessed using DPPH (Tepe et al. 2005). The potential of *A. spinosa* extracts to delay lipid peroxidation was evaluated using a β-carotene/linoleic acid bleaching test and FRAP reducing power test, which assesses the ability of the extracts to reduce the Fe^{3+}ion to Fe^{2+} ion. Results of the study showed that except for Chwihia branches extract, all extracts exhibit a strong ability to scavenge oxygen free radicals. Results of the study suggested that leaves extracts are more effective than branches extract. There is a well-established link between antioxidant activity and the abundance of these bioactive chemicals. However, certain limits must be considered when comparing the content and composition of polyphenols in Argan leaves and branches aqueous extract and their antioxidant activity. The synthesis of secondary metabolites is an ingenious strategy plants use to control their environment and adapt to biotic and abiotic conditions. Therefore, the geographical origin, the period of collection of plant material and the phenotype of the Argan tree are the major parameters that have a significant impact on the chemical composition of the plant (Bourhim et al. 2021), which could explain the difference in activity between the same plant from two different regions.

This study investigated the effect of different extracts of *A. spinosa* (1 mg/ml) on thrombin-induced platelet aggregation and bleeding time under *in vitro* conditions. Contrary to the Chwihia branches extract, which exhibits a shallow antiplatelet effect, all other extracts demonstrate a significant reduction in platelet aggregation and a prolonged tail bleeding time. Similar studies on some medicinal plants have been conducted and reported that inhibition of platelet aggregation is not always associated with a change in bleeding time. Mekhfi et al. (2008) showed that *A. spinosa* oil inhibits platelet aggregation without affecting bleeding time. However, Ferreira et al. (1999) reported that in addition to its antiplatelet effect, isolated quinones of *Auxemma oncocalyx Taub* cause a significant decrease in bleeding time. This difference in the results suggested that different compounds have different modes of action. Based on all these data, the tested aqueous extracts of *A. spinosa* (leaves and branches) have a more potent antiaggregating effect than its oil. This can be attributed to their difference in solubility. Indeed, *A. spinosa* oil could act just at the level of the cell membrane, while the constituents of aqueous extracts can penetrate inside the cell. According to Rand et al. (1988), fatty acids can regulate platelet function by modulating the number of their precursors and changing cell membrane fluidity.

In the cascade of coagulation, activated partial thromboplastin time and prothrombin time are the basic blood measurements to assess the risk of bleeding and thrombosis. APTT is linked to the intrinsic and/or common pathways of plasma coagulation and is used to detect deficiencies in factors II, V, VIII, IX, X, XI and XII. PT mainly explores clothing factors of the extrinsic pathway (Kim et al. 2013; Sayari et al. 2016). The current study showed that leaves

of *A. spinosa* significantly prolong the PT and APTT, suggesting that these extracts exert an intense action on the extrinsic and intrinsic pathways of plasmatic coagulation.

Functional abnormalities of platelets or thrombopathies produce hemorrhagic clinical manifestations and an extension of bleeding time similar to thrombocytopenia. The hemorrhagic syndrome may affect one or more steps, including adhesion, secretion, activation, aggregation and coagulant hemostasis activity (Nurden et al. 2007). In the current study, we suggest that the extension of bleeding time induced by *A. spinosa* leaves would be caused in part, probably, by the inhibition of platelet aggregation. Consequently, these extracts may be able to prevent cardiovascular and thrombotic complications. This shows this plant's special interest, which is widely consumed by the Moroccan population.

Epidemiological studies suggested that high consumption of polyphenols is associated with reduced risk of cardiovascular disease (Nardini et al. 2007). Furthermore, sterols can increase the release of prostacyclin "PGI2" by vascular smooth muscle cells. This molecule acts as a platelet antiaggregator by stimulating adenylate cyclase and cAMP production (Awad et al. 2001). Another study shows that sterols present in margarine significantly inhibits platelet aggregation and adhesion time after collagen activation (Kozłowska-Wojciechowska et al. 2003). Margarine-containing sterols can play a vital role in the prevention of cardiovascular diseases.

Flavonoids, whose richness is demonstrated by both types of extracts prepared in this study, and their beneficial properties against cardiovascular risk are well documented (Kumar and Pandey 2013). According to Pignatelli et al. (2000), flavonoids quercetin and myricetin inhibited platelet aggregation induced by different agonists such as ADP, arachidonic acid and collagen.

Many routes, such as arachidonic acid way, phospholipase C signalling pathway, mobilization of intraplatelet Ca^{++} and other enzymatic activities, are proposed to explain the antiaggregant action of flavonoids. These compounds may act by stopping the thromboxane A_2 production by blocking the cyclooxygenase "COX", phospholipase A_2 or the thromboxane A_2 synthetase (Faggio et al. 2017) or inhibiting the interaction of thromboxane A_2 with its receptor (Guerrero et al. 2005). In addition, Nardini et al. (2007) reported that reduced phospholipase C activity may be leading to the breakdown of the cytoplasmic inositol trisphosphate (Sheu et al. 2004). Finally, the cytoplasmic Ca^{++}, which plays a key role in platelet activity, is indeed reduced, and it was reported that quercetin has been shown to inhibit calcium mobilization (Pignatelli et al. 2000). On the other hand, flavonoids are also able to activate adenylate cyclase and guanylate cyclase or inhibit phosphodiesterases. These enzymatic activities inhibition can promote the accumulation of cAMP and cGMP. This accumulation causes a decrease in granular secretion and, thus, an inhibition of platelet aggregation (Landolfi et al. 1984).

Moreover, Faggio et al. (2017) demonstrate that polyphenols enhance the synthesis of nitrogen monoxide. By stimulating guanylate cyclase, this molecule causes an increase in the level of intraplatelet cGMP leading to an inhibition of platelet aggregation. Tyrosine kinase proteins contribute massively to regulating platelet function from the initial phase of activation to the final step of aggregation, and an *in vitro* study has shown that quercetin reduced phosphorylation (Hubbard et al. 2003).

Finally, the activation of blood platelets produces some reactive oxygen derivatives via NADPH oxidase activation. These reactive oxygen derivatives can stimulate platelet aggregation by activating a kinase protein or inhibiting tyrosine phosphatase (Nardini et al. 2007). Inhibition of platelet aggregation by phenolic compounds is achieved by reducing endogenous peroxides or storing endogenous antioxidants. Flavonoids can trap (or recover) free radicals such as superoxide anion hydroxyl radicals by transferring hydrogen (Procházková et al. 2011). A previous study showed that flavonoids such as quercetin and catechin decrease collagen-induced human platelet aggregation by inhibiting the platelet production of hydrogen peroxide (Pignatelli et al. 2000). In the same way, Freedman et al. (2001) reported that the consumption of grape juice significantly decreases the production of superoxide anion by platelets.

Other mechanisms are also proposed, such as the inhibition of the binding of Von Willbrand factor to its specific receptor and also the change in the conformation of the IIb-IIIa glycoprotein fibrinogen receptor, responsible for the aggregation of the platelets (Mruk et al. 2000).

Conclusion

In conclusion, the results of this study showed an *in vitro* antioxidant, antiaggregant and anticoagulant effect of two aqueous extracts of *A. spinosa* (leaves and branches) harvested from the Oriental Region of Morocco. These activities may be related to many active phytochemical Compounds present in the extract. These original results suggest that *A. spinosa* may be considered a vibrant source of antiplatelet, anticoagulant and antioxidant compounds, capable of preventing thrombotic complications of cardiovascular diseases.

Conflict of interest statement

The authors declare that there is no conflict of interest.

References

Alam, M. N., Bristi, N. J., & Rafiquzzaman, M. (2013). Review on *in vivo* and *in vitro* methods evaluation of antioxidant activity. *Saudi Pharmaceutical Journal, 21*(2), 143-152.

Amirou, A., Bnouham, M., Legssyer, A., Ziyyat, A., Aziz, M., Berrabah, M., & Mekhfi, H. (2018). Effects of *Juglans regia* Root Bark Extract on Platelet Aggregation, Bleeding Time, and Plasmatic Coagulation: *In Vitro* and *Ex Vivo* Experiments. *Evidence-based complementary and alternative medicine : eCAM*, *2018*, 7313517. https://doi.org/10.1155/2018/7313517.

Amirou, A., Legssyer, A., Ziyyat, A., Mohammed, A., Bnouham, M., et al. (2022). Antithrombotic activity of flavonoid fractions of *Juglans regia* root bark through inhibiting platelet aggregation and plasmatic coagulation. *Arabian Journal of medicinal and Aromatic Plants, 8*(3), 94-114.

Awad, A., Smith, A., & Fink, C. (2001). Plant sterols regulate rat vascular smooth muscle cell growth and prostacyclin release in culture. *Prostaglandins, Leukotrienes and Essential Fatty Acids (PLEFA), 64*(6), 323-330.

Bekkouch, O., Harnafi, M., Touiss, I., Khatib, S., Harnafi, H., Alem, C., & Amrani, S. (2019). *In Vitro* Antioxidant and *In Vivo* Lipid-Lowering Properties of *Zingiber officinale* Crude Aqueous Extract and Methanolic Fraction: A Follow-Up Study. *Evidence-Based Complementary and Alternative Medicine : eCAM*, *2019*, 9734390. https://doi.org/10.1155/2019/9734390

Ben Mansour, R., Ben Slema, H., Falleh, H., Tounsi, M., Kechebar, M. S. A., Ksouri, R., & Megdiche-Ksouri, W. (2018). Phytochemical characteristics, antioxidant, and health properties of roasted and unroasted Algerian argan (*Argania spinosa*) oil. *Journal of Food Biochemistry, 42*(5), e12562.

Berrougui, H., Ettaib, A., Gonzalez, M. H., De Sotomayor, M. A., Bennani-Kabchi, N., & Hmamouchi, M. (2003). Hypolipidemic and hypocholesterolemic effect of argan oil (*Argania spinosa* L.) in Meriones shawi rats. *Journal of Ethnopharmacology, 89*(1), 15-18.

Bnouham, M., Bellahcen, S., Benalla, W., Legssyer, A., Ziyyat, A. & Mekhfi, H. (2008). Antidiabetic Activity Assessment of *Argania spinosa* Oil. *Journal of Complementary and Integrative Medicine*, *5*(1). https://doi.org/10.2202/1553-3840.1180

Bourhim, T., Villareal, M. O., Couderc, F., Hafidi, A., Isoda, H., & Gadhi, C. (2021). Melanogenesis promoting effect, antioxidant activity, and UPLC-ESI-HRMS characterization of phenolic compounds of argan leaves extract. *Molecules, 26*(2), 371.

Buvaneswari, K., Ramamoorthy, D., & Velanganni, J. (2011). Preliminary phytochemical and antimicrobial activity studies on the leaves of the Indian plant *Thevetia neriifolia* Juss. *World Journal of Agricultural Sciences, 7*(6), 659-666.

Charrouf, Z., & Guillaume, D. (1999). Ethnoeconomical, ethnomedical, and phytochemical study of *Argania spinosa* (L.) Skeels. *Journal of Ethnopharmacology, 67*(1), 7-14.

Cherki, M., Berrougui, H., Drissi, A., Adlouni, A., & Khalil, A. (2006). Argan oil: which benefits on cardiovascular diseases? *Pharmacological Research, 54*(1), 1-5.

de la Rosa, L. A., Alvarez-Parrilla, E., & Shahidi, F. (2011). Phenolic compounds and antioxidant activity of kernels and shells of Mexican pecan (*Carya illinoinensis*). *Journal of Agricultural and Food Chemistry, 59*(1), 152-162.

Ebrahimi, F., Torbati, M., Mahmoudi, J., & Valizadeh, H. (2020). Medicinal plants as potential hemostatic agents. *Journal of Pharmacy & Pharmaceutical Sciences, 23*, 10-23.

El Haouari, M., & Mekhfi, H. (2017). Antiplatelet aggregation effects of extracts from *Arbutus unedo* leaves. *Plant Science Today, 4*(2), 68-74.

El Haouari, M., & Rosado, J. A. (2016). Medicinal plants with antiplatelet activity. *Phytotherapy Research, 30*(7), 1059-1071.

Faggio, C., Sureda, A., Morabito, S., Sanches-Silva, A., Mocan, A., Nabavi, S. F., & Nabavi, S. M. (2017). Flavonoids and platelet aggregation: A brief review. *European Journal of Pharmacology, 807*, 91-101. doi: 10.1016/j.ejphar.2017.04.009

Ferreira, M., Nunes, O., Fujimura, A., Pessoa, O., Lemos, T., & Viana, G. (1999). Inhibition of platelet activation by quinones isolated from *Auxemma oncocalyx* Taub. *Research Communications in Molecular Pathology and Pharmacology, 106*(1-2), 97-107.

Freedman, J. E., Parker III, C., Li, L., Perlman, J. A., Frei, B., et al. (2001). Select flavonoids and whole juice from purple grapes inhibit platelet function and enhance nitric oxide release. *Circulation, 103*(23), 2792-2798.

Gadi, D., Bnouham, M., Aziz, M., Ziyyat, A., Legssyer, A., et al. (2009). Parsley extract inhibits *in vitro* and *ex vivo* platelet aggregation and prolongs bleeding time in rats. *Journal of Ethnopharmacology, 125*, 170-174. doi: 10.1016/j.jep.2009.05.014

Guerrero, J., Lozano, M., Castillo, J., Benavente-Garcia, O., Vicente, V., & Rivera, J. (2005). Flavonoids inhibit platelet function through binding to the thromboxane A2 receptor. *Journal of Thrombosis and Haemostasis, 3*(2), 369-376.

Hagerman, A. E. (1988). Extraction of tannin from fresh and preserved leaves. *Journal of Chemical Ecology, 14*(2), 453-461. doi: 10.1007/BF01013897

Hubbard, G. P., Wolffram, S., Lovegrove, J. A., & Gibbins, J. M. (2003). The role of polyphenolic compounds in the diet as inhibitors of platelet function. *Proceedings of the Nutrition Society, 62*(2), 469-478.

Jesus, R. S., Piana, M., Freitas, R. B., Brum, T. F., Alves, C. F., et al. (2018). *In vitro* antimicrobial and antimycobacterial activity and HPLC-DAD screening of phenolics from *Chenopodium ambrosioides* L. *Brazilian Journal of Microbiology, 49*, 296-302.

Kim, D.W., Sapkota, K., Choi, J.H., Kim, Y.S., Kim, S., & Kim, S.J. (2013). Direct acting antithrombotic serine protease from brown seaweed *Costaria costata*. *Process Biochemistry, 48*(2), 340-350.

Kozłowska-Wojciechowska, M., Jastrzębska, M., Naruszewicz, M., & Foltyńska, A. (2003). Impact of margarine enriched with plant sterols on blood lipids, platelet function, and fibrinogen level in young men. *Metabolism, 52*(11), 1373-1378.

Kumar, S., & Pandey, A. K. (2013). Chemistry and biological activities of flavonoids: an overview. *The Scientific World Journal*, *2013*, 162750. https://doi.org/10.1155/2013/162750

Landolfi, R., Mower, R. L., & Steiner, M. (1984). Modification of platelet function and arachidonic acid metabolism by bioflavonoids: structure-activity relations. *Biochemical Pharmacology, 33*(9), 1525-1530.

Li, T., Yuan, D., Yuan, J. (2020). Antithrombotic Drugs—Pharmacology and Perspectives. In: M. Wang (eds.) *Coronary Artery Disease: Therapeutics and Drug Discovery. Advances in Experimental Medicine and Biology*, vol 1177. Singapore Springer. DOI: https://doi.org/10.1007/978-981-15-2517-9_4.

Mekhfi, H., Belmekki, F., Ziyyat, A., Legssyer, A., Bnouham, M., & Aziz, M. (2012). Antithrombotic activity of argan oil: An *in vivo* experimental study. *Nutrition, 28*(9), 937-941. doi: 10.1016/j.nut.2011.11.032

Mekhfi, H., Gadi, D., Bnouham, M., Ziyyat, A., Legssyer, A., & Aziz, M. (2008). Effect of Argan Oil on Platelet Aggregation and Bleeding Time: A Beneficial Nutritional Property. *Journal of Complementary and Integrative Medicine, 5*(1). doi: 10.2202/1553-3840.1164

Mekhfi, H., Haouari, M. E., Legssyer, A., Bnouham, M., Aziz, M., et al. (2004). Platelet anti-aggregant property of some Moroccan medicinal plants. *Journal of Ethnopharmacology, 94*(2-3), 317-322. doi: 10.1016/j.jep.2004.06.005

Mercolini, L., Protti, M., Saracino, M. A., Mandrone, M., Antognoni, F., & Poli, F. (2016). Analytical profiling of bioactive phenolic compounds in Argan (*Argania spinosa*) Leaves by Combined Microextraction by Packed Sorbent (MEPS) and LC-DAD-MS/MS. *Phytochemical Analysis, 27*(1), 41-49.

Morel, O., Kessler, L., Ohlmann, P., & Bareiss, P. (2010). Diabetes and the platelet: toward new therapeutic paradigms for diabetic atherothrombosis. *Atherosclerosis, 212*(2), 367-376.

Moukal, A. (2004). L'arganier, *Argania spinosa* L. (skeels), usage thérapeutique, cosmétique et alimentaire. *Phytotherapie, 2*(5), 135-141. doi: 10.1007/s10298-004-0041-2

Mruk, J. S., Webster, M. W., Heras, M., Reid, J. M., Grill, D. E., & Chesebro, J. H. (2000). Flavone-8-acetic acid (Flavonoid) profoundly reduces platelet-dependent thrombosis and vasoconstriction after deep arterial injury *in vivo*. *Circulation, 101*(3), 324-328.

Mu, H., Battsetseg, B., Ito, T., Otani, S., Onishi, K., & Kurozawa, Y. (2010). Effects of Asian dust storm on health-related quality of life: a survey immediately after an Asian dust storm event in Mongolia. *International Journal of Health Research, 3*(2), 87-92.

Nardini, M., Natella, F., & Scaccini, C. (2007). Role of dietary polyphenols in platelet aggregation. A review of the supplementation studies. *Platelets, 18*(3), 224-243. doi: 10.1080/09537100601078083

Nijveldt, R. J., Van Nood, E., Van Hoorn, D. E., Boelens, P. G., Van Norren, K., & Van Leeuwen, P. A. (2001). Flavonoids: a review of probable mechanisms of action and potential applications. *The American Journal of Clinical Nutrition, 74*(4), 418-425.

Nurden, P., Dreyfus, M., Favier, R., Négrier, C., Schlégel, N., & Sie, P. (2007). Centre de référence des pathologies plaquettaires. *Archives de Pédiatrie (Paris), 14*(6), 679-682.

Pignatelli, P., Pulcinelli, F. M., Celestini, A., Lenti, L., Ghiselli, A., Gazzaniga, P. P., & Violi, F. (2000). The flavonoids quercetin and catechin synergistically inhibit platelet function by antagonizing the intracellular production of hydrogen peroxide. *The American Journal of Clinical Nutrition, 72*(5), 1150-1155.

Procházková, D., Boušová, I., & Wilhelmová, N. (2011). Antioxidant and prooxidant properties of flavonoids. *Fitoterapia, 82*(4), 513-523.

Raal, A., Meos, A., Hinrikus, T., Heinämäki, J., Romāne, E., et al. (2020). Dragendorff's reagent: Historical perspectives and current status of a versatile reagent introduced over 150 years ago at the University of Dorpat, Tartu, Estonia. *Die Pharmazie-An International Journal of Pharmaceutical Sciences, 75*(7), 299-306.

Rai, V., Pai, V. R., Kedilaya, P., & Hegde, S. (2013). Preliminary phytochemical screening of members of Lamiaceae family: *Leucas linifolia, Coleus aromaticus* and *Pogestemon patchouli. International Journal of Pharmaceutical Science Review and Research, 21*(1), 131-137.

Rammal, H., Bouayed, J., Younos, C., & Soulimani, R. (2009). Notes ethnobotanique et phytopharmacologique d'*Argania spinosa* L. *Phytotherapie, 7*(3), 157-160.

Rand, M. L., Hennissen, A. A., & Hornstra, G. (1988). Effects of dietary palm oil on arterial thrombosis, platelet responses and platelet membrane fluidity in rats. *Lipids, 23*(11), 1019-1023.

Rosendaal, F. R., & Raskob, G. E. (2014). On world thrombosis day. *The Lancet, 9955*(384), 1653-1654.

Sayari, N., Balti, R., Mansour, M. B., Amor, I. B., Graiet, I., Gargouri, J., & Bougatef, A. (2016). Anticoagulant properties and cytotoxic effect against HCT116 human colon cell line of sulfated glycosaminoglycans isolated from the Norway lobster (*Nephrops norvegicus*) shell. *Biomedicine & Pharmacotherapy, 80*, 322-330.

Sheu, J.R., Hsiao, G., Chou, P.H., Shen, M.Y., & Chou, D.-S. (2004). Mechanisms involved in the antiplatelet activity of rutin, a glycoside of the flavonol quercetin, in human platelets. *Journal of Agricultural and Food Chemistry, 52*(14), 4414-4418.

Tepe, B., Daferera, D., Sokmen, A., Sokmen, M., & Polissiou, M. (2005). Antimicrobial and antioxidant activities of the essential oil and various extracts of *Salvia tomentosa* Miller (Lamiaceae). *Food Chemistry, 90*(3), 333-340.

Effect of human β-Globin second intron on transient gene expression in mammalian cell lines

Kevin Kumar Vijayakumar, Humera Khathun Abdul Hameed, Shakila Harshavardhan[*]

Department of Molecular Microbiology, School of Biotechnology, Madurai Kamaraj University, Palkalai Nagar, Madurai, Tamil Nadu

ABSTRACT

Exogenous protein expression in mammalian cells is necessary to produce therapeutic proteins and modern medical applications like developing DNA vaccines and gene therapy. This study examines the human-Globin (hBG) second intron's capacity for intron-mediated enhancement (IME) in various mammalian cell lines. Our study's main aim is to investigate the effect of the incorporation and arrangement of the second intron of the human Beta-globin gene into the pVAX-1 expression cassette on improving the expression of foreign genes. Two plasmids were constructed, one with the hBG second intron positioned upstream and the other downstream in the expression cassette. EGFP expression was evaluated at the mRNA and protein levels after transfection using Lipofectamine 2000 using One-way ANOVA analysis. Results showed that the pVAX-1 harbouring the hBG second intron did not lead to enhanced transient EGFP expression and did not exhibit Intron Mediated Enhancement (IME) in tested mammalian cell lines. Further investigations are necessary to understand factors contributing to the lack of enhancement and explore alternative intron options for optimizing foreign gene expression in cell lines.

* Corresponding author

E-mail: mohanshakila.biotech@mkuniversity.org (H. Shakila)

1 Introduction

Mammalian cell lines are crucial for the manufacture of complicated biopharmaceuticals. Production in mammalian cells improves the quality and effectiveness of biologics, including antibodies, growth factors, and many more, by facilitating complex post-translational changes (Tan et al. 2021). Similarly, foreign gene expression in mammalian cells is critical in gene therapy and DNA vaccine development. An effective expression vector with appropriate regulatory elements is necessary to create a functional protein. Polyadenylation (Poly-A) signals, promoters, upstream enhancers, and terminators are common components of the expression cassette found in various expression systems to increase or optimize gene expression in mammalian cells (Barrett et al. 2012). The promoter sequence in the expression vector determines the expression efficiency of the protein of interest. Thus, to effectively express foreign genes at high levels, it is necessary first to develop an optimal promoter (Wang et al. 2017; Dou et al. 2021; Grose et al. 2021). In addition to an optimal promotor, noncoding enhancer sequences such as introns can boost transcript levels by influencing transcription rates, nuclear mRNA export, transcript stability, translational efficiency, and mRNA degradation, a phenomenon called Intron-Mediated Enhancement (IME)(Carron et al. 2021). Many commercial vectors include heterologous introns, which are known to dramatically increase exogenous gene

expression depending on the gene type and cell line (Samadder et al. 2008; Bartlett et al. 2009; Gallegos and Rose 2015; Laxa 2017). Furthermore, studies have demonstrated that promoter-proximal introns can improve the initiation of transcription and the processivity of RNA polymerase II, thereby increasing pre-mRNA synthesis. Studies have also shown that for effective 3'-end cleavage and polyadenylation, the 3'-splice acceptor intronic region is necessary (Furger et al. 2002; Noe Gonzalez et al. 2021).

Previous research has shown that the hBG introns enhance foreign gene expression in various cell types (Kang et al., 2005; Haddad-Mashadrizeh et al., 2009; Pereverzev et al., 2014). In this study, we investigated whether the presence of the second intron of hBG in the expression cassette and its position within the cassette impacted its IME potential. Accordingly, we constructed mammalian expression plasmids based on pVAX-1 with hBG second intron and evaluated the transient expression in five cell lines viz., CHO-K1, HEK-293, HELA, NRK-52E, and NIH-3T3.

2 Materials and Method

2.1 Plasmid construction for transient expression

The hBG gene containing the second intron was amplified and sequenced using human genomic DNA as a template. The sequence-verified DNA was used as the template for cloning the hBG second
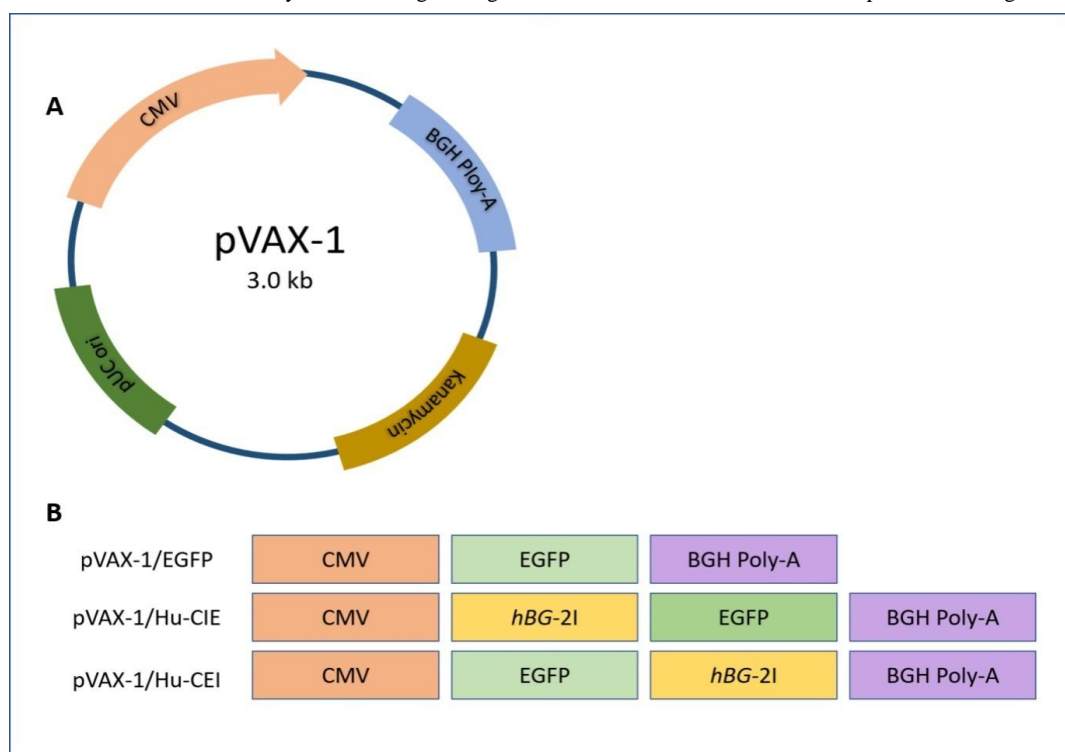
Figure 1 Plasmid pVAX-1/Hu-CIE and pVAX-1/Hu-CEI construction (A) A vector map of the plasmid pVAX-1; (B) A schematic illustration of an intron-cloned and intron-less plasmid; CMV - human cytomegalovirus immediate-early promoter; BGH Poly-A - bovine growth hormone polyadenylation signal; EGFP - enhanced green fluorescent protein; hBG-2I - hBG second intron

Table 1 Primer sets used for hBG second intron sequencing and plasmid construction

Gene	Primer	Sequence	Restriction site
hBG second intron	Forward	5'- TGAGTGAGCTGCACTGTG -3'	-
	Reverse	5'- TCTTTGCCAAAGTGATGG -3'	-
	Forward-1	5' -ATATGCTAGCTGAGTGAGCTG -3'	NheI
	Reverse-1	5'- ATATCTTAAGTCTTTGCCAAAGTG -3'	AflII
	Forward-2	5'- TATATGAATTCTGAGTGAGCTGC -3'	EcoRI
	Reverse-2	5'- TATATTCTAGATCTTTGCCAAAGTG -3'	XbaI
EGFP	Forward	5'- TATGAAGCTTATGGTGAGCAAGGG -3'	HindIII
	Reverse	5'- ATGCGGATCCTTACTTGTACAGCT -3'	BamHI

intron into the mammalian expression vector. The intron and intron-less pVAX-1-based expression plasmids were constructed based on our previously reported methodology (Vijayakumar et al. 2023). Briefly, the EGFP sequence with HindIII and BamHI restriction sites was PCR amplified and cloned into pVAX-1 to generate a control plasmid with no intron (pVAX-1/EGFP). Two plasmids with intron viz., pVAX-1/Hu-CIE and pVAX-1/Hu-CEI, were prepared by PCR amplifying and cloning hBG gene containing second intron with NheI and AflII restriction sites and EcoRI and XbaI restriction site respectively into pVAX-1/EGFP. A schematic diagram of the intron-less plasmid and hBG gene containing second intron positioning in the expression cassette of the expression vectors is shown in the Figure 1, and the primers used for intron sequencing and plasmid construction are given in Table 1.

2.2 Cell culture, Transfection

The cell lines utilized throughout this study were procured from NCCS Pune and were carefully maintained and cultured in a humid incubation environment at 37°C with 5% CO_2. The panel of cell lines encompassed HEK-293, HELA, NRK-52E, NIH-3T3, and CHO-K1 cells. Specifically, HEK-293, HELA, NRK-52E, and NIH-3T3 cells were cultured and maintained in Dulbecco's

Modified Eagle Medium (DMEM), while CHO-K1 cells were cultured and maintained in the RPMI medium. These culture media were supplemented with 10% foetal bovine serum (FBS) and 1X Penicillin-Streptomycin (Pen-Step) antibiotics to support optimal cell growth and viability. A day before transfection, the appropriate amount of exponentially growing cells were seeded in the complete media in 6-well plates. During the transfection process, the entire media was removed, and the cells were subsequently rinsed with 1X phosphate-buffered saline (PBS). The transient transfection of cell lines was conducted using Lipofectamine 2000 (ThermoFisher). The transfection involved using pVAX-1/EGFP (control plasmid) or pVAX-1/Hu-CIE or pVAX-1/Hu-CEI plasmids at a ratio of 1:2 (plasmid to Lipofectamine), following the instructions provided by the manufacturer. The transfection experiments were conducted in triplicate to ensure the accuracy of the results.

2.3 Fluorescent Microscopy and RT-PCR

For qualitative analysis, the Olympus CKX53 inverted fluorescent microscope was used to observe green fluorescence, and RTq-PCR was used for quantitative analysis to determine the presence of EGFP in cells transfected with the plasmid. TRIZOL was used to

Table 2 Real-time PCR primers used for relative quantification of EGFP mRNA transcript

Host system	Gene	Primer	Sequence	NCBI Accession number
-	EGFP	Sense	5'- AAGCTGACCCTGAAGTTCATCTGC -3'	-
		Antisense	5'- CTTGTAGTTGCCGTCGTCCTTGAA -3'	
Human	GAPDH	Sense	5'- GTCTCCTCTGACTTCAACAGCG -3'	NM_001289745.3
		Antisense	5'- ACCACCCTGTTGCTGTAGCCAA -3'	
Mouse	GAPDH	Sense	5'- TTCACCACCATGGAGAAGGC -3'	BC023196.2
		Antisense	5'- GGCATGGACTGTGGTCATGA -3'	
Rat	GAPDH	Sense	5'- TGGGGCTGGCATTGCTCTTA -3'	XM_032885257
		Antisense	5'- CTGGGTGGTCCAGGGTTTCT -3'	
Chinese Hamster	GAPDH	Sense	5'- GAAAGCTGTGGCGTGATGG -3'	NM_001244854.2
		Antisense	5'- CATACTTGGCAGGTTTCTCCAG -3'	

extract the total RNA, and Takara's PrimeScript™ RT Master Mix was then used to quantify and convert the extracted total RNA to cDNA. Utilizing Takara's TB Green® Premix Ex TaqTM II (Tli RNase H Plus) following the manufacturer's instructions, RTq-PCR was performed on a Himedia InstaQ48m real-time PCR instrument. The relative mRNA expression level of EGFP was quantified using the GAPDH gene as an internal control (Table 2), and the calculation of the fold change was performed using the $2^{-\Delta\Delta Ct}$ method. Briefly, 2μl of 50ng/μl cDNA, 10μl of 2X Master mix, 0.8μl of 10mM primers (0.4μM each), and 6.4μl of PCR grade water was added to a final volume of 20μl. PCR conditions for EGFP expression were as follows: an initial denaturation step at 95°C for 30 seconds, followed by denaturation at 95°C for 5 seconds, and subsequent annealing/extension at 60°C for 35 seconds. This cycle was repeated for a total of 40 times. Subsequently, a melt curve analysis was performed to assess the PCR amplification's efficacy.

2.4 Western Blot

To gain further insights into the EGFP expression at the protein level, western blot analysis was performed on HEK-293 cells. The following western blot protocol was used for this study (Subbarayan et al. 2018). Briefly, the protocol entailed trypsinizing the cells and then centrifuging them for 10 minutes at 500 x g at 4 °C. The resulting cell pellet was re-suspended in 400 μl of ice-cold lysis buffer. 4 μl of a mixture of protease inhibitors were added. The remaining proteins were carefully isolated after further incubation and centrifugation, and the total protein content was assessed using a bicinchoninate test. A total of 30 g of protein extract was resolved using sodium dodecyl sulphate-polyacrylamide (SDS-PAGE) gel electrophoresis, followed by subsequent transfer onto nitrocellulose membranes. Each membrane was subjected to incubation with primary anti-EGFP antibody [F56-6A1.2.3] (Abcam, #ab184601) and anti-GAPDH antibody [6C5] with the Loading Control (Abcam, #ab8245) at a 1:1000 dilution, followed by goat anti-mouse IgG H+L secondary antibody (ThermoFisher #31430) at a 1:5000 dilution.

2.5 Statistical analysis

All experimental data of biological triplicates were represented as the mean and standard deviation from the three experiments. Statistical significance between groups was calculated using One-way ANOVA analysis using GraphPad Prism (9.0) (**** $p < 0.001$).

3 Results and Discussions

3.1 Influence of human β-Globin second intron in transgene expression

Two different sets of plasmids were created to examine the effects of the hBG second intron on transgene expression in mammalian cell lines. The intron was positioned upstream in the expression cassette of the first plasmid, pVAX-1/Hu-CIE, between the CMV promoter and the EGFP sequence and downstream in the expression cassette of the second plasmid, pVAX-1/Hu-CEI, between the EGFP sequence and the BHG Poly A-tail. The pVAX-1/EGFP plasmid without an intron was used as the control plasmid for comparison. Comparing cells transfected with pVAX-1/Hu-CIE to those transfected with pVAX-1/EGFP, there was no discernible difference in the levels of EGFP transcripts. Concerning the location of the intron inside the expression cassette, CHO-K1, HEK-293, and NRK-52E cells transfected with pVAX-1/Hu-CEI as opposed to pVAX-1/EGFP showed a significant reduction in EGFP transcript levels. In a similar vein, CHO-K1 and NRK-52E cells transfected with pVAX-1/Hu-CEI showed noticeably lower levels of EGFP transcripts than pVAX-1/Hu-CIE. Between pVAX-1/Hu-CEI and the intron-less control plasmid pVAX-1/EGFP, however, there was no appreciable difference in the expression of EGFP between HELA and NIH-3T3 cells (Figures 2 and 3).

Furthermore, Western blot analysis extended the validation of the observed expression pattern to the proteome level. Remarkably, the Western blot findings for all HEK-293 cells subjected to transfection exhibited concordance with their corresponding RTq-PCR outcomes, affirming the direct correspondence between protein expression and mRNA levels. In the pVAX-1/Hu-CIE group, EGFP expression was not significantly altered compared to the control group with the intron-less plasmid pVAX-1/EGFP. However, the EGFP expression was substantially lower in the pVAX-1/Hu-CEI group compared to the control intron-less group and the pVAX-1/Hu-CIE group (Figure 4).

It is well known that introns can affect heterologous gene expression in many ways, including transcription rate, mRNA export, polyadenylation, and mRNA decay (Bonnet and Palancade 2015; Misra and Green 2016; Schlautmann and Gehring 2020; Watts et al. 2021). Kang et al. (2005) have shown enhanced murine cytomegalovirus (MCMV) promotor activity with hBG second intron and stronger expression when compared to the human cytomegalovirus (HCMV) promoter (Kang et al. 2005). Similarly, Haddad-Mashadrizeh et al. (2009) have reported a synergistic effect of hBG second intron and Kozak sequence on the expression level of human factor IX (hFIX) in CHO cells (Haddad-Mashadrizeh et al. 2009). However, we discovered no substantial enhancement in exogenous EGFP expression by the hBG second intron in all cells in our current investigation (Figure 2-4).

Regarding intron positioning in the expression cassette, multiple studies have reported increased gene expression by inserting an intron between the gene's promoter and the gene of interest, and no enhancement in gene expression or even decreased gene expression at the 3' UTR (Furger et al. 2002; Agarwal and Ansari

pVAX-1/EGFP   **pVAX-1/Hu-CIE**   **pVAX-1/Hu-CEI**
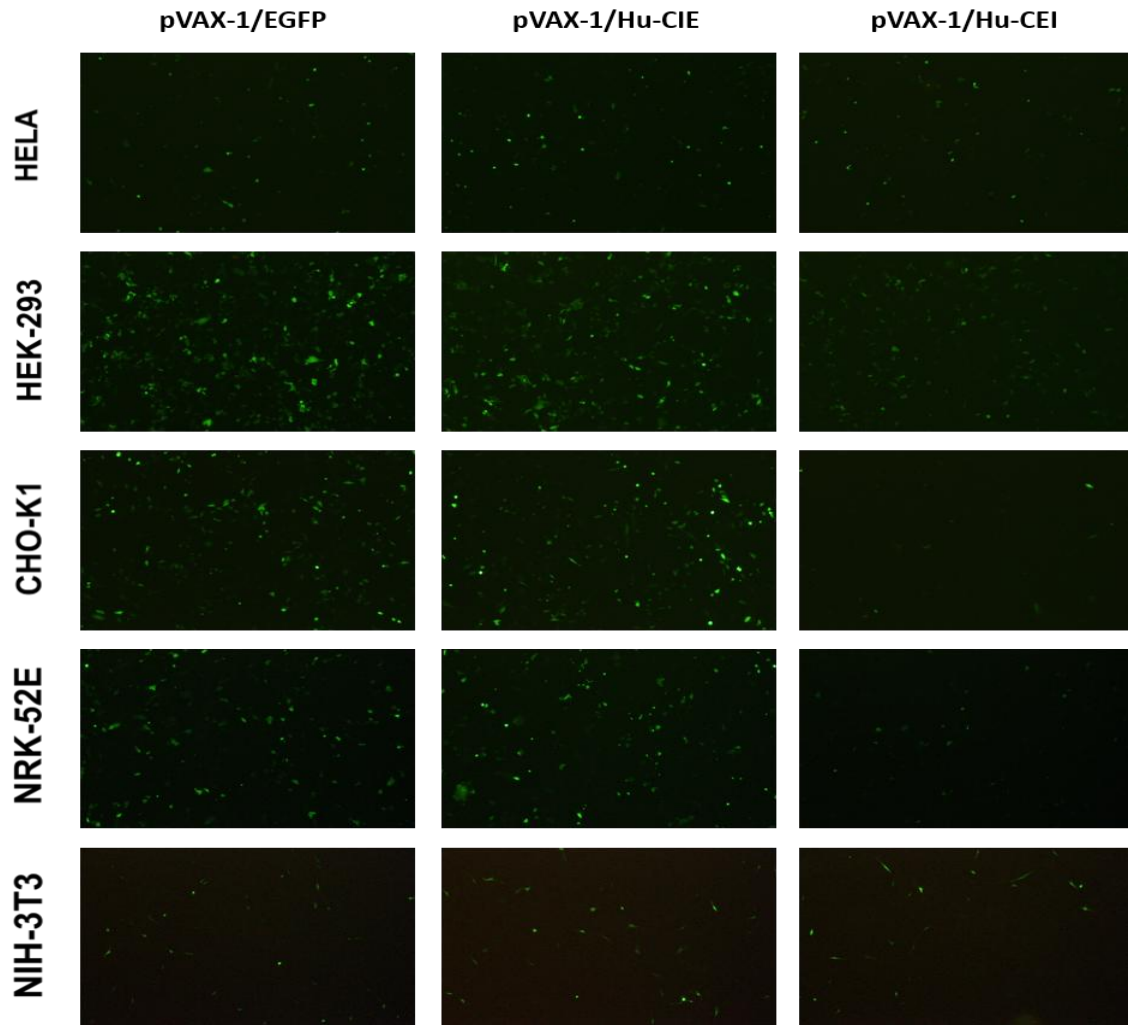
Figure 2 Expression of EGFP in CHO-K1, HEK-293, HELA, NRK-52E, and NIH-3T3 cells transfected with pVAX-1/E or pVAX-1/Hu-CIE or pVAX-1/Hu-CEI plasmid.
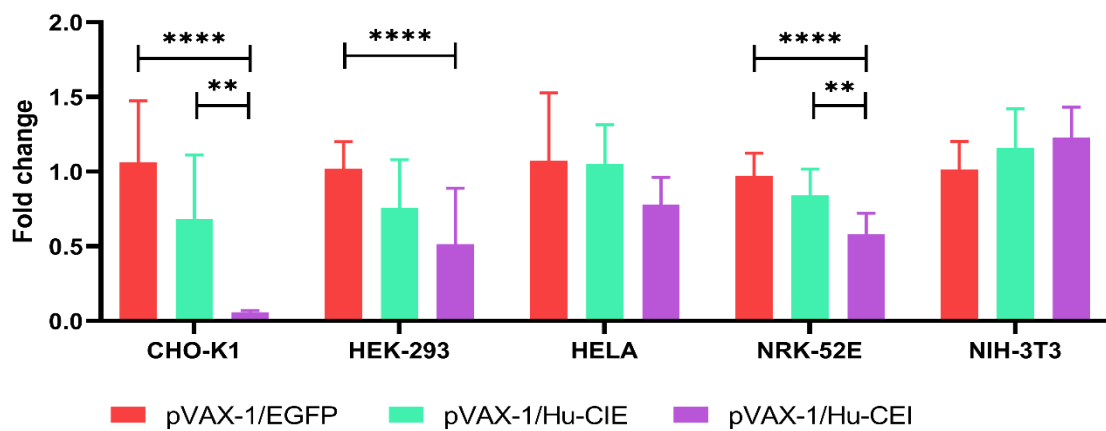
Figure 3 One-Way ANOVA analysis of transient EGFP expression in CHO-K1, HEK-293, HELA, NRK-52E, and NIH-3T3 cells transfected with pVAX-1/E or pVAX-1/Hu-CIE or pVAX-1/Hu-CEI using GraphPad Prism (9.0)(**** $p < 0.001$).
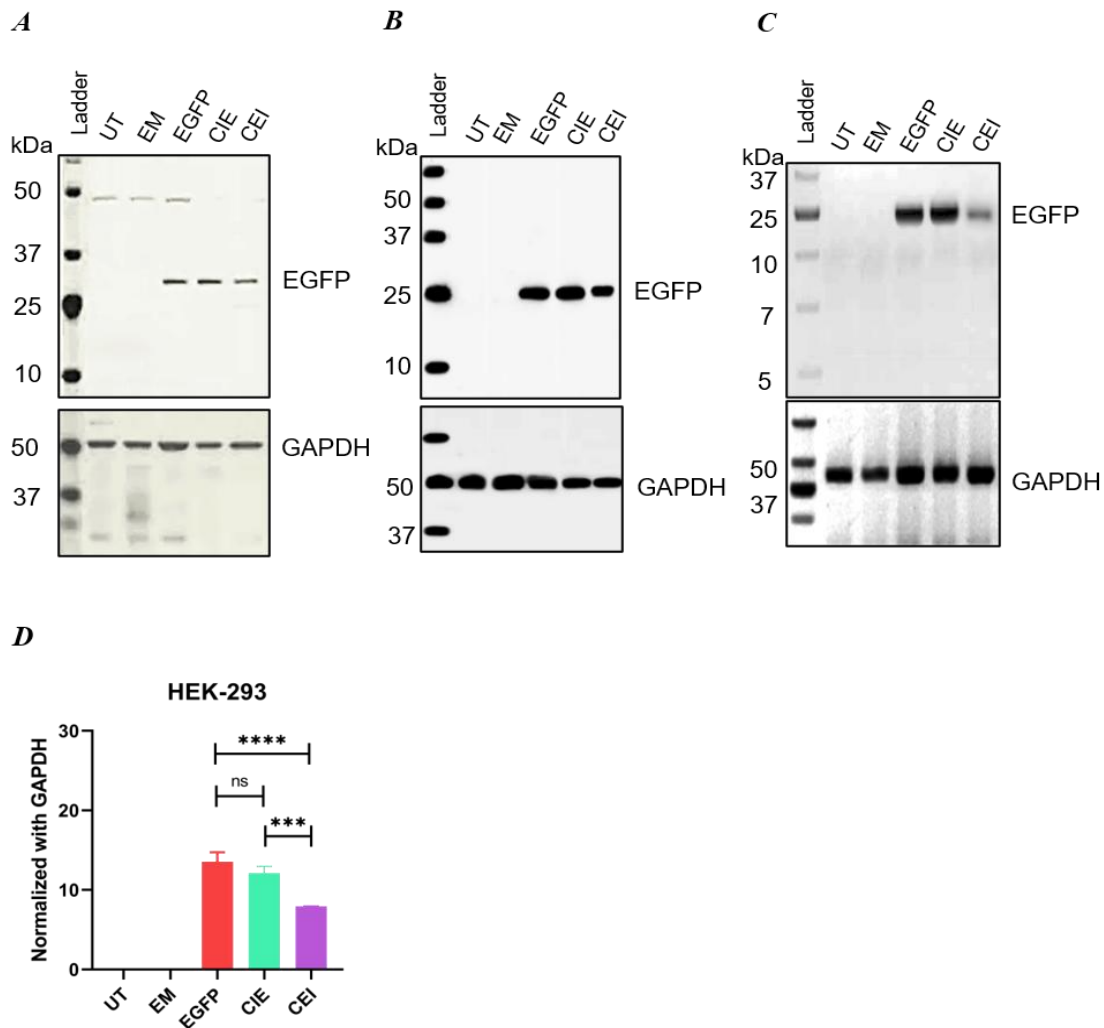
Figure 4 Western Blot confirmation of transient expression of EGFP in HEK-293 (A) First set; (B) Second set; (C) Third set; UT - Untreated; EM - Empty vector; EGFP, pVAX-1/EGFP; CIE - pVAX-1/Hu-CIE; CEI - pVAX-1/Hu-CEI, and (D) One-Way ANOVA analysis of transient EGFP expression in HEK-293 followed by the Bonferroni multiple comparison test using GraphPad Prism (**** $p < 0.001$).

2016). Consistent with previous studies, our results demonstrated similar patterns in EGFP expression in cells transfected with the plasmid carrying the hBG second intron located downstream within the expression cassette (Figures 2 and 3). A plausible rationale behind this expression discrepancy might be the increased distance between the transcription start site and the recognition sites of U1 snRNA within the intron. When the intron is positioned distantly from the transcription start site, the association between the human Transcription Factor II (TFIIH), U1 snRNA, and RNA Polymerase II (Pol-II) may not occur efficiently, leading to a compromised transcription re-initiation efficiency (Bieberstein et al. 2012; Almada et al. 2013; Engreitz et al. 2014).

Another possible explanation could be the rapid degradation of mRNA by Nonsense-Mediated Decay (NMD). The impact of introns on nuclear export and nonsense-mediated mRNA decay (NMD) has been ascribed to the interaction between ribosomes and the Exon Junction Protein Complex (EJC). If a premature termination codon is detected, the EJC binds to mRNA upstream at the exon-exon junction and may enter the nucleus and change cytoplasmic mRNA metabolism by NMD (Le Hir et al. 2000; Schlautmann and Gehring 2020; Lejeune 2022). However, Pereverzev et al. (2014) showed that the hBG second intron in 3' UTR of the expression cassette can improve exogenous GFP expression by 1.8-fold, contradicting our findings and earlier studies. According to the research, the enhanced expression was due to a shorter distance between termination codons and exon junctions of less than 50 nucleotides, which reduced the risk of mRNA decay via NMD (Pereverzev et al. 2014).

Conclusion

Including introns in gene expression constructs could affect the expression of the target gene, depending on the specific intron sequence and placement, particularly when located near the 5' UTR in the expression cassette between the promotor and the gene. We believe that selecting the optimal promoter, intron, gene, and intron position, along with other factors, including chromosomal position, physiological conditions, and cell type, can enable introns to enhance gene expression. When introns are utilized, cautious vector design is required because cryptic splicing signals have the potential to result in abnormal processing of the mRNA transcript, which can lead to decreased translation levels and inadequate or defective protein products.

Author's contribution

Shakila Harshavardhan and Kevin Kumar Vijayakumar conceived and planned the study. Kevin Kumar Vijayakumar and Humera Khathun Abdul Hameed did the experiments and data analysis. The paper was written and proofread by Shakila Harshavardhan and Kevin Kumar Vijayakumar.

Conflict of interest

The authors did not declare any possible conflict of interest.

Reference

Agarwal, N., & Ansari, A. (2016). Enhancement of Transcription by a Splicing-Competent Intron Is Dependent on Promoter Directionality. *PLoS Genet, 12*(5), e1006047. doi:10.1371/journal.pgen.1006047

Almada, A. E., Wu, X., Kriz, A. J., Burge, C. B., & Sharp, P. A. (2013). Promoter directionality is controlled by U1 snRNP and polyadenylation signals. *Nature, 499*(7458), 360-363. doi:10.1038/nature12349

Barrett, L. W., Fletcher, S., & Wilton, S. D. (2012). Regulation of eukaryotic gene expression by the untranslated gene regions and other noncoding elements. *Cellular and Molecular Life Sciences, 69*(21), 3613-3634. doi:10.1007/s00018-012-0990-9

Bartlett, J. G., Snape, J. W., & Harwood, W. A. (2009). Intron-mediated enhancement as a method for increasing transgene expression levels in barley. *Plant Biotechnology Journal, 7*(9), 856-866. doi:https://doi.org/10.1111/j.1467-7652.2009.00448.x

Bieberstein, N. I., Carrillo Oesterreich, F., Straube, K., & Neugebauer, K. M. (2012). First exon length controls active chromatin signatures and transcription. *Cell reports, 2*(1), 62-68. doi:10.1016/j.celrep.2012.05.019

Bonnet, A., & Palancade, B. (2015). Intron or no intron: a matter for nuclear pore complexes. *Nucleus, 6*(6), 455-461. doi:10.1080/19491034.2015.1116660

Carron, J., Torricelli, C., Silva, J. K., de Oliveira Coser, L., Lima, C. S. P., & Lourenco, G. J. (2021). Intronic variants of MITF (rs7623610) and CREB1 (rs10932201) genes may enhance splicing efficiency in human melanoma cell line. *Mutation Research/Fundamental and Molecular Mechanisms of Mutagenesis, 823*, 111763.

Dou, Y., Lin, Y., Wang, T. Y., Wang, X. Y., Jia, Y. l., & Zhao, C. P. (2021). The CAG promoter maintains high-level transgene expression in HEK293 cells. *FEBS Open Bio, 11*(1), 95-104.

Engreitz, J. M., Sirokman, K., McDonel, P., Shishkin, A. A., Surka, C., et al. (2014). RNA-RNA interactions enable specific targeting of noncoding RNAs to nascent Pre-mRNAs and chromatin sites. *Cell*, *159*(1), 188–199. https://doi.org/10.1016/j.cell.2014.08.018

Furger, A., O'Sullivan, J. M., Binnie, A., Lee, B. A., & Proudfoot, N. J. (2002). Promoter proximal splice sites enhance transcription. *Genes & development, 16*(21), 2792-2799. doi:10.1101/gad.983602

Gallegos, J. E., & Rose, A. B. (2015). The enduring mystery of intron-mediated enhancement. *Plant Science, 237*, 8-15. doi:10.1016/j.plantsci.2015.04.017

Grose, C., Putman, Z., & Esposito, D. (2021). A review of alternative promoters for optimal recombinant protein expression in baculovirus-infected insect cells. *Protein Expression and Purification, 186*, 105924.

Haddad-Mashadrizeh, A., Zomorodipour, A., Izadpanah, M., Sam, M. R., Ataei, F., et al. (2009). A systematic study of the function of the human beta-globin introns on the expression of the human coagulation factor IX in cultured Chinese hamster ovary cells. *The journal of gene medicine*, *11*(10), 941–950. https://doi.org/10.1002/jgm.1367

Kang, M., Kim, S., Lee, S., Lee, Y., Lee, J.H., Shin, H., & Kim, Y.S. (2005). Human β-globin second intron highly enhances expression of foreign genes from murine cytomegalovirus immediate-early promoter. *Journal of Microbiology and Biotechnology, 15* (3), 544-550..

Laxa, M. (2017). Intron-Mediated Enhancement: A Tool for Heterologous Gene Expression in Plants? *Frontiers in Plant Science, 7*. doi:10.3389/fpls.2016.01977

Le Hir, H., Izaurralde, E., Maquat, L. E., & Moore, M. J. (2000). The spliceosome deposits multiple proteins 20-24 nucleotides upstream of mRNA exon-exon junctions. *The EMBO journal, 19*(24), 6860-6869. doi:10.1093/emboj/19.24.6860

Lejeune, F. (2022). Nonsense-mediated mRNA decay, a finely regulated mechanism. *Biomedicines, 10*(1), 141.

Misra, A., & Green, M. R. (2016). From polyadenylation to splicing: Dual role for mRNA 3' end formation factors. *RNA biology, 13*(3), 259-264. doi:10.1080/15476286.2015.1112490

Noe Gonzalez, M., Blears, D., & Svejstrup, J. Q. (2021). Causes and consequences of RNA polymerase II stalling during transcript elongation. *Nature reviews Molecular cell biology, 22*(1), 3-21.

Pereverzev, A. P., Markina, N. M., et al. (2014). [Intron 2 of human beta-globin in 3'-untranslated region enhances expression of chimeric genes]. *Russian Journal of Bioorganic Chemistry, 40*(3), 293-296. doi:10.1134/s106816201403011x

Samadder, P., Sivamani, E., Lu, J., Li, X., & Qu, R. (2008). Transcriptional and post-transcriptional enhancement of gene expression by the 5′ UTR intron of rice rubi3 gene in transgenic rice cells. *Molecular Genetics and Genomics, 279*, 429-439.

Schlautmann, L. P., & Gehring, N. H. (2020). A Day in the Life of the Exon Junction Complex. *Biomolecules, 10*(6), 866.

Subbarayan, R., Murugan Girija, D., & Ranga Rao, S. (2018). Gingival spheroids possess multilineage differentiation potential. *Journal of Cellular Physiology, 233*(3), 1952-1958. doi:https://doi.org/10.1002/jcp.25894

Tan, E., Chin, C. S. H., Lim, Z. F. S., & Ng, S. K. (2021). HEK293 cell line as a platform to produce recombinant proteins and viral vectors. *Frontiers in bioengineering and biotechnology, 9*, 796991.

Vijayakumar, K. K., Rajandran, A., Lumumba, S., & Harshavardhan, S. (2023). In silico characterization of Melittin from Apis cerana indica and evaluation of melittin intron for transgene expression in mammalian cells. *Journal of Applied Biology and Biotechnology, 11*(3), 153-159.

Wang, W., Jia, Y. L., Li, Y. C., Jing, C. Q., Guo, X., et al. (2017). Impact of different promoters, promoter mutation, and an enhancer on recombinant protein expression in CHO cells. *Scientific reports*, *7*(1), 10416. https://doi.org/10.1038/s41598-017-10966-y.

Watts, A., Sankaranarayanan, S., Watts, A., & Raipuria, R. K. (2021). Optimizing protein expression in heterologous system: strategies and tools. *Meta Gene, 29*, 100899.

CrossMark
click for updates

Journal of Experimental Biology and Agricultural Sciences

http://www.jebas.org

Development of the bacterial consortia for the degradation of benzo[a]pyrene, pyrene from hydrocarbons waste

Beema Kumari [iD], Ram Chandra* [iD]

Department of Environmental Microbiology, School for Environmental Sciences, Babasaheb Bhimrao Ambedkar University (A Central University), Lucknow-226025, Uttar Pradesh-226025, India

ABSTRACT

The environment is heavily populated with polycyclic aromatic hydrocarbons (PAHs), which are dangerous to human health. Degradation and cleaning of PAH chemicals from water and soil regions are crucial due to their chemical and biological impacts and persistent nature. In this study, we found that a very efficient bacterial consortium A-LOBP-19A+LOP-9 (99.62%) for benzo[a]pyrene up to 1000ppm and B-LOP-9 +GWP-2 (93.8%) for pyrene up to 2000ppm concentration degradation and it was done in MSM medium with isolated bacterial strains and incubated at 37° C for 50 days and 30 days respectively. This consortium consisting of the *Mycobacterium vaanbaalenii* GWP-2 (ON715011), *Staphylococcus aureus* LOP-9(ON715121), and *Stutzerimonas stutzeri* (LOBP-19A) OP389146, and these have capabilities of mentioned PAHs. The HPLC analysis suggested that both benzo[a]pyrene and pyrene degraded through peaks by both consortia. Degraded metabolites were identified by GC-MS and reported the presence of Phthalic acid, Naphthalene, 1,4-benzodicarboxylic acid, Butoxyacetic acid, Benzeneacetic acid and benzo [a]pyrene-1,6-dione. Thus, the study demonstrated efficient bacterial community enhancement for PAHs (benzo[a]pyrene, pyrene) decomposition, and these can be further explored for the cleanup of hydrocarbons pollution.

* Corresponding author

E-mail: prof.chandrabbau@gmail.com (Ram Chandra)

1 Introduction

Leakage of petroleum products during oil exploration, disposal, and transportation from drilling sites to refineries harms surrounding agricultural areas and aquatic bodies (Johnston et al. 2019). Accidental and intentional leakage, as well as natural environmental pollution, have presented a significant risk to flora and fauna by introducing harmful compounds into the food chain, including the combinations of various hydrocarbons, metals, and so on (Militon et al. 2010); complex chemical composition, petrol product can have several adverse impacts (Aguilera et al. 2010). Toxicity depends on the secretion of petrol products, dose, route, and organisms, and it can cause rapid death (Kumari and Chandra 2022; Donald et al. 2023). Some oil products have the potential for bio-accumulation within sensitive sea species and transfer to the next phase of the food chain via trophic transfer (Perhar and Arhonditsis 2014). Furthermore, because of the higher expense of secure and appropriate dumping, this problem is exacerbated by improper disposal methods (Rahman et al. 2009). As a result of harmful petroleum contamination, developing a bioremediation technique is critical to disinfecting harmed areas. Because exogenously functional microorganisms typically refuse to carry out the desired stage in an unknown environment, the achievement of biodegradation technology mainly depends on the degrading abilities of various species of microorganisms (Diaz-Ramrez et al. 2003; Venosa and Zhu 2003). Petroleum products showing hydrocarbons became acquainted, demonstrating selection enhancement and hereditary changes (Patowary et al. 2016). Habitual microorganisms can react to pollution containing hydrocarbons in only a brief amount of time and have an advanced biological degradation rate than populations that have never been exposed to such circumstances (Murphy et al. 2021). As a result, the isolation of naturally occurring microorganisms with oil-degrading capacity from an explicitly polluted environment may hold the possibility for the remediation of such contaminated areas. Indeed, such microorganisms are widely regarded as the most efficient hydrocarbon-degrading agents in that environment (Patowary et al. 2016). Although an individual microbe can only process a restricted spectrum of hydrocarbon substrates, the degradation of complex hydrocarbon mixtures generally requires the collaboration of multiple species of bacteria (Das and Chandran 2011). As a result, conglomerations of heterogeneous communities and diverse enzyme capacities are needed to speed up and amplify the value and scope of petrol product degradation (Ozaki et al. 2007). Despite the occurrence of the diverse range of aromatic compounds demeaning microbial organisms, the establishment of particular bacteria on hydrocarbon substrates may be limited by a variety of variables, such as substrate resistance and low solubility of hydrophobic substances in water-based, which limits the potential to

biological degradation (Joutey et al. 2013; Zakaria et al. 2021). Some species of the microorganism may release key degrading enzymes and growth factors, whereas some species may be capable of producing biosurfactants, resulting in increased solubilization of polar aromatic compounds for enhanced consumption by bacteria (Patowary et al. 2016).

The study's objective was to develop bacterial consortia from hydrocarbon-contaminated soil from the diesel spilling site in Lucknow, India and create an effective degradation of the inhabitant oil spill region. Three bacterial isolates, namely LOP-9, GWP-2 and LOBP-19A, were selected from two distinct hydrocarbon-contaminated areas, which were chosen for efficient crude oil degradation; this method was described and accepted in the previous study (Kumari et al. 2022; Kumari and Chandra 2023). The consortium, which comprises three bacterial strains, namely *Mycobacterium vaanbaalenii* GWP-2 (ON715011), *Staphylococcus aureus* LOP-9(ON715121), and *Stutzerimonas stutzeri* (LOBP-19A) OP389146 were identified based on their 16s-rRNA sequencing (identified by 16s rRNA sequencing). Consortium A, comprised of LOBP-19A and LOP-9, showed degradation up to 99.62% of benzo[a]pyere after 50 days of incubation, consortia B prepared by LOP-9 and GWP-2 strains with pyrene, which was 93.8% degraded within 30days. FTIR (Fourier transform infrared) and GCMS (Gas chromatography-mass spectrometer) techniques were analyzed, which demonstrates that these consortia eliminated several kinds of petroleum hydrocarbons, including various aliphatic and aromatic hydrocarbons, in comparison to abiotic control.

2 Materials and Methods

2.1 Chemical and reagents

Benzo[a]pyrene (99%) was bought from TCI (Tokyo Chemical Industry) India Pvt. Ltd. Loba Chemie Pvt Ltd provided the HPLC grade 99.8% acetone.

2.2 Sample collection

A diesel-contaminated soil sample was collected from a fuel leaking area near the Charbagh railway station (Lat N 26°49'48.9648" Long E 80°55'26.0436"), Lucknow, Uttar Pradesh, India. Ten grams of soil were collected in autoclaved plastic poly-bag and stored at 4°C until further investigation.

2.3 Preparation of stock solution

In a sterilized individual glass vial, benzo[a]pyrene and pyrene were dissolved in acetone and made a concentration of 1000 ppm for stock production. Before use, the amber vial was airtight, covered in aluminium foil, and kept in the dark at 4°C.

Figure 1 Sample sites A) Hydrocarbons contaminated soil B) Petrochemical plant effluent

2.4 Preparation of medium and inoculum

MSM media was prepared, and fresh bacterial culture with carbon source in individual conical flasks and inoculated with GWP-2, LOP-9 and LOBP -19 A strains , labelled and incubated at 37°C and 130rpm orbital shaker for five days. Bacterial growth should be 1.00 OD by spectrophotometer for biodegradation assay at 600nm OD. Bacterial strains have been isolated as described in the previous study (Kumari et al. 2022; Kumari and Chandra 2023).

2.5 Preparation of bacterial consortia of pyrene and benzo[a]pyrene

Two flasks were prepared to contain 150ml MSM medium, one for benzo[a]pyrene and the second for pyrene degradation by LOBP-19A+LOP-9 and LOP-9+GWP-2 bacterial consortia, respectively. 1000ppm benzo[a]pyrene and 2000 ppm pyrene were included in the prepared medium flask and left for complete evaporation of acetone in the flasks. 1ml LOP-9 and GWP-2 bacterial culture inoculated in pyrene flask, and LOBP-19A and LOP-9 bacterial strains inoculated in benzo[a]pyrene flask. Both flasks were incubated at 37°C, 140 rpm orbital shaker temperature will different for both flasks because benzo[a]pyrene have not easily degrade in a few days, so that benzo[a]pyrene flask was incubated

for 50 days and pyrene flask for 30 days. Consortium bacterial growth was checked every 5 days intervals, and the growth curve in OD was observed by spectrophotometer at 600nm. The total benzo[a]pyrene and pyrene degradation analysis were performed with the total standard concentration in HPLC (Aziz et al. 2018; Mandal and Das 2017).

$$\% \text{ of Degradation} = (C_0\text{-Ce})/C_0 \times 100$$

Where C_0=initial conc. of degradation compound (ppm)

Ce= final conc. of degraded compound (ppm)

2.6 Sample extraction (Liquid-liquid)

The extraction of different compounds in the liquid medium by separating funnel or centrifugation methods is called liquid-liquid extraction. Benzo[a]pyrene and pyrene from bacterial growth culture were extracted (liquid-liquid extraction) with ethyl acetate (1:1), and the organic phase was collected and re-extracted with the same amount of ethyl acetate, and managed organic phase and left for complete evaporation. The evaporated part was diluted in 2ml ethyl acetate and filtered by 0.22μm (Schneider et al. 2021). An aliquot of this sample was prepared containing ethyl acetate solution before HPLC and GCMS analysis.

2.7 HPLC analysis

The distribution of the analysis (sample) throughout a mobile phase (eluent) and a stationary phase (column packing material) is the foundation of the HPLC separation principle. The molecules are retarded while passing through the stationary phase, based on the chemical structure of the molecule. A sample's "on-column" time is analyzed by the precise intermolecular interactions between the sample's molecules and the packing material (Lunn 2005).

Degraded compounds were monitored via HPLC unit (LC-20AP, SHIMADZU, JAPAN) with a C18 column (150 mm × 4.5 µm) with dual λ absorbance detector, and the sample was input by the manual injector. The mobile phase is an isocratic solution flowing at a constant rate of 1.5 mL/min at room temperature. Each analysis continued for a total of 15 minutes. (Nzila et al. 2022).

2.8 Quantitative assay (GCMS analysis)

In the quantitative assay, 50 days old bacterial crude culture (LOBP-19A+LOP-9) and LOP-9+GWP-2 culture incubated for 30 days with the concentration of 1000ppm benzo[a]pyrene and pyrene (2000ppm), respectively, residual were analyzed by GCMS. A negative control was also prepared to compare bacterial strains using GCMS peaks (Minuti et al. 2006; Di Lorenzo et al. 2019). GCMS technique was also carried out as described in a previous study (Kumari et al. 2022).
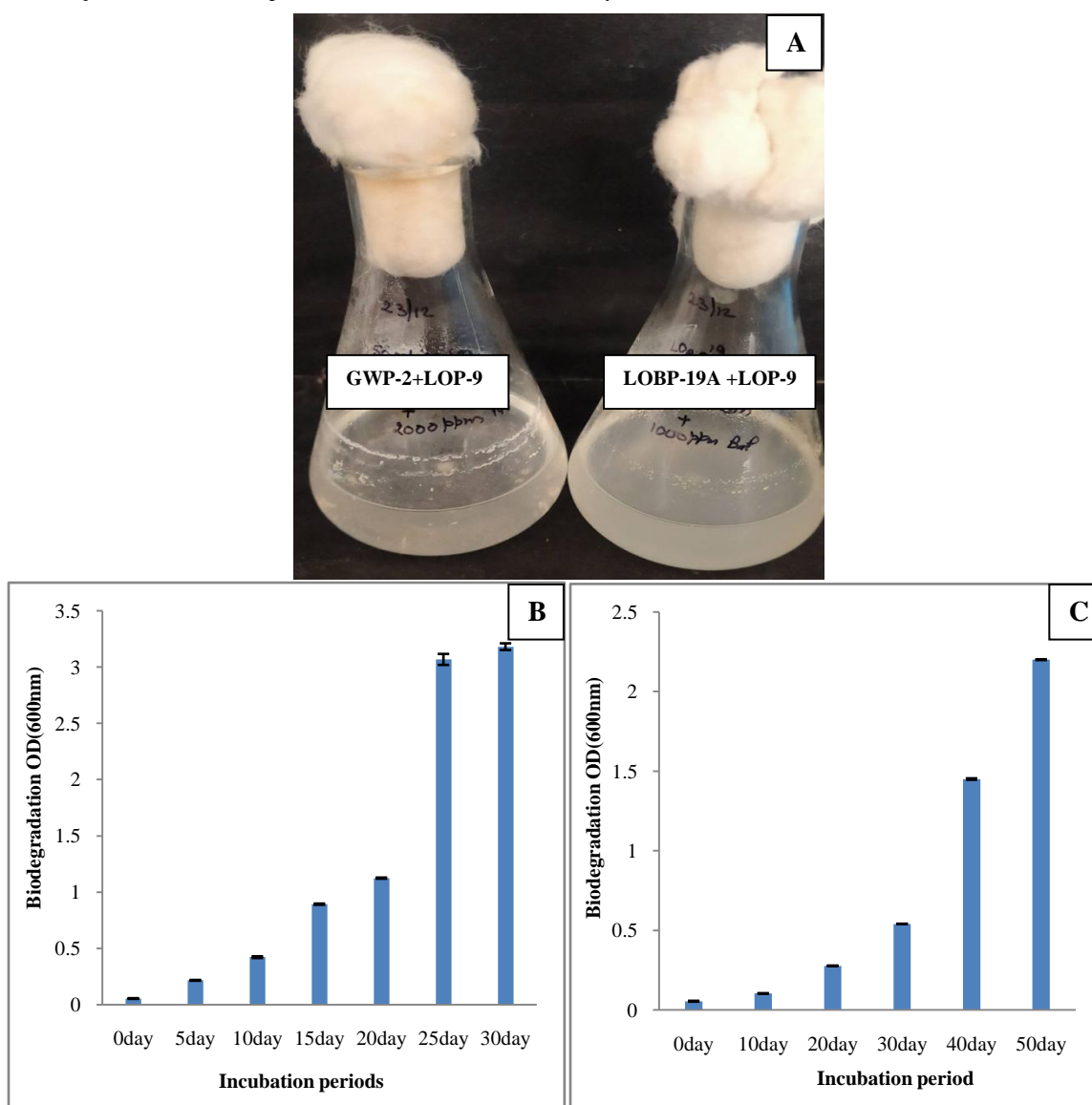
Figure 2 A Biodegradation of benzo[a]pyrene and pyrene; B. Consortia growth OD by spectrophotometer
[a. GWP-2+LOP-9; b. LOBP-19A + LOP-9]

Table 1 Percentage of benzo[a]pyrene and pyrene degradation

S.No.	Strains	Degradation (%)
1.	LOP-9	99.3%
2.	GWP-2	97.9%
3.	LOBP-19A	87.5%
4.	LOBP19A+LOP-9(Consortia A) benzo[a]pyrene	99.62%
5.	LOP-9+GWP-2(Consortia B) pyrene	93.8%

2.9 FTIR analysis

Using KBr, IR spectra were collected using a Shimadzu IR affinity-1 FTIR spectrophotometer and the sample was prepared using centrifugal at 10,000 rpm for 10 minutes. The supernatant was preserved via a vacuum dryer. The dried product was extensively combined with KBr after being coarsely powdered. The spectral resolution was 4 cm, and the spectral area was between 3500 and 700 cm^{-1} (Selvi et al. 2014).

2.10 Statistical analysis

In statistical analysis, the T-test was applied to compare the means of benzo[a]pyrene and pyrene degrading bacterial consortia. MS Excel was used to examine the study data and calculate the significance level for each parameter.

3 Results and discussion

3.1 Degradation of benzo[a]pyrene and pyrene by bacterial consortia

Two bacterial consortiums were prepared, in which pyrene was degraded 93.8% in the 30 days and benzo[a]pyrene 99.62% degraded in the 50-day incubation period. The bacterial growth in the biodegradation experiments is shown in Figure 2; the pyrene degradation assay observed that the OD of the LOP-9+GWP-2 consortium was 3.180.03 after 30 days and 2.240.009 after 50 days for the LOP-9+LOBP-19A consortium (optical density checked by spectrophotometer). The removal of benzo[a]pyrene and pyrene was preceded by a prolonged biodegradability lag period, indicating that the lack of benzo[a]pyrene and pyrene removal during the incubation period may be due to poor degradation rates rather than a lack of benzo[a]pyrene and pyrene degradable capacity.

The maximum consortium (*Pseudomonas sp.* ASDP1, *Burkholderia sp.* ASDP2, and *Rhodococcus sp.* ASDP3) rate of growth has been reported to be 0.060/h, both inorganic and organic nutrients, as well as various surfactants, did not affect pyrene degradation (Vaidya et al. 2017). Significantly PAHs degradation has been previously reported increased by mixture of *Selenastrum capricornutum* and *Mycobacterium* sp. strain A1-PYR culture (Ghosal et al. 2016). A previously reported study suggested that

consortium degraded 41% of benzo[a]pyrene concentration within 8 days (Aziz et al. 2018).

3.2 HPLC analysis

High-performance liquid chromatography (HPLC) quantification indicated that 99.62% benzo[a]pyrene degraded by LOBP-19A and LOP-9 bacterial consortia, and 93.8% pyrene was degraded by LOP-9 and GWP-2 bacterial consortia as compared with used standard concentration (Figure 3C). Bacterial consortium degradation rate were compared with single bacterial strains degradation of benzo[a]pyrene and pyrene (Table 1).

In previous research, pyrene and benz[a]pyrene degradation have been shown in *M. Luteus*, and BaP is degraded by *Bacillus spp.*, including *B. cereus* and *B. vireti* (Nzila et al. 2023; Mohandass et al. 2012). According to Kristanti and Hadibarata (2015), 59% of BaP disappeared in just 20 days. In anaerobic conditions, strain PYR1 has been reported to degrade 94% of pyrene within 15 days and to decompose benzo[a]pyrene after 35 days (Yan et al. 2017). In the current research, degradation of benzo[a]pyrene by the bacterial consortium (LOBP19-A+LOP-9) was given 99.62% degradation, significantly higher than single bacterial strains LOBP-19A. LOP-9 and GWP-2 consortium had a 93.8% degradation rate, which decreased compared to single strain LOP-9 and GWP-2 (described in previous studies).

3.3 GCMS analysis

A qualitative and quantitative examination of their GC traces can illustrate the assessment of benzo[a]pyrene and pyrene degraded residual. The results of this GCMS demonstrated that pyrene and benzo[a]pyrene in a 250-mL flask of MSM broth were degraded into a variety of by-products as a result of the action of the bacterial strains LOBP-19A+LOP-9 and LOP-9+GWP-2. These residual metabolites' GC-MS analysis identified various substances.

These metabolites helped in pyrene degrading metabolic pathways and co-metabolism (Figure 4 D). Metabolites compared with used standard pyrene in the concentration in 2000ppm from 1000ppm standard in acetone concentration. Pyrene showed in GC-MS at 23.15 RT in the chromatogram, and pyrene disappeared in LOP-9 and GWP-2 bacterial consortium after 30 30-day incubation period.
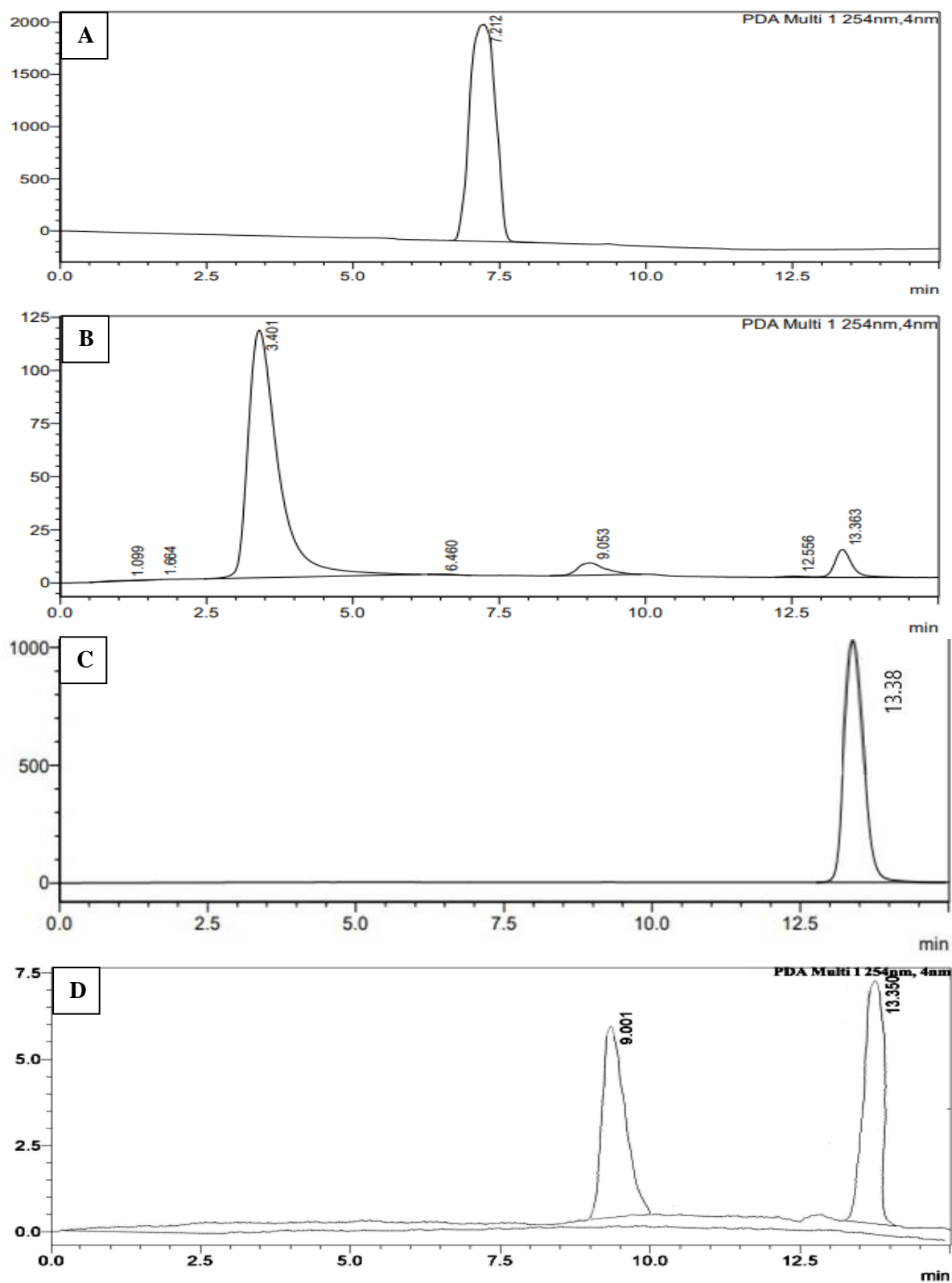
Figure 3 HPLC chromatogram A. Benzo[a]pyrene Std, B. Consortia (LOP-9+LOBP-19A), C. Pyrene Std, and D. Consortia (LOP-9+GWP-2)
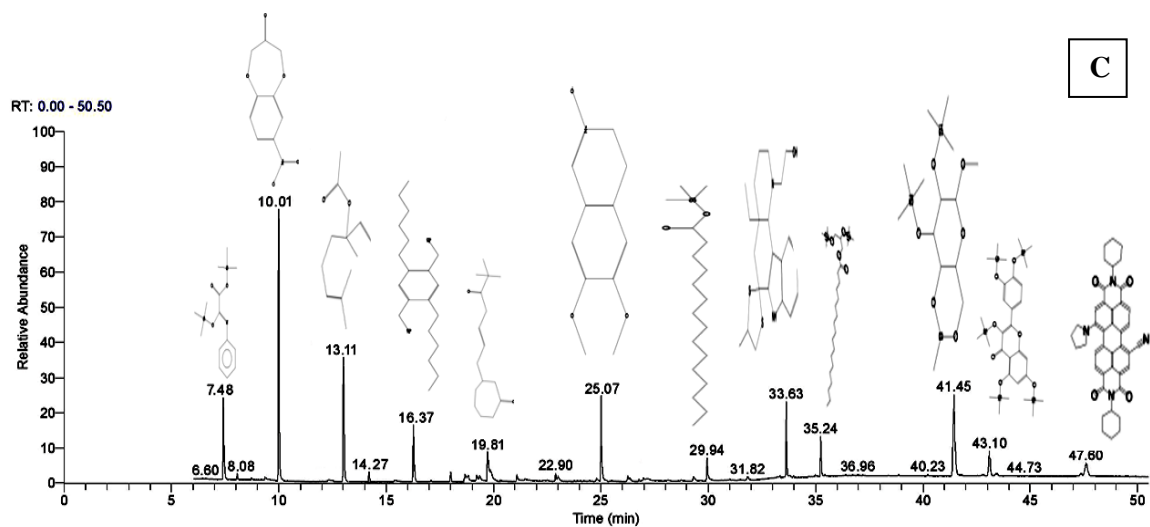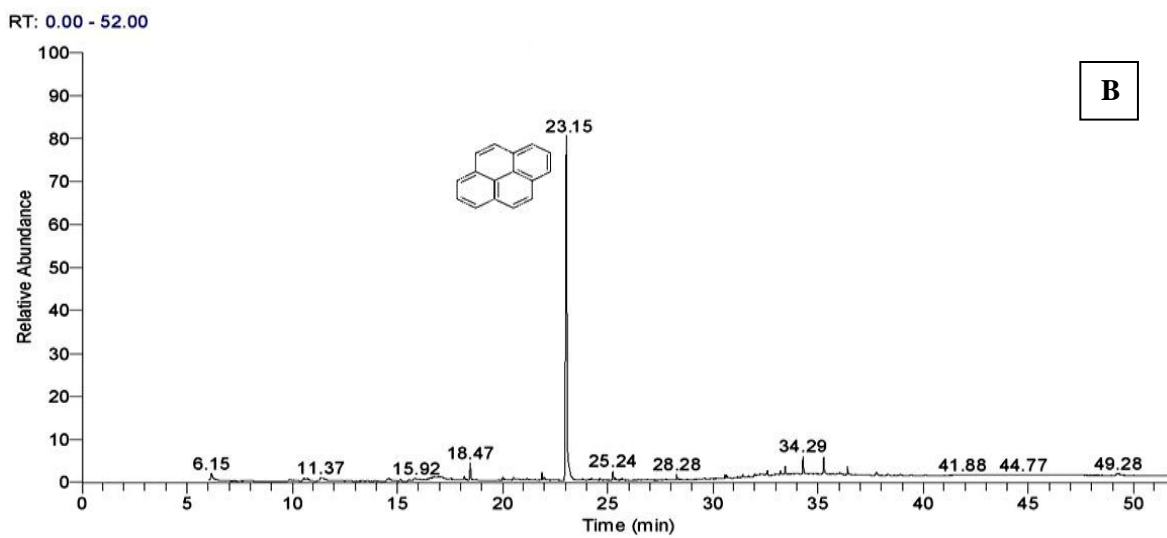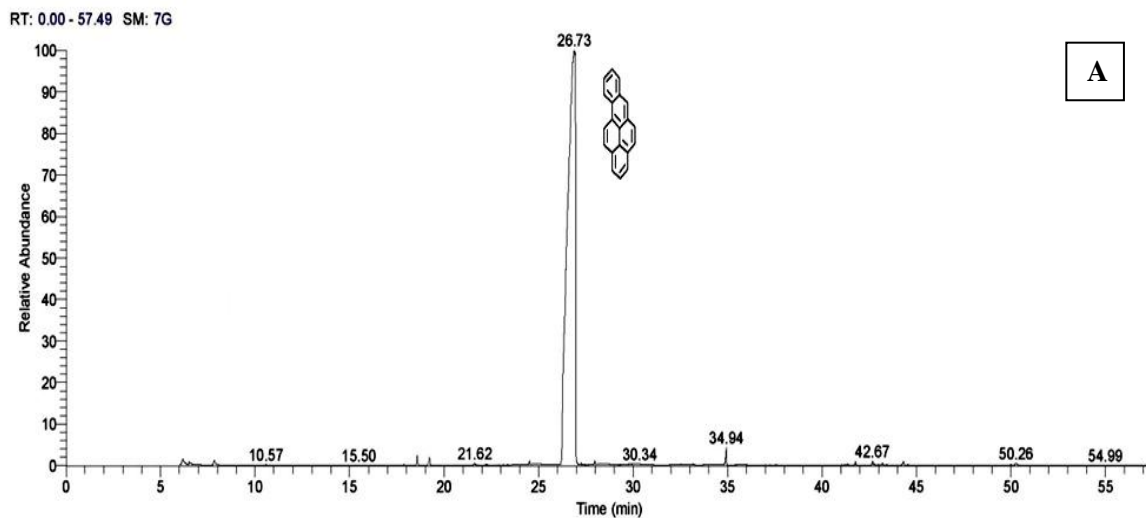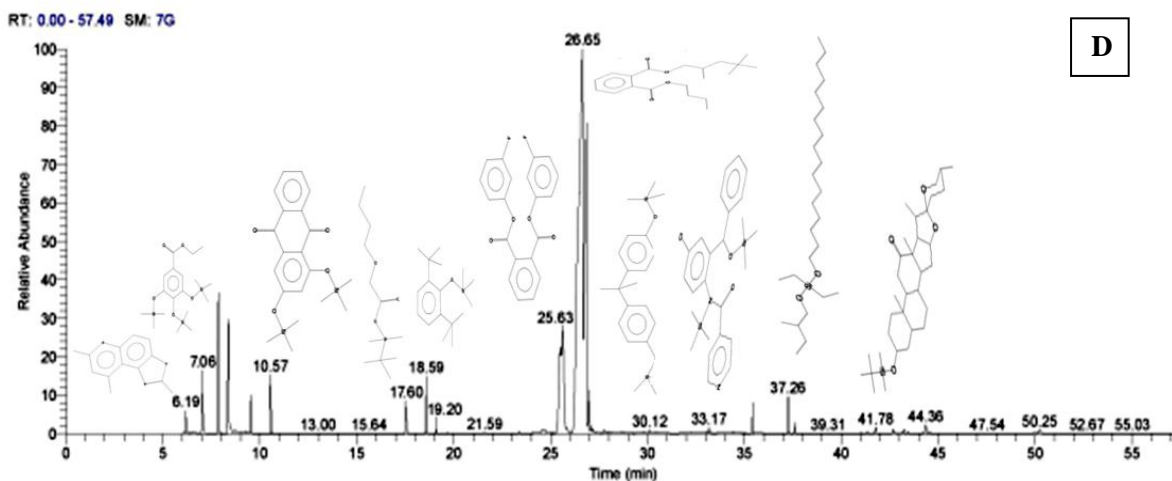
Figure 4 Chromatogram of consortia A. Benzo[a]pyrene std., B. Pyrene std., C. Consortia [LOBP-19A+LOP-9],
D. Consortia [LOP-9+GWP-2].

Table 2 Metabolic product of Consortia B (LOP-9+GWP-2)

S. No.	RT	Metabolites (GWP-2+ LOP-9) (after 50 days)	Toxicity
1.	6.19	p-toluenesulfonamide	Irritating to eyes, respiratory system and skin
2.	7.06	3,4,5-trihydroxybenzoic acid ethyl ester	skin and eye irritation
3.	10.57	1,3-dihydroxyanthraquinone	Oral and dermal toxicity
4.	17.60	Butoxyacetic acid	Respiratory, oral and eye irritation
5.	18.59	2,6-bis(tert butyl)phenol	Bronchospasm and pulmonary oedema
6.	19.20	Phthalic acid	Carcinogenic, malformations and reproductive toxicity
7.	19.71	Oxalic acid	Headache, dizziness, nausea and vomiting, convulsions, coma
8.	21.59	Naphthalene	Hemolytic anemia and methemoglobinemia
9.	23.38	Cyclohexane 1,3,5-trimethyl-2-octadecyl	-
10.	24.61	1,4-benzodicarboxylic acid	Irritate the nose, throat and lungs
11.	25.63	Phthalic acid	Carcinogenic, malformations and reproductive toxicity
12.	26.65	Terephthalic acid	Irritate the nose, throat and lungs
13.	27.92	9-octadecenoic acid	-
14.	30.12	Bisphenol	Cytotoxicity, genotoxicity, reproductive toxicity, dioxin-like effects, and neurotoxicity
15.	32.75	9,12-octadecadienoic acid	-
16.	37.26	Silane diethyldecylcloxydodecyloxy	Reproductive and developmental toxicity
17.	41.05	Diethyl(pentafluorobenzyloxy) tetradecycloxy	-

GC-MS chromatogram of the organic compound separated of benzo[a]pyrene degrading metabolites by LOBP-19A and LOP-9 bacterial consortium showed major and minor peaks indicating the occurrence of two bacterial (LOBP-19A+LOP-9) constituents (Figure 4C). The pyrene degrading constituents were characterized by comparing the mass spectra of the constituents with the NIST library. The same compound, oleic acid (cis -9-octadecenoic acid), had been reported in ethanol extract at 10.73 RT (retention time) and methanoic extraction at 13.9 RT by *Staphylococcus aureus* and *Stenotrophomonas maltophilia* in the previous study and present study was at 27.92 RT   in ethyl acetate extraction on bacterial viability (Nor et al. 2015). Hexadecanoic acid was found at 23.64 and 27.00 RT in this study, and previous studies have been found at 32.61 and produced by *B. cereus* strain VASB1/TS bacterial constituents (Bayat et al. 2015).

Table 3 Metabolites of consortium (LOP-9+LOBP-19A)

S. No.	RT	Metabolites (LOP-9+LOBP-19A)	Toxicity
1.	6.36	1,2,3,4-tetramethyl-5-(chloromethyl)benzene	Skin and eye irritation
2.	7.46	5,6,7,8-tetrahydro-8,8-dimethyl-2-indolizinecarboxylic acid methyl ester	-
3.	9.05	Butanedioic acid (succinic acid)	*Slight skin irritant and a strong eye irritant*
4.	10.01	Benzo[a]pyrene-1,6-dione	*Carcinogenic, malformations and reproductive toxicity*
5.	11.82	Benzene,[3-chloro-2-propenyl)oxy]-(CAS)	*Irritate the nose, throat and lungs*
6.	13.11	3-acetoxy-3,7-dimethyloocta-1,6-diene	-
7.	14.27	t-butyl 3-(3-methyl-1-butenoxy) propanoate	*Reproductive toxicity*
8.	16.37	2,5-bis(bromomethyl)-1,4-dihexylbenzene	*Severe skin burns and eye damage*
9.	17.30	1-nitro-4-octanol	*Carcinogenicity*
10.	19.81	3-(6,6-dimethyl-5-oxohept-2-enyl)-cycloheptanone	-
11.	21.10	Propenoic acid	Acute eye and dermal irritation effects
12.	22.90	1-heptacosanol	*Oral/Parenteral Toxicity*
13.	23.01	Hexadecane,2-methyl-(CAS)	*CNS depression and gastrointestinal tract irritation*
14.	23.64	Hexadecanoic acid, dimethyl ester	*Low acute toxicities*
15.	25.07	6,7-dimethoxy-3,4-dihydroisoquinoline-N-oxide	Specific *target organ toxicity*
16.	27.00	Hexadecanoic acid	Thrombotic activity
17.	29.94	Tridecanoic acid, trimethyl ester	-
18.	31.82	1,2-dimethylpropyl trifluoroacetate	*Oral/Parenteral Toxicity*
19.	33.63	1,2-dibenzoylbenzo[e]indolizine	
20.	34.09	Benzeneacetic acid	*Specific target organ toxicity*
21.	35.24	2,3-bis [trimethylsilyl] oxypropyl stearate	*Acute toxicity, inhalation*
22.	41.45	Dithioerythritol	*Respiratory tract irritation*
23.	43.10	3,5,7-tri(trimethylsiloxy)-2-[3,4-di(trimethylsiloxy)phenyl]-4H-1-benzopyran-4-one	-
24.	47.60	5[4-(acetylthio)butyl]-15butyl-10,20-diphenylporphyrin	*Slight skin and eye irritation*

Note- According to GC-MS NIST library compound

Table 4 Metabolites functional group

S. No.	Wave number (cm^{-1})	Functional group	GWP-2 + LOP-9	LOBP-19A + LOP-9
1.	3000-2000	Aliphatic C-H Stretching (alkenes, alkanes)	2954.27 (cm^{-1})	2973.39(cm^{-1})
2.	1800-1700	Anhydried simple aliphatic(C=O) stretch,ester,ketone	1731.96 (cm^{-1})	1783(cm^{-1})
3.	1500-1400	C-H aromatic compound, aliphatic group	1447.47 (cm^{-1})	1439.12, (cm^{-1})
4.	1400-1200	C-O carboxy esters, ethers, aromatics, alcohol ether	1374.4 (cm^{-1})	1372.8, 1209.37 (cm^{-1})
5.	1100-1000	C-O bond alkanes, hydroxyl group(O-H)	1097.39 (cm^{-1})	1075.47(cm^{-1})
6.	1000-900	C=C bending (alkene)	938.27(cm^{-1})	975.73(cm^{-1})
7.	900-800	C=C and aromatic ring, C-H bending bending (alkene) inorganic band	847.04(cm^{-1})	884(cm^{-1})
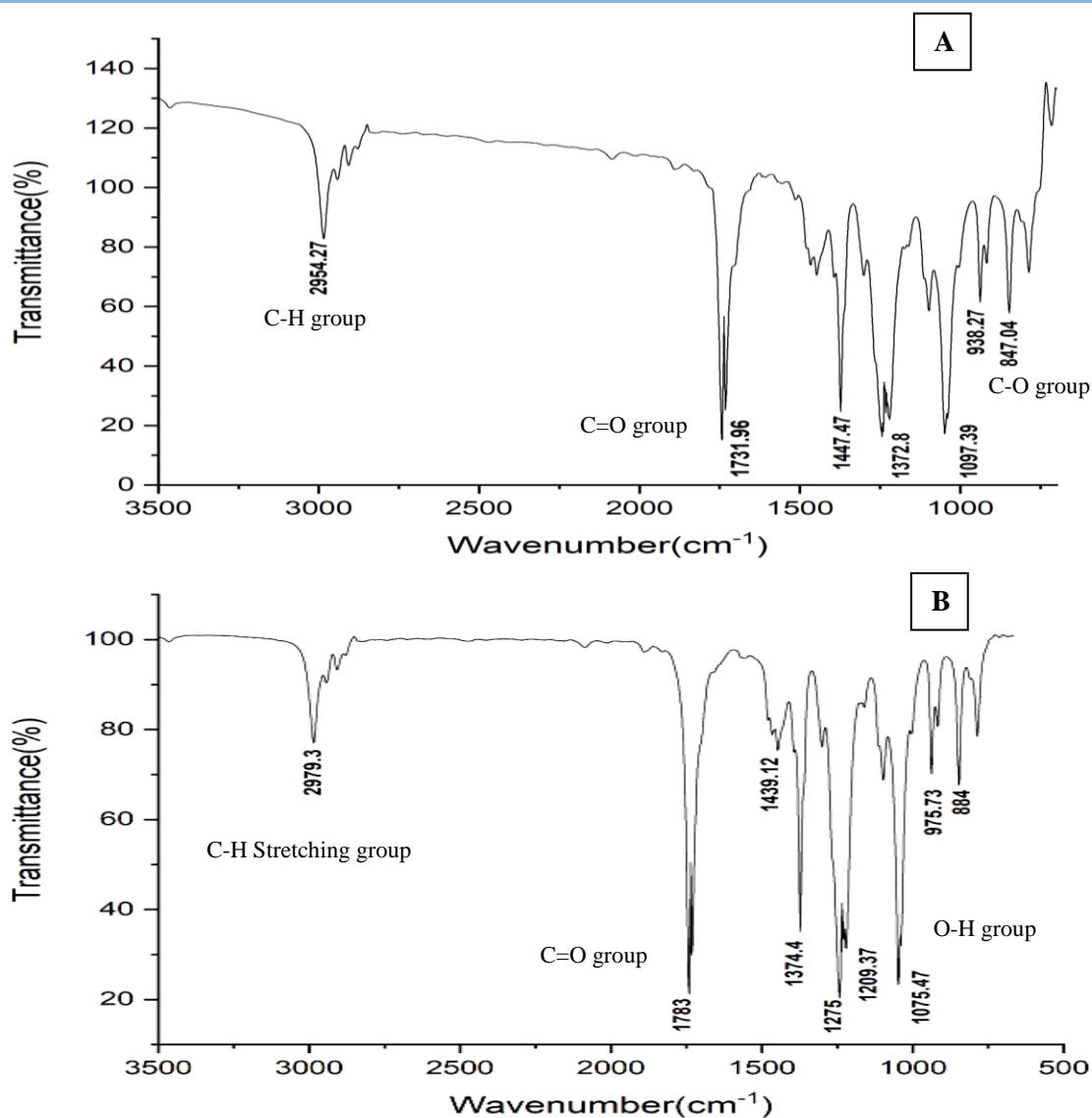
Figure 5 FTIR analysis A. GWP-2+LOP-9 consortia, B. LOBP-19+LOP-9 consortia)

3.4 FTIR analysis

FTIR spectra of pyrene, benzo[a]pyrene degrading metabolites acquired during the degradation phase were compared to demonstrate the change in functional groups between the two compounds and Figure 5 displayed the results. FTIR was used to analyze two bacterial consortium metabolites of degraded benzo[a]pyrene and pyrene. Previous studies reported O-H, C-O, O-H, C-C and C-H vibration in aromatics functional groups (Agrawal and Shahi 2017). In this study, the active group of degrading metabolites (pyrene and benzo[a]pyrene) FTIR graph and Table 4 are represented below (figure 5).

The FTIR library analyzed degrading metabolite's functional groups and bonds. Peaks and wave numbers detailed in the table are 2954.27 (cm^{-1}) in GWP-2+LOP-9 bacterial consortia and 2973.39 (cm^{-1}) produced in LOBP-19A+LOP-9 consortia; these wave numbers were identified as Aliphatic C-H Stretching (alkenes, alkanes) in FTIR library.

Conclusion

The bacterial consortium enriched in MSM and bacterial strains (LOBP-19A, LOP-9 and GWP-2) were used for capable of degrading to different PAHs as pyrene at 2000 ppm and benzo[a]pyrene at 1000 ppm of concentration from 1000ppm standard concentration in acetone. Two consortiums were prepared; one was LOP-9+GWP-2 strains with 2000ppm pyrene, and the second was LOBP-19A+LOP-9 strains with 1000ppm benzo[a]pyrene on environmental conditions. The study proved

that consortium (LOBP-19A and LOP-9) had the better result as compared to single strains, and high benzo[a]pyrene degradation was found (99.62%) where, as LOP-9+GWP-2 consortia had low degradation (93.8%) rate as compared to single bacterial strains pyrene degradation and standard of pyrene (2000ppm) and benzo[a]pyrene (1000ppm). The degradation rate and residual products were identified by HPLC and GCMS, respectively. LOBP-19A+LOP-9 was degraded benzo[a]pyrene, and its degraded metabolites are benzo [a]pyrene-1,6-dione, Butanedioic acid (succinic acid), 2,5-bis(bromomethyl)-1,4-dihexylbenzene, Benzeneacetic acid; besides LOP-9 and GWP-2 bacterial consortium degraded pyrene and degraded metabolites are Naphthalene, 1,4-benzodicarboxylic acid, Terephthalic acid, 9-octadecenoic acid, and these metabolites were degraded with the help of bacterial enzymes secretion and identified by GC-MS. Both aromatic hydrocarbons (pyrene and benzo[a]pyrene) were degraded by bacterial consortium and C-H Stretching (alkenes, alkanes), C-O carboxy esters, ethers, aromatics, alcohol ether and C-O bond alkanes, hydroxyl group (O-H) groups are identified by FTIR analysis which were produced by bacterial consortium degradation. These bacterial consortia may be efficient in the degradation of pyrene and benzo[a]pyrene, and the study may play a significant role in the breakdown of further PAHs. The current study demonstrates the prospective PAHs-degrading bacterial consortium under environmental conditions, which is economical and beneficial to environmental promotion.

Conflict of interest

The authors declare no conflict of interest.

References

Agrawal, N., & Shahi, S. K. (2017). Degradation of polycyclic aromatic hydrocarbon (pyrene) using novel fungal strain *Coriolopsis byrsina* strain APC5. *International Biodeterioration & Biodegradation*, *122*, 69-81.

Aguilera, F., Méndez, J., Pásaro, E., & Laffon, B. (2010). Review on the effects of exposure to spilled oils on human health. *Journal of Applied Toxicology, 30*(4), 291-301.

Aziz, A., Agamuthu, P., Alaribe, F. O., & Fauziah, S. H. (2018). Biodegradation of benzo [a] pyrene by bacterial consortium isolated from mangrove sediment. *Environmental technology*, *39*(4), 527-535.

Bayat, Z., Hassanshahian, M., & Hesni, M. A. (2015). Enrichment and isolation of crude oil degrading bacteria from some mussels collected from the Persian Gulf. *Marine Pollution Bulletin*, *101*(1), 85-91.

Das, N., & Chandran, P. (2011). Microbial degradation of petroleum hydrocarbon contaminants: an overview. *Biotechnology research international*, *2011*, 941810. https://doi.org/10.4061/2011/941810.

Di Lorenzo, R. A., Lobodin, V. V., Cochran, J., Kolic, T., & Besevic, S. (2019). Fast gas chromatography-atmospheric pressure (photo) ionization mass spectrometry of polybrominated diphenylether flame retardants. *Analytica chimica acta*, *1056*, 70-78.

Díaz-Ramírez, I. J., Ramírez-Saad, H., Gutiérrez-Rojas, M., & Favela-Torres, E. (2003). Biodegradation of Maya crude oil fractions by bacterial strains and a defined mixed culture isolated from *Cyperus laxus* rhizosphere soil in a contaminated site. *Canadian Journal of Microbiology*, *49*(12), 755-761.

Donald, C. E., Nakken, C. L., Sørhus, E., Perrichon, P., & Jørgensen, K. B. (2023). Alkyl-phenanthrenes in early life stage fish: differential toxicity in Atlantic haddock (*Melanogrammus aeglefinus*) embryos. *Environmental Science: Processes & Impacts*, *25*(3), 594-608.

Ghosal, D., Ghosh, S., Dutta, T. K., & Ahn, Y. (2016). Current State of Knowledge in Microbial Degradation of Polycyclic Aromatic Hydrocarbons (PAHs): A Review. *Frontiers in microbiology*, *7*, 1369. https://doi.org/10.3389/fmicb.2016.01369.

Johnston, J. E., Lim, E., & Roh, H. (2019). Impact of upstream oil extraction and environmental public health: A review of the evidence. *Science of the Total Environment*, *657*, 187-199.

Joutey, N. T., Bahafid, W., Sayel, H., & El Ghachtouli, N. (2013). Biodegradation: involved microorganisms and genetically engineered microorganisms. *Biodegradation-life of science*, *1*, 289-320.

Kristanti, R. A., & Hadibarata, T. (2015). Biodegradation and identification of transformation products of fluorene by ascomycete fungi. *Water, Air, & Soil Pollution*, *226*, 1-6.

Kumari, B., Chandra, H., & Chandra, R. (2022). Detection of pyrene degrading bacterial strains (LOP-9 *Staphylococcus aureus* and GWP-2 *Mycobacterium vaanbaalenii*) and their metabolic products. *Cleaner Chemical Engineering*, *4*, 100080.

Kumari, B., & Chandra, R. (2022). A Review on Bacterial Degradation of Benzo[a]pyrene and Its Impact on Environmental Health. *Journal of Experimental Biology and Agricultural Sciences*, *10*(6), 1253–1265. https://doi.org/10.18006/2022.10(6).1253.1265

Kumari, B., & Chandra, R. (2023). Benzo [a] pyrene degradation from hydrocarbon-contaminated soil and their degrading

metabolites by Stutzerimonas stutzeri (LOBP-19A). *Waste Management Bulletin*, *1*(3), 115-127.

Lunn, G. (2005). *HPLC methods for recently approved pharmaceuticals*. John Wiley & Sons.

Mandal, S. K., & Das, N. (2017). Biodegradation of benzo [a] pyrene by Rhodotorula sp. NS01 strain isolated from contaminated soil sample. *Research Journal of Pharmacy and Technology*, *10*(6), 1751-1757.

Militon, C., Boucher, D., Vachelard, C., Perchet, G., Barra, V., et al. (2010). Bacterial community changes during bioremediation of aliphatic hydrocarbon-contaminated soil. *FEMS Microbiology Ecology*, *74*(3), 669-681.

Minuti, L., Pellegrino, R. M., & Tesei, I. (2006). Simple extraction method and gas chromatography–mass spectrometry in the selective ion monitoring mode for the determination of phenols in wine. *Journal of Chromatography A*, *1114*(2), 263-268. https://doi.org/10.1016/j.chroma.2006.02.068

Mohandass, R., Rout, P., Jiwal, S., & Sasikala, C. (2012). Biodegradation of benzo [a] pyrene by the mixed culture of *Bacillus cereus* and *Bacillus vireti* isolated from the petrochemical industry. *Journal of Environmental Biology*, *33*(6), 985.

Murphy, S. M., Bautista, M. A., Cramm, M. A., & Hubert, C. R. (2021). Diesel and crude oil biodegradation by cold-adapted microbial communities in the Labrador Sea. *Applied and Environmental Microbiology*, *87*(20), e00800-21.

Nor, N. M., Hadibarata, T., Zubir, M. M. F. A., Lazim, Z. M., Adnan, L. A., & Fulazzaky, M. A. (2015). Mechanism of triphenylmethane Cresol Red degradation by Trichoderma harzianum M06. *Bioprocess and Biosystems Engineering*, *38*, 2167-2175.

Nzila, A., Musa, M. M., Afuecheta, E., Al-Thukair, A., Sankaran, S., Xiang, L., & Li, Q. X. (2023). Benzo [A] Pyrene Biodegradation by Multiple and Individual Mesophilic Bacteria under Axenic Conditions and in Soil Samples. *International Journal of Environmental Research and Public Health*, *20*(3), 1855.

Nzila, A., Musa, M. M., Afuecheta, E., Thukair, A., Sankaran, S., Xiang, L., & Li, Q. X. (2022). Benzo [a] pyrene biodegradation by multiple and individual mesophilic bacteria in axenic conditions and in soil samples. *bioRxiv*, 2022-05.

Ozaki, S., Kishimoto, N., & Fujita, T. (2007). Change in the predominant bacteria in a microbial consortium cultured on media containing aromatic and saturated hydrocarbons as the sole carbon source. *Microbes and Environments*, *22*(2), 128-135.

Patowary, K., Patowary, R., Kalita, M. C., & Deka, S. (2016). Development of an efficient bacterial consortium for the potential remediation of hydrocarbons from contaminated sites. *Frontiers in microbiology*, *7*, 1092.

Perhar, G., & Arhonditsis, G. B. (2014). Aquatic ecosystem dynamics following petroleum hydrocarbon perturbations: A review of the current state of knowledge. *Journal of Great Lakes Research*, *40*, 56-72.

Rahman, P. K., Pasirayi, G., Auger, V., & Ali, Z. (2009). Development of a simple and low cost microbioreactor for high-throughput bioprocessing. *Biotechnology letters*, *31*, 209-214.

Schneider, Y. K., Jørgensen, S. M., Andersen, J. H., & Hansen, E. H. (2021). Qualitative and quantitative comparison of liquid–liquid phase extraction using ethyl acetate and liquid–solid phase extraction using poly-benzyl-resin for natural products. *Applied Sciences*, *11*(21), 10241.

Selvi, A., Salam, J. A., & Das, N. (2014). Biodegradation of cefdinir by a novel yeast strain, *Ustilago* sp. SMN03 isolated from pharmaceutical wastewater. *World Journal of Microbiology and Biotechnology*, *30*, 2839-2850.

Vaidya, S., Jain, K., & Madamwar, D. (2017). Metabolism of pyrene through phthalic acid pathway by enriched bacterial consortium composed of *Pseudomonas*, *Burkholderia*, and *Rhodococcus* (PBR). *3 Biotech*, *7*, 1-15.

Venosa, A. D., & Zhu, X. (2003). Biodegradation of crude oil contaminating marine shorelines and freshwater wetlands. *Spill Science & Technology Bulletin*, *8*(2), 163-178.

Yan, Z., Zhang, Y., Wu, H., Yang, M., Zhang, H., Hao, Z., & Jiang, H. (2017). Isolation and characterization of a bacterial strain *Hydrogenophaga* sp. PYR1 for anaerobic pyrene and benzo [a] pyrene biodegradation. *RSC advances*, *7*(74), 46690-46698.

Zakaria, N. N., Gomez-Fuentes, C., Abdul Khalil, K., Convey, P., Roslee, A. F. A., et al. (2021). Statistical optimization of diesel biodegradation at low temperatures by an Antarctic marine bacterial consortium isolated from non-contaminated seawater. *Microorganisms*, *9*(6), 1213.

CrossMark
click for updates

Journal of Experimental Biology and Agricultural Sciences

http://www.jebas.org

Acclimation to warm temperatures modulates lactate and malate dehydrogenase isozymes in juvenile *Horabagrus brachysoma* (Günther)

Rishikesh S. Dalvi[1,2,*] iD, Asim K. Pal[2], Dipesh Debnath[2,3] iD

[1]Department of Zoology, Maharshi Dayanand College (University of Mumbai), Parel, Mumbai-400012, Maharashtra, India
[2]Division of Fish Nutrition and Biochemistry, Central Institute of Fisheries Education, Versova, Mumbai-400061, Maharashtra, India
[3]ICAR-Central Inland Fisheries Research Institute, Regional Centre, HousefedComplex, Dispur, Guwahati–781 006, Assam, India

ABSTRACT

Differential expression of isozymes enables fish to tolerate temperature fluctuations in their environment. The present study explores the modulation of lactate dehydrogenase (LDH) and cytoplasmic malate dehydrogenase (sMDH) isozyme expression in the heart, muscle, brain, liver, gill, and kidney of juvenile *Horabagrus brachysoma* after 30 days of acclimation at 26, 31, 33, and 36°C. LDH and sMDH zymography were performed using native polyacrylamide gel electrophoresis. The zymography revealed five distinct bands of LDH isoenzymes (labelled from cathode to anode as LDH-A_4, LDH-A_3B_1, LDH-A_2B_2, LDH-A_1B_3, and LDH-B_4) and three distinct bands of sMDH isoenzymes (labelled from cathode to anode as sMDH-A_2, sMDH-AB, and sMDH-B_2), with considerable variation in their expression in the tissues. Acclimation to the test temperatures did not influence the expression patterns of LDH or sMDH isozymes. Densitometric analysis of individual isozyme bands revealed a reduction in the densities of bands containing the LDH-B and sMDH-B molecules, while the densities of bands containing the LDH-A and sMDH-A molecules increased in the gills and muscle, indicating the role of these organs in adaptive responses to thermal acclimation. However, the total densities of the LDH and sMDH isozymes increased with higher acclimation temperatures, indicating that adaptation to increased temperatures in *H. brachysoma* is primarily characterised by quantitative changes in isozyme expression.

* Corresponding author

E-mail: rishi.dalvi@gmail.com (Rishikesh S. Dalvi)

Peer review under responsibility of Journal of Experimental Biology and Agricultural Sciences.

1 Introduction

Most fish species being poikilothermic animals, fluctuations in the water temperature profoundly influence their metabolism, behaviour, migration, growth, reproduction, and ultimately survival. However, every fish species has a unique adaptive capacity, both behavioural and physiological, to endure the temperature change in their environment. Their physiology is modulated in a variety of ways, with the rise and fall in temperature extending the thermal tolerance range of the species (Ficke et al. 2007; McKenzie et al. 2021). The biochemical mechanism for temperature adaptations in fish involves modulations in the activities of metabolic enzymes, the lipid composition of cellular membranes, quantitative changes in total or specific protein in different organs, and the manifestation of isozymes that allow for continuous functions under altered temperature conditions (Seddon 1997; Morgan et al. 2022). Most enzymes that play an important role in adaptive response in fish are linked to energy-producing pathways, such as glycolysis, gluconeogenesis, pentose phosphate pathway, Kreb's cycle, respiratory chain, digestion, and protein metabolism (Guillen et al. 2019; Volkoff and Rønnestad 2020; Li et al. 2023). Organisms often produce isozymes that allow them to adapt and function at altered environmental temperatures (Tattersall et al. 2012; Sejian et al. 2018). The adaptive responses to thermal acclimation involve both qualitative and quantitative changes in the metabolic enzymes. Quantitative changes involve the production of varying quantities of an enzyme, while qualitative changes involve the kinds of enzymes that are produced (Schulte 2004; Tattersall et al. 2012). The outcome of these adaptative processes is to maintain a constant metabolic function at altered environmental temperatures.

Fish acclimated to warm and cold temperatures may differ in the rates of their gene expression, resulting in different amounts of an enzyme being synthesized (Schulte 2004; Badr et al. 2023). The channel catfish (*Ictalurus punctatus*) after cold acclimation showed a two-fold increase in its liver weight, size of cell, total protein, and activity of enzymes including cytochrome oxidase, lactate dehydrogenase, citrate synthase, glucose-6-phosphate dehydrogenase (G6PDH), and 6-phosphogluconate dehydrogenase (Kent et al. 1988). Similarly, quantitative changes in liver G6PDH were detected by immunodetection technique during cold acclimation in *I. punctatus* (Seddon 1997). An alternative to the quantitative theory is the synthesis of qualitatively distinct molecules, in which the warm and cold-acclimated fish would differ mainly in the proportion of the genotype being expressed, such that the populations express isozymes that are qualitatively different (Schulte 2004; Luo et al. 2022). A direct correlation between isozyme expression and temperature acclimation was reported in the brain acetylcholinesterase (AChE) of the trout (*Salmo gairdnerii*) with two variants, namely warm-variant and cold-variant, of which only the warm-variant occurred during

warm acclimation (17°C) and the cold-variant occurred only during cold acclimation (2°C), while both isozymes (variants) were present during acclimation at an intermediate temperature (12°C) (Baldwin and Hochachka 1970). In contrast, no changes were reported in the level of isozymes in *Gillichthys mirabilis, Ameiurus nebulosus, Gibbonsia elagans, G. metzi*, and *G.montereyensis* in response to changes in environmental temperatures (Somero 1975). While the concept of on-off isozyme control, which accounts for the quantitative and qualitative changes, is intriguing, another plausible hypothesis of temperature-dependent conformational changes in the enzymes has been suggested (Poly 1997; Aswani and Trabucco 2019). Studies on the orthologs of LDH have shown the importance of pH and osmolytes (low-molecular-mass organic solutes) in maintaining the structural and functional characteristics of enzymes (Somero 2004).

Horabagrus brachysoma is an endemic catfish with a natural range in the rivers of Kerala (Ali et al. 2007), Karnataka (Bhat 2001), and the Northern Western Ghats in Maharashtra (Katwate et al. 2012). The catfish is propagated for small-scale aquaculture (Raghavan et al. 2016) and is valued for the ornamental fish trade (Ali et al. 2007; Sureshkumar 2013). In earlier research on *H. brachysoma*, it was reported that acclimation to increasing temperatures from 15 to 36 °C increased the heat tolerance and metabolic rates, with optimal physiological performance between 31 and 33 °C (Dalvi et al. 2009); the correlation of its elevated heat tolerance with the elevated HSP70 after acclimation at 20 and 30 °C (Dalvi et al. 2012); and the modulation of metabolic enzymes and HSP70 with increasing temperatures (Dalvi et al. 2017).

With the escalating concerns about global warming and its effect on ecosystems, research is now focused on understanding the molecular mechanisms that help organisms adapt to changing climatic conditions (McCaw et al. 2020; Aubry and Williams 2022). A vast literature documents the efforts that have been made to understand such adaptive responses. However, there is a dearth of information on the adaptive mechanisms of fish endemic to India. The current study was therefore undertaken to understand the modulation of lactate dehydrogenase (LDH) and cytoplasmic malate dehydrogenase (sMDH) isozymes for thermal adaptation in *H. brachysoma* acclimated at 26, 31, 33, and 36°C.

2 Materials and methods

2.1 Experimental fish and experimental setup

Juveniles of *H. brachysoma* (Average length 10.35 ± 2.78 cm) were procured from Aquatic World, Mumbai, India, and transported live with proper aeration to the wet laboratory of the Central Institute of Fisheries Education, Mumbai, India. The fish were given a prophylactic dip in salt solution (2%) and then acclimatized to laboratory conditions (26 ± 1 °C) for 30 days,

during which the fish were daily fed with live *tubifex* worms *ad libitum*. The experimental setup consisted of 24 fish equally distributed in 4 thermostatic aquariums (6 fish per test temperature; water capacity 52 L; sensitivity ± 0.2°C) maintained at 26°C. One of the aquariums maintained at 26 °C was used as the control. Acclimation to elevated temperatures of 31, 33, and 36°C and maintenance of the fish were done as described earlier by Dalvi et al. (2009), and Dalvi et al. (2017). After 30 days of acclimation, the fish were fasted for 24 hours before sampling.

2.2 Sample preparation and protein estimation

Following 30 days of acclimation, fish from the test temperatures were anaesthetized with 50 μL^{-1} clove oil and dissected to extract the tissues, such as gill, brain, heart, kidney, liver, and muscle. The tissues were immediately washed twice with chilled phosphate buffer (50 mM, pH 7.2), blotted on filter paper, weighed, and homogenised (20% weight/volume) individually in chilled phosphate buffer (50 mM, pH 7.2, with 0.1 mM PMSF, and 0.25M sucrose) using a glass homogenizer kept in an ice bath. Individual tissue homogenates were centrifuged for 20 minutes at 10,000 rpm at 4°C, the supernatants of each tissue homogenate were collected separately in a glass vial and kept at -20°C until use. The protein contents in each supernatant were determined using the Bradford (1976) method with bovine serum albumin as a standard.

2.3 Electrophoresis and zymography

Lactate dehydrogenase (LDH) and cytoplasmic malate dehydrogenase (sMDH) isozymes in various tissues were resolved using non-denaturing polyacrylamide gel electrophoresis (ND-PAGE) in a vertical slab gel electrophoresis apparatus (Microkin, TechnoSource, Mumbai, India) with a discontinuous system following the method of Walker (2002). The LDH isozymes were resolved using ND-PAGE with 5% stacking and 10% separating gels, while the sMDH isozymes were resolved using ND-PAGE with 5% stacking and 12% separating gels. Since the concentration of LDH and sMDH varied in different tissues, the amount of protein to be loaded on the PAGE for good resolution of the isozymes was different for each tissue (Figures 2 and 5). However, aliquots of the supernatant with equal protein concentrations were loaded on the gel for each tissue to be tested at different acclimation temperatures. Two to three replicates of each tissue from different test temperatures were electrophoresed simultaneously on the ND-PAGE with a constant voltage (50V) for 3 hrs at 4°C. The LDH and sMDH isozymes were visualized by activity staining in the gel following the methods described by Pasteur et al. (1988), with modifications. Briefly, the LDH gels were incubated in a solution containing 0.5 M Tris-HCl buffer (pH 7.5), NAD (3%), NBT (0.4%), PMS (0.01%), and sodium lactate (0.2 N). Similarly, the sMDH gels were incubated in a solution of 0.5 M Tris-HCl buffer (pH 7.5), NAD (3%), NBT (0.4%), PMS

(0.01%), and malic acid (0.2 N). The gels were incubated for 30 minutes at 30°C. Human serum was loaded into the gels for LDH isozyme for comparison and standardization of the procedure. No artifacts were observed in the gels that were stained in buffer without the substrates for LDH and sMDH. The stained gels were rinsed with distilled water and images were captured using a gel documentation system (Syngene, UK). The LDH and sMDH isoenzymes were nomenclated following Shaklee et al. (1990). The absolute integrated optical density (IOD) of each isoenzyme band was quantified using the Gel-pro analyzer (version 4.5, Media Cybernetics, USA) and represented as area density per μg protein. The densities of all isoenzyme bands in a lane for each tissue tested were summed to investigate the change in the total activities of the enzymes at different acclimation temperatures.

2.4 Statistical analysis

The area densities of each isozyme type and the summed densities of the isoenzymes for an organ of fish acclimated to the four experimental temperatures were compared via one-way ANOVA using Statistical Package for the Social Sciences (version 16.0, USA). Duncan's multiple range tests were used to determine the differences among treatment means at P<0.05. The data presented in the figures are expressed as the mean ± standard error of the mean (SEM).

3 Results

3.1 Lactate dehydrogenase (LDH)

Five distinct LDH isoenzymes were observed in *H. brachysoma*, with considerable variation in their expression patterns in different tissues (Figure 1). The LDH isoenzymes were nomenclated as LDH-A_4, LDH-A_3B_1, LDH-A_2B_2, LDH-A_1B_3, and LDH-B_4 based on their relative electrophoretic mobility. A distinct anodal band (LDH-B_4) was observed in the liver, and a single cathodal band (LDH-A_4) was observed in the muscle. However, in the liver, electrophoresis with higher protein concentrations (5 or 10μg) revealed three faintly stained heterotetramers (LDH-A_3B_1, LDH-A_2B_2, and LDH-A_1B_3) in addition to the homotetramer of LDH-B (LDH-B_4), while in the muscle, the heterotetramers were not detected at higher protein concentrations (5 or 10μg) (Data not shown). The heart, brain, gills, and kidney showed the presence of all five isozymes, consisting of homotetramers and heterotetramers of the LDH-A and LDH-B subunits, but the IODs of each isoenzyme differed for each tissue. The LDH-C isoenzyme was not detected in any of the tissues investigated.

When a specific tissue between fish acclimated at 26, 31, 33, and 36°C was compared, although the LDH isozyme expression patterns remained consistent (Figure 2), the IODs of each LDH isozyme type showed variations (Figure 3). The IODs of all the LDH isozymes
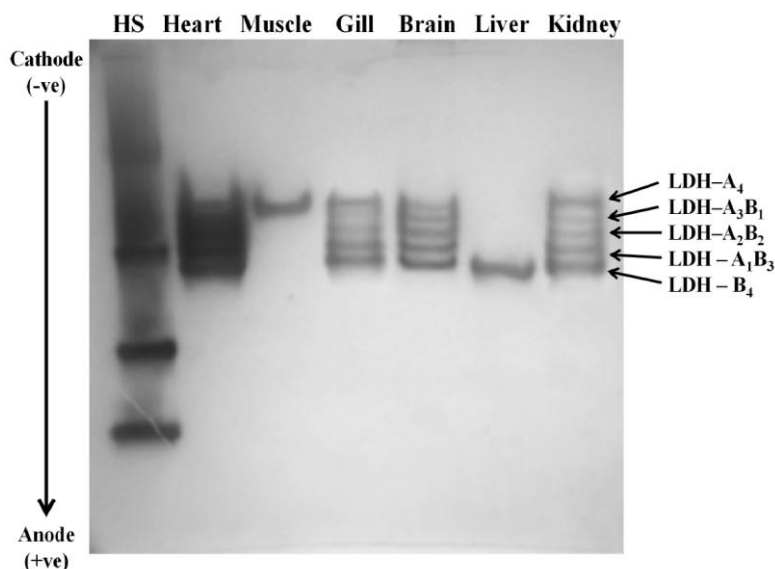
Figure 1 Comparison of lactate dehydrogenase isozyme expression in heart, skeletal muscle, gill, brain, liver, and kidney tissues of *H. brachysoma* acclimated at 26°C.The amount of protein loaded on the gel for each tissue were, heart: 2 μg, skeletal muscle: 2 μg, gill: 10 μg, brain: 5 μg, liver: 2μg, and kidney: 5 μg. The tetrameric lactate dehydrogenase represented by five isozymes are labelled from cathode to anode as LDH-A$_4$, LDH-A$_3$B$_1$, LDH-A$_2$B$_2$, LDH-A$_1$B$_3$, and LDH-B$_4$. Human serum (HS) was loaded in the first well for comparison and standardization of the procedure.

Figure 2 Comparison of lactate dehydrogenase isozyme expression in brain, gill, kidney, liver,muscle, and heart tissues of *H. brachysoma* acclimated to the test temperatures. The amount of protein loaded on the gel for each tissue were, brain- 5 μg, gill- 10 μg, kidney- 5 μg, liver- 5 μg, skeletal muscle- 2μg, and heart- 2 μg.

Figure 3 Area densities (IODs) of lactate dehydrogenase isozyme in in brain, gill, kidney, liver,muscle, and heart tissues of *H. brachysoma* acclimated to the test temperatures. Value expressed as area density/µg of protein. Data represents mean ± SE, n=6. The bars with the asterisk '*' indicate significant (P<0.05) differences among the test temperatures.

significantly increased (*P*<0.05) in the kidney, liver, muscle, and heart tissues at either 33 and/or 36℃. In the brain, the IODs of LDH-A_4, LDH-A_3B_1, and LDH-A_2B_2 significantly (*P*<0.05) increased at 33 and 36℃ than at lower temperatures. In the gills, the IODs of LDH-A_4, LDH-A_3B_1, and LDH-A_2B_2 significantly (P<0.05) increased, while the IOD of LDH-B_4 significantly (P<0.05) decreased at 33 and 36℃. A significant increase (P<0.05) was also observed in the LDH-A_2B_2 and LDH-A_1B_3 in the kidney and the LDH-A_2B_2 in the gill at 31℃ and higher temperatures. The total densities (sum of IODs) of the LDH isozyme significantly (P<0.05) increased in the kidney at 31℃ and higher acclimation temperatures, in the liver and muscle at 33 and 36℃, and in the heart at 36℃ (Figure 7A).

3.2 Cytoplasmic malate dehydrogenase (sMDH)

Three distinct sMDH isoenzymes were observed in different tissues of *H. brachysoma*, with considerable variation in their expression patterns (Figure 4). The MDH is a multimeric enzyme made up of dimers or tetramers of subunits with molecular weights ranging from 30 to 35 kDa (Goward and Nicholls 1994). The sMDH isozymes were nomenclated from the cathode to the anode as sMDH-A_2, sMDH-AB, and sMDH-B_2. The muscle and heart predominantly expressed sMDH-AB and sMDH-B_2, while the liver expressed sMDH-A_2 and sMDH-AB isozymes. Although all three sMDH isozymes were expressed in the gill, brain, and kidney, considerable differences were observed in their IODs in the selected tissues.
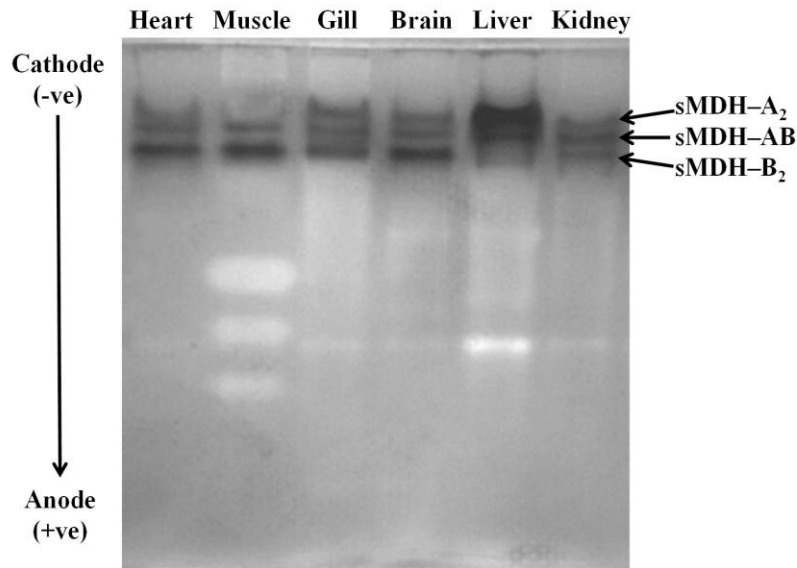
Figure 4 Comparison of cytoplasmic malate dehydrogenase isozyme expression in heart, skeletal muscle, gill, brain, liver, and kidney tissues of *H. brachysoma* acclimated at 26°C. The dimeric matate dehydrogenase represented by three isozymes are labelled from cathode to anode as sMDH-A$_2$, sMDH-AB, and sMDH-B$_2$. The amount of protein loaded on the gel for each tissue were, heart- 10 μg, skeletal muscle- 10 μg, gill- 20 μg, brain- 10 μg, liver- 5 μg, and kidney- 10 μg.
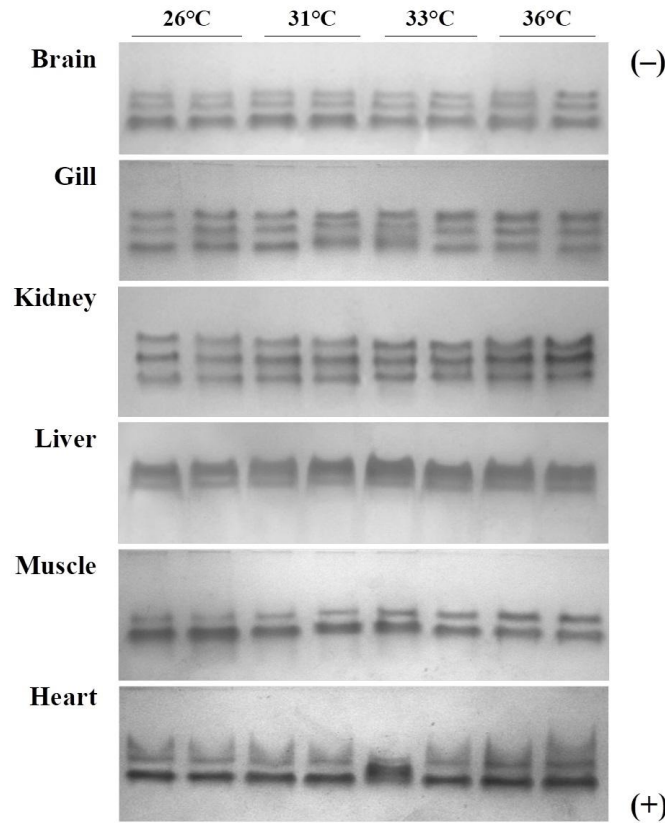
Figure 5 Comparison of cytoplasmic malate dehydrogenase isozyme expression in brain, gill, kidney, liver, muscle, and heart tissues of *H. brachysoma* acclimated to the test temperatures.The amount of protein loaded on the gel for each tissue were, brain- 10 μg, gill- 20 μg, kidney- 10 μg, liver- 5 μg, skeletal muscle- 10 μg, and heart- 10 μg.

When a specific tissue between fish acclimated at 26, 31, 33, and 36°C was compared, although the sMDH isozyme expression patterns remained consistent (Figure 5), the IODs of each MDH isozyme type showed variations (Figure 6). The sMDH-A_2 significantly ($P<0.05$) increased in the gills, kidney, and liver tissues, while the sMDH-AB significantly ($P<0.05$) increased in the gills, kidney, muscle, and heart tissues either at 33 and/or 36°C. However, in the muscle, the sMDH-B_2 significantly decreased ($P<0.05$) in fish acclimated at 36°C. The total densities (sum of IODs) of the sMDH isozymes significantly increased ($P<0.05$) in the gills, kidney, liver, and heart at 33 and/or 36°C, but not in the brain and muscle tissues (Figure 7B).
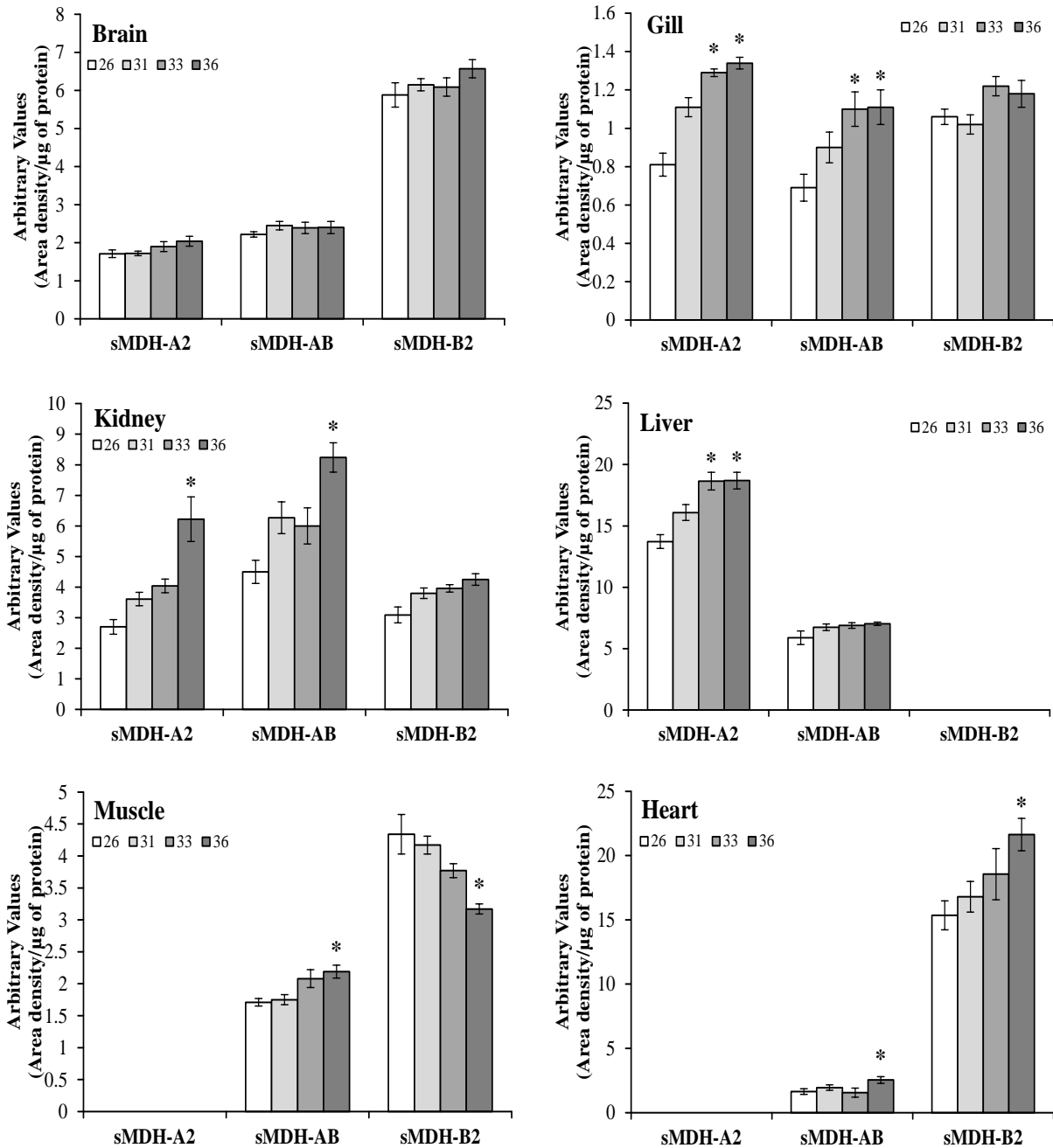
Figure 6 Area densities (IODs) of cytoplasmic malate dehydrogenase isozyme in brain, gill, kidney, liver, muscle, and heart tissues of *H. brachysoma* acclimated to the test temperatures. Value expressed as area density/µg of protein. Data represents mean ± SE, n=6. The bars with the asterisk '*' indicate significant (P<0.05) differences among the test temperatures.

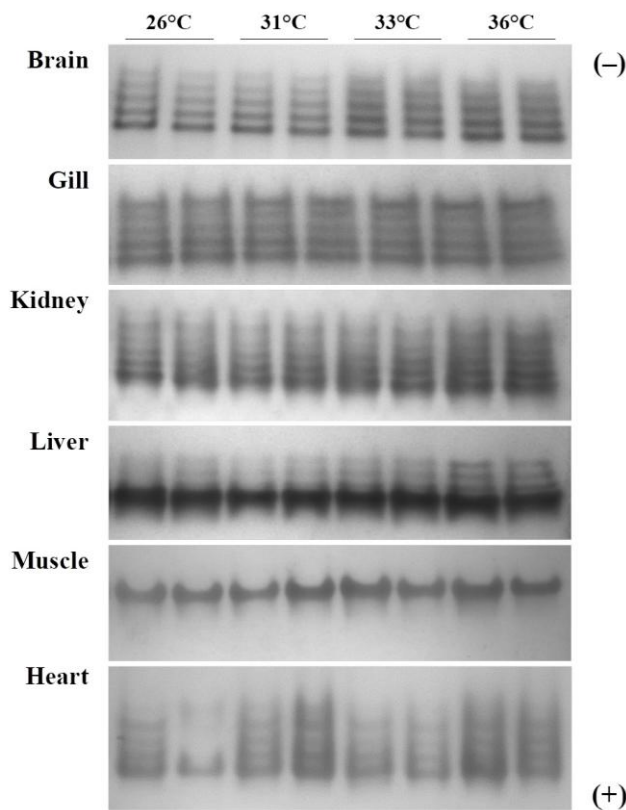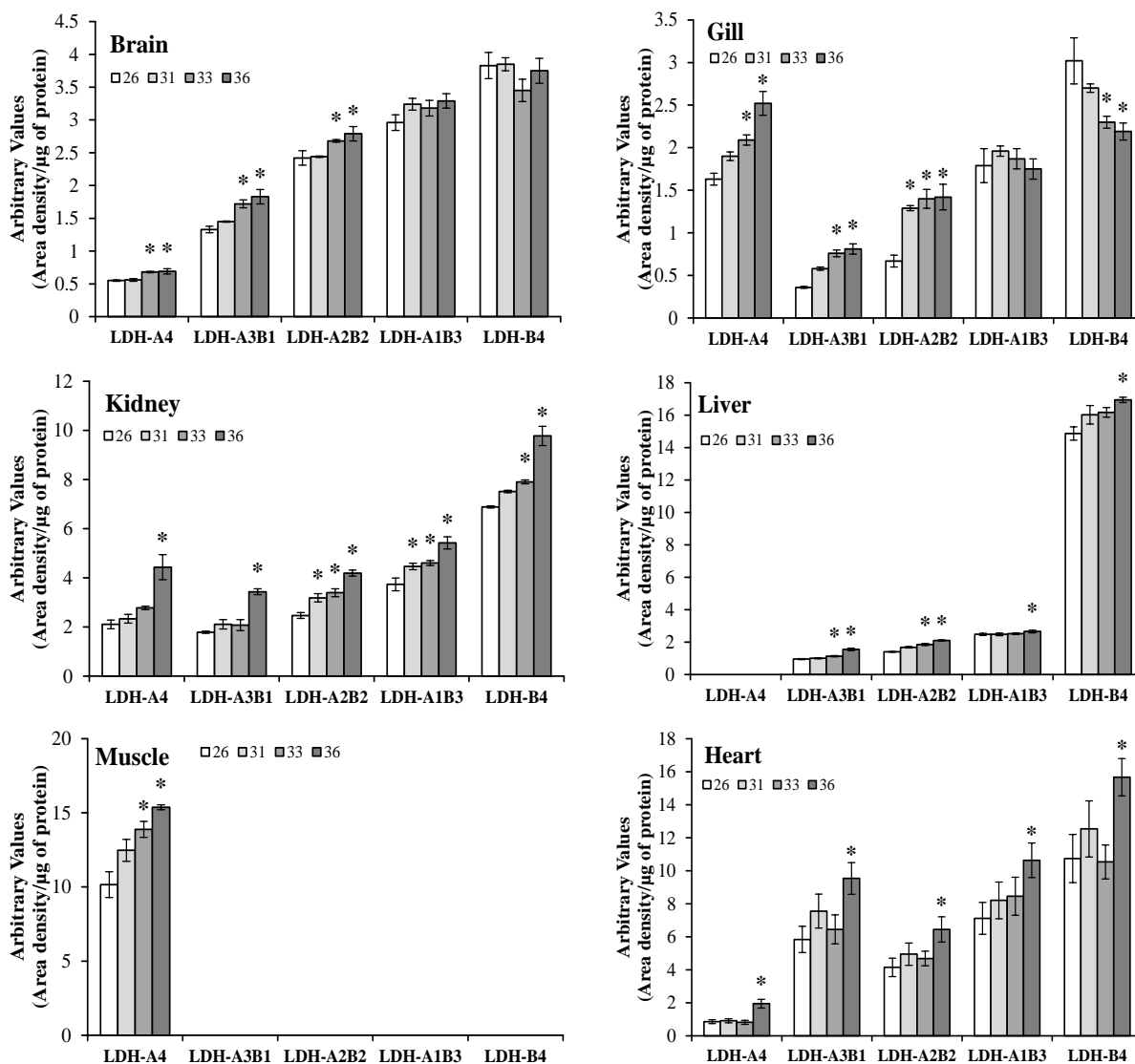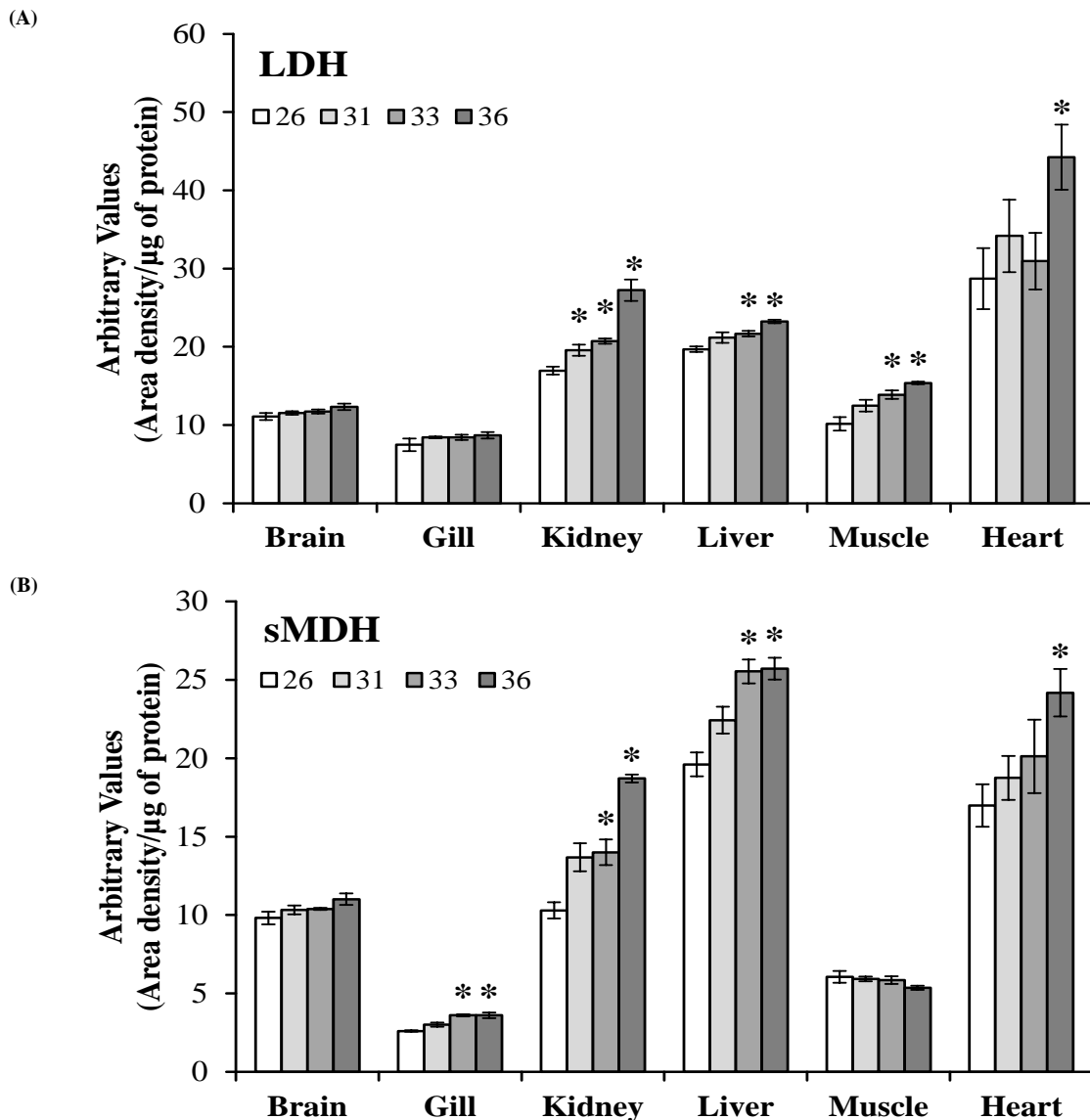Figure 7 Summed area densities (IODs) of lactate dehydrogenase (A) and cytoplasmic malate dehydrogenase (B) isozyme expressed in brain, gill, kidney, liver, muscle, and heart tissues of *H. brachysoma* acclimated to the test temperatures. Value expressed as area density/µg of protein. Data represents mean ± SE, n=6. The bars with the asterisk '*' indicate significant (P<0.05) differences among the test temperatures.

4 Discussion

LDH is the most widely researched enzyme in fish. It is a cytosolic enzyme that catalyses the interconversion of lactate to pyruvate in the final step of anaerobic glycolysis and also the conversion of lactate to glucose during gluconeogenesis (Zakhartsev et al. 2004; Koenekoop and Åqvist 2023). It is a tetrameric protein that is controlled by three distinct genes viz., LDH-A*, LDH-B*, and LDH-C*. The random combination of these gene products results in the formation of different isoenzymes that are known to have a tissue-specific distribution. In fish, the LDH-A is chiefly expressed in tissues with anaerobic glycolysis, like the skeletal muscle; the

LDH-B is chiefly expressed in tissues with aerobic metabolism, such as the heart and/or liver; and the LDH-C is typically expressed in the liver or eyes, often co-occurring with the LDH-B (de Almeida-Val and Val 1993; Ahmad 2009). In the present study, the normal (not reverse) electrophoretic mobility of the LDH-A and LDH-B subunits in *H. brachysoma* is similar to those reported earlier in most teleost fishes (Markert and Faulhaber 1965; Rao et al. 1989; Ferreira et al. 1991; El-alfy et al. 2008). Differences observed in the expression patterns of LDH isozymes in the selected tissues of *H. brachysoma* (Figure 1) indicate restricted or preferential subunit assembly as an adaptation strategy to meet metabolic demands (aerobic or anaerobic) (Coquelle et al.

2007) or restricted expression of the subunit in the tissue (Murphy et al. 1990; Ahmad 2009). Our observations on the expression patterns of the LDH-A and LDH-B subunits in different tissues are similar to those in the catfishes *Clarias batrachus* and *Heteropneustes fossilis* (Triveni and Rao 1986) and the murrel *Channa punctata* (Ahmad 2009). The LDH-C gene is predominantly expressed in the liver or the eyes of most teleost fishes (Rao et al. 1989; Powers and Schulte 1998; Schulte 2004). It is noteworthy that in the present study, the LDH-C was not detected in liver tissue.

In this study, the expression patterns of LDH (Figure 2) and sMDH (Figure 5) isozymes were consistent in *H. brachysoma* acclimated to increasing temperatures. The findings of this study are similar to those reported for LDH in the loach *Misgurnus fossilis* (Ozernyuk et al. 1994) and crucian carp *Carassius carassius* (Vornanen 1994) during seasonal temperature changes and in the cod *Gadus morhua* acclimated to 4°C and 12°C (Zakhartsev et al. 2004). Recently, Luo et al. (2022) showed that exposure to cold (13°C) or heat (23°C) shock did not influence the muscle LDH isozyme expression pattern in Amur sturgeon (*Acipenser schrenckii*). Aswani and Trabucco (2019) observed that the two isozymes of brain AChE (a 59 Kda monomer and a 244 Kda tetramer) in *Tilapia mossambica* acclimated to 25 and 37°C had similar electrophoretic mobility and intensity but differed in their Kms, thermal stability, and activation energy, and suggested that the temperature adaptation of brain AChE in *T. mossambica* involves the aggregation-dissociation of the two isozymes. However, in the present study, the sum densities of the isozymes in different tissues increased at either 33 and/or 36°C, indicating enhanced expression of their respective genes at higher temperatures. In the case of LDH, such a phenomenon may indicate temperature-induced metabolic reorganization towards aerobic or anaerobic metabolism at warm temperatures (Somero 1973; Lannig et al. 2003). Thus, the higher LDH densities (or activities) detected in all tissues of *H. brachysoma* acclimated to 36°C imply that the fish were in an anaerobic state of metabolism at this temperature, as observed in our earlier study (Dalvi et al. 2017). An earlier study on LDH in different tissues of goldfish (*Carassius auratus*) revealed increased expression of specific LDH isoforms during cold acclimation, indicating that metabolic adjustments can be achieved, at least partially, by modifying protein concentration (Hochachka 1965). Quantitative changes in the muscle LDH and brain sMDH, as determined by staining intensities in the gel, were reported in *Lepomis cynellus* acclimated at 5 and 25°C (Wilson et al. 1975). Similarly, acclimation to cold temperatures resulted in a reduction in the specific concentration of LDH in cod (*G. morhua*) liver and white muscle (Zakhartsev et al. 2004). However, contrary to our results, exposure of Amur sturgeon (*A. schrenckii*) to heat shock (23°C) decreased the intensity of a

specific LDH-2 band during the 72-hour exposure period (Luo et al. 2022), indicating a species-specific response to thermal stress.

In the present study, the IODs of LDH-A_4 increased in all tissues with increasing acclimation temperatures, except for the liver. The tissue-specific distributions of LDH isozymes indicate functional divergence, as LDH-A is ideally suited for pyruvate reduction and LDH-B and LDH-C are ideally suited for lactate oxidation (Schulte 2004). Since LDH-A_4 is predominantly responsible for the conversion of pyruvate to lactate, i.e., anaerobic glycolysis, and LDH-B_4 is responsible for the conversion of lactate to pyruvate, i.e., gluconeogenesis and aerobic metabolism, it is suggested that different LDH isozymes have different functional significance (Powers and Schulte 1998). Studies on gene coding loci for LDH-A_4 in *Misgurnus fossilis* acclimated to 5 and 18°C reported that the qualities of total and LDH-A mRNA isolated from white skeletal muscle significantly increased after acclimation to 18°C compared to 5°C (Smirnova et al. 2002). Therefore, the results of this study may indicate increased production of LDH-A_4 and an enhanced pyruvate metabolism pathway in *H. brachysoma* acclimated to higher temperatures.

In this study, the LDH-B_4 isozyme decreased significantly ($P<0.05$) in the gills of *H. brachysoma* with increasing acclimation temperatures (Figure 6). Crawford and Powers (1989) compared two environmentally distinct populations of *Fundulus heteroclitus* and observed that the northern population (14.1°C) had twice the concentration of LDH-B_4 enzyme (EC 1.1.1.27) and its mRNA than the southern population (31.7°C). In a subsequent experiment, Segal and Crawford (1994) observed that when these two populations of *F. heteroclitus* were acclimated to 10°C and 20°C, both populations exhibited 1.3-fold higher levels of the LDH-B_4 enzyme at 10°C compared to 20°C, suggesting that the variations in 10°C acclimated fish are caused by differences in the protein stability of LDH-B allozymes between the northern and southern populations. Organs such as the heart or gill may first encounter reduced aerobic scope, oxygen deprivation, anaerobiosis, and energy failure at increasing temperatures (Ern et al. 2023). In our study, the reduction in LDH-B_4 and increase in LDH-A_4 isozymes in the gills with increasing acclimation temperatures indicate that warm temperatures induce the production of thermostable LDH-A molecules, profoundly affecting the respiratory organs. However, further investigation is required to confirm the thermostability of LDH-A in *H. brachysoma*.

In the present study, the sMDH isozyme expression pattern varied in different tissues of *H. brachysoma* (Figure 4). Results of this study are consistent with those reported for sMDH in *Leporinus friderici*, *Hoplias malabaricus*, and *Pimelodus maculatus* (Monteiro et al. 1998), *Leiostomus xanthurus* (Schwantes and Schwantes 1982a; Schwantes and Schwantes 1982b), and the

Astyanax fasciatus (De Luca et al. 1983), demonstrating variable expression of MDH-A and MDH-B subunits in different tissues. Schwantes and Schwantes (1982a, 1982b) first reported thermal adaptation in teleosts by two sMDH gene loci, with the sMDH-A* encoding a thermostable isoform and the sMDH-B* encoding a thermolabile isoform. A comparison of sMDH between eastern Pacific barracudas (*Sphyraena idiastes*, *S. argentea*, *S.ensis*, and *S.lucasana*) from different latitudes revealed that variations in the proportion of thermostable and thermolabile sMDH isozymes are crucial for temperature adaptation and that the lack of thermolabile isoforms can be a specific trait in species adapted to warm temperatures (Lin and Somero 1995a). Thermostable sMDH-A expression is reported in Sciaenids (*Micropogonias furnieri*, *Cynoscion striatus*, and *Macrodon ancylodon*) (Coppes et al. 1987), Amazon cichlid fishes (*Astronotus ocellatus*, *Cichla monoculus*, *Geophagus cffharreri*, *Cichlassoma severum*, and *Mesonauta insignis*) (Farias and Almeida-Val 1992), Eastern Pacific barracuda (*Sphyraena* spp)(Lin and Somero 1995a), *Gillichthys mirabilis* (Lin and Somero 1995b), and Characiformes and Perciformes fishes (Monteiro et al. 1998). In our study, the sMDH-A$_2$ isozyme increased significantly ($P<0.05$) in the gills, kidney, and liver tissues, and the sMDH-B$_2$ isozyme decreased significantly ($P<0.05$) in the muscle at 33 and 36°C (Figure 6), indicating differential expression of the thermostable sMDH-A sub-unit in the tissues for sustained metabolic functions at elevated temperatures.

Conclusion

In this study, the suite of LDH and sMDH isozymes expressed in various tissues remained unchanged regardless of acclimation temperatures. However, an increase in the sum density and the densities (IODs) of isozymes with LDH-A and sMDH-A sub-units was observed with increasing acclimation temperatures. Our results suggest that the strategies for thermal adaptation in *H. brachysoma* involve quantitative changes in the LDH and sMDH isozymes. Further, the reduction in the levels of the LDH-B and sMDH-B molecules and the increase in the LDH-A and sMDH-A molecules in the gill and muscle tissues indicate that the adaptive responses to thermal acclimation are governed by and restricted to these organs.

Acknowledgement

Conflicts of interest and financial disclosures

The authors state that they have no conflicts of interest.

References

Ahmad, R. (2009). Functional and adaptive significance of differentially expressed lactate dehydrogenase isoenzymes in tissues of four obligatory air-breathing *Channa* species. *Biologia*, *64*(1), 192–196. https://doi.org/10.2478/s11756-009-0017-7

Ali, P. A., Raghavan, R., & Prasad, G. (2007). Threatened fishes of the world: *Horabagrus brachysoma* (Gunther, 1864) (Bagridae). *Environmental Biology of Fishes*, *78*(3), 221. https://doi.org/10.1007/s10641-006-0022-4

Aswani, V., & Trabucco, D. (2019). Biochemical adaptation in brain acetylcholinesterase during acclimation to sub-lethal temperatures in the eurythermal fish *Tilapia mossambica*. *Scientific Reports*, *9*(1), 19762. https://doi.org/10.1038/s41598-019-56066-x

Aubry, L. M., & Williams, C. T. (2022). Vertebrate phenological plasticity: From molecular mechanisms to ecological and evolutionary implications. *Integrative and Comparative Biology*, *62*(4), 958–971. https://doi.org/10.1093/icb/icac121

Badr, A., Haverinen, J., & Vornanen, M. (2023). Tissue-specific differences and temperature-dependent changes in Na, K-ATPase of the roach (*Rutilus rutilus*). *Aquaculture*, *563*, 738963. https://doi.org/10.1016/j.aquaculture.2022.738963

Baldwin, J., &Hochachka, P. W. (1970). Functional significance of isoenzymes in thermal acclimatization. Acetylcholinesterase from trout brain. *Biochemical Journal*, *116*(5), 883–887. https://doi.org/10.1042/bj1160883

Bhat, A. (2001). A new report of Horabagrus brachysoma Jayaram, family Bagridae in Uttara Kannada District, Karnataka. *Journal of the Bombay Natural History Society*, *98*(2), 294–295.

Bradford, M. M. (1976). A rapid and sensitive method for the quantitation of microgram quantities of protein utilizing the principle of protein-dye binding. *Analytical Biochemistry*, *72*(1–2), 248–254. https://doi.org/10.1006/abio.1976.9999

Coppes, Z. L., Schwantes, M. L. B., & Schwantes, A. R. (1987). Adaptative features of enzymes from family Sciaenidae (Perciformes)—I. Studies on soluble malate dehydrogenase (s-MDH) and creatine kinase (CK) of fishes from the south coast of Uruguay. *Comparative Biochemistry and Physiology. Part B: Comparative Biochemistry*, *88*(1), 203–209. https://doi.org/10.1016/0305-0491(87)90101-5

Coquelle, N., Fioravanti, E., Weik, M., Vellieux, F., & Madern, D. (2007). Activity, stability and structural studies of lactate dehydrogenases adapted to extreme thermal environments. *Journal of Molecular Biology*, *374*(2), 547–562. https://doi.org/10.1016/j.jmb.2007.09.049

Crawford, D. L., & Powers, D. A. (1989). Molecular basis of evolutionary adaptation at the lactate dehydrogenase-B locus in the fish *Fundulusheteroclitus*. *Proceedings of the National Academy of Sciences of the United States of America*, *86*(23), 9365–9369. https://doi.org/10.1073/pnas.86.23.9365

Dalvi, R. S., Pal, A. K., Tiwari, L. R., Das, T., & Baruah, K. (2009). Thermal tolerance and oxygen consumption in *Horabagrus brachysoma* (Gunther) acclimated to different temperatures. *Aquaculture*, *29*, 116–119. https://doi.org/10.1016/j.aquaculture.2009.06.034

Dalvi, R. S., Pal, A. K., Tiwari, L. R., & Baruah, K. (2012). Influence of acclimation temperature on the induction of heat-shock protein 70 in the catfish *Horabagrus brachysoma* (Günther). *Fish Physiology and Biochemistry*, *38*(4), 919–927. https://doi.org/10.1007/s10695-011-9578-9

Dalvi, R. S., Das, T., Debnath, D., Yengkokpam, S., Baruah, K., Tiwari, L. R., & Pal, A. K. (2017). Metabolic and cellular stress responses of catfish, *Horabagrus brachysoma* (Günther) acclimated to increasing temperatures. *Journal of Thermal Biology*, *65*, 32–40. https://doi.org/10.1016/j.jtherbio.2017.02.003

de Almeida-Val, V. M. F., & Val, A. L. (1993). Evolutionary trends of LDH isozymes in fishes. *Comparative Biochemistry and Physiology Part B: Comparative Biochemistry*, *105*(1), 21–28. https://doi.org/10.1016/0305-0491(93)90164-Z

De Luca, P. H., Schwantes, M. L. B., & Schwantes, A. R. (1983). Adaptative features of ectothermic enzymes—IV. Studies on malate dehydrogenase of *Astyanax fasciatus* (Characidae) from lobo reservoir (São Carlos, São Paulo, Brasil). *Comparative Biochemistry and Physiology Part B: Comparative Biochemistry*, *74*(2), 315–324. https://doi.org/10.1016/0305-0491(83)90019-6

El-Alfy, S. H., Abdelmordy, M. B., & Salama, M. S. (2008). Lactate dehydrogenase isozymes in tilapiine fishes (Cichlidae): Tissue expression and genetic variability patterns. In *Proceedings of the 8th International Symposium on Tilapia in Aquaculture* (pp. 181–197).

Ern, R., Andreassen, A. H., & Jutfelt, F. (2023). Physiological mechanisms of acute upper thermal tolerance in fish. *Physiology*, *38*(3), 141–158. https://doi.org/10.1152/physiol.00027.2022

Farias, I. P., & Fonseca de Almeida-Val, V. M. F. (1992). Malate dehydrogenase (sMDH) in Amazon cichlid fishes: Evolutionary features. *Comparative Biochemistry and Physiology Part B: Comparative Biochemistry*, *103*(4), 939–943. https://doi.org/10.1016/0305-0491(92)90219-H

Ferreira, N. C. D. A., De Almeida-Val, V. M. F., & Schwantes, M. L. B. (1991). Lactate dehydrogenase (LDH) in 27 species of Amazon fish: Adaptive and evolutive aspects. *Comparative Biochemistry and Physiology Part B: Comparative Biochemistry*, *100*(2), 391–398. https://doi.org/10.1016/0305-0491(91)90392-Q

Ficke, A. D., Myrick, C. A., & Hansen, L. J. (2007). Potential impacts of global climate change on freshwater fisheries. *Reviews in Fish Biology and Fisheries*, *17*(4), 581–613. https://doi.org/10.1007/s11160-007-9059-5

Goward, C. R., & Nicholls, D. J. (1994). Malate dehydrogenase: A model for structure, evolution, and catalysis. *Protein Science*, *3*(10), 1883–1888. https://doi.org/10.1002/pro.5560031027

Guillen, A. C., Borges, M. E., Herrerias, T., Kandalski, P. K., de Arruda Marins, E., et al. (2019). Effect of gradual temperature increase on the carbohydrate energy metabolism responses of the Antarctic fish *Notothenia rossii*. *Marine Environmental Research*, *150*, 104779. https://doi.org/10.1016/j.marenvres.2019.104779

Hochachka, P. W. (1965). Isoenzymes in metabolic adaptation of a poikilotherm: Subunit relationships in lactic dehydrogenases of goldfish. *Archives of Biochemistry and Biophysics*, *111*(1), 96–103. https://doi.org/10.1016/0003-9861(65)90327-9

Katwate, U., Raut, R., Khot, M., Paingankar, M., & Dahanukar, N. (2012). Molecular identification and ecology of a newly discovered population of sun catfish *Horabagrus brachysoma* from northern Western Ghats of India. *ISRN Zoology*, *2012*, 1–9. https://doi.org/10.5402/2012/419320

Kent, J., Koban, M., & Prosser, C. L. (1988). Cold-acclimation-induced protein hypertrophy in channel catfish and green sunfish. *Journal of Comparative Physiology. Part B*, *158*(2), 185–198. https://doi.org/10.1007/BF01075832

Koenekoop, L., & Åqvist, J. (2023). Principles of cold adaptation of fish lactate dehydrogenases revealed by computer simulations of the catalytic reaction. *Molecular Biology Evolution*, *40*(5), msad099. https://doi.org/10.1093/molbev/msad099

Lannig, G., Eckerle, L., Serendero, I., Sartoris, F.-J., Fischer, T., Knust, R., Johansen, T., & Pörtner, H.O. (2003). Temperature adaptation in eurythermal cod (*Gadus morhua*): A comparison of mitochondrial enzyme capacities in boreal and Arctic populations. *Marine Biology*, *142*(3), 589–599. https://doi.org/10.1007/s00227-002-0967-6

Li, Q. Q., Zhang, J., Wang, H. Y., Niu, S. F., Wu, R. X., Tang, B. G., Wang, Q. H., Liang, Z. B., & Liang, Y. S. (2023). Transcriptomic response of the liver tissue in Trachinotusovatus to acute heat stress. *Animals*, *13*(13), 2053. https://doi.org/10.3390/ani13132053

Lin, J. J., & Somero, G. N. (1995a). Thermal adaptation of cytoplasmic malate dehydrogenases of eastern Pacific barracuda (*Sphyraena*spp): The role of differential isoenzyme expression. *Journal of Experimental Biology*, *198*(2), 551–560. https://doi.org/10.1242/jeb.198.2.551

Lin, J. J., & Somero, G. N. (1995b). Temperature-dependent changes in expression of thermostable and thermolabile isozymes of cytosolic malate dehydrogenase in the eurythermal goby fish *Gillichthys mirabilis*. *Physiological Zoology*, *68*(1), 114–128. https://doi.org/10.1086/physzool.68.1.30163921

Luo, L., Zhao, Z., Zhang, R., Guo, K., Wang, S., Xu, W., & Wang, C. (2022). The effects of temperature changes on the isozyme and Hsp70 levels of the Amur sturgeon, *Acipenser schrenckii*, at two acclimation temperatures. *Aquaculture*, *551*, 737743. https://doi.org/10.1016/j.aquaculture.2021.737743

Markert, C. L., & Faulhaber, I. (1965). Lactate dehydrogenase isozyme patterns of fish. *Journal of Experimental Zoology*, *159*(3), 319–332. https://doi.org/10.1002/jez.1401590304

McCaw, B. A., Stevenson, T. J., & Lancaster, L. T. (2020). Epigenetic responses to temperature and climate. *Integrative and Comparative Biology*, *60*(6), 1469–1480. https://doi.org/10.1093/icb/icaa049

McKenzie, D. J., Zhang, Y., Eliason, E. J., Schulte, P. M., Claireaux, G., Blasco, F. R., Nati, J. J. H., & Farrell, A. P. (2021). Intraspecific variation in tolerance of warming in fishes. *Journal of Fish Biology*, *98*(6), 1536–1555. https://doi.org/10.1111/jfb.14620

Monteiro, M. D. C., Schwantes, M. L. B., Schwantes, A. R., & Silva, M. R. D. A. (1998). Thermal stability of soluble malate dehydrogenase isozymes of subtropical fish belonging to the orders Characiformes, Siluriformes and Perciformes. *Genetics and Molecular Biology*, *21*(2), 191–199. https://doi.org/10.1590/S1415-47571998000200004

Morgan, R., Andreassen, A. H., Åsheim, E. R., Finnøen, M. H., Dresler, G., Brembu, T., Loh, A., Miest, J. J., & Jutfelt, F. (2022). Reduced physiological plasticity in a fish adapted to stable temperatures. *Proceedings of the National Academy of Sciences of the United States of America*, *119*(22), e2201919119. https://doi.org/10.1073/pnas.2201919119

Murphy, R. W., Sites, J. W., Buth, D. G., & Haufler, C. H. (1990). Proteins I: isozyme electrophoresis. In D. M. Hillis & C. Moritz (Eds.), *Molecular systematics* (pp. 45–126). Sinauer Associates, Sunderland, MA.

Ozernyuk, N. D., Klyachko, O. S., & Polosukhina, E. S. (1994). Acclimation temperature affects the functional and structural properties of lactate dehydrogenase from fish (*Misgurnusfossilis*) skeletal muscles. *Comparative Biochemistry and Physiology Part B: Comparative Biochemistry*, *107*(1), 141–145. https://doi.org/10.1016/0305-0491(94)90236-4

Pasteur, N., Pasteur, G., Bonhomme, F., Catalan, J., & Britton-Davidian, J. (1988). *Practical isozyme genetics*. Ellis Horwood Ltd., Chichester, England.

Poly, W. J. (1997). Nongenetic variation, genetic-environmental interactions and altered gene expression. I. Temperature, photoperiod, diet, pH and sex-related effects. *Comparative Biochemistry and Physiology. Part A, Physiology*, *117*(1), 11–66. https://doi.org/10.1016/s0300-9629(96)00366-0

Powers, D. A., & Schulte, P. M. (1998). Evolutionary adaptations of gene structure and expression in natural populations in relation to a changing environment: A multidisciplinary approach to address the million-year saga of a small fish. *Journal of Experimental Zoology*, *282*(1–2), 71–94. https://doi.org/10.1002/(SICI)1097-010X(199809/10)282:1/2<71::AID-JEZ11>3.0.CO;2-J

Raghavan, R., Philip, S., Ali, A., Katwate, U., & Dahanukar, N. (2016). Fishery, biology, aquaculture and conservation of the threatened Asian Sun catfish. *Reviews in Fish Biology and Fisheries*, *26*(2), 169–180. https://doi.org/10.1007/s11160-016-9418-1

Rao, M. R. K., Padhi, B. K., & Khuda-Bukhsh, A. R. (1989). Lactate dehydrogenase isozymes in fifty-two species of teleostean fishes: Taxonomic significance of Ldh-C gene expression. *Biochemical Systematics and Ecology*, *17*(1), 69–76. https://doi.org/10.1016/0305-1978(89)90045-8

Schulte, P. M. (2004). Changes in gene expression as biochemical adaptations to environmental change: A tribute to Peter Hochachka. *Comparative Biochemistry and Physiology. Part B, Biochemistry and Molecular Biology*, *139*(3), 519–529. https://doi.org/10.1016/j.cbpc.2004.06.001

Schwantes, M. L. B., & Schwantes, A. R. (1982a). Adaptative features of ectothermic enzymes—I. Temperature effects on the malate dehydrogenase from a temperate fish *Leiostomusxanthurus*. *Comparative Biochemistry and Physiology Part B: Comparative Biochemistry*, *72*(1), 49–58. https://doi.org/10.1016/0305-0491(82)90009-8

Schwantes, M. L. B., & Schwantes, A. R. (1982b). Adaptative features of ectothermic enzymes—II. The effects of acclimation

temperature on the malate dehydrogenase of the spot, *Leiostomusxanthurus*. *Comparative Biochemistry and Physiology Part B: Comparative Biochemistry*, *72*(1), 59–64. https://doi.org/10.1016/0305-0491(82)90010-4

Seddon, W. L. (1997). Mechanisms of temperature acclimation in the channel catfish Ictalurus punctatus: Isozymes and quantitative changes. *Comparative Biochemistry and Physiology Part A: Physiology*, *118*(3), 813–820. https://doi.org/10.1016/S0300-9629(97)87356-2

Segal, J. A., & Crawford, D. L. (1994). LDH-B enzyme expression: The mechanisms of altered gene expression in acclimation and evolutionary adaptation. *American Journal of Physiology-Regulatory, Integrative and Comparative Physiology*, *267*(4), R1150–R1153. https://doi.org/10.1152/ajpregu.1994.267.4.R1150

Sejian, V., Bhatta, R., Gaughan, J. B., Dunshea, F. R., &Lacetera, N. (2018). Review: Adaptation of animals to heat stress. *Animal*, *12*(s2), s431–s444. https://doi.org/10.1017/S1751731118001945

Shaklee, J. B., Allendorf, F. W., Morizot, D. C., & Whitt, G. S. (1990). Gene nomenclature for protein-coding loci in fish. *Transactions of the American Fisheries Society*, *119*(1), 2–15. https://doi.org/10.1577/1548-8659(1990)119<0002:GNFPLI>2.3.CO;2

Smirnova, Y. A., Zinov'eva, R. D., & Ozernyuk, N. D. (2002). Effect of thermal acclimation on the expression of gene coding for lactate dehydrogenase A 4. In Loach Skeletal Muscle. *Biology bulletin of the Russian Academy of Sciences, 29*, 207–211.

Somero, G. N. (1973). Thermal modulation of pyruvate metabolism in the fish *Gillichthys mirabilis*: The role of lactate dehydrogenases. *Comparative Biochemistry and Physiology Part B: Comparative Biochemistry*, *44*(1), 205-206. https://doi.org/10.1016/0305-0491(73)90357-x

Somero, G. N. (2004). Adaptation of enzymes to temperature: Searching for basic "strategies".*Comparative Biochemistry and Physiology. Part B, Biochemistry and Molecular Biology*, *139*(3), 321–333. https://doi.org/10.1016/j.cbpc.2004.05.003

Somero, G. N. (1975). The role of isozymes to adaptation varying temperature. In C. L. Markert (Ed.), *Isozymes II. Physiological function* (pp. 221–234). Academic Press, New York.

Sureshkumar, S., Ranjeet, K., & Radhakrishnan, K. V. (2013). Live handling and domestication of selected indigenous ornamental fishes of India. *International Journal of Fisheries and Aquatic Studies*, *1*(5), 08–11.

Tattersall, G. J., Sinclair, B. J., Withers, P. C., Fields, P. A., Seebacher, F., Cooper, C. E., & Maloney, S. K. (2012). Coping with thermal challenges: Physiological adaptations to environmental temperatures. *Comprehensive Physiology*, *2*(3), 2151–2202. https://doi.org/10.1002/cphy.c110055

Triveni, A., & Rao, P. R. (1986). Tissue distribution and characterization of LDH isozymes in two fishes of the order Cypriniformes. *Proceedings of Indian Academy of Science: Animal Sciences*, *95*(2), 255–262. https://doi.org/10.1007/BF03179584

Volkoff, H., & Rønnestad, I. (2020). Effects of temperature on feeding and digestive processes in fish. *Temperature*, *7*(4), 307–320. https://doi.org/10.1080/23328940.2020.1765950

Vornanen, M. (1994). Seasonal adaptation of crucian carp (*Carassius carassius* L.) heart: Glycogen stores and lactate dehydrogenase activity. *Canadian Journal of Zoology*, *72*(3), 433–442. https://doi.org/10.1139/z94-061

Walker, J. M. (2002). Nondenaturing polyacrylamide gel electrophoresis of proteins. In J. M. Walker (Ed.), *The Protein Protocols Handbook* (pp. 57–60). Humana Press, Totowa, N.J.

Wilson, F. R., Champion, M. J., Whitt, G. S., & Prosser, C. L. (1975). Isozyme patterns of in tissues of temperature-acclimated fishes. In C. L. Market (Ed.), *Isozymes II, Physiological function* (pp. 193–206). Academy Press, New York.

Zakhartsev, M., Johansen, T., Pörtner, H. O., & Blust, R. (2004). Effects of temperature acclimation on lactate dehydrogenase of cod (*Gadus morhua*): Genetic, kinetic and thermodynamic aspects. *Journal of Experimental Biology*, *207*(1), 95–112. https://doi.org/10.1242/jeb.00708

Journal of Experimental Biology and Agricultural Sciences

Effect of the Nucleotide and Turmeric Extract Supplementation and different Cage Floors on the Blood Profile and Physiological Status of Broiler Chicken

Elly Tugiyanti[1*] ⓘ, Ismoyowati[1] ⓘ, Rosidi[1] ⓘ, Dadang Mulyadi Saleh[1] ⓘ,
Soegeng Heriyanto[2] ⓘ, Tri Laras Wigati[3] ⓘ

[1]Department of Animal Production, Faculty of Animal Science, Universitas Jenderal Soedirman, Banyumas 53122, Indonesia
[2]Department of Animal Production, Faculty of Animal Science, Universitas Wijayakusuma, Banyumas 53152, Indonesia
[3]Magister Program Faculty of Animal Science, Universitas Jenderal Soedirman, Banyumas 53122, Indonesia

ABSTRACT

Climate change has been responsible for the high prevalence of heat stress (HS) among broiler chickens. In this research, efforts are made to curb the negative impact of HS on chickens by modifying the feed and cage floor. The blood profile and physiological responses of broiler chickens supplemented with nucleotide and turmeric powder and kept in different floor cages were recorded (litter, slatted, and combination of slat-litter). A total of 245 broiler day-old chicks (DOC) were randomly allotted to seven treatment groups of the combined supplementation of nucleotide and turmeric extract and different types of cage floor (litter, slate, combination of slat-litter) for 35-day maintenance. Each treatment was replicated five times. The supplementation of nucleotide and turmeric extract into feed and different types of cage floor did not significantly affect (P>0.05) body temperature, respiratory rate, pulse rate, lien index, PVC, TPP, heterophils, lymphocyte, and monocyte, but significantly affected (P<0.05) the erythrocyte level, hemoglobin, leukocyte, rectal temperature and the index of bursa fabricius of broilers. Results of this study concluded that the combined treatments of supplementing nucleotide and turmeric extract in feed and using slat-floored cages tend to reduce the comfort of broiler chickens.

* Corresponding author

E-mail: ellytugiyantipurwokerto@gmail.com (Elly Tugiyanti)

1 Introduction

The recent climate change has caused prevalent heat stress (HS) among broiler chickens. Temperature above 29° C is hot for a chicken and can lead to heat stress. Heat stress (HS) occurs when the amount of heat produced by an animal surpasses its capacity to dissipate the heat to the surrounding environment. When the environmental temperature rises above the thermoneutral zone, birds typically reduce their physical activity and feed intake (FI) to limit heat production (HP), as well as increase their panting and water consumption to favour heat loss by evaporation Brugaletta et al. (2022).

In addition to causing evident changes in chicken behaviour, HS negatively acts upon metabolism and general homeostasis and impairs the functionality of the digestive system (Rostagno 2020). Birds reduce feed consumption and nutrient digestibility in a hot environment to limit metabolic heat production. High humidity makes it increasingly difficult for birds to cool themselves and evaporate water off their respiratory systems. Stress reduces feed intake and growth and impairs immune response and function, resulting in high disease susceptibility. Heat exposure causes several physiological impairments in birds, including oxidative stress, weight loss, immunosuppression, and dysregulated metabolism. Broiler chickens must live comfortably in a proper environment, known as the thermoneutral zone, with a temperature of 20-25°C and 50% humidity (Omomowo and Falayi 2021; Kpomasse et al. 2021). Indonesia has a humid tropical climate with temperatures between 28 - 38°C in the dry season and 25 - 29°C during the rainy season. Humidity during the dry season is around 40 -70%, while humidity during the rainy season is about 80 - 100%. In addition, areas that have a humid tropical climate will receive a lot of solar radiation (Mustamin et al. 2019).

In addition to heat stress, the prohibition of antibiotic growth promoters (AGP) has negatively affected the broiler industry. AGPs have been well documented as a widely used supplement to improve broilers' performance and food conversion rates because broilers are very susceptible to disease (Untari et al. 2021). AGP is offered to chickens from the age of 2-4 days to prevent infections that are responsible for broilers' poor immunity against disease, high mortality rate, slow growth rate, and declining physiological status and productivity (Manafi 2015; Ravindran and Reza Abdollahi 2021). Accordingly, there has been increasing development of natural compounds extracted from herbal plants as a source of antioxidants and as a substitute for AGP in broiler diets (Gharechopogh et al. 2021; Mnisi et al. 2022). Turmeric (*Curcuma longa*) is one of the most commonly used herbal plants, and it possesses immunomodulators, antiinflammation, and antioxidant properties (Irshad et al. 2018; Chanda and Ramachandra 2019). As a member of the Zingiberaceae family, turmeric contains an element known as curcumin. The distinctive bulb of curcumin

[1,7-bis (4-hydroxy 3- methoxyphenyl)- 1,6-heptadiene-3,5-dione; diferulylmethane] allows the plant to retain its economic value (Salah et al. 2019). The use of turmeric as a feed additive has been reported to induce positive effects on the performance and immunity of broiler chickens, even during heat stress (Al-Jaleel 2012; Sugiharto 2020; Lagua and Ampode 2021). Despite this, studies have also reported that turmeric powder supplementing produces subpar effects compared to AGP on broilers (Nagar et al. 2021).

Combining turmeric extract and nucleotide as a feed additive is expected to optimize the performance of broiler chickens. As the basic building blocks of nucleic acids (RNA and DNA), nucleotides consist of a sugar molecule (ribose in RNA or deoxyribose in DNA) bonded to a phosphate group and a nitrogen-containing base. The bases used in DNA are adenine (A), cytosine (C), guanine (G) and thymine (T). In RNA, the base uracil (U) replaces thymine. DNA and RNA molecules are polymers made up of long chains of nucleotides. Nucleotides can be synthesized in cells by de novo pathway from precursor amino acids, including glutamine, formate, glycine, and aspartic acid. Broiler chickens that experience heat stress cannot synthesize nucleotides in sufficient amounts, thus experiencing stunted cell growth, especially epithelial cells in the intestine (intestinal villi) and reduced metabolism, absorption, digestibility and performance, which all lead to less body weight (Aldiyanti et al. 2022).

Nucleotide is vital in energy metabolism, coenzyme formation, and cell defence mechanisms (Dawood et al. 2018). Previous research by Mohamed et al. (2020) has demonstrated that the supplementation of 0.1% nucleotide has improved performance and reduced *Clostridium perfringens* infection in broiler chickens. Meanwhile, 1.5% supplementation tends to boost growth and enhance the intestinal morphology of broiler chickens (Trairatapiwan et al. 2017). Furthermore, supplementing nucleotide to swine has been reported to improve immune response and the well-being of broiler chickens' digestive tracts, making nucleotide a potential alternative for AGP (Adedokun and Olojede 2019).

Tugiyanti et al. (2022) studied the effect of the combination of 0.5 g nucleotide and 0.6 g turmeric powder and reported the inability of this supplementation to significant improvement in the immune response of broiler chickens kept in battery cage, which was closely related to poultry welfare (Zhao et al. 2014; Mesa et al. 2017) The comfort of animals in the cage depends on the microclimate as well as the types of flooring inside the cage (Adler et al. 2020). Broiler farmers in Indonesia commonly use litter floor, slat floor, or slat-litter floor combinations.

Litter floor cage using husk is the most used type of floor in the broiler industry in Indonesia. Litter floor has some drawbacks,

such as poorly managed litter, which can cause respiratory disease and dermatitis on the feet and breasts (Çavuşoğlu et al. 2018). Meanwhile, keeping litter husk dry and unspoiled in the litter cage is difficult because broiler chickens drink water frequently (Petek et al. 2014). Wet litter will increase microorganism activities in fermenting organic materials, which further triggers heat release and negatively affects broilers' welfare, performance, and quality of carcass (De Jong et al. 2014; Petek et al. 2014; Saleh et al. 2021). Slatted floor systems resulted in higher body weights, reduced total feed consumption, lower feed conversion ratio, and less incidence of foot pad and hock joint deformations in broiler chickens (Eratalar 2021; Topal and Petek 2021). Although a slatted floor cage provides better air circulation, its design often makes broilers slip and bruise their feet and wings, deteriorating the carcass quality. Slatted-floor cages are mainly used in an open coop for chicken production (Heitmann et al. 2020). Considering that cage temperature is closely related to the cage floor, the production of nucleotides, and the health of digestive organs, this research aims to investigate the physiological response to heat stress of broiler chickens supplemented with nucleotide and turmeric powder and kept in different types of cage floors litter, slat, and slat-litter combination.

2 Materials and Methods

2.1 Birds and Experimental Design

A total of 245 broiler day-old chicks (DOC) were randomly allotted to seven treatment groups. Each group was replicated five times, and each cage unit contained seven DOC. The treatments were the combined supplementation of nucleotide and turmeric extract and the types of floors for poultry maintenance (litter, slat, and combination of slat-litter). The details of the formulated groups were as follows:

A: Basal feed (control) three floor types

B: Basal feed + nucleotide 0.5g/kg feed + turmeric powder 0.6g/kg feed+ litter floor

C: Basal feed + nucleotide 0.5g/kg feed + turmeric powder 0.6g/kg feed+ slatted floor

D: Basal feed + nucleotide 0.5g/kg feed + turmeric powder 0.6g/kg feed+ (slat-litter) floor combination

E: Basal feed + nucleotide 1g/kg feed + turmeric powder 1g/kg feed + litter floor

F: Basal feed + nucleotide 1g/kg feed + turmeric powder 1g/kg feed + raised cage

G: Basal feed + nucleotide 1g/kg feed + turmeric powder 1g/kg feed + (slat-litter) floor combination

2.2 Birds Diet and Husbandry

The basal diet used in this research for broiler chickens during the starter period was a commercial diet with formulation given in Table 1 containing 21% protein and 3,100 kcal/kg ME, while the basal diet at the finisher period had 19% protein and 2,900 kcal/kg ME.

Table 1 Feed formulation of the feed used in the experiment

Ingredients (%)	Starter diet (%)	Finisher diet (%)
Maize	53.6	62.5
Soya bean meal	35.6	29.2
Meat bone meal	5.0	5.0
Palm oil	3.1	1.2
Stone Grounded	0.64	0.4
Dicalcium phosphate (DCP)	0.44	0.5
Premix	1.6	1.3
Calculated Analysis		
Crude protein (%)	21	19
Crude Fibre (%)	2.57	2.6
Lysine	1.20	0.70
Methionine	0.71	0.50
Metabolizable energy (kcal/kg)	3100	2900

The nucleotides used were BioNutrend, produced by Wuhan Sunhy Biology Co. Ltd., China. The average nucleotide composition was 27.4% adenine, 22.6% guanine, 22.8% cytosine and 27.1% thymine, and the turmeric extract was Herbana brand produced by PT, Deltomed Laboratories. The broilers were maintained at 19-32°C with a 292mm precipitation rate, 95 % humidity, and 10 km/h wind velocity. Broilers were supplemented with vitamins and vaccines at their appropriate age and kept in 30 units per cage, each measuring 1.5x1.5x1 m for 35 days. Feed and water were provided *ad libitum*.

2.3 Blood Profile Measurement

The blood sample was collected to measure erythrocyte, leukocytes, and leukocyte differential using a 3-ml pipette, EDTA vacutainer, *ice pack* and *cool box*. At the end of the maintenance period, venipuncture was conducted on the wing using the pipette and the blood was put into an EDTA vacutainer and shaken to prevent blood clotting, then put into an ice box prefilled with an ice pack. The erythrocyte count was performed by drawing the blood sample using an erythrocyte pipette up to 0.5 ml/µl and incorporating Hayem's solution up to 11 ml/µl. After that, the solution was homogenized, and then some drops were put into the improved Neubauer counting chamber sealed with cover glass. The erythrocyte was counted using a microscope with 100x magnification and a hand counter. The erythrocyte differential counts were conducted by placing a drop of blood onto the counting chamber, covered with a cover glass, and counting the number of leukocytes under the microscope.

The hemoglobin concentration was evaluated by matching acid hematin solution with a standard coloured solution found in Sahl's hemoglobin meter according to the methods described by Dein (1984). The Sahli (1902) method is based on converting hemoglobin to acid haematin (brown colour) and then visually matching its colour against a solid glass standard. Diluted hydrochloric acid was mixed into a graduated cylinder with 20µl of the blood sample, and distilled water was added until the colour of the diluted blood sample matched the glass standard. The blood sample's hemoglobin level determined the dilution, as Philippe (2009) described.

2.4 Physiological Response Measurement

Body temperature was measured on the broiler's back using an infrared thermometer (Codenoll digital infrared laser thermometer). The rectal temperature was measured by inserting a digital thermometer into the broiler's rectum (Suprayogi et al. 2017) to a depth of 1/3 of the rectum until the thermometer beeped. The respiratory rate was measured by calculating the breath or looking at the broiler's chest movement within 10 seconds. The pulse frequency was obtained by placing a stethoscope onto the

broiler's left chest and counting the pulse for one minute (Hartono et al. 2002). Meanwhile, the ratio of bursa fabricius to the spleen was obtained after the broilers were sacrificed at the age of 35 days. The Bursa fabricius and spleen were weighed and divided by the broiler's body weight.

2.5 Statistical Analysis

This experimental research was conducted in a completely randomized design (CRD). All data were subjected to one-way ANOVA using the SPSS 25.00 (SPSS Ltd., Surrey, UK). Duncan's test would ensue when significant differences were observed across all variables measured at the probability of $P < 0.05$ for all treatment groups.

3 Results and Discussion

3.1 Blood profile

The effects of nucleotide, turmeric powder, and floor types on broilers' blood profile (erythrocyte, hemoglobin, PCV, Total plasma proteins, leukocytes, and leukocyte differential) are presented in Table 2. The values for the red series and hematimetric indexes were calculated for RBC (2.20 ± 0.06 - $2.93\pm0.07 \times10^6/\mu L$), PCV ($21.33\pm2.31$-$28.33\pm1.5\%$), Hb ($5.91\pm0.25$-$9.93\pm0.67$ g/dL), TPP (3.53 ± 0.12-3.80 ± 0.20fL). The values of white series were WBC (8.52 ± 1.00 - $14.25\pm3.92/\mu L$), heterophils (59.67 ± 16.80- 77.33 ± 6.43 %), monocytes (2.67 ± 1.53-4.33 ± 0.58 %), lymphocytes (16.67 ± 6.66- 31.00 ± 9.85 %). Blood profile data in this study were within the normal range (Aldiyanti et al., 2022).

Tugiyanti et al. (2022) and Aldiyanti et al. (2022) stated that blood is an essential component for the physiological regulation of the body and an indicator of poultry health. While leukocytes are part of the immune system against some infectious diseases, erythrocytes determine physiology. Leukocytes are divided into agranulocytes (lymphocytes and monocytes) and granulocytes (basophils, eosinophils, and heterophils). Lymphocytes are the most abundant leukocytes in chickens, and their size varies from small to large, as in mammals (Colin et al. 2015). According to Yuniwarti (2015), erythrocytes function in gas exchange and oxygen distribution into cells and are used by cells for metabolic processes. Oxygen is essential in producing adenosine triphosphate (ATP), the energy for cells to metabolize (Salin et al. 2015). The process of forming new erythrocytes daily requires precursors to synthesize new cells, including iron, vitamins, and amino acids, while the hormone erythropoietin regulates the cell formation process.

Supplementing nucleotide and turmeric extract to broiler chickens kept in cages with different types of floors resulted in a non-significantly different effect (P>0.05) on the erythrocyte,

Table 2 The effect of feed treatment on the blood profile of broiler chickens

Parameter	A	B	C	D	E	F	G	Sig.
Erythrocyte (10^6/µl)	2.75±0.15[c]	2.93±0.07[c]	2.77±0.23[c]	2.67±0.36[bc]	2.20±0.06[a]	2.35±0.03[ab]	2.40±0.07[ab]	0.003
HB (g/dL)	9.6±0.36[d]	8.75±0.37[c]	9.93±0.67[d]	7.87±0.64[b]	7.33±0.23[b]	5.91±0.25[a]	6.13±0.03[a]	0.006
PCV (%)	24.33±3.21	28.33±1.53	27.33±4.93	24.67±5.03	21.33±2.31	22.00±2.00	23.67±2.51	0.159
TPP (g/dL)	3.80±0.20	3.67±0.12	3.73±0.23	3.67±0.23	3.67±0.12	3.53±0.12	3.67±0.12	0.597
Leukocyte (/µl)	14.25±3.92[b]	11.70±0.11[b]	8.52±1.00[a]	14.06±4.83[b]	13.68±5.02[b]	12.73±0.04[b]	11.12±0.02[b]	0.007
Heterophils (%)	68.33±1.68	73.67±8.39	59.67±16.80	64.67±10.26	65.33±8.08	77.33±6.43	70.25±10.23	0.427
Lymphocyte (%)	19.33±8.02	30.00±8.72	31.00±9.85	23.00±10.15	28.67±10.21	16.67±6.66	21.33±10.21	0.319
Monocyte (%)	4.33±0.58	4.33±0.58	3.67±0.58	3.00±1.73	4.00±1.73	2.67±1.53	3.67±1.73	0.488

Data are mean of five replicates; ± Standard Error of mean; A: Basal Feed (control); B: nucleotide 0.5 g + turmeric powder 0.6 g + litter floor; C: nucleotide 0.5 g + turmeric powder 0.6 g + slatted floor; D: nucleotide 0.5 g + turmeric powder 0.6 g + (latted+litter) floor combination; E: nucleotide 1 g + turmeric powder 1 g + litter floor; F: nucleotide 1 g + turmeric powder 1 g + slatted floor; G: nucleotide 1 g + turmeric powder 1 g + (slat-litter) floor combination; Values without common superscripts letters in row differ significantly at LSD P<0.05

hemoglobin, and PCV levels, as presented in Table 2. Turmeric extract helps the nucleotide trigger the hypothalamus for inhibiting heat stress, facilitating the erythropoiesis process and preventing the delay of hemoglobin synthesis (Sugiharto et al. 2011). According to Hafez et al. (2022), the antioxidant properties of curcumin reduce free radicals and improve immune performance and haematology. The red blood cell count in the present research was 2.20 and 2.35 x10^6/dl in the E and F groups, respectively, but the hemoglobin level was slightly under 10.26-10.71 g/dL as reported by Daudu et al. (2020). Meanwhile, Ifelayo et al. 2020) reported PCV slightly lower than 30.83-32.33%.

Supplementing nucleotide and turmeric extract to broiler chickens kept in cages with different types of floors resulted in a non-significant difference (P>0.05) in the levels of erythrocyte, hemoglobin, and PCV (Table 2). Different types of cage floors generate different temperatures inside the cage, but this did not affect broiler chickens' levels of erythrocyte, hemoglobin and PCV. Turmeric extract helps the nucleotide trigger the hypothalamus for inhibiting heat stress, using the erythropoiesis process and preventing declining hemoglobin synthesis (Zhang et al. 2015; Balakrishnan et al. 2023). According to Hafez et al. (2022) curcumin's antioxidant properties reduce free radicals and improvchickens' immune performance and haematology. The red blood cell count in the present research was 2.42-2.84 x10^6/dl, but the hemoglobin level was slightly under 10.26-10.71 g/dL, as Daudu et al. (2020) reported. Meanwhile, Kafi et al. (2017) reported PCV slightly lower than 31.50-32.50%.

Total protein plasma (TPP), leukocytes, and leukocyte differential (lymphocyte and monocyte) are important indicators in broiler chickens to evaluate their health status and protein metabolism regarding the activities of some body organs like the liver and kidneys. The phagocytosis process by leukocytes will protect the body from diseases (Rosales and Uribe-Querol 2017). The total plasma protein and leukocyte levels in broiler chickens depend on some conditions, including stress, physiological activities, nutrition, and age. Previous study reported the range of total plasma protein (TPP) was 4.17±0.05-4.27±0.05 g/dL (Ifelayo et al. 2020), leukocytes was 11.18-14,78 x10^9/L (Makeri et al. 2017), leukocyte differential (lymphocyte) was 58.00±4.80-71.00-6.60%, and monocyte was 5.25± 1.50-7.75-3.90% (Aldiyanti et al. 2022). In this research, TPP, leukocytes and leukocyte differential were not significantly different (P>0,05) from these studies. The absence of increasing TPP or declining leukocytes and leukocytes differential and non-existent variation in temperature across different types of cage floor demonstrated that broiler chickens were healthy and not suffering from bacterial infection (Salam et al. 2013; Saputro et al. 2013). Different cage temperatures because of different types of floor did not cause protein aggregation and imbalance in the overall protein homeostasis in the cells.

3.2 Physiological Status

The thermal comfort (TC) zone for chickens is characterized by a range of environmental temperatures within which chickens have minimal and nearly constant energy expenditure for maintaining body temperature (Chang et al. 2018). The thermoregulatory system adjusts physiological responses to increase or decrease body heat loss. Outside of the TC zone is a situation characterized by heat or cold stress where birds adjust their metabolism to compensate for their energy balance (Liu et al. 2021; Belkhanchi et al. 2023).

Body temperature and rectal temperature are the indicators of comfort in broiler chickens. According to Skomorucha and

Sosnówka-Czajka (2017), chickens' average body and rectal temperature is 41-42°C and 41.4-41.9°C, respectively. In this study, broiler chickens' body and rectal temperatures were lower than those of previous studies (Table 3). Moe et al. (2017) stated that chickens' body temperature would drop by 2°C after one-minute handling. Furthermore, the results of the analysis of variance of this study showed that supplementing nucleotide and turmeric extract into feed and different types of floor used in chicken cages did not significantly affect (P>0,05) the body temperature but had a significant effect (P<0,05) on the rectal temperature of broiler chickens. This is because rectal temperatures are considered the peripheral temperature, the most similar to the core body temperature, which is easily affected by the environmental temperature. This study recorded the temperature of the litter floor was 28.9-30.3°C, the slatted floor was 27.8-30.2°C, and the combined slat-litter floor was 28.7-30.2°C. The litter floor, slatted floor, and the combination of slat-litter floor combination resulted in different microclimate temperatures inside the cage (Li et al. 2017). When the environmental temperature is high, the rectal temperature will increase. In other words, rectal temperature manifests a thermoregulation mechanism in chickens to balance the generated heat and emitted heat to maintain the ideal body temperature. In addition, the supplementation of nucleotide and turmeric extract can improve the performance of digestive tracts and help support the proper functions of the thermoregulation system and physiological response in broiler chickens (Taylor et al. 2014; Trairatapiwan et al. 2017). To maintain the ideal body temperature, chickens either increase or decrease heat loss (Taylor et al. 2014).

The thermoregulation system in broiler chickens is related to the molecular functions of broiler chickens' hormone and nerve system(Ruuskanen et al. 2021). Thyroid hormones (THs, triiodothyronine, T3 and thyroxine, T4) are the most important hormones in regulating thermogenesis (Sawicka-Gutaj et al.

(2022). Chickens that suffer from heat stress will experience a declining synthesis of nucleotide that results in low production and release of thyroid hormones; consequently, chickens have a high body temperature (Bruno et al. 2011; Balakrishnan et al. 2023). The supplementation of nucleotide and turmeric extract would improve the comfort of broiler chickens. Broiler chickens living within the comfortable thermal zone have a constant heat production and balanced heat loss to maintain the ideal body temperature (Chang et al. 2018).

In addition to body and rectal temperatures, panting is a commonly used physiological response by a distressed chicken (Iftitah et al. 2022). When a broiler chicken is panting, it will draw heavy and rapid breaths with an open mouth, which causes water loss through evaporation that will help limit heat stress due to high temperature or vigorous physical activities (Kang et al. 2020). Respiratory rate (RR) and pulse rate (PR) are the physiological responses that can be utilized to evaluate the impact of the thermal environment on the thermoregulation status in broiler chickens. RR and PR in this study were within the normal range (Table 3.), which, as reported in the previous study, was 19.90 breath/minute, and the pulse rate was 67.41 ± 7.22 beats/min (Ijadunola et al. 2020; Bello et al. 2022). The analysis of variance showed that the supplementation of nucleotide and turmeric extract into feed and the use of different types of cage floor did not significantly affect (P>0,05) RR and PR. It demonstrated that both supplementation and different floors successfully inhibited heat stress in broiler chickens, so RR and PR did not increase and were relatively similar across treatments. The constant RR and PR showed that broiler chickens' thermoregulation system (Hypothalamus, hypophyses, autonomic nervous system) usually functions (Nawaz et al. 2021).

The lymphatic organs in poultry's immune system consist of the primary and secondary lymphoids. Bursa fabricius is the primary organ, and the spleen is the secondary lymphatic organ (Toivanen

Table 3 The effect of treatments on the physiological status and percentage of bursa fabricius and spleen

Parameter	Feed treatment							Sig.
	A	B	C	D	E	F	G	
Body temperature	37.49±1.18	38.05±0.53	38.25±1.28	37.80±1.58	36.85±1.36	38.02±0.99	37.78±1.28	0.618
Rectal temperature	40.75±0.86[b]	39.80±0.15[a]	39.98±0.18[a]	40.28±0.38[ab]	40.01±0.12[a]	39.98±0.14[a]	40.06±0.03[a]	0.047
Respiratory rate (times/minute)	27.25±3.93	28.40±2.86	27.45±3.64	28.30±4.24	26.50±4.33	28.40±3.42	27.80±3.00	0.062
Pulse (times/minute)	69.75±4.27	69.48±4.06	70.04±7.65	84.95±11.44	70.78±7.93	73.69±8.84	72.45±6.89	0.074
%Bursa Fabrisius	2.26±0.02[a]	2.36±0.04[bc]	2.38±0.03[c]	2.39±0.03[c]	2.33±0.02[b]	2.38±0.03[c]	2.34±0.03[b]	0.000
%Spleen	0.15±0.04	0.11±0.02	0.15±0.01	0.14±0.02	0.14±0.01	0.13±0.01	0.14±0.01	0.083

Data are mean of five replicates; ± Standard Error of mean; A : basal feed (control); B: nucleotide 0.5 g + turmeric powder 0.6 g + litter floor; C: nucleotide 0.5 g + turmeric powder 0.6 g + slatted floor; D: nucleotide 0.5 g + turmeric powder 0.6 g + (latted+litter) floor combination; E: nucleotide 1 g + turmeric powder 1 g + litter floor; F: nucleotide 1 g + turmeric powder 1 g + slatted floor; G: nucleotide 1 g + turmeric powder 1 g + (slat-litter) floor combination.

1998; Berthault et al. 2018). The index of bursa fabricius (BFI) and lien index (LI) of broiler chickens in this study were 2.26-2.39% and 0.11±-0.15% (Table 3). BFI and LI in this study were higher than those of Hakim et al. (2021), reporting that BFI and LI in broiler chickens supplemented with nucleotide were only 0.044-0.047% and 0.112-0.146%, respectively. The result of the analysis of variance showed that the supplementation of nucleotide and turmeric extract and different types of floors did not significantly affect (P>0,05) LI, but this combination significantly affected (P<0,05) the BFI of broiler chickens. This is because the average temperatures of the litter floor, slatted floor, and slat-litter floor combination were different, impacting the index of bursa fabricius differently (Kusnadi 2009). These results follow the findings of Hirakawa et al. (2020) that high environmental temperature can cause the weight loss of several lymphatic organs such as bursa fabricius, spleen, and thymus, and therefore, less lymphocyte production. The average temperature of litter floor cage in the morning, afternoon and night was 23.98±2.38℃, 31.8±3.47℃, and 21.84±1.23℃ respectively. While the average temperature of the slatted floor in the morning, afternoon, and night was 22.98±2.81℃, 30.14±2.88℃, and 20.32±1.67℃, respectively, the slat-litter floor was 22.76±1.94℃, 30.3±2.32℃, and 21.03±2.68℃, respectively. The excessive reactive oxygen species (ROS) resulting from heat stress (HS) has imposed unwanted effects on the immune balance of organs immune systems (Hirakawa et al. 2020; Liu et al. 2021). Bursa Fabricius is the central organ of the immune system in broiler chickens that can produce lymphocyte B and antibodies specific to complete the immune-specific response and play important roles in maintaining the immune system of poultry (Liu et al. 2021). Nucleotide and turmeric extract keep the BFI high, thus producing a high level of lymphocytes. As a result, the antibody produced by the lymphocyte (like gamma globulin) is relatively high. Curcumin inhibits the dysfunction of liver mitochondria and damaged mtDNA and stimulates the thioredoxin mitochondria system in broiler chickens, which undergo heat stress (Zhang et al. 2018).

The spleen is the biggest peripheral lymphatic organ in chickens, which play an important role in the antibacterial and antiviral immune response against antigen obtained by the chickens. The development of peripheral lymphatic organs is closely related to maintaining immune function (Liao and Padera 2013; Zhang et al. 2019). The effects of the treatment were not different on LI because the chickens were in healthy conditions during the observation. The role of the spleen in the defence system is related to the immunology response against antigen that can reach blood circulation to defend against the invasion of organisms or toxins before they spread. Furthermore, the spleen is the organ where antibody-producing cells are maturing. In addition to being a defence system against microorganisms, the spleen is the central location where macrophage degrades old erythrocyte cells and

reacts against the antigens carried in the bloodstream while performing immunological filtration to blood (Lewis et al. 2019).

Conclusions

The supplementation of nucleotide and turmeric extract into feed, and different types of cage floor did not significantly affect (P>0.05) body temperature, respiratory rate, pulse rate, lien index, PVC, TPP, and heterophils, lymphocyte, monocyte, but significantly affected (P<0.05) erythrocyte level, hemoglobin, leukocyte, the rectal temperature and the index of bursa fabricius of broilers. The combined supplementation of nucleotide and turmeric extract in feed and the types of cage floor tend to reduce the comfort of broiler chickens.

Author contributions

ET, I., and R. contributed to designing the research model data analysis and wrote the paper. D. M. S., S. H. and T. L. W. contributed to enrich the discussion.

Conflict of interest

The authors state no conflict of interest.

Data availability statement

The data sets generated during the current study are available from the corresponding author on reasonable request

References

Adedokun, S. A., & Olojede, O. C. (2019). Optimizing gastrointestinal integrity in poultry: The role of nutrients and feed additives. *Frontiers in Veterinary Science, 5*, (348), 1-11. https://doi.org/10.3389/fvets.2018.00348

Adler, C., Tiemann, I., Hillemacher, S., Schmithausen, A. J., Müller, U., Heitmann, S., Spindler, B., Kemper, N., & Büscher, W. (2020). Effects of a partially perforated flooring system on animal-based welfare indicators in broiler housing. *Poultry Science*, *99*(7), 3343–3354. https://doi.org/10.1016/j.psj.2020.04.008

Aldiyanti, A., Tugiyanti, E., & Hartoyo, B. (2022). Blood profile and carcass production of broiler chickens given nucleotides and

turmeric extract in feed. *Buletin Peternakan*, *46*(4), 235-242. https://doi.org/10.21059/buletinpeternak.v46i4.76789

Al-Jaleel, R. A. A. (2012). Use of turmeric (*Curcuma longa*) on the performance and some physiological traits on the broiler diets. *The Iraqi Journal of Veterinary Medicine, 36*(1)*, 51-57.*

Balakrishnan, K. N., Ramiah, S. K., & Zulkifli, I. (2023). Heat shock protein response to stress in poultry: A Review. *Animals*, *13*(2), 317. https://doi.org/10.3390/ani13020317

Belkhanchi, H., Younes, Z., Maryama, H., & Ousama I. (2023). Formulation, optimization of a poultry feed and analysis of spectrometry, biochemical composition and energy facts.*South African Journal of Chemical Engineering*, *44*(1), 31-41. https://doi.org/10.1016/j.sajce.2023.01.005

Bello, K., Irekhore, O., Adeitan, O., Yusuf, A., & Bada, B. (2022). Physiological response, haematology and stress condition of scavenging chickens in cement production areas. *Journal of Applied Animal Welfare Science*, 1–12. https://doi.org/10.1080/10888705.2021.2021531

Berthault, C., Larcher, T., Härtle, S., Vautherot, J. F., Trapp-Fragnet, L., & Denesvre, C. (2018). Atrophy of primary lymphoid organs induced by Marek's disease virus during early infection is associated with increased apoptosis, inhibition of cell proliferation and a severe B-lymphopenia. *Veterinary Research*, *49*(1), 1-18. https://doi.org/10.1186/s13567-018-0526-x

Brugaletta, G., Teyssier, J. R., Rochell, S. J., Dridi, S., & Sirri, F. (2022). A review of heat stress in chickens. Part I: Insights into physiology and gut health. *Frontiers in physiology*, *13*, 934381. https://doi.org/10.3389/fphys.2022.934381.

Bruno, A. N., Carneiro-Ramos, M. S., Buffon, A., Pochmann, D., Ricachenevsky, F. K., Barreto-Chaves, M. L. M., & Sarkis, J. J. F. (2011). Thyroid hormones alter the adenine nucleotide hydrolysis in adult rat blood serum. *BioFactors*, *37*(1), 40–45. https://doi.org/10.1002/biof.133

Çavuşoğlu, E., Petek, M., Abdourhamane, I. M., Akkoc, A., & Topal, E. (2018). Effects of different floor housing systems on the welfare of fast-growing broilers with an extended fattening period. *Archives Animal Breeding*, *61*(1), 9–16. https://doi.org/10.5194/aab-61-9-2018

Chanda, S., & Ramachandra, T. V. (2019). *Phytochemical and Pharmacological Importance of Turmeric (Curcuma longa): A Review*. *A Journal of Pharmacology*, *9*(1), 16–23.

Chang, Y., Wang, X.J., Feng, J.H., Zhang, M.H., Diao, H.J., Zhang, S.S., Peng, Q.Q., Zhou, Y., Li, M., & Li, X. (2018). Real-time variations in body temperature of laying hens with increasing ambient temperature at different relative humidity levels. *Poultry Science*, *97*(9), 3119–3125. https://doi.org/10.3382/ps/pey184

Colin, P.Y., Kintses, B., Gielen, F., Miton, C.M., Fischer, G., et al. (2015). Ultrahigh-throughput discovery of promiscuous enzymes by picodroplet functional metagenomics. *Nature communications*, *6*(1), 10008.

Daudu, O. M., Kpachi, J., Clement, N. J., Odegbile, O. E., Salihu, E. A., & Ademu, L. A. (2020). Thermoregulatory, growth and blood indices of broiler chicks fed betaine hydrochloride supplemented diets under high ambient temperature Nigerian Society for Animal Production Nigerian Journal of Animal Production. *Nigerian Journal of Animal Production*, *47*(4), 58–63.

Dawood, M. A. O., Koshio, S., & Esteban, M. Á. (2018). Beneficial roles of feed additives as immunostimulants in aquaculture: a review. *Reviews in Aquaculture, 10*(4), 950–974.https://doi.org/10.1111/raq.12209

Dein, F. (1984). *Laboratory Manual of Avian Hematology*. Association of Avian Veterinarian, East North Port, USA

De Jong, I. C., Gunnink, H., & Van Harn, J. (2014). Wet litter not only induces footpad dermatitis but also reduces overall welfare, technical performance, and carcass yield in broiler chickens. *Journal of Applied Poultry Research*, *23*(1), 51–58. https://doi.org/10.3382/japr.2013-00803

Eratalar, S.A. (2021). The effects of plastic slatted floor and a deep- litter system on the growth performance of hybrid Pekin ducks. *Archives Animal Breeding, 64(1), 1-6.* https://doi: 10.5194/aab-64-1-2021.

Gharechopogh, A. M., Fakhraei, J., Hosseini, S. A., Yarahmadi, H. M., & Lotfollahian, H. (2021). Performance, immune responses, and blood biochemistry of broiler chickens fed with plant growth compound. *Tropical Animal Science Journal*, *44*(1), 62–70. https://doi.org/10.5398/tasj.2021.44.1.62

Sawicka-Gutaj, N., Gruszczyński, D., Zawalna, N., Nijakowski, K., et al. (2022). Microbiota alterations in patients with autoimmune thyroid diseases: A systematic review. *International Journal of Molecular Sciences*, *23*(21), 13450. https://doi.org/10.3390/ijms232113450

Hafez, M. H., El-Kazaz, S. E., Alharthi, B., Ghamry, H. I., Alshehri, M. A., Sayed, S., Shukry, M., & El-Sayed, Y. S. (2022). The Impact of Curcumin on Growth Performance, Growth-Related Gene Expression, Oxidative Stress, and Immunological Biomarkers in Broiler Chickens at Different Stocking Densities.

Animals : an open access journal from MDPI, *12*(8), 958. https://doi.org/10.3390/ani12080958

Hakim, R. L., Mahfudz, L. D., & Muryani, R. (2021). Penambahan nukleotida pada ransum broiler yang dipelihara pada suhu lingkungan berbeda terhadap performa organ imunitas. *Jurnal Sain Peternakan Indonesia*, *16*(2), 164–170. https://doi.org/10.31186/jspi.id.16.2.164-170

Hartono, M., Suharyati, S., & Santosa, P. E. (2002). *Dasar fisiologi ternak*. Fakultas Pertanian, Universitas Lampung.

Heitmann, S., Stracke, J., Adler, C., Ahmed, M. F. E., Schulz, J., Büscher, W., Kemper, N., & Spindler, B. (2020). Effects of a slatted floor on bacteria and physical parameters in litter in broiler houses. *Veterinary and Animal Science*, *9*, 100115 https://doi.org/10.1016/j.vas.2020.100115

Hirakawa, R., Nurjanah, S., Furukawa, K., Murai, A., Kikusato, M., Nochi, T., & Toyomizu, M. (2020). Heat stress causes immune abnormalities via massive damage to effect proliferation and differentiation of lymphocytes in broiler chickens. *Frontiers in Veterinary Science*, *7(46),1-13*. https://doi.org/10.3389/fvets.2020.00046

Ifelayo, I. I., Onize, I. H., Faith, U., & Wodi, S. M. (2020). Haematology and serum biochemistry of broiler strains (Cobbs and Arbor-acre) fed ginger (*Zingiber officinale*). *GSC Biological and Pharmaceutical Sciences*, *11*(2), 320–326. https://doi.org/10.30574/gscbps.2020.11.2.0145

Iftitah, D., Arisandi, B., Widyani, R. R. R., & Juniah, J. (2022). Physiological Conditions of Broiler Chickens During Transportation with Vitamin Treatment and Distance Difference. *JurnalIlmu-Ilmu Peternakan*, *32*(3), 313–327. https://doi.org/10.21776/ub.jiip.2022.032.03.02

Ijadunola, T. I., Popoola, M. A., Bolarinwa, M. O., Ayangbola, K. A., & Omole, C. A. (2020). Effects of supplemental Vitamins E and C on growth performance and physiological responses of broiler chicken under environmental heat stress. *Nigerian Journal Animal Science*, *22*(3), 17–25. https://doi.org/10.1080/13625187.2020.1774537

Irshad, S., Muazzam, A., Larke, M., & Dalrymple, B. (2018). *Curcuma longa* (Turmeric): An auspicious spice for antibacterial, phytochemical and antioxidant activities. *Pakistan Journal of Pharmaceutical Sciences*, *31*(6), 2689–2696.

Kafi, A., Uddin, M. N., Uddin, M. J., Khan, M. M. H., & Haque, E. (2017). Effect of dietary supplementation of turmeric (*Curcuma longa*), ginger (*Zingiber officinale*) and their combination as feed additives on feed intake, growth performance and economics of

broiler. *International Journal of Poultry Science*, *16*(7), 257–265. https://doi.org/10.3923/ijps.2017.257.265

Kang, S., Kim, D. H., Lee, S., Lee, T., Lee, K. W., Chang, H. H., Moon, B., Ayasan, T., & Choi, Y. H. (2020). An acute, rather than progressive, increase in temperature-humidity index has severe effects on mortality in laying hens. *Frontiers in Veterinary Science*, *7, (2020),* 568093.doi.org/10.3389/fvets.2020.568093

Kpomasse, C.C., Oke, O.E., Houndonougbo, F.M., & Tona, K.(2021). Broiler production challenges in the tropics: A review. *Veterinary Medicine and Science, 7, 831–842*. https://doi.org/10.1002/vms3.435.

Kusnadi, E. (2009). Perubahan malonaldehida hati, bobot relatif bursa fabricius dan rasio heterofil/limfosit (h/l) ayam broiler yang diberi cekaman panas. *Media Peternakan*, *32*(2), 81–87.

Lagua, E. B., & Ampode, K. M. B. (2021). Turmeric powder: Potential alternative to antibiotics in broiler chicken diets. *Journal of Animal Health and Production*, *9*(3), 243–253. https://doi.org/10.17582/journal.jahp/2021/9.3.243.253

Lewis, S. M., Williams, A., & Eisenbarth, S. C. (2019). Structure and function of the immune system in the spleen. *Science Immunology*, *33*(4), 1–12. https://doi.org/10.1126/sciimmunol.aau6085

Li, H., Wen, X., Alphin, R., Zhu, Z., & Zhou, Z. (2017). Effects of two different broiler flooring systems on production performances, welfare, and environment under commercial production conditions. *Poultry Science*, *96*(5), 1108–1119. https://doi.org/10.3382/ps/pew440

Liao, S., & Padera, T. P. (2013). Lymphatic function and immune regulation in health and disease. *Lymphatic Research and Biology*, *11*(3), 136–143. https://doi.org/10.1089/lrb.2013.0012

Liu, W. C., Ou, B. H., Liang, Z. L., Zhang, R., & Zhao, Z. H. (2021). Algae-derived polysaccharides supplementation ameliorates heat stress-induced impairment of bursa of Fabricius via modulating NF-κB signaling pathway in broilers. *Poultry Science*, *100*(8). https://doi.org/10.1016/j.psj.2021.101139

Makeri, H. K., Ayo, J. O., Aluwong, T., & Minka, N. S. (2017). Daily rhythms of blood parameters in broiler chickens reared under tropical climate conditions. *Journal of Circadian Rhythms*, *15*(1), 1-8. https://doi.org/10.5334/jcr.151

Manafi, M. (2015). Comparison study of a natural non-antibiotic growth promoter and a commercial probiotic on growth performance, immune response and biochemical parameters of broiler chicks. *Journal of Poultry Science*, *52*(4), 274–281. https://doi.org/10.2141/jpsa.0150027

Mesa, D., Muniz, E., Souza, A., & Geffroy, B. (2017). Broiler-housing conditions affect the performance. *Revista Brasileira de Ciencia Avicola*, *19*(2), 263–272. https://doi.org/10.1590/1806-9061-2016-0346

Mnisi, C.M., Mlambo, V., Gila, A., Matabane, A.N., Mthiyane, D.M.N., et al. (2022). Antioxidant and antimicrobial properties of selected phytogenics for sustainable poultry production. *Applied Sciences, 13*(1), 1-17. https://doi.org/10.3390/app13010099

Moe, R. O., Bohlin, J., Flø, A., Vasdal, G., & Stubsjøen, S. M. (2017). Hot chicks, cold feet. *Physiology and Behavior*, *179*, 42–48. https://doi.org/10.1016/j.physbeh.2017.05.025

Mohamed, F. F., Hady, M. M., Kamel, N. F., & Ragaa, N. M. (2020). The impact of exogenous dietary nucleotides in ameliorating *Clostridium perfringens* infection and improving intestinal barriers gene expression in broiler chicken. *Veterinary and Animal Science*, *10*, 1-9. https://doi.org/10.1016/j.vas.2020.100130

Mustamin, T., Rahim, R., Baharuddin, & Mulyadi, R. (2019). Air temperature and humidity outdoor analysis of buildings in panakukang makassar. *IOP Conference Series: Materials Science and Engineering*, *620* (2019), 1-8. https://doi.org/10.1088/1757-899X/620/1/012104

Nagar, M. K., Shende, K., Dhuria, R. K., Manzer, H., & Surendra, S. (2021). Effect of turmeric (*curcuma longa*) powder and synbiotic as alternative to antibiotic growth promoter on the growth performance and mortality of broiler chicks. *Journal of Animal Research*, *11*(1), 167–172. https://doi.org/10.30954/2277-940x.01.2021.22

Nawaz, A. H., Amoah, K., Leng, Q. Y., Zheng, J. H., Zhang, W. L., & Zhang, L. (2021). Poultry response to heat stress: Its physiological, metabolic, and genetic implications on meat production and quality including strategies to improve broiler production in a warming world. *Frontiers in Veterinary Science, 8*, 699081. https://doi.org/10.3389/fvets.2021.699081

Omomowo, O. O., & Falayi, F. R. (2021). Temperature-humidity index and thermal comfort of broilers in humid tropics. *Agricultural Engineering International: CIGR Journal*, *23* (3), 101-110.

Petek, M., Üstüner, H., & Yeşilbağ, D. (2014). Effects of stocking density and litter type on litter quality and growth performance of broiler chicken. *Kafkas Universitesi Veteriner Fakultesi Dergisi*, *20*(5), 743–748. https://doi.org/10.9775/kvfd.2014.11016

Philippe (2009). *Clinical and biomedical sciences of tropical diseases*. Stichting van Openbaar Nut., 2: 701

Ravindran, V., & Reza Abdollahi, M. (2021). Nutrition and digestive physiology of the broiler chick: State of the art and outlook. *Animals, 11* (10), 2795. https://doi.org/10.3390/ani11102795

Rosales, C., & Uribe-Querol, E. (2017). Phagocytosis: A Fundamental Process in Immunity. In *BioMed Research International, 2017, 18*, https://doi.org/10.1155/2017/9042851

Ruuskanen, S., Hsu, B. Y., & Nord, A. (2021). Endocrinology of thermoregulation in birds in a changing climate. *Molecular and Cellular Endocrinology*, *519*, 111088. https://doi.org/10.1016/j.mce.2020.111088

Rostagno, M. H. (2020). Effects of heat stress on the gut health of poultry. *Journal of Animal Science*, *98*(4), 1-41.https://doi.org/10.1093/jas/skaa090

Sahli, H. (1902). *Lehrbuch der klinischen untersuchungs-methoden*. Leipzig, Wien, Franz Deuticke.

Salah A.S., Mahmoud M.A., Ahmed-Farid O.A., & El-Tarabany M.S. (2019). Effects of dietary curcumin and acetylsalicylic acid supplements on performance, muscle amino acid and fatty acid profiles, antioxidant biomarkers and blood chemistry of heat-stressed broiler chickens. *Journal of Thermal Biology, 84*, 259–265. doi: 10.1016/j.jtherbio.2019.07.002.

Salam, S., Sunarti, D., & Isroli, I. (2013). Physiological responses of blood and immune organs of broiler chicken fed dietary black cumin powder (*nigella sativa*) during dry seasons. *Journal of the Indonesian Tropical Animal Agriculture*, *38*(3), 185–191. https://doi.org/https://doi.org/10.14710/jitaa.38.3.185-191

Saleh, A. A., Shukry, M., Farrag, F., Soliman, M. M., & Abdel-Moneim, A. M. E. (2021). Effect of feeding wet feed or wet feed fermented by bacillus licheniformis on growth performance, histopathology and growth and lipid metabolism marker genes in broiler chickens. *Animals*, *11*(1), 1–14. https://doi.org/10.3390/ani11010083

Salin, K., Auer, S. K., Rey, B., Selman, C., & Metcalfe, N. B. (2015). Variation in the link between oxygen consumption and ATP production, and its relevance for animal performance. *Proceedings of the Royal Society B: Biological Sciences*, *282*(1812), 20151028.

Saputro, B., Santosa, P. E., & Kurtini, T. (2013). Pengaruh cara pemberianv aksin nd live pada broiler terhadap titer antibodi, jumlah sel darah merah dan sel darah putih. *Jurnal Ilmiah Peternakan Terpadu*, *2*(3), 43–48.

Skomorucha, I., & Sosnówka-Czajka, E. (2017). Physiological parameters in broiler chickens reared under different housing

systems during a period of high temperatures. *Acta Scientiarum Polonorum Zootechnica*, *16*(3), 25–34. https://doi.org/10.21005/asp.2017.16.3.04

Sugiharto, S. (2020). Alleviation of heat stress in broiler chicken using turmeric (*Curcuma longa*) - a short review. *Journal of Animal Behaviour and Biometeorology, 8* (3), 215–222. https://doi.org/10.31893/JABB.20028

Sugiharto, S., Isroli, I., Widiastuti, E., & Prabowo, N. S. (2011). Effect of turmeric extract on blood parameters, feed efficiency and abdominal fat content in broilers. *Journal of the Indonesian Tropical Animal Agriculture*, *36*(1), 21–26. https://doi.org/https://doi.org/10.14710/jitaa.36.1.21-26

Suprayogi, A., Alaydrussani, G., & Ruhyana, A. Y. (2017). Rate, respiration rate, and body temperature values of lactating dairy cattle in pangalengan. *Jurnal Ilmu Pertanian Indonesia*, *22*(2), 127–132. https://doi.org/10.18343/jipi.22.2.127

Taylor, N. A. S., Tipton, M. J., & Kenny, G. P. (2014). Considerations for the measurement of core, skin and mean body temperatures. *Journal of Thermal Biology, 46*, 72–101. https://doi.org/10.1016/j.jtherbio.2014.10.006

Toivanen, P. (1998). Bursa of Fabricius. In P. J. Delves (Ed.), *Encyclopedia of Immunology (Second Edition)* (pp. 393–396). Elsevier. https://doi.org/https:/doi.org/10.1006/rwei.1999.0105

Topal, E. & Petek, M. (2021) Effects of fully or partially slatted flooring designs on the performance, welfare and carcass characteristics of broiler chickens, *British Poultry Science, 62(6), 804-809.* https://doi.org/10.1080/00071668.2021.1934399

Trairatapiwan, T., Lertpatarakomol, R., Jaipeng, P., & Paditporn, K. (2017). Effect of nucleotides supplementation on growth performance, humoral immunity, and intestinal morphological structure of broiler chickens. *Journal of Mahanakorn Veterinary Medicine*, *12*(1), 1–10.

Tugiyanti, E., Susanti, E., Ismoyowati, I., & Rosidi, R. (2022). Effect of nucleotides and turmeric extract on blood protein and body weight of broiler kept in open cages. *IOP Conference Series: Earth and Environmental Science*, *1001*(2022), 012005. https://doi.org/10.1088/1755-1315/1001/1/012005

Yuniwarti, E. Y. W. (2015). Profil darah ayam broiler setelah vaksinasi AI dan pemberian berbagai kadar VCO. *ANATOMI FISIOLOGI*, *23*(1), 38-46.

Untari, T., Herawati, O., Anggita, M., Asmara, W., Wahyuni, A. E. T. H., & Wibowo, M. H. (2021). The effect of Antibiotic Growth Promoters (AGP) on antibiotic resistance and the digestive system of Broiler Chicken in Sleman, Yogyakarta. In *BIO Web of Conferences* (Vol. 33, p. 04005). EDP Sciences.

Zhang, J., Bai, K. W., He, J., Niu, Y., Lu, Y., Zhang, L., & Wang, T. (2018). Curcumin attenuates hepatic mitochondrial dysfunction through the maintenance of thiol pool, inhibition of mtDNA damage, and stimulation of the mitochondrial thioredoxin system in heat-stressed broilers. *Journal of Animal Science*, *96*(3), 867–879. https://doi.org/10.1093/jas/sky009

Zhang, J. F., Hu, Z. P., Lu, C. H., Yang, M. X., Zhang, L. L., & Wang, T. (2015). Dietary curcumin supplementation protects against heat-stress-impaired growth performance of broilers possibly through a mitochondrial pathway. *Journal of Animal Science*, *93*(4), 1656–1665. https://doi.org/10.2527/jas.2014-8244

Zhang, Q., Sun, X., Wang, T., Chen, B., Huang, Y., Chen, H., & Chen, Q. (2019). The postembryonic development of the immunological barrier in the chicken spleens. *Journal of Immunology Research*, *4*,1-10. https://doi.org/10.1155/2019/6279360

Zhao, Z. G., Li, J. H., Li, X., & Bao, J. (2014). Effects of housing systems on behaviour, performance and welfare of fast-growing broilers. *Asian-Australasian Journal of Animal Sciences*, *27*(1), 140–146. https://doi.org/10.5713/ajas.2013.13167

CrossMark
click for updates

Journal of Experimental Biology and Agricultural Sciences

Length-Weight Relationship and Condition Factor of *Oreochromis niloticus* (Linnaeus, 1758) in Selected Tropical Reservoirs of Ekiti State, Southwest Nigeria

Olagbemide P. T.[1, 2*] iD, Owolabi O. D.[2]

[1]Department of Biological Sciences, AfeBabalola University, Ado-Ekiti, Nigeria
[2]Department of Zoology, University of Ilorin, Ilorin; Nigeria

ABSTRACT

In Ekiti State, southwest Nigeria, *Oreochromis niloticus* is significant to live. This investigation was conducted to improve its sustainable management and access the length-weight relationship and condition factor of *O. niloticus* across important reservoirs in Ekiti State from November 2017 to October 2019. Collected specimens were weighed to the nearest gram, while the entire lengths were measured to the closest centimetre. Log-transformed regression was used to determine the fish's growth pattern in the reservoirs. The gradient comparison was done using the T-test. The length and weight of the species in the reservoirs showed a significant association. All length-weight relationships had r^2 values greater than 0.8150 and were significant at $P < 0.05$. In the length-weight relationship of *O. niloticus*, the values of the exponent b in Egbe, Ero, and Ureje reservoirs varied from 2.45 to 2.87, 3.02 to 3.20, and 2.45 to 2.82, respectively. The results of regression coefficient b obtained showed that in the combined season, male, female and combined sexes from the Ero reservoir had isometric growth patterns with growth exponent b values of 3.18, 3.20 and 3.19 respectively that were not statistically different from 3. These results contradicted the negative allometric growth pattern in the Egbe and Ureje reservoirs. The condition factor during the dry season ranged from 1.93-2.05, 2.05-2.11, and 1.93-2.03 for fish in Egbe, Ero, and Ureje reservoirs, respectively while in the rainy season, it ranged from 2.00-2.02; 2.08-2.09 and 1.96-2.01 respectively. The fish species studied in the reservoirs lived above-average life and thus indicate that the prevailing ecological conditions in the reservoirs were not beyond the forbearance range for the fish species since their condition factors were within the range considered adequate for freshwater fishes in tropical waters.

* Corresponding author

E-mail: olagbemidept@abuad.edu.ng (Olagbemide P. T.)

1 Introduction

Fish production plays a vital role in providing livelihoods, employment, and income, and it is also a very cheap source of proteinous foods to the riparian communities and over two million people who live in Ekiti state, Nigeria. It is significant to the Nigerian economy and contributes over US$ 1 billion to its gross domestic product (Fasae and Isinkaye 2018). Fishing and marketing of fish are very lucrative ventures contributing to Nigeria's food security, poverty alleviation, and economic growth. 3–4% of Nigeria's annual GDP comprises the fishing and aquaculture industries (Subansighe et al. 2021). The fish industry also plays a significant role in meeting the nation's nutritional needs by providing around 50% of the food derived from animals and as an indispensable part of the nation's economy (Subansighe et al. 2021). *O. niloticus* is one of significant global economic importance fish species and is raised in at least 85 nations worldwide, making it the second most significant category of farmed fish after carp (Burden 2014). It is considered to be one of the most important fish species in tropical and subtropical aquaculture (FAO 2012). It is the most prevalent species of fish in the waterways of the Ekiti State, and consumers choose it as their top protein source, especially in low-income households due to its undeniable market demand (Olagbemide and Owolabi 2023).

Nigerians' reservoirs contribute significantly to the nation's total indigenous fish production (Komolafe et al. 2014). Although its annual domestic harvest is projected to be 450,000 metric tons, Nigeria is one of the developing world's top fish importers, bringing in nearly 900,000 metric tons of fish (George 2020). Human activities, including industrial, urban, farming, and residential pollution, negatively affect the quality of the environment with its accompanying biological, ecological, and sociological consequences have put Nigerians' water bodies under increasing threat (Ouma 2015). Reservoirs in Ekiti State are sources of potable water, fish, and recreation centres but also receive inputs from domestic and agricultural activities. These various anthropogenic activities are likely to adversely affect the biology of the fish in the reservoirs. Thus, effective management of aquatic resources must be fully adopted to close the gap between fish demand and availability in the State. Biometric relationships are frequently used in fisheries management to convert field data into the proper indices (RobiulHasan et al. 2021). The length-weight relationship (LWR) is a crucial tool for managing and assessing fisheries (Tran et al. 2021), conducting growth studies and providing valuable data related to the habitat and aquatic ecosystem simulations (Moutopoulos and Stergiou 2002). Physiologically, fish size is more important than age because various environmental and physiological aspects depend more on size than age. As a result, size variation significantly affects fisheries knowledge and population trends (Alonso-Fernández et al. 2021) and is among the most basic fisheries data metrics

(Mehmood et al. 2021). Hence, LWR offers helpful information about fish species in a specific geographic area (Olopade et al. 2018). Although LWRs are similar among fish species, they may differ due to hereditary body form and physiological parameters and fluctuate seasonally (De Giosa et al. 2014). Even in the same species living in different areas, the growth process that determines the length and mass of fish might differ due to various biotic and abiotic factors (Nazek et al. 2018).

The fish condition factor (K) acts as a physiological indicator of the well-being of the fish (Ajibare and Loto 2022). According to Olopade et al. (2018), it assesses various biological and environmental parameters, including extent of fitness, gonad maturation, and appropriateness of environment concerning nutritional condition. It refers to the relative fatness of the individual fish, which represents stored energy. When comparing the two populations subjected to particular feeding densities, climatic circumstances and other influences, condition factors are valuable (Fafioye and Ayodele 2018). It helps assess fish's feeding frequency, age, and growth pace (Ndimele et al. 2010). The condition factors of fish species are used to understand their life cycles, manage fish populations appropriately and preserve environmental equilibrium (Imam et al. 2010). Biotic and abiotic environmental conditions strongly influence condition factors and can be used as a metric to evaluate the state of the fish-supporting aquatic ecosystem (Famoofo and Abdul 2020).

Despite numerous studies on the length-weight association and condition factor for fish in Nigerian water bodies (Imam et al. 2010; Ndimele et al. 2010; Ayoade 2011; Ikongbeh et al. 2012; Dan-Kishiya 2013; Fagbuaro 2015; Kareem et al. 2015; Fagbuaro et al. 2016; Kareem et al. 2016; Moslen and Miebaka 2017; Omotayo et al. 2018; Laurat et al. 2019; Oladimeji et al. 2020; Olatunde 2020; Mohammud et al. 2020), but the reports on length-weight relationship and condition factor of *O. niloticus* from Ekiti State reservoirs are scarce. This study compares the length-weight relationship and differences in the condition factor of *O. niloticus* from Egbe, Ero and Ureje reservoirs in Ekiti State, southwest Nigeria, to improve sustainable fishing management.

2 Materials and Methods

2.1 Area of Study

Ekiti State is situated between latitudes 7° 15 and 8° 5' North of the equator and between longitudes 4° 45' to 5° 45' East of the International Meridian, and Kwara, Kogi, and Osun States are its neighbours to the North, east, and south, respectively. Three largest reservoirs of the State included in this study are Egbe reservoir, located between latitudes 7° 36'N North and longitude 5° 35' East of the equator; Ero reservoir at Ikun-Ekiti, Moba Local, located between latitudes 7° 15' N and longitude 5° 31' E; and Ureje
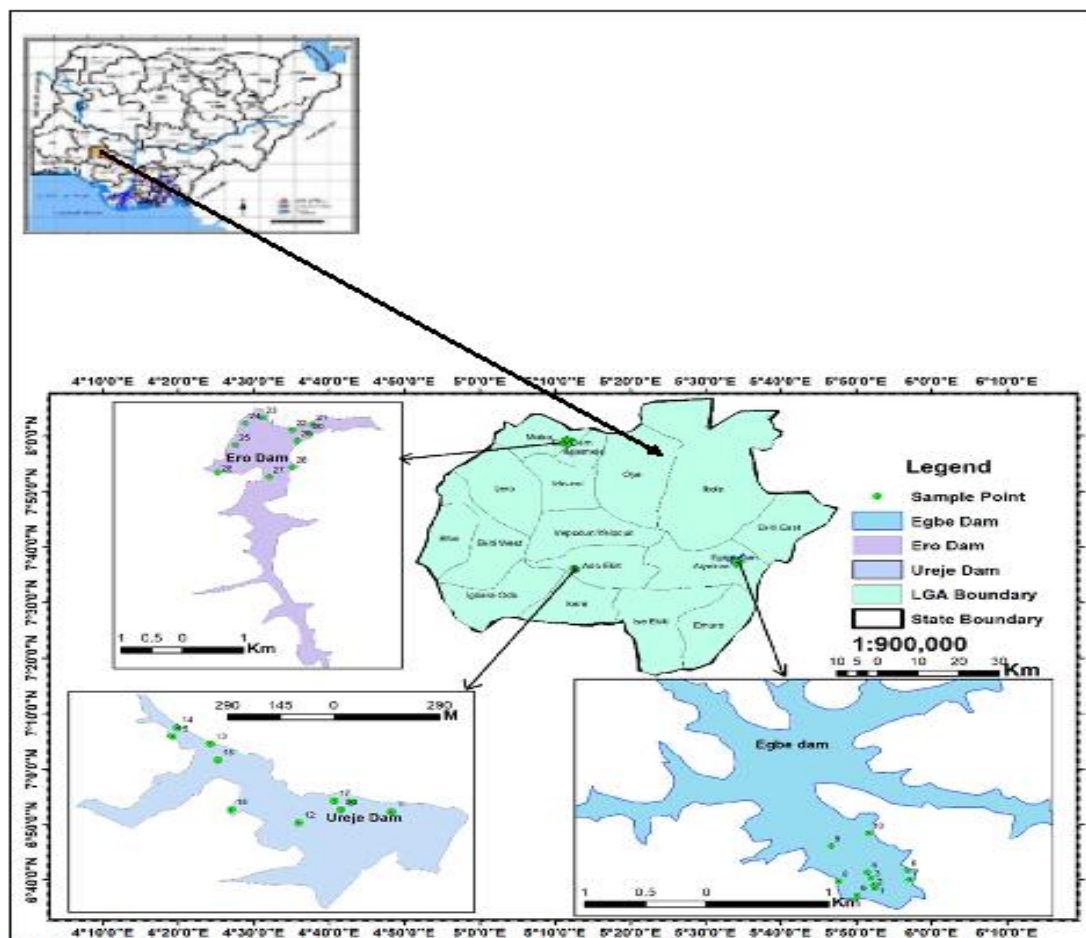
Figure 1 Map of Ekiti State showing the locations of the Reservoirs (Egbe, Ero, and Ureje), southwest Nigeria

reservoir, located between latitude $7^o 35^{'}$ N and longitude $5^o 13^{'}$ E. (Figure 1). Ekiti State reservoirs are very significant and central to the economy of the State's people as they are water sources for domestic and agricultural purposes. Further, these reservoirs are sources of livelihood for the rural fishermen and market women and also a major source of animal protein for the populace, especially the rural dwellers who feed on fish from the reservoirs.

2.2 Sample Collections, Identification and Laboratory Procedures

Permission was obtained from the Ekiti State Water Corporation, and ethical clearance was acquired from the University of Ilorin ethical committee. Samples of *O. niloticus* were collected monthly from the landing sites of Egbe, Ero, and Ureje reservoirs with the help of fishermen working on these reservoirs during both dry (November-March) and rainy season (April-October) of 2017 to 2019 to explore the effect of season on the fish growth pattern. The rainy season is characterized by rainfalls, high relative humidity, lower temperature and reduced photoperiod, while during the dry

season, there is no rainfall, relative humidity is low, and temperature and photoperiod are higher. The fishermen used gill nets left overnight with surface marker buoys for easy relocation. Fish were given labels and identification numbers before being transported to the laboratory in ice-packed containers for further analysis. Fish experts at the Zoology Department, Ekiti State University, Ado-Ekiti, Nigeria, validated the fish samples' identity in the laboratory using the standard identification key developed by FAO (2009) and Olaosebikan and Raji (2013).

Blotting paper was used to remove water from the fish body, and with the aid of a measuring board, the total length (TL), the tip of the head (mouth closed) to the expanded tail fins of each fish, was determined to the nearest 0.1 centimetres (cm). Using an Ohaus CS 5000 model digital top-loading balance, the fish body weight was taken to the nearest g. The genital papillae were visually inspected to determine the fish's sexes, which was later confirmed by dissecting the fish's belly to view the gonads. The male fish has only one opening (a urine pore) in the genital papilla, located directly behind the anus, while the female possesses two (oviduct

and urinary pore). Additionally, the transverse slit of the genital papilla was used to distinguish males from females, whereas the longitudinal slit was used to identify females (Wangatia 2012). The equation below was used to represent the relationship between fish length (L) and weight (W):

$W = aL^b$ ……………………………... (1) (Kahraman et al. 2014).

Before the calculations, the equation mentioned above (1) and data were turned into logarithms. As a result, equation 1 becomes:

$\text{Log } W = \log a + b \log L$... (2) (Zar 1984).

W = fish's weight in grams (g)

L is the fish's total length in centimetres (cm)

a = is the intercept of the regression.

b = Regression slope coefficient (Pauly 1983).

The parameter, a, is a scaling factor for the fish species' weight at length. The shape parameter b refers to the fish species' particular body type. The exponent's value, b, provides biological information on the pattern of fish growth (Abobi 2015). A linear regression of the logarithms of fish length and weight generated the "a" and "b" values. According to Yilmaz et al. (2012), an isometric growth is ascribed when b is not significantly different from 3 and an allometric change is implied when the difference between b and 3 is statistically significant at P <0.05 (Morey et al. 2003).

$ts = (b-3)/s_b$ …………………….……………………………. (3)

 where ts = Student's t-test, b = slope, and s_b = standard error of the slope. Because the fish grows isometrically, the b value of 3 was chosen for comparison and as a reference.

The 95 percent confidence interval (CI) of 'b' was obtained using the equation (Egbal et al. 2011).

$CI = b \pm (1.96 \times SE)$…………………………………………… (4)

where SE stands for "b's standard error."

Using the method published by Pauly (1983), the condition factor, which indicates the level of fish welfare in the Egbe, Ero, and Ureje reservoirs for each month, was calculated for each fish species:

$100W/L^b$ is the condition factor (K).   …………..……………. (5)

Where W is the weight in grams (g), L is the total length of the fish (cm), and b is the calculated LWR growth coefficient.

The condition factor of fish is related to both male and female body types. The calculation was done separately for male and female fish to obtain their statistical differences. According to Bolognini et al. (2013), the data reported were the mean values of the samples collected over two years.

2.3 Statistical Analysis

All statistical analyses were deemed significant at $P < 0.05$. One-way analysis of variances (ANOVA) was performed to compare the means of K of *O. niloticus* among the examined reservoirs. A t-test was used at a predetermined significant level ($P < 0.05$) to determine whether the b-values from the linear regression analysis varied significantly from the optimal value (b=3). This study used Microsoft Office Excel and the Statistical Package for Social Sciences, version 23.

3 Results and Discussion

3.1 Length-weight relationships (Combined seasons)

Fish length-weight relationship studies are a useful resource for characterizing the biological characteristics of the fish species. *Oreochromis niloticus* in the Egbe, Ero, and Ureje reservoirs had mean total lengths of 18.66 ± 0.21, 20.11 ± 0.09, and 18.14 ± 0.13 cm and mean weights of 139.17 ± 4.73, 173.35 ± 2.14, and 117.73 ± 4.76 grams, respectively. Results presented in Table 1 revealed the sample size and the length-weight features, and Figure 2 displays scatter plots or regression graphs of the total length and weight relationships of the species in the reservoirs. Since the body weight of fish species increases as total length increases (Tah et al. 2012; Ezekiel and Abowei 2014), the high coefficient of determination value calculated in the evaluation of LWRs over the mean year in the reservoirs validates or explains the quality and reliability of the LWR model or linear regression for the fish species, thus, according to Nazek et al. (2018), the extrapolation of body weight in future catches can be done in Egbe, Ero, and Ureje for the observed size range in the reservoirs. All the reservoirs had a significant relationship at $P < 0.05$ for *O. niloticus*. Negative allometric growth was reported for *O. niloticus* in all reservoirs except Ero, indicating that *O. niloticus* in Egbe and Ureje reservoirs has a slimmer growth rate. Positive allometric growth indicates the fish gets robust, weightier, and deeper-bodied as its length increases as opposed to isometric growth, which means the fish's length and weight increase at the same rate. *O. niloticus* showed isometric growth (b = 3) in the Ero reservoir. This shows that b-values could vary amongst the different populations of similar species. Bernard et al. (2010) found a similar isometric growth pattern (b = 3.04) for *O. niloticus* in the Egah River, Kogi State, Nigeria. In contrast, Getso et al. (2017) discovered a negative allometric coefficient (b) ranging from 0.1441 to 0.8058 for the same species in Nigeria's Wudil River of Kano State. Similarly, Lauret et al. (2019) found a negative allometric coefficient (0.332 female, 0.365 male) for *O. niloticus* in the lower river Benue, Nigeria. However, most fishes

Table 1 The regression assessment of the correlation between *O. niloticus* body weight and total length from studied reservoirs in Ekiti State, Nigeria

	N	Mean TL	Mean BW	a	B	SE (b)	Cl (b)	Growth Type	R^2	P value of r	t value	K
Egbe (CS)	634	18.66	139.17	0.249	2.75	0.056	2.64-2.86	- Allometric	0.93	5.6×10^{-47}	-4.46	2.01
Egbe (CSM)	409	18.02	126.92	0.241	2.78	0.074	2.63-2.93	- Allometric	0.93	1.64×10^{-29}	-2.97	1.99
Egbe (CSF)	225	19.29	151.43	0.261	2.71	0.088	2.54-2.88	- Allometric	0.94	2.8×10^{-18}	-3.30	2.03
Egbe (CR)	368	18.39	134.47	0.263	2.71	0.059	2.59-2.83	- Allometric	0.93	2.34×10^{-40}	-4.92	2.01
Egbe(MR)	252	17.89	130.52	0.284	2.65	0.066	2.52-2.78	- Allometric	0.94	1.82×10^{-28}	-5.30	2.00
Egbe (FR)	116	18.90	138.41	0.217	2.87	0.130	2.62-3.12	- Allometric	0.90	4.8×10^{-13}	-1.00	2.02
Ero (CS)	610	20.11	173.35	0.143	3.19	0.037	3.12-3.26	Isometric	0.98	6.9×10^{-97}	5.14	2.09
Ero (CSM)	406	20.11	172.57	0.144	3.18	0.049	3.08-3.28	Isometric	0.97	2.42×10^{-56}	3.67	2.07
Ero (CSF)	204	20.11	174.13	0.141	3.20	0.057	3.09-3.31	Isometric	0.97	4.30×10^{-40}	3.51	2.10
Ero (CR)	354	19.80	164.97	0.174	3.05	0.064	2.92-3.18	Isometric	0.94	2.57×10^{-45}	0.78	2.09
Ero (MR)	245	19.78	163.85	0.169	3.07	0.085	2.90-3.24	Isometric	0.93	1.04×10^{-29}	0.82	2.08
Ero (FR)	109	19.81	166.10	0.177	3.02	0.100	2.82-3.22	Isometric	0.95	1.55×10^{-17}	0.20	2.09
Ureje (CS)	640	18.14	117.73	0.321	2.58	0.067	2.45-2.71	- Allometric	0.88	1.07×10^{-28}	-6.27	2.09
Ureje (CSM)	358	18.07	115.67	0.317	2.60	0.085	2.43-2.77	- Allometric	0.87	8.62×10^{-19}	-4.71	2.07
Ureje (CSF)	282	18.21	119.80	0.329	2.57	0.109	2.36-2.78	- Allometric	0.89	4.93×10^{-11}	-3.94	2.10
Ureje (CR)	374	17.36	106.35	0.379	2.46	0.086	2.29-2.63	- Allometric	0.83	1.23×10^{-13}	-6.28	2.09
Ureje (MR)	208	17.08	102.40	0.383	2.45	0.117	2.22-2.68	- Allometric	0.85	1.45×10^{-8}	-4.70	2.08
Ureje (FR)	166	17.64	110.29	0.366	2.49	0.146	2.20-2.78	- Allometric	0.82	1.24×10^{-6}	-3.49	2.09
Egbe (CD)	266	18.92	143.88	0.330	2.52	0.081	2.36-2.68	- Allometric	0.92	6.63×10^{-18}	-5.92	1.98
Egbe(MD)	157	18.15	123.31	0.361	2.45	0.094	2.27-2.63	- Allometric	0.94	6.68×10^{-11}	-5.85	1.93
Egbe (FD)	109	19.69	164.45	0.246	2.77	0.133	2.51-3.03	- Allometric	0.91	2.05×10^{-10}	-1.73	2.05
Ero (CD)	256	20.43	181.73	0.158	3.11	0.066	2.98-3.24	Isometric	0.96	1.42×10^{-42}	1.67	2.08
Ero (MD)	161	20.44	181.30	0.174	3.02	0.089	2.85-3.19	Isometric	0.95	1.98×10^{-23}	0.22	2.05
Ero (FD)	95	20.42	182.16	0.148	3.17	0.088	3.00-3.34	Isometric	0.97	2.62×10^{-19}	1.93	2.11
Ureje (CD)	266	18.92	129.12	0.309	2.63	0.092	2.45-2.81	- Allometric	0.89	1.31×10^{-18}	-4.02	1.98
Ureje (MD)	150	19.06	128.94	0.347	2.53	0.113	2.31-2.75	- Allometric	0.89	9.73×10^{-10}	-4.16	1.93
Ureje (FD)	116	18.78	129.30	0.240	2.82	0.135	2.56-3.04	- Allometric	0.89	6.52×10^{-11}	-1.33	2.03

CS= combined seasons both sexes, CSM = combined seasons male, CSF= combined seasons Female, CR = Combined sexes rainy season, MR = Rainy season male, FR = Rainy season female, CD = combined sexes dry season, MD = Dry season male, FD = Dry season female, TL = overall length (cm), BW = Body mass (g), SE = Standard error; Cl = confidence intervals of b; K = Condition factor, N = number of samples.
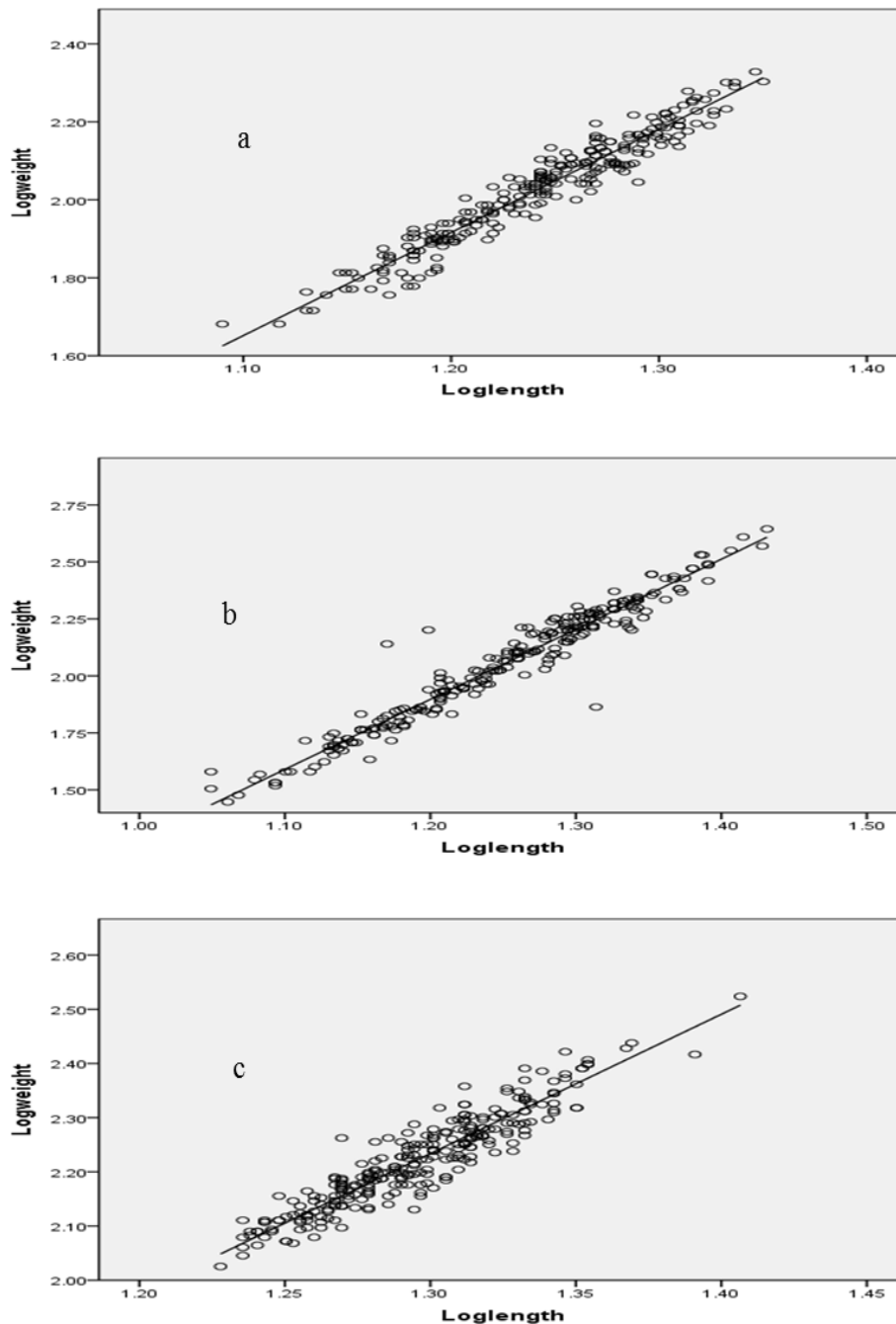
Figure 2 Length and weight relationships of *O. niloticus* in (a) Egbe, (b) Ero and (c) Ureje reservoirs

do not display isometric growth in real life or under natural conditions since their size changes as they develop or grow, making them heavier in one season and lighter in the following. Le Cren (1951) concluded that the existing relationship between the length and weight of fish may deviate from the ideal value (3.0), which certain environmental parameters or fish-related factors may cause. The productivity of the immediate environment of fish species greatly determines the degree of deviation from b. Highly productive aquatic settings typically encourage positive allometric development, and low productivity conditions facilitate negative allometric growth (Thomas et al. 2003). The environmental conditions of the habitat may be responsible for the variations in fish species' growth. This observed variation in fish development is consistent with the findings of Adeyemi et al. (2009), who discovered that fish growth pattern fluctuation is a common occurrence in tropical and subtropical waters due to environmental

variations, spawning, and nutrient composition variations. Therefore, there is a direct proportionality between the length and weight of fish species and their environmental conditions, and this relationship varies according to the species. Consequently, even while fish growth pattern varies depending on the species, as this study's observations show, it might fluctuate significantly among the same species living in different geographic regions. These results are confirmed by Armstrong et al. (2004) and Gerritsen et al's. (2006) findings and showed that some biological parameters vary over constrained geographic regions. In the Kashmir Himalayas, the Crucian carp (*Carassius carassius*) exhibited positive allometric growth in the Manasbal and Anchar lakes and isometric growth in the Dal Lake (Zargar et al. 2012). Ahmed (2016) also communicated both allometric and isometric growth in freshwater snow trout (*Schizothorax niger*) from Dal Lake. According to Moslen and Miebaka (2017), the variations in the b values for the same species may result from variations in fish conditions and habits, ages and development rates, maturation stages, availability of food, and biological factors. As a result, the differences in the values of b found among the three reservoirs within the same species (*Oreochromis niloticus*) could be due to the different environmental changes experienced in the reservoirs during sampling. However, the b values of *O. niloticus* in the three reservoirs were consistent with the range 2.5 and 3.5 published by Gayanilo and Pauly (1997) for the majority of tropical fish species, as well as the range 2-4 often recorded for tropical freshwater fish species (Thomas et al. 2003). The range of the 95 percent

confidence interval for the exponent "b" in the length-weight relationships in the reservoirs under study was 2.2 to 2.3, which was similar to the range (2.1–2.3) discovered by Dan-Kishiya (2013) in *O. niloticus* in a tropical lake in Abuja, Nigeria. In this study, the effects of sex on the variation of b showed no significant difference (P < 0.05). However, the b values were higher in females than the male fish in the three studied reservoirs. Equations describing the length-weight association for both sexes in this study are (i) fish in Egbe reservoir (n = 634), log W = 0.25 + 2.75 log L (r = 0.93), (ii) fish in Ero reservoir, (n = 610), Log W = 0.14 + 3.19 log L (r = 0.97) and fish in Ureje reservoir (n = 640), log W = 0.32 + 2.58 log L (r = 0.88).

3.2 Length-weight associations by seasons

The b values of the fish in the reservoirs were higher during the rainy season than the dry season, which indicates that season may have an impact on the LWRs reported in this study, even if there was no statistically significant difference (P > 0.05) between the dry and rainy seasons.

3.3 Condition Factor

Figure 3 shows the monthly fluctuations in K of *O. niloticus* in the three reservoirs during the dry and rainy seasons. The lowest average K values for the Egbe reservoir in combined sexes during the dry season (1.79 ± 0.03) were witnessed in November 2018, and the highest mean K value was 2.12 ± 0.04 in March 2018. In
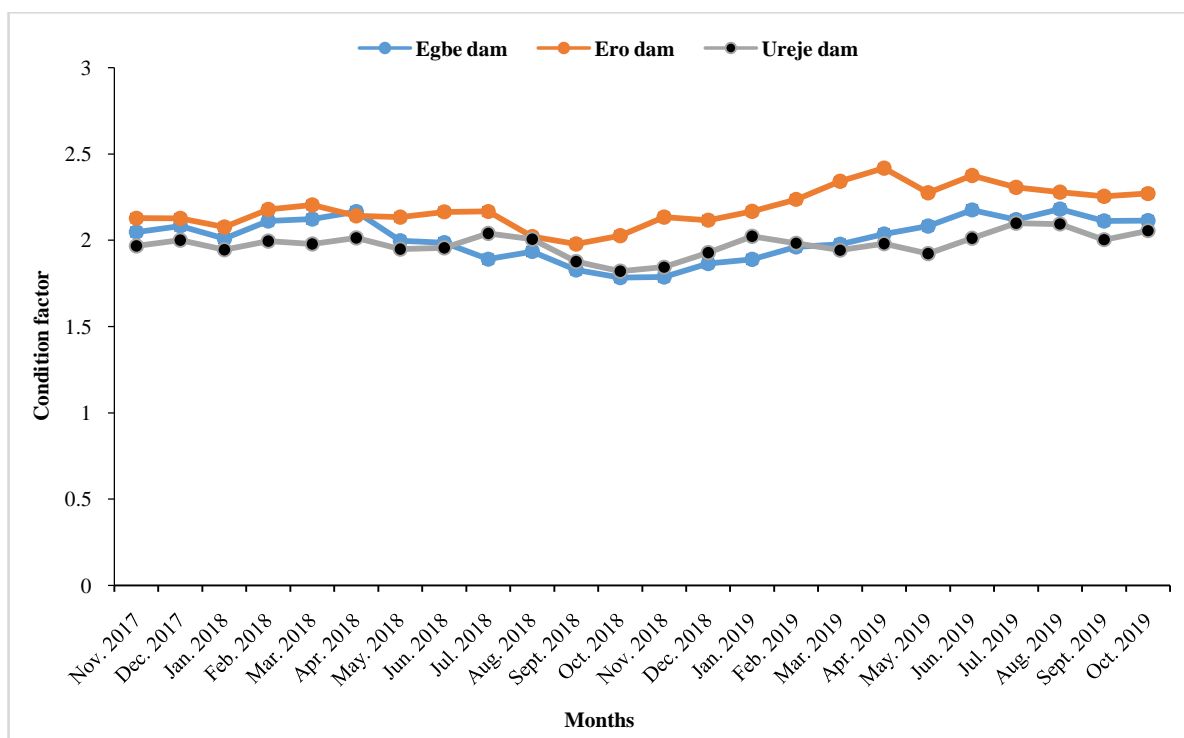

Figure 3 Monthly Changes in *O. niloticus* Condition Factors in Studied Water Reservoirs

the Ero reservoir, the lowest mean K values for combined sexes during the dry season (2.08 ± 0.04) were observed in January 2018, and the highest K values (2.34 ± 0.08) were reported in March 2019. In the case of the Ureje reservoir, the lowest mean K values for combined sexes during the dry season (1.84 ± 0.04) were witnessed in November 2018, and the highest K values (2.02 ± 0.03) were reported in January 2019. A significant difference at P < 0.05 existed in mean K values for combined sexes in all the months during the dry seasons between Ero and Ureje reservoirs. Between Egbe and Ero reservoirs, significant differences existed in mean K values at P < 0.05 in March, November-December, 2018 and January-March, 2019 while between Egbe and Ureje reservoirs, significant differences existed in mean K values at P < 0.05 in February-March, 2018 and January 2019.

The lowest mean K values in the Egbe reservoir for combined sexes during the rainy season (1.78 ± 0.03) were observed in October 2018, and the highest K value was 2.18 ± 0.02 in June and August 2019. In the Ero reservoir, the lowest mean K value for combined sexes during the rainy season (1.98 ± 0.02) was observed in September 2018 and the highest value of 2.42 ± 0.11 in April 2019. The lowest mean K values in the Ureje reservoir for combined sexes during the rainy season (1.82 ± 0.03) were observed in October 2018, and the highest (2.10 ± 0.04) was observed in July 2019. Significant difference at P < 0.05 existed in mean K values for combined sexes in May, June and July, September-October, 2018; April-July and September-October, 2019 between Egbe and Ero reservoirs. Between Ero and Ureje reservoirs, the significant difference at P < 0.05 existed in mean K values for combined sexes in April-June, September-October, 2018 and April-October, 2019. In April, July 2018 and May-June and September 2019, significant differences existed at P < 0.05 in mean K values between Egbe and Ureje reservoirs. The mean values of K in the three reservoirs during the dry and rainy seasons

ranged from 1.85 ± 0.05 to 2.42 ± 0.12 and based on the health status and the fish condition factor measure of Barnham and Baxter (1998), who gave 1.6 K value as outstanding, 1.4 as good; 1.2 as fair; 1.0 as deprived and 0.8 as extremely poor. Furthermore, Ujjania et al. (2012) reported that fish condition factor equal or greater than 1 signifies adequate feeding and healthy surroundings. Hence, the mean value of condition factors of *O. niloticus* acquired in the reservoirs during this study suggests that the fish in the reservoirs were living above average life and thus indicates that the prevalent ecological conditions in the reservoirs were not beyond the forbearance range for the fish species. Ekpo et al. (2013) found a comparable high K value (1.24) for *Epinephelus aeneus* from the Qua Iboe River estuary, Akwa Ibom State, southern Nigeria, and *Hepsetus odoe* from the Ado Ekiti, Ogbomoso, and Eleiyele Reservoirs were reported to have K > 1 by Idowu (2013), Adedokun et al. (2013), and Kareem et al. (2016), respectively. However, the K value in this study is less than the 2.9 to 4.8 reported by Bagenal and Tesch (1978) for mature freshwater fish and within the range (1.97-2.63) documented by Outa et al. (2014) in the same fish species in Lake Naivasha. During the dry and rainy seasons, the monthly variations in K of *O. niloticus* from the reservoirs may be due to different environmental conditions that vary from month to month.

In the Egbe reservoir, there was a significant difference in the K values between the dry and rainy seasons at P < 0.05, while there was no difference at P < 0.05 in the K values between the dry and rainy seasons in the Ero or Ureje reservoirs.

Table 2 shows seasonal fluctuations in the condition factor of the male, female, and mixed sexes during the dry and rainy seasons. For combined sexes, the highest mean seasonal K value during the dry season was obtained in Ero reservoir (2.08 ± 0.02), while the lowest mean seasonal K value was obtained in Egbe and Ureje reservoirs

Table 2 Mean Seasonal variations in the condition factor in male, female and combined sexes of *O. niloticus* from studied water reservoirs in Ekiti State, southwest Nigeria

	Condition Factor											
	Combined sexes				Male				Female			
Reservoirs	N	Min	Max	Mean	N	Min	Max	Mean	N	Min	Max	Mean
Dry season												
Egbe	266	1.54	2.45	1.98 ± 0.02[a]	157	1.61	2.45	1.93 ± 0.03[a]	109	1.5	2.29	2.03 ± 0.02[a]
Ero	256	1.69	2.56	2.08 ± 0.02[b]	161	1.69	2.56	2.05 ± 0.03[b]	95	1.81	2.35	2.11 ± 0.02[a]
Ureje	266	1.24	2.45	1.98 ± 0.02[a]	150	1.24	2.35	1.93 ± 0.03[a]	116	1.62	2.53	2.01 ± 0.03[a]
Rainy season												
Egbe	368	1.65	2.58	2.01 ± 0.01[a]	252	1.65	2.58	2.00 ± 0.02[a]	116	1.70	2.42	2.02 ± 0.03[a]
Ero	354	1.74	2.58	2.09 ± 0.01[b]	245	1.74	2.58	2.08 ± 0.02[b]	109	1.76	2.42	2.09 ± 0.02[b]
Ureje	374	1.54	2.70	2.00 ± 0.02[a]	208	1.24	2.70	1.96 ± 0.03[a]	166	1.62	2.53	2.01 ± 0.03[a]

Means with different superscripts along a row are significantly different at P < 0.05

(1.98 ± 0.02). Significant differences existed at P < 0.05 between the average seasonal values of K in Egbe and Ero reservoirs and between Ero and Ureje reservoirs during the dry season. In Egbe reservoir, the mean seasonal K values were 1.98 ± 0.02, 1.93 ± 0.03 and 2.03 ± 0.02 for combined sexes, males and females. The mean seasonal K values were 2.08 ± 0.02, 2.05 ± 0.03, and 2.11 ± 0.02 for combined sexes, males and females, respectively, in the Ero reservoir, while the mean seasonal K values in *O. niloticus* in the Ureje reservoir were 1.98 ± 0.02, 1.93 ± 0.03, and 2.05 ± 0.03 for combined sexes, males and females respectively. A significant difference at P < 0.05 existed in the mean seasonal K values between males of Egbe and Ero reservoirs and between the males of Ureje and Ero reservoirs, while the females showed no significant difference in mean K values among the reservoirs.

During the rainy season, the highest mean seasonal K value (2.09 ± 0.01) for combined sexes was obtained in the Ero reservoir, while the lowest mean seasonal K value (2.00 ± 0.02) was obtained in the Ureje reservoir. Significant differences existed at P < 0.05 between the mean seasonal values of K in Egbe and Ero reservoirs and between Ero and Ureje reservoirs. In the Egbe reservoir, the mean seasonal K values were 2.01 ± 0.01, 2.00 ± 0.02, and 2.02 ± 0.03 for combined sexes, males and females, respectively. The mean seasonal K values were 2.09 ± 0.01, 2.08 ± 0.02, and 2.09 ± 0.02 for combined sexes, males and females, respectively, in the Ero reservoir, while the mean seasonal K values in *O. niloticus* in the Ureje reservoir were 2.00 ± 0.02, 2.01 ± 0.03, and 1.96 ± 0.03 for combined sexes, males and females respectively. A significant difference existed in the mean seasonal K values at P < 0.05 between males and females of the Egbe and Ero reservoirs and between the males and females of the Ero and Ureje reservoirs.

The fish in the reservoirs were in a better physiological state during the rainy season than during the dry season, as indicated by the mean K values during the rainy season, which were typically higher than those during the dry season. This seasonal variation in K may be related to the availability of food and nutrients brought into the reservoirs by runoffs during the rains from residential houses around the reservoirs. Thus, increasing food availability in reservoirs and makes more food available to fish. The observed differences in the mean K values between the dry and the rainy seasons, the rainy period recorded a relatively higher K value than the dry season could also be explained in terms of the dissolved oxygen. Dissolved oxygen levels were higher during the rainy season (Olagbemide and Owolabi 2019), and thus, the water became well-saturated with oxygen, leading to the effective functioning of the fish's metabolic processes. Shinkafi and Ipimiolu (2010), Ibrahim et al. (2011), Keyombe et al. (2017), and Mohd and Khaironizam (2019) reported similar higher value of condition factors during the rainy season than the dry season. According to Gomiero and de Souza Braga (2005), the availability of food and enhancement throughout their gonad growth

contributed to their superior condition during the rainy season, and Samat et al. (2008) revealed that specific external influences, such as variations in temperature and photoperiod, may have an impact on fish condition. This agrees with Alam et al. (2013) when they examined fish from freshwater in Bangladesh and recounted that fish exhibited extreme stoutness in the summer and rainy seasons owing to suitable environmental conditions. Therefore, the natural fluctuations or differences in K of fish must be considered when interpreting its values.

Conclusion

Although the condition factor varied between reservoirs, it was still within the productive and healthy range, and the b values of the fish in the three reservoirs were within the range frequently recorded for tropical freshwater fish species. Therefore, the information from this study will benefit future ecological research and fishery management in Ekiti State in line with the preservation, restoration, and management methods for fish species in the reservoirs.

Acknowledgements

Conflict of interests

The authors have no conflict of interest to disclose.

Funding

References

Abobi, S. M. (2015). Weight-length models and relative condition factors of nine (9) freshwater fish species from the Yapei stretch of the White Volta, Ghana. *Elixir Applied Zoology*, *79*, 30427–31.

Adedokun, M. A., Fawole, O. O., & Ayandiran, T. A. (2013). Allometry and condition factors of African pike "*Hepsetusodoe*" Actinopterygii in a lake. *African Journal of Agricultural Res*earch, *8,* 3281–3284.

Adeyemi, S. O., Bankole, N. O., Adikwu, I. A., & Akombu, P. M. (2009). Age, growth and mortality of some commercially important fish species of the Gbedikere Lake, Kogi State, Nigeria. *International Journal of Lakes and Rivers*, *2*(1), 45–51.

Ahmed, I. (2016). Length-weight relationship and Condition Factor of Freshwater Snow Trout, *Schizothorax Niger* (Heckel 1838) from Dal Lake of Kashmir Himalayas. *Journal of Ecophysiology and Occupatinal Health, 16*(1-2), 22–26.

Ajibare, A. O., & Loto, O. O. (2022). Length-weight relationship and condition factor of Sarotherodon*Melanotheron* and *Tilapia Guineensis* in Lagos Lagoon, Nigeria. *Agrosearch*, *21*(1&2), 57-66.

Alam, M. M., Jahan, S. N., Hussain, M. A., De, M., Goutham-Bharathi, M. P., Magalhães, A. L. B., Mazlan, A. G., & Simon, K. D. (2013). Length-length relationship, length-weight relationship and condition factor of freshwater fish species of Bangladesh. *Aquaculture, Aquarium, Conservation & Legislation International Journal of the Bioflux Society*, *6*(5), 498 – 509.

Alonso-Fernández, A., Otero, J., & Bañón, R. (2021). Indicators of body size variability in a highly developed small-scale fishery: Ecological and management implications, *Ecological Indicators*, *121,* 107141. DOI: https://doi.org/10.1016/j.ecolind.2020.107141.

Armstrong, M. J., Gerritsen, H. D., Allen, M., McCurdy, W. J., & Peel, J. A. D. (2004). Variability in maturity and growth in a heavily exploited stock: cod (*Gadus morhua* L.) in the Irish Sea. *ICES Journal of Marine Sci*ence, *61,* 98–112. DOI: https://sci-hub.ru/10.1016/j.icesjms.2003.10.005

Ayoade, A. A. (2011). Length-weight relationship and diet of African Carp *Labeogunensis* (Boulenger, 1910) in Asejire Lake Southwestern Nigeria. *Journal of Fisheries and Aquatic Science*, *6,* 472-478.

Bagenal, T.B., & Tesch, F.W. (1978). Age and Growth. In: T. Bagenal (Ed.) *Methods for Assessment of Fish Production in Fresh Waters, 3rd Edition*. IBP Handbook No. 3, Blackwell Science Publications, Oxford.

Barnham, P. C., & Baxter, A. (1998). Condition Factor for Salmonid Fish. *Journal of Fisheries* Notes, 1– 3. https://pdf4pro.com/amp/view/condition-factor-k-for-salmonid-fish-a93.html

Bernard, E., Bankole, N. O., Akande, G. R., Adeyemi. S., & Ayo-Olalusi, C. I. (2010). Organoleptic characteristics, length-weight relationship and condition factor of *Oreochromis niloticus* in Egah River at Idah L.G.A of Kogi State, Nigeria. *Internet Journal of Food Safety, 12,* 62-70.

Bolognini, L., Domenichetti, F., Grati, F., Polidori, P., Scarcella, G., & Fabi, G. (2013). Weight-Length Relationships for 20 Fish Species in the Adriatic Sea. *Turkish Journal of   Fisheries and Aquatic Sciences, 13,* 555-560.

Burden, D. (2014). *Tilapia profile*. International and special project, Extension value added agriculture and Agricultural Marketing Resource centre, Iowa State University. Pp 1-4.

Dan-Kishiya, A. S. (2013). Length-weight relationship and condition factor of five fish species from a tropical water supply reservoir in Abuja, Nigeria. *American Journal of Research Communication, 1*(9), 175-187.

De Giosa, M., Czerniejewski, P., & Rybczyk, A. (2014). Seasonal changes in condition factor and weight-length relationship of invasive carassiusgibelio (Bloch, 1782) from Leszczynskie Lakeland, Poland. *Advances in Zoolo*gy, *2014*, *678763*. DOI: https://doi.org/10.1155/2014/678763

Egbal, O. A., Mohammed, E. A., & Afra, A. A. (2011). Length-weight relationships and condition factors of six fish species in Atbara River and Khashm El-Girba Reservoir, Sudan. *International Journal of Agriculture Sciences*, *3* (1), 65-70.

Ekpo, E. I., Mandu, A., Ibok, E., & Nkwoji, J. N. (2013). Food and feeding habits and condition factor of fish species in Qua Iboe River estuary, AkwaIbom State, southeastern Nigeria. *International Journal Fisheries and Aquatic Studies*, *2*(2), 38-46.

Ezekiel, E. N., & Abowei, J. F. N. (2014). A study of length-weight relationship and condition factor of *Hepsetusodoe* (Bloch, 1794) from Amassoma flood plains. *Annals Biological Sci*ences, *2*(2), 10–17.

Fafioye, O., & Ayodele, O. (2018). Length-eight relationship and condition factor of four commercial fish species of Oyan Lake, Nigeria. *Examines in Marine Biology and Oceanography*, *2*(4), EIMBO.000543.2018.

Fagbuaro, O. (2015). Morphometric characteristics and meristic traits of *Tilapia Zillii* from three major dams of a Southwestern state, Nigeria. *Continental Journal of Biological Sciences, 8* (1), 1–7. DOI: 10.5707/cjbiolsci.2015.8.1.1.7.

Fagbuaro, O., Oso, J. A., Ola-Oladimeji, F. A., Olafusi, T., & Akinyemi, O. (2016). Comparative biometric variations of two Cichlidae: *Oreochromis niloticus* and *Tilapia zillii* from a dam in Southwestern Nigeria. *American Journal of Research Communication*, *4*(5): 119-   129.

Famoofo, O. O., & Abdul, W. O. (2020). Biometry, condition factors and length-weight relationships of sixteen fish species in

Iwopin freshwater ecotype of Lekki Lagoon, Ogun State, Southwest Nigeria. *Heliyon, 6*(1), e02957.

FAO. (2009). *Oreochromis niloticus*. In Rakocy, J. E. (Ed.) Cultured aquatic species fact sheets. Text by and compiled by Valerio Crespi and Michael New. Retrieved from https://www.fao.org/fishery/docs/CDrom/aquaculture/I1129m/file/en/en_niletilapia.htm.

FAO. (2012). The State of World Fisheries and Aquaculture 2012. FAO Fisheries and Aquaculture Department, Rome, Italy. Retrieved from https://www.fao.org/3/i2727e/i2727e.pdf.

Fasae, K. P., & Isinkaye, M. O. (2018). Radiological risks assessment of ^{238}U, ^{232}Th and ^{40}K in fish feeds and catfish samples from selected fish farms in Ado-Ekiti, Nigeria. *Journal of Radiation Research and Applied Sciences*, 11: 317-322. DOI: https://doi.org/10.1016/j.jrras.2018.05.002.

Gayanilo, F. C., & Pauly, D. (1997). *FAO-ICLARM stock assessment tools* (FiSAT). Reference manual, FAO Computerized Information Series (Fisheries). No. 8. Rome; p.262. Retrieved from https://agris.fao.org/agris-search/search.do?recordID=XF1998081063.

George, S. M. D. (2020). The Profitability of Fish Production by Co-Operative Society Members in Rivers State, Nigeria. *Global Journal of Management and Business Research*, *20*(B10), 41–127.

Gerritsen, H. D., McGrath, D., & Lordan, C. A. (2006). Simple method for comparing age–length keys reveals significant regional differences within a single stock of haddock (*Melanogrammusaeglefinus*). *ICES Journal of Marine Sci*ence, *63*, 1096–1100.

Gesto, B. M., Abdullahi, J. M., & Yola, I. A. (2017). Length-weight relationship and condition factor of *Clarias gariepinus* and *Oreochromis niloticus* of Wudil River, Kano, Nigeria. *Journal of Tropical Agriculture, Food, Environment and Extension, 16*(1), 1 – 4.

Gomiero, L.M., & de Souza Braga, F.M. (2005) The Condition Factor of Fishes from Two River Basins in São Paulo State, Southeast of Brazil. *Acta Scientiarum-Biological Sciences*, 27: 73-78.

Ibrahim, B. U., Auta, J., Balogun, J. K., Bolorunduro, P. I., & Umar, R. (2011). Length-Weight Relationship and Condition Factor of *Clarias anguillaris* (Family: Claridae) in Kontagora Reservoir, Niger State, Nigeria. *Nigerian Journal of Basic and Applied Science*, 19(2): 299-303.

Idowu, E. O. (2013). Studies on age and growth of African Pike, *Hepsetusodoe* in Ado Ekiti Reservoir. *IOSR Journal of Pharmacy and Biological Sciences* (IOSR-JPBS), *8*(3), 75–82.

Ikongbeh, O. A., Ogbe, F. G., & Solomon, S. G. (2012). Length-weight relationship and condition factor of *Bagrus docmac* from Lake Akata, Benue state, Nigeria. *Journal of Animal and Plant Sciences, 15,* 2267-2274.

Imam, T. S., Bala, U., Balarabe, M. L., & Oyeyi, T. I. (2010). Length-weight relationship and condition factor of four fish species from Wasai Reservoir in Kano, Nigeria. *African Journal of General Agriculture, 6* (3), 125-130.

Kahraman, A. E., Göktürk, D. & Aydin, E. (2014). Length-weight relationships of five fish species from the Sakarya River, Turkey. *Annual Research and Review in Biology*, *4*(15)*,*   2476-2483.

Kareem, O. K., Olanrewaju, A. N., & Orisasona, O. (2015). Length-weight relationship and condition factor of *Chrysichthys nigrodigitatus* and *Schilbemystus* in Erelu Lake, Oyo State, Nigeria. *Journal of Fisheries and Livestock Production, 3,* 150.

Kareem, O. K., Olanrewaju, A. N., Osho, E. F., Orisasana, O., & Akintunde, M. A. (2016). Growth patterns and condition factor of Hepsetusodoe (Bloch, 1794) captured in Eleiyele Lake, Southwest, Nigeria. *Fisheries and Aquaculture Journal*, *7*(3)*,* 1–4.

Keyombe, J. L., Malala, J. O., Waithaka, E., Lewo; R. M., & Obwanga, B. O. (2017). Seasonal changes in length-weight relationship and condition factor of *Nile tilapia*, *Oreochromis niloticus* (Linnaeus, 1758) (Cichlidae) in Lake Naivasha, Kenya. *International Journal of Aquatic Biology*, *5*(1), 7-11.

Komolafe, O. O., Arawomo, G. A. O., Idowu, E. O., & Adedeji. A. A. (2014). Status and Economic Impact of the Fisheries of Osinmo Reservoir, Ejigbo, Nigeria, *Ife Journal of Science*, *16*(2), 309-317.

Laurat, H. T., Isiyaku, M. S., & Akange, E. T. (2019). Length-weight relationships and condition factor of *Oreochromis niloticus* and *Citharinus citharus* in lower river Benue, Nigeria. *International Journal of Fisheries and Aquatic Studies*, *7*(6), 21-25.

Le Cren, E. D. (1951). The length-weight relationship and seasonal cycle in gonad weight and condition in the Perch (*Perca fluviatilis*). *Journal of Animal Ecology*, *20,* 201-219.

Mehmood, S., Ahmed, I., & Ali, M. N. (2021). Length-weight relationship, morphometric and meristic controlling elements of three freshwater fish species inhabiting North Western Himalaya. *Egyptian Journal of Aquatic Biology & Fisheries*, *25*(6)*,* 243 – 257.

Mohammud, A. Y., Taofik, B., Babangida, A., & Salim, A. M. (2020). Length-weight relationship, condition factor and growth of *Alestesbaremose* (Joaniss, 1835) in Zobe Dam,   Katsina. *Fudma Journal of Sciences*, *4*(1), 24 - 28.

Mohd, I. C. A., & Khaironizam M. Z. (2019). Length-Weight Relationships, Condition Factor and Growth Parameters of *Periophthalmus chrysospilos* (Bleeker, 1852) (Gobiiformes: Gobiidae) in Bayan Bay, Penang, Malaysia. *Sains Malaysiana*, *48*(2), 271–279.

Morey, G., Morantai, J., Massut, E., Grau, A., Linde, M., Riera, F., & Morales, N. B. (2003). Weight-length relationships of littoral to lower slope fishes from the western Mediterranean, *Fisheries Research*, *62*, 89–96. DOI: https://doi.org/10.1016/S0165-7836(02)00250-3

Moslen, M., & Miebaka, C. A. (2017). Length-weight relationship and condition factor of *Mugil cephalus* and *Oreochromis niloticus* from a Tidal creek in the Niger Delta, Nigeria. *Archives of Agriculture and Environmental Science*, *2*(4), 287-292.

Moutopoulos, D. K., & Stergiou, K. I. (2002). Length-weight and length-length relationships of fish species from Aegean Sea (Greece). *Journal of Applied Ichthyology, 18*, 200-203. DOI: https://doi.org/10.1046/j.1439-0426.2002.00281.x

Nazek, J., Ghassan, Y. Carol, S., & Mohammad H. E. (2018). Length-weight relationships and relative condition factor of fish inhabiting the marine area of the Eastern Mediterranean city, Tripoli-Lebanon. *The Egyptian Journal of Aquatic Research*, *44*(4), 299-305.

Ndimele, P. E., Kumolu-Johnson, C. A., Aladetohun, N. F., & Ayorinde, O. A. (2010). Length-weight relationship, condition factor and dietary composition of *Sarotherodon melanotheron*, Ruppell, 1852 (Pisces: Cichlidae) in Ologe Lagoon, Lagos, Nigeria. *Agriculture and Biology Journal of North America, 1*, 584-590.

Oladimeji, F. A. O., Oladimeji, T. E., & Oyewole, O. S. (2020). Estimation of weight- length relationship and condition factor of two dominant fish species in Egbe dam, Southwestern Nigeria. *Uttar Pradesh Journal of Zoology*, *41*(11), 152-159.

Olagbemide, P. T., & Owolabi, O. D. (2019). Assessment of Physico-Chemical Parameters and Their Pollution Implications on the Major Dams in Ekiti State. *International Journal of Ecotoxicology and Ecobiology*, *4*(2), 58-72.

Olagbemide, P. T., & Qwolabi, O. D. (2023). Assessment of metal contamination in *Oreochromis niloticus* from Ekiti State's major Dams, Southwest, Nigeria and its human health Implications. *Abuad International Journal of Natural and Applied Sciences*, *3*(1), 1–15. https://doi.org/10.53982/aijnas.2023.0301.01-j

Olaosebikan, B. D., & Raji, A. (2013). *Field guide to Nigerian freshwater fishes.* Revised Edition. Federal College of Freshwater Fisheries Technology. New Bussa. Nigeria, pp.144.

Olatunde, O. (2020). Length-Weight Relationship of *Tilapia zillii* Fish Species Collected from Egbe Reservoir, Ekiti State, Southwest Nigeria. *Science Letter, 8*(1), 43-47.

Olopade, O.A., Dienye, H.E., Jimba, B., Bamidele, N. A., & Taiwo, I. O.(2018). Length–weight relationship and condition factor of Guinean Tilapia *Coptodon guineensis* (Günther, 1862) from the New Calabar River and Buguma Creek, Nigeria. *Punjab University Journal of Zoology*, *33*(1), 42-46. DOI: http:dx.doi.org/10.17582/pujz/2018.33.1.42.46

Omotayo F., Oluwadare, A., & Modupe, A. M. (2018). Length-Weight Relationship and Condition Factor of Two Species of Tilapia and One Species of Mormyrops from a Tropical Dam in a Southwestern State, Nigeria. *Journal of Ecology and Natural Resour*ces, *2*(2), 124. DOI: https://doi.org/10.23880/jenr-16000124

Ouma S. O. (2015). Physico-chemical and bacteriological quality of water from five rural catchment areas of Lake Victoria basin in Kenya. M. Sc. Thesis in Science (Biotechnology) in the School of Pure and Applied Sciences of Kenyatta University, Kenya. Retrieved from https://ir-library.ku.ac.ke/handle/123456789/13434?show=full

Outa N. O., Kitaka N., & Njiru J.M. (2014). Length-weight relationship, condition factor, length at first maturity and sex ratio of Nile tilapia, *Oreochromis niloticus* in Lake Naivasha, Kenya. *International Journal of Fisheries and Aquatic Studies*, *2*(2), 67-72.

Pauly, D. (1983). Some simple methods for the assessment of tropical fish stock. FAO fish *Technical paper, 234*, 52.

RobiulHasan, M., Mamun, A.A., & Yeamin Hossain, M. (2021). Biometric indices of eleven mangrove fish species from southwest Bangladesh. *The Egyptian Journal of Aquatic Research*, *47*(2), 207–213.DOI: https://doi.org/10.1016/j.ejar.2020.11.002

Samat, A., Shukor, M. N., Mazlan, A. G., Arshad, A., & Fatimah, M.Y. (2008). Length-Weight Relationship and Condition Factor of *Pterygoplichthys pardalis* (Pisces: Loricariidae) in Malaysia Peninsula. *Research Journal of Fisheries and Hydrobiology*, *3*, 48-53.

Shinkafi, B. A., & Ipinjolu, J. K. (2010).. Morphometric Relationships and Relative Condition Factor of *Auchenoglanis occidentalis* (Cuvier and Valenciennes) from River Rima, North-Western Nigeria. *Journal of Fisheries International, 5*, 61-66.

Subasinghe, R., Siriwardena, S.N., Byrd, K., Chan, C.Y., et al. (2021). Nigeria fish futures. Aquaculture in Nigeria: Increasing Income, Diversifying Diets and Empowering Women. Report of the scoping study, Penang, Malaysia: World Fish. Program Report: 2021-16. Retrieved from https://hdl.handle.net/20.500.12348/4951.

Tah, L. G., Gooré Bi, G., & Da Costa, K. S. (2012). Length-weight relationships for 36 freshwater fish species from two tropical reservoirs: Ayamé I and Buyo, Côte d'Ivoire. *International Journal*

of Tropical Biology and Conservation / Revista De Biología Tropical, 60(4): 1847-1856.

Thomas, J., Venu, S., & Kurup, B. M. (2003). Length-weight relationship of some deep-sea fish inhabiting the continental slope beyond 250 m depth along the west coast of India. *NAGA ICLARM Quarterly*, *26* (2), 17–21.

Tran, H. D., Nguyen, H. H., & Ha, L. M. (2021). *Length–weight relationship and condition factor of the mudskipper (Periophthalmus modestus) in the Red River Delta. Regional Studies in Marine Science, 46, 101903*.DOI: https://doi.org/10.1016/j.rsma.2021.101903

Ujjania, N. C., Kohli, M. P. S., & Sharma, L. L (2012). Length-weight relationship and condition factors of Indian major carps (*Catlacatla, Labeorohita* and *Cirrhinus mrigala*) in Mahi Bajaj Sagar, India. *Research Journal of Biology*, *2*(1), 30-36.

Wangatia, V. M. (2012). Assessment of parasite infection in Nile Tilapia (*Oreochromis niloticus*) from Ziwa Dam, Eldoret- Kenya.

Community Disaster Interventions (CDI), Kenya; PO Box 36143 – 00200, Nairobi (Kenya). Retrieved from https://www.academia.edu/9481337/Assessment_of_parasite_infec tion_in_Nile_Tilapia_Oreochromis_niloticus_from_Ziwa_Dam_El doret_Kenya

Yilmaz, S., Yazıcıoğlu, O., Erbas_aran, M., Esen, S., Zengin, M., & Polat, N. (2012). Length weight relationship and relative condition factor of white bream, *Blicca bjoerkna* (L., 1758), from Lake Ladik, Turkey. *Journal Black Sea/Mediterranean Environment*, *18*(3)*,* 380–387.

Zar, J.H. (1984). Biostatistical Analysis. Practice Hall, New Jersey, pp. 718.

Zargar, U. R., Yousuf, A. R., Mushtaq, B., & Jan, D. (2012). Length–Weight Relationship of the Crucian carp, *Carassiuscarassius* in Relation to Water Quality, Sex and Season in Some Lentic Water Bodies of Kashmir Himalayas. *Turkish Journal of Fisheries and Aquatic Sciences*, 12: 683-689.

Journal of Experimental Biology and Agricultural Sciences

Acid Rain and Seed Germination: A Predictive Model Using ML-based CART Algorithm

Vasundhara Arora[1], Bikram Jit Singh[2] iD, Navneet Bithel[3] iD, Tapan Kumar Mukherjee[4] iD,
Sushil Kumar Upadhyay[5] iD, Rippin Sehgal[5] iD, Raj Singh[5*] iD

[1]Department of Botany C.C.S. University, Meerut, UP, India
[2]Department of Mechanical Engineering, MM Engineering College, Maharishi Markandeshwar (Deemed to be University) Mullana-Ambala, 133207, Haryana, India
[3]Department of Botany and Microbiology, Gurukul Kangri University, Haridwar -249404, Uttrakhand, India
[4]Department of Biotechnology, Amity University, Major Arterial Road, Action Area II-36, 37, 38, Rajarhat, New Town, Kolkata,West Bengal 700156, India
[5]Department of Bio-Sciences and Technology, Maharishi Markandeshwar (Deemed to be University), Mullana-Ambala, 133207, Haryana, India

ABSTRACT

The impact of acid rain on the germination of seeds is a significant concern in agricultural and environmental studies. Acid rain, characterized by elevated acidity levels due to pollutants like sulfur dioxide and nitrogen oxides, can adversely affect the germination process of various plant species. The objective of this study was to evaluate the impact of simulated acid rain (SAR) on the germination of Brinjal (*Solanum melongena* Linn.) and Cowpea (*Vigna unguiculata* ssp. *cylindrica* L. Walpers) crops. The experiments were conducted using eight plastic trays of approximately 25 cm. x 30 cm dimensions. Four trays were used for experiments with brinjal seeds (Set I), while the other four were used for cowpea seeds (Set II). One tray from each set was used as positive control and treated with normal pH 5.6, while the other three trays from each batch were treated with SAR solutions of pH 4.5, 3.5, and 2.5. Brinjal seed germination percentage and seed vigor were inferior to Cowpea seeds. The seeds treated with SAR (pH 4.5, 3.5, and 2.5) showed hindered seed germination. Furthermore, a more significant inhibitory effect was observed at lower pH values. The mean germination percentage of seeds was highest for standard SAR (pH 5.6) in the case of Brinjal seeds, while it was recorded lowest for Cowpea seeds. The results indicate that plants do not respond uniformly to SAR. To investigate the behavior of the simulated acid rain data, a Machine Learning-based Decision Tree Algorithm was employed to identify and optimize conditions. Cowpea was predicted to get 95% seed germination, whereas brinjal would only

* Corresponding author

E-mail: dr.rajsingh09@gmail.com (Raj Singh)

be 64% in acid rain of pH value 5.05 for 36 hours. In conclusion, utilizing a Machine Learning-based CART algorithm has provided valuable insights into predicting the germination behavior of seeds under the influence of acid rain.

GRAPHICAL ABSTRACT
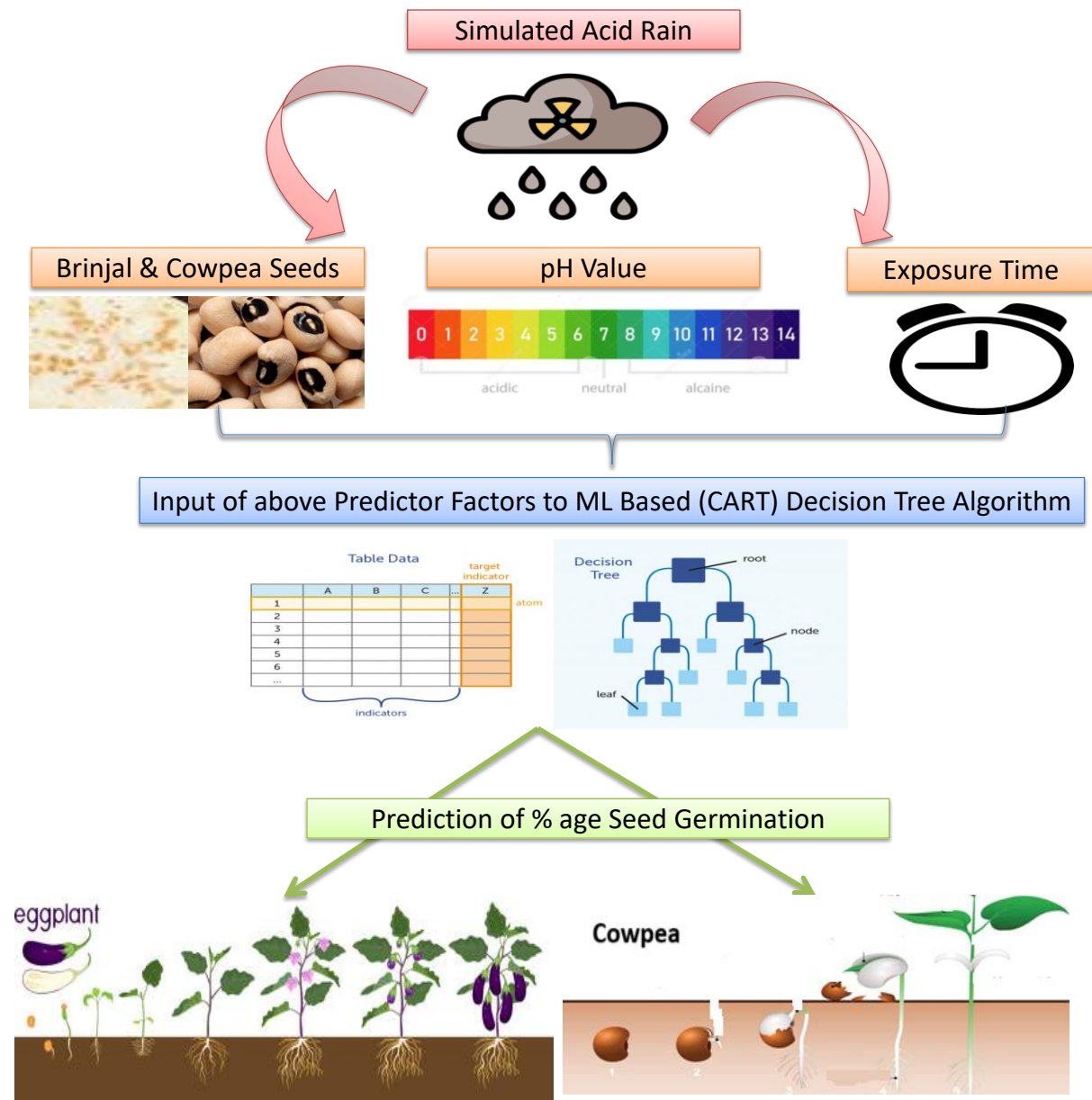
1 Introduction

Acid rain refers to precipitation that contains acidic compounds resulting from various sources. The term "acid deposition" is more accurate, including dry and wet deposition (Lee 1988; Burns et al. 2016). Pure rainwater has a pH of 5.6 as it contains dissolved carbon dioxide, but when the pH of rainwater falls below 5.6, it is referred to as acid rain (Park et al. 2015). In some cases, the pH of rain and fog water can drop as low as 2.2, as reported in Wheeling, West Virginia, and Pitlochry, Scotland (McCormick 2013). The increase in natural water and soil acidity is a global issue due to nitrogen and sulfur oxides resulting from atmospheric pollution

(Shi et al. 2021). The various gases react with water, oxygen, and other chemicals to produce different compounds causing acidity. Among these, H_2SO_4 primarily contributes to acidic precipitation (60-70%), followed by HNO_3 (30-40%) and HCl. Acid rain can also deteriorate monuments and building materials (Altae 2022).

While studying the impact of simulated acid rain on nutrient cycling and the ratios of Mg, Al, Ca, N, and P in tea plants in a subtropical plantation, Hu et al. (2019) found varied effects on plant growth. The levels of Mg and Ca decreased in the soil and within plant tissues with increasing acidity; in contrast, Al concentration increased. The study highlighted the complex interactions between acid rain and nutrient dynamics within the ecosystem and focused on the potential consequences on plant health and soil fertility. Depending on the acidity of precipitation and the plant species being studied, the leaf chlorophyll content was reduced by 6.71% per pH among deciduous species compared to evergreen species. This underscores the differential sensitivity of various plant types to changes in pH levels, emphasizing the need for tailored approaches to understanding and mitigating the impacts of acid rain on diverse ecosystems (Li et al. 2021; Du et al. 2017). Acid rain can cause various adverse effects, including large irregular lesions on leaf surfaces, hyperplasia, hypertrophy, and yield reduction (Arora et al. 2022). Ulrich et al. (1980) reported that changes in soil resulting from acid rain led to the death of fine roots. Some studies have shown the effects of acid rain on seed germination and seedling growth of different plant species, including Anitha and Ramanujam (1992), Verma and Prakash (1999), Tyagi (2006), Akinci and Akinci (2010), and Verma et al. (2010). A few studies have also reported the indirect effects of acid rain on plants through the soil microorganisms and abiotic environment in the soil rhizosphere. Acid deposition affects plant-associated microorganisms' distribution, composition, abundance, function, and activity. It can influence the dynamics of some substances in the soil in ways that may be detrimental to plants (Zhang et al. 2023).'

Some authors have examined the effect of pH and time on the germination of Brinjal and Cowpea seeds. For instance, Kumar et al. (2014) inferred that a pH range of 6-7 was optimal for germinating Brinjal seeds, while Sodhi and Singh (2013) discovered that an incubation period of 24-48 hours was ideal for germinating Cowpea seeds. In the present case, the algorithm's decision criteria for splitting nodes were adapted to access the particularities of brinjal and cowpea. It accounted for factors such as water pH levels and relevant time for each crop. CART can generate trees of varying complexity based on the data and relationships within each crop's ecosystem. The algorithm may discover unique patterns in brinjal and cowpea growth that aren't present in other crops, leading to different tree structures and depths. This enables the creation of models tailored to the intricacies of each crop, leading to more accurate predictions and

actionable insights for optimizing their cultivation. Singh et al. (2018) and Singh and Sodhi (2015) developed a model for predicting Brinjal and Cowpea seed germination based on pH, time, and temperature, respectively. The incidence of acidic rain events has become more frequent in the Indo-Gangetic plains and Indian summer monsoon (Bisht et al. 2015; Majumdar et al. 2022). Industrialization of the National Capital Region in India and burning post-harvested crop residues have significantly contributed to this issue.

Therefore, this investigation evaluated the impact of simulated acid rain on the germination of Brinjal and Cowpea seeds, which are significant crops grown in Meerut, UP, India. This study emphasizes the significance of developing predictive models to forecast germination under different environmental conditions through CART algorithms, which are still to be explored. Gathered experimental data was analyzed appropriately through behavioral and predictive analysis for percentage germination. This study strategically regressed the simulated acid rain data for necessary behavioral investigation. It utilized a corresponding Machine Learning Decision Tree Algorithm to identify and optimize the conditions for properly germinating these plants. This analysis's findings can further help improve crop yield and productivity.

2 Materials and Methods

The seeds of Brinjal (*Solanum melongena* Linn.) and Cowpea (*Vigna unguiculata* L. Wapl.) were obtained from a National Seeds Corporation (NSC), Meerut, Uttar Pradesh, India. Pusa-1 and Gomati varieties of Brinjal and Cowpea were utilized, respectively.

2.1 Preparation of Plant Material

According to the Lee et al. (1980) methodology, approximately 25cm X 30cm eight plastic trays measuring were utilized for this study. The trays were filled with garden soil and kept moist for one week to maintain proper moisture levels. Four trays were designated for the Brinjal seed experiments (Set I), and the remaining four were used for the Cowpea seed experiments (Set II). Each tray of the experimental set I contained 20 seeds arranged in four rows of five seeds each. The seeds were spaced evenly apart. Before sowing, the seeds were sterilized with 0.1% $HgCl_2$ for two minutes and then rinsed thoroughly with distilled water to ensure good health. The trays in Set II were also planted analogously but with Cowpea seeds instead.

2.2 Preparation of Acid Solutions for SAR Experiments

A solution consisting of concentrated H_2SO_4 and HNO_3 (purchased from Merck) in a 7:3 (v/v) ratio was created to conduct the analysis. To obtain the aqueous solutions of predefined pH values (5.6, 4.5, 3.5, and 2.5), the concentrated stock solution was diluted with distilled water following the standard procedure of Lee et al.

(1980). The pH of the working acid solution for SAR experiments was then measured using a digital pH meter (EI-111).

2.3 Treatment of seeds with SAR

In each set, one tray was designated as the control, and the seeds were treated with distilled water, while the other four trays were treated with different pH values. For Set I (with Brinjal seeds), four trays were treated with predefined aquatic solutions of pH 5.6, 4.5, 3.5, and 2.5, respectively. A similar treatment was carried forward for Set II (with Cowpea seeds), respectively.

2.4 The Germination Response of Seeds to SAR

The seeds typically began to sprout within a day, and the emergence of a 1-2mm root was considered a successful germination. The number of germinated seeds was recorded daily until no further germination occurred. The seedlings were given treatments every alternate day, alternating between distilled water and the required solution. This procedure was conducted for six days. The germination percentage, mean germination frequency and seed vigor were calculated using the collected data.

$$\text{Germination percentage} = \frac{\text{Number of seed germinated}}{\text{Total no.of seeds}} \text{ X } 100$$

Mean germination frequency =

$$\frac{\text{Naximum no.of seed germinated}}{\text{Minimum period in which maximum germinatedis achivedv}} \text{ X } 100$$

It represents the rate of germination

The following formula determined seed vigour (an index of seed germination).

$$\text{Seed vigour} = \frac{\sum \text{Quotient of daily counts}}{\text{No.of days of germination}}$$

2.5 Data Analysis Techniques

The data obtained from the seed germination experiment was analyzed using various methods to gain meaningful insights. Multi-regression analysis was used to determine the effect of pH and time on the seed germination percentages for Brinjal and Cowpea plants. Main-effect plots were created to show the variation in germination percentage by considering one factor at a time. Regression statistics were generated to ensure the accuracy of the mode-fitment, and statistical equations were modelled to describe the overall germination behaviour. A heat map was used to illustrate necessary trends and effects.

A Machine Learning (ML) based Classification and Regression Trees (CART) algorithm was used to predict the germination percentage for predictive analysis. This algorithm was used to identify the optimal pH and time conditions for maximum seed germination of Brinjal and Cowpea plants. The CART algorithm

selects a split point for each feature, using a metric such as Gini impurity or information gain to determine the best split. It can handle categorical and continuous input features, missing values, binary and multi-class classification tasks, and regression tasks. The algorithm's output was validated by plotting diagonal scatter plots for actual versus predicted values. Using these tools and techniques will provide a better understanding of the factors affecting seed germination behavior and help to determine optimal conditions for seed germination in agricultural practices.

3 Results

Compared to Cowpea seeds, Brinjal seeds' germination percentage and seed vigor were poorer. The use of SAR (pH 4.5) treatment had a significant inhibitory effect on the germination of both varieties of seeds. The treatment of seeds with higher pH SAR (pH 3.5 and 2.5) also reduced seed germination, with a more significant inhibitory effect observed with decreasing pH levels. In the case of brinjal, the mean germination percentage was highest with standard SAR treatment (pH 5.6) but was lowest for cowpea. A decrease in seed vigour was regularly observed for both plants as the pH decreased. As shown in Table 1, maximum seed vigour was observed in the control (pH 5.6) for both species.

3.1 Findings

The data collected was analyzed in two phases to evaluate the results comprehensively. The first phase focused on comprehending and normalizing the variations in germination related to the independent variables by conducting an appropriate "Behavioral Analysis." In the second phase, "Predictive Analysis" was performed using a Machine Learning (ML)-based Tree Algorithm to make necessary predictions about germination.

3.1.1 Phase-I: Behavioural Analysis

Both inferential and descriptive analyses are important for comprehensively understanding and analyzing data. Descriptive statistics can provide valuable insights into a dataset, such as the results of an experiment that examined the effect of pH, time, and their interaction on the germination percentage of Brinjal and Cowpea plants (Table 1). In this experiment, the predictors or independent variables were the pH levels and time duration, while the dependent variable or response was the germination percentage. The experiment used pH levels of 2.5, 3.5, 4.5, and 5.6 and time durations of 24, 48, 72, 96, 120, and 144 hours (Figure 1).

For brinjal, the germination percentage ranged from 0% to 30%, and for cowpea, it ranged from 10% to 100%. The data in the plot shows that as the pH level and time duration increased, the germination percentage also increased for both the selected plants. Cowpea had a germination percentage of 100% at pH 5.6 and a duration of 120 and 144 hours, while brinjal had a germination

Table 1 Effect of treatment with simulated acid rains (SAR) on germination percentage, mean germination frequency and seed vigour of Brinjal seeds and Cowpea seeds

Responses	Hours	pH							
		Brinjal seeds				Cowpea seeds			
		5.6*	4.5	3.5	2.5	5.6*	4.5	3.5	2.5
Seed Germination in Percentage (%)	24	5.00	Nil	Nil	Nil	40.00	25.00	20.00	10.00
	48	30.00	20.00	10.00	10.00	90.00	50.00	45.00	45.00
	72	30.00	20.00	10.00	10.00	90.00	70.00	70.00	70.00
	96	30.00	20.00	15.00	10.00	95.00	70.00	70.00	70.00
	120	30.00	20.00	15.00	10.00	100.00	70.00	65.00(R)	65.00(R)
	144	30.00	20.00	15.00	10.00	100.00	70.00	65.00(R)	65.00(R)
Mean Germination Frequency		25.00	8.33	3.12	4.16	16.66	19.44	19.44	19.44
Seed Vigor		5.16	3.33	2.16	1.66	15.50	11.83	11.16	11.83

* Treatment with a solution of pH 5.6 is regarded as a control in this experiment; R = Rotting of seedling, and 'Nil' represented no seed germination.
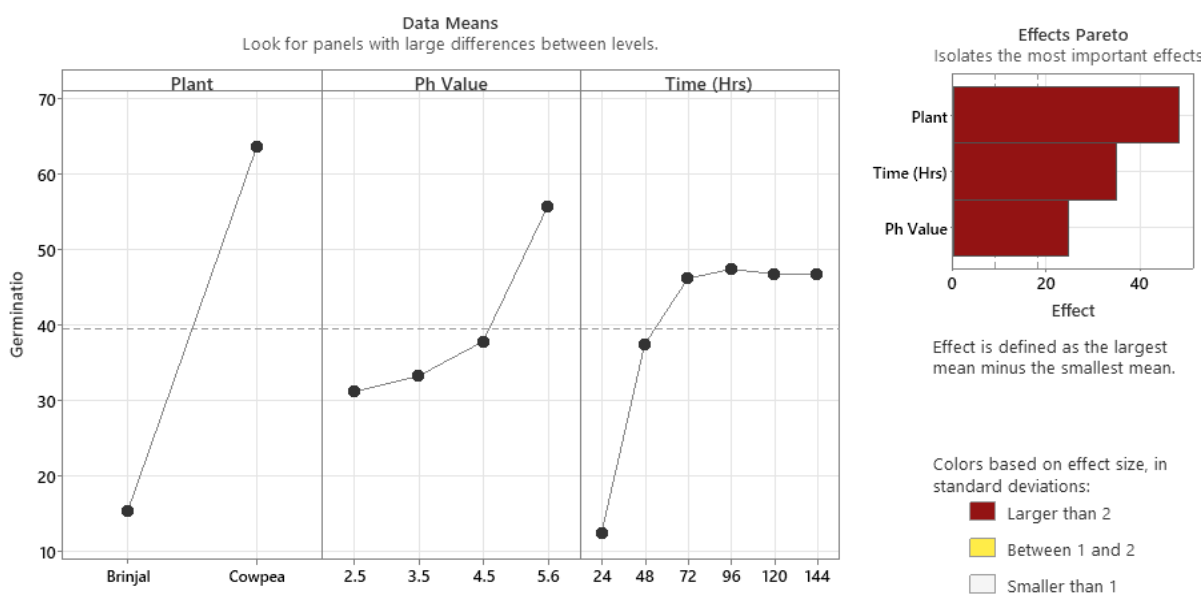
Figure 1 Main Effect Plots for Germination

percentage of only 30% under similar conditions. These data revealed that cowpea had a higher germination percentage than brinjal, which suggested that cowpea was more tolerant to changes in pH levels and time duration. Further, on the right side of the plot, the Pareto chart examines the relative impact of each predictive factor on response (i.e. germination percentage). A Huge difference (more than 40%) was observed due to Plant Type (Cowpea surpassed the brinjal), followed by Time duration (more than 30%) and ended with pH value (more than 20% difference in

germination percentage). Overall, this plot delineates the importance of pH level and time duration on the germination percentage of plants (as observed from the sample data collected) and highlights the differences in germination behavior between different plant species.

Descriptive analysis has some limitations, such as it cannot be used to generalize findings beyond the collected dataset and does not provide a basis for making predictions or drawing inferences about
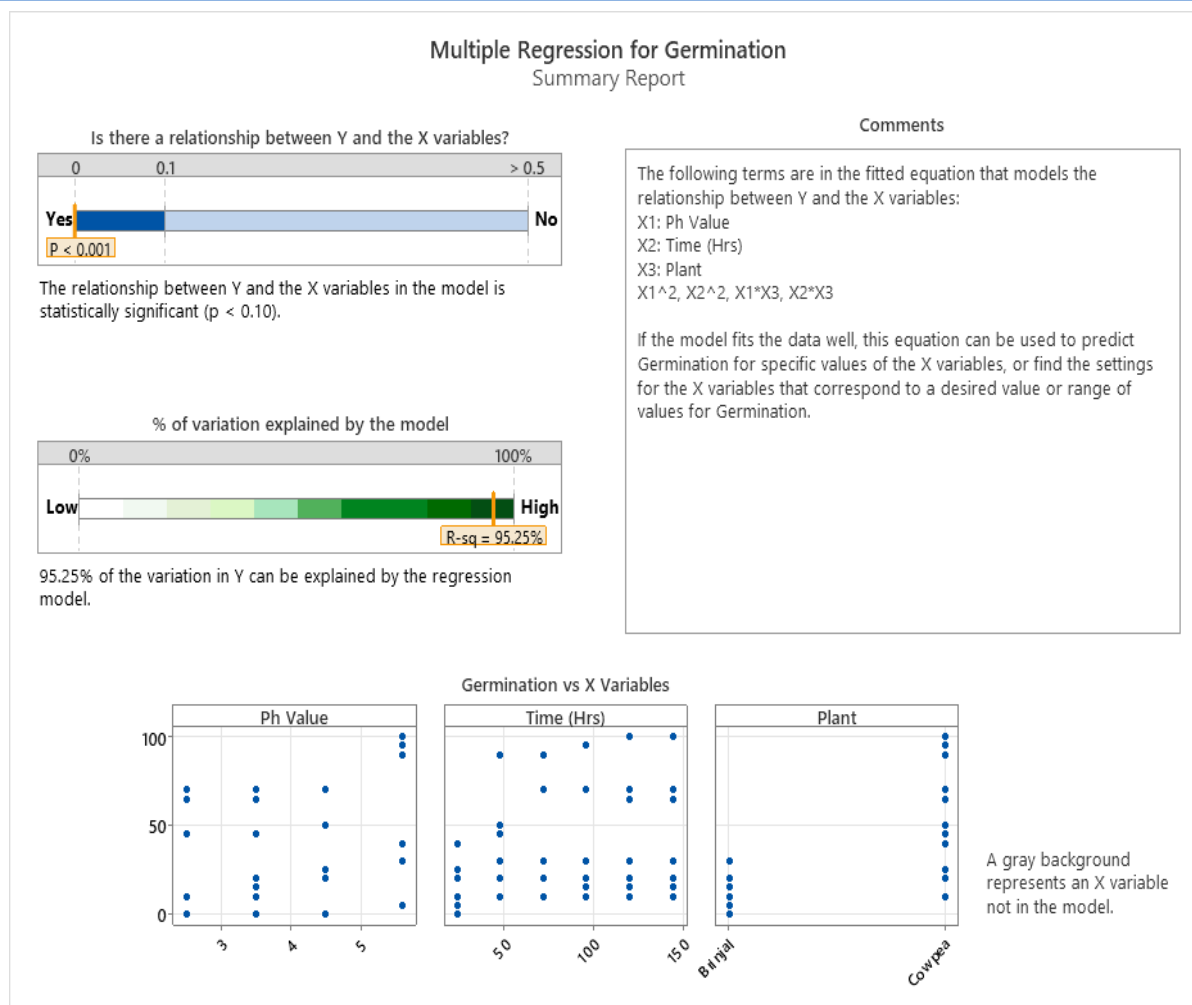
Figure 2 Summary Report for Percentage Germination

the population from which the data was collected. On the other hand, inferential statistics can help to determine the significance of differences or relationships observed in a dataset and can be used to make predictions and draw conclusions about a population. Cowpea was more sensitive to acid rain than brinjal, while percentage germination increased in both crops with increased pH value and time. However, it enhanced abruptly when pH varied from 4.5 to 5.6 and time raised to 72 hours, respectively.

This regression output from Minitab statistical software presents a regression model's coefficients and statistical information (Figure 2). The coefficient for pH Value is -21, which means that for every unit increase in the pH value, the predicted value of the response variable (percentage germination) decreases by 21 units, holding all other variables constant. This coefficient is statistically significant at the 0.05 significance level (p-value = 0.047). The coefficient for Time (Hrs.) is 1.086, which suggests that for every one-hour increase in time, the predicted value of the response variable increases by 1.086 units, holding all other variables

constant. This coefficient is also statistically significant (p-value = 0). The regression model incorporates a categorical predictor variable named "Plant," encompassing two levels: Brinjal (used as the reference level) and Cowpea. The coefficient for the Cowpea level of the Plant variable is 48.33, which means that the predicted value of the response variable for cowpea is higher than brinjal by 48.33 units, holding all other variables constant.

The model includes interaction terms between pH Value and Time (Hrs.). The coefficient for the pH Value*pH Value interaction term is 3.53, which means that the effect of pH Value on the response variable changes depending on the level of pH Value. This coefficient is statistically significant (p-value = 0.007). The coefficient for the Time (Hrs.)*Time (Hrs.) interaction is 0.005038, which means that the effect of Time (Hrs.) on the response variable changes depending on the level of Time (Hrs.). This coefficient is also statistically significant (p-value = 0). Overall, all the Xs and their squares substantially relate to the given Y (as p-value < 0.001). The R-squared (R-sq) value is
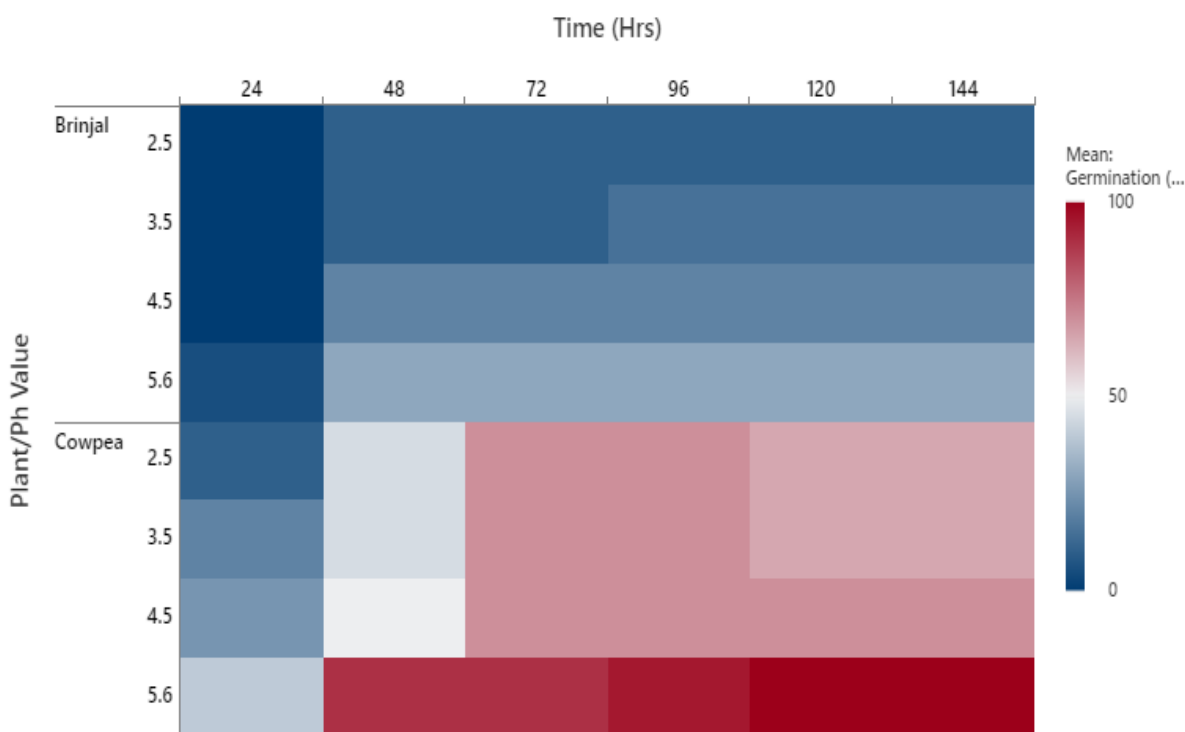
Figure 3 Heat Map for Percentage Germination

92.25%, indicating that the predictor variables can explain 92% of the variation in the response variable. In brief, the high R-squared and adjusted R-squared values indicate that the predictor variables in the model are good at explaining the variation in the response variable, and the model has an excellent fit to the data. Necessary variations of all the independent variables concerning the dependent one have been plotted in Figure 2.

For more precise insights, a heat map has been delineated between predictors (pH level and Duration) and response (Germination in percentage) with 95% confidence (Figure 3). These maps are graphical representations of data that use colors to indicate the magnitude of a variable.

According to Borner and Chen (2018), heat maps are a valuable tool for identifying patterns and trends in large data sets, as they allow for easy identification of areas of high or low response values. In a heat map, the intensity of the color corresponds to the value of the variable being represented. In a heat map of germination data, areas with a high percentage of germination would be represented by intense colors (red), while cooler areas would be represented by less intense colors (blue). According to Schiffer and Ha (2017), using color in heat maps can make it easier for users to identify patterns and trends in the data. Results presented in Figure 3 revealed that in cowpeas with a pH value of 5.6, maximum germination would be found in the time range from 48 hrs to 144 hrs, while the brinjal has only 50% germination at these predictor settings. The colour scale is used for percentage germination (shown on the left side of the map) for necessary interpretation. The decrease in pH will decrease germination capability in both plants. Time after around 72 hrs did not have much effect on brinjal, whereas Cow pea shows a continuous increase in germination up to 144 hrs. The two-dimensional map region is suitably divided among assorted colour shades (highlighting various levels of percentage germination) for corresponding predictor values.

To generalize, necessary statistical equations generated by Minitab at the end have been used (Figure 4). Two independent quadratic equations for predicting germination behaviour (w.r.t each plant) have been regressed with 95% confidence.

These equations have quantified the behavior of percentage germinations for each plant w.r.t. pH and time suitably and will provide needed information to practitioners or bio-scientists for future research. In the case of brinjal, percentage germination was directly proportional to pH value and its square, whereas cowpea showed inversely proportional relation with pH value but directly proportional to time and its quadratic term. The square of pH value also directly highlighted its relation with germination, which made it more sensitive than brinjal. Regression models allow us to understand the relationships between the predictor and response variables. This can provide insights into the factors that influence the response variable (Germination) and help identify areas for improvement.

X1: Ph Value   X2: Time (Hrs)   X3: Plant

Plant	Final Equations
Brinjal	Germination (%) = $9.6 - 22.97 X1 + 0.956 X2 + 3.534 X1^2 - 0.005038 X2^2$
Cowpea	Germination (%) = $20.1 - 18.98 X1 + 1.215 X2 + 3.534 X1^2 - 0.005038 X2^2$

Figure 4 Modelled Equations for Brinjal and Cowpea Plants

3.1.2 Phase-2: Predictive Analysis

Predictive analysis through machine learning (ML) based Tree Algorithms has become popular in various fields, including biosciences, biomaterials, finance, healthcare, and marketing (Qian et al. 2020). Tree Algorithms, such as Decision Trees and Random Forests, can handle categorical and continuous variables, making them highly versatile and effective for predicting outcomes (Yin et al. 2019). The ML-based Decision Tree Algorithm has been applied in the present case for more accurate and precise predictions for percentage germination. It will help predict germination percentage in plants exposed to environmental stressors such as acid rain. The model will utilize under-study predictors such as pH value, time of exposure and plant species to provide accurate predictions. Using such models can assist farmers and scientists in understanding the impacts of acid rain on plant growth and provide insights into potential mitigation strategies.

Table 2 provides information related to the Classification and Regression Trees (CART) Algorithm to predict the germination percentage of plants based on their pH value, time (hours), and type of plant. The CART® method uses node splitting to divide the data into smaller groups based on the independent variables. The splitting is done so that the variability within the groups is minimized. The method uses the least squared error to select the best split at each node. The breakup of that results in the lowest sum of squared errors is chosen. The analysis identifies the optimal tree that best fits the data.

Table 3 encapsulates the response (Percentage germination) for the given dataset. The percentage germination has a mean of 39.5%, a standard deviation of 30.35, and ranges from 0 to 100, respectively. The first quartile (Q1) is 11.25, the median is 30, and the third quartile (Q3) is 70 for germination. This table provides valuable information on the response variable's central tendency, variability, and range. The mean and median values give an idea of the typical value of the response variable, while the standard deviation indicates the degree of variation in the data. The quartile values provide information on the data's spread and help identify outliers.

In conclusion, this information can help understand the distribution of the percentage germination variable and select appropriate statistical methods for predicting the data suitably. Next, a line plot (Figure 5) has been drawn with R-squared values (in percentage) and the Number of Terminal Nodes (of a corresponding Tree Diagram).

The Minitab provides different tree structures for appropriate decision-making at different Number of Nodes, but the best fit will be the one having maximum R-squared value with minimum nodes (complexity). In the current study, the 4-Node Tree Diagram has been shortlisted for further predictions, as it will provide around 81.9% R-squared value with a less complex tree structure.

The Optimal Tree Diagram for percentage germination has been delineated through Minitab, as it is a helpful tool for decision-making since it allows the visualization of the decision tree model and helps identify the critical variables and their relationships to the outcome variable (Figure 6). The diagram provides a clear and intuitive representation of the decision-making process and helps identify the optimal path (based on the available data). The decision

Table 2 4 Node CART Regression Settings for Percentage Germination

Node splitting	Least squared error
Optimal tree	Within 1 standard error of maximum R-squared
Model validation	10-fold cross-validation
Rows used	48

Table 3 Response Information

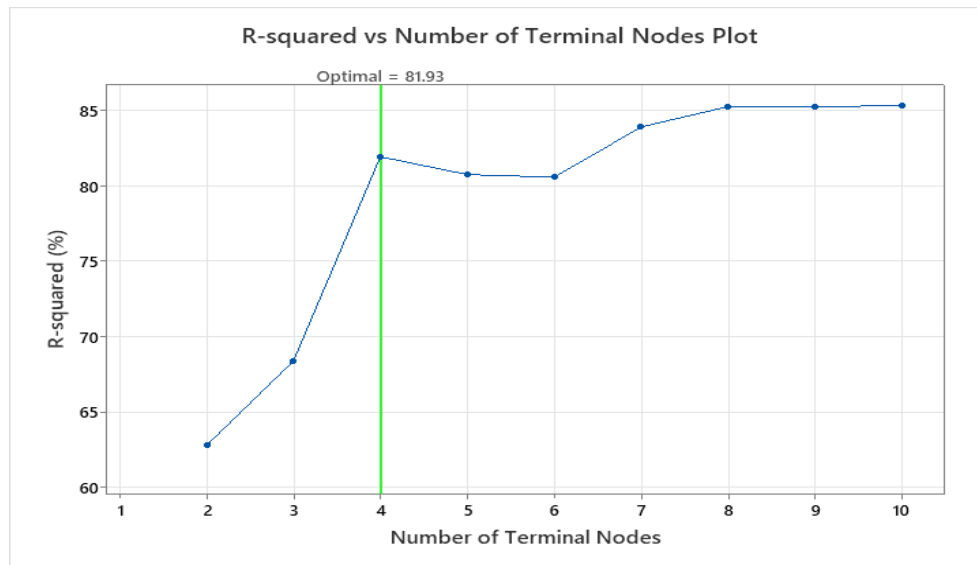| Mean	StDev	Minimum	Q1	Median	Q3	Maximum
39.5833	30.3496	0	11.25	30	70	100

Figure 5 Line Plot to Select Optimal Decision Tree
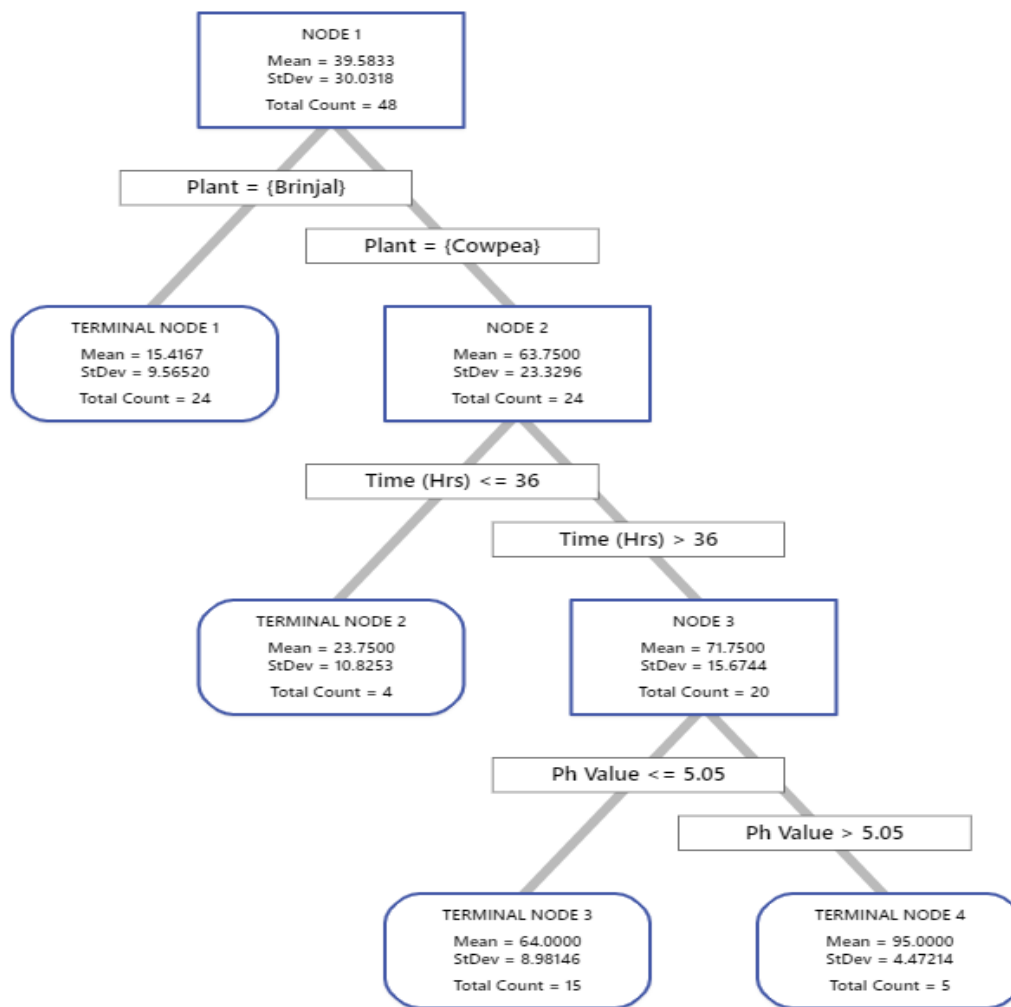
Figure 6 Optimal Decision Tree

Table 4 Model Summary While Training and Testing

Total predictors	3	
Important predictors	3	
Number of terminal nodes	4	
Minimum terminal node size	4	

Statistics	Training	Test
R-squared	90.82%	81.93%
Root mean squared error (RMSE)	9.0997	12.7670
Mean squared error (MSE)	82.8038	162.9955
Mean absolute deviation (MAD)	7.3056	8.8456
Mean absolute percent error (MAPE)	0.3030	0.3352

tree algorithm is a machine learning technique that recursively partitions data based on feature values, creating a tree-like structure to make decisions or predictions. Several studies have demonstrated the usefulness of Optimal Tree Diagrams in decision-making (De Ste Croix et al. 2016). The optimal tree diagram aims to predict the percentage germination of Brinjal and Cowpea plants under different conditions of pH value and time (in hours) using a dataset of 48 observations. The tree starts at Node-1, which represents the mean and standard deviation of the response variable (percentage germination) for the entire dataset. The mean percentage germination for the dataset is 39.58%, and the standard deviation is 30.03. The tree splits into two branches based on the type of plant, i.e. Brinjal and Cowpea.

Terminal Node-1 represents the mean and standard deviation of the response variable for the subset of observations that correspond to Brinjal plants. The mean percentage germination for Brinjal plants is 15.41, and the standard deviation is 9.56. Node-2 represents the mean and standard deviation of the response variable for the subset of observations that correspond to Cowpea plants. The mean percentage germination for Cowpea plants is also 15.41, and the standard deviation is 9.56. Further, The tree splits the Cowpea branch into two branches based on the time (in hours) variable. Terminal Node-2 represents the mean and standard deviation of the response variable for the subset of observations corresponding to Cowpea plants exposed to less than or equal to 36 hours of simulated acid rain. The mean percentage germination for these plants is 23.75, and the standard deviation is 10.82. The total count of observations in this terminal node is 4. Node-3 represents the mean and standard deviation of the response variable for the subset of observations corresponding to Cowpea plants exposed to more than 36 hours of simulated acid rain. The mean percentage germination for these plants is 71.7, and the standard deviation is 15.67. The total count of observations in this node is 20.

Finally, Node-3 is split into two terminal nodes based on the pH value variable. Terminal Node-3 represents the mean and standard

deviation of the response variable for the subset of observations corresponding to Cowpea plants that were exposed to more than 36 hours of simulated acid rain and had a pH value of less than or equal to 5.05. The mean percentage germination for these plants is 64, and the standard deviation is 8.98. The total count of observations in this terminal node is 15. Terminal Node-4 represents the mean and standard deviation of the response variable for the subset of observations corresponding to Cowpea plants exposed to more than 36 hours of simulated acid rain and with a pH value of more than 5.05. The mean percentage germination for cowpeas is 95, and the standard deviation is 4.472. The total count of observations in this terminal node is 5. This decision tree can help predict Brinjal and Cowpea plants' percentage germination under different pH values and time conditions. It can also be used to identify which factors are most important in predicting germination, as the tree splits are based on the importance of these variables.

Further, Table 4 quoted the model summary for a decision tree model with three important predictors and four terminal nodes. The model has been evaluated on both training and test data. The R-squared value for the training set is 90.82%, indicating that the model explains a substantial portion of the variance in the data. The R-squared value for the test set is slightly lower at 81.93%, indicating that the model may have some degree of overfitting. The root mean squared error (RMSE) is 9.0997 for the training set and 12.7670 for the test set. The lower RMSE value for the training set suggests that the model fits the training data better than the test data.

The mean squared error (MSE) is 82.8038 for the training set and 162.9955 for the test set. This indicates that the model has a higher error level on the test set than the training set. The mean absolute deviation (MAD) is 7.3056 for the training set and 8.8456 for the test set. The mean absolute percent error (MAPE) is 0.3030 for the training set and 0.3352 for the test set. These values measure the model's accuracy in predicting the response variable. In brief, the
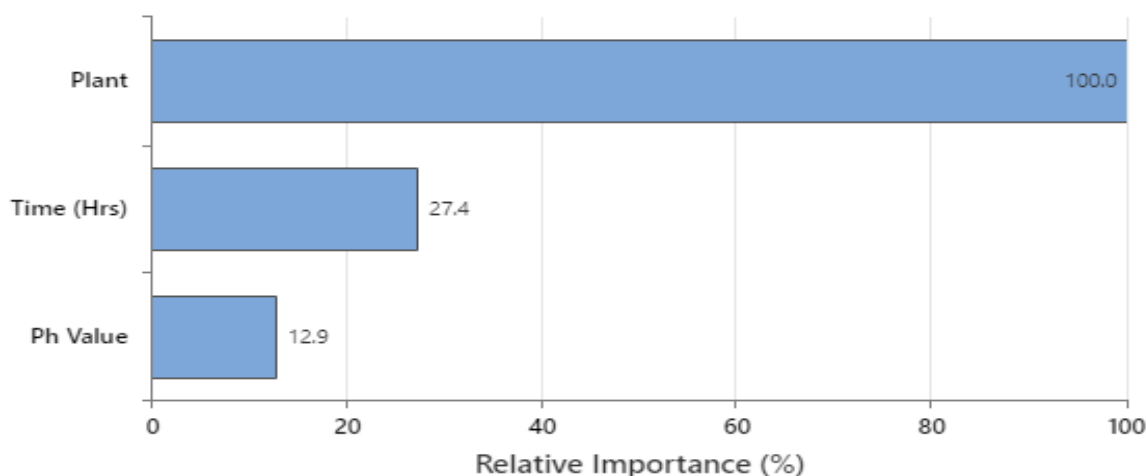
Variable importance measures model improvement when splits are made on a predictor. Relative importance is defined as % improvement with respect to the top predictor.

Figure 7 Relative Significance of Predictors

model seems to perform well on the training set but may have some degree of overfitting (which can be ignored). The performance on the test set is slightly lower, indicating that the model may not generalize well to new data, but it is insufficient to add any substantial error in the final prediction.

Additionally, the relative importance of predictors is determined based on their contribution to the model's predictive accuracy. It helps to identify the most important predictors that significantly impact the response variable and can be used to improve the model's accuracy. The horizontal bar graph illustrated in Figure 7 uncovered that the top predictor is 'Plant' with a relative

importance of 100%, which means that it has the highest impact on the response variable compared to other predictors.

The relative importance of 'pH value' is 12.9%, and the relative importance of 'Time (Hrs.)' is 27.4% respectively. This suggests that both 'pH Value' and 'Time (Hrs.)' also have some influence on the response variable (percentage germination), but they are not as significant as the 'Plant' predictor.

In the CART (Classification and Regression Tree) algorithm, the scatter plots of response fits versus actual values are used to evaluate the performance of the model (Figure 8). These plots
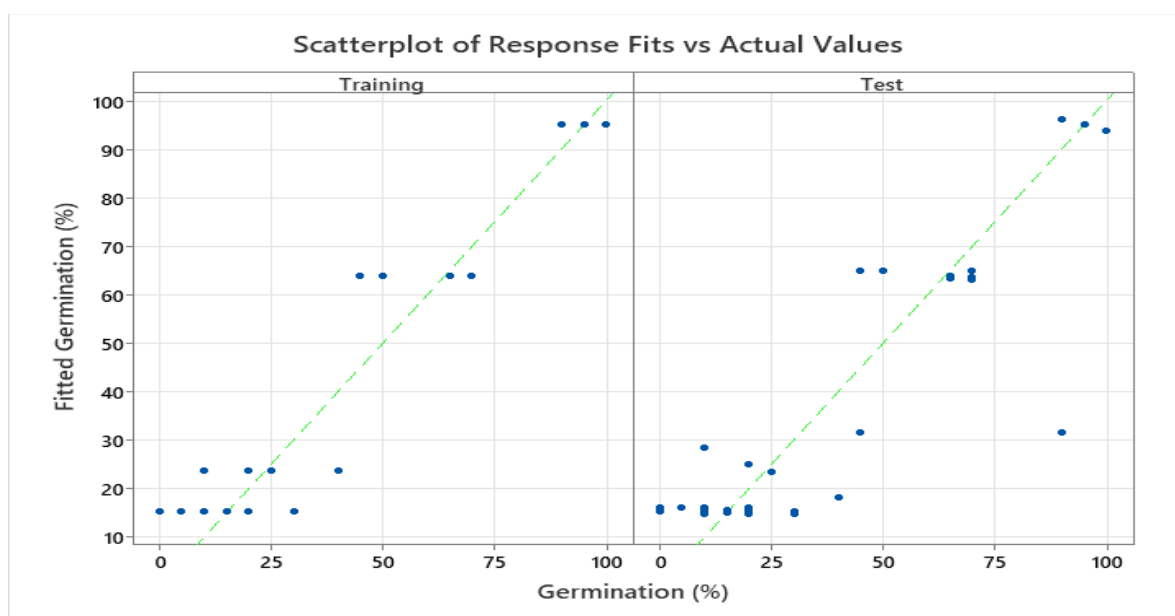

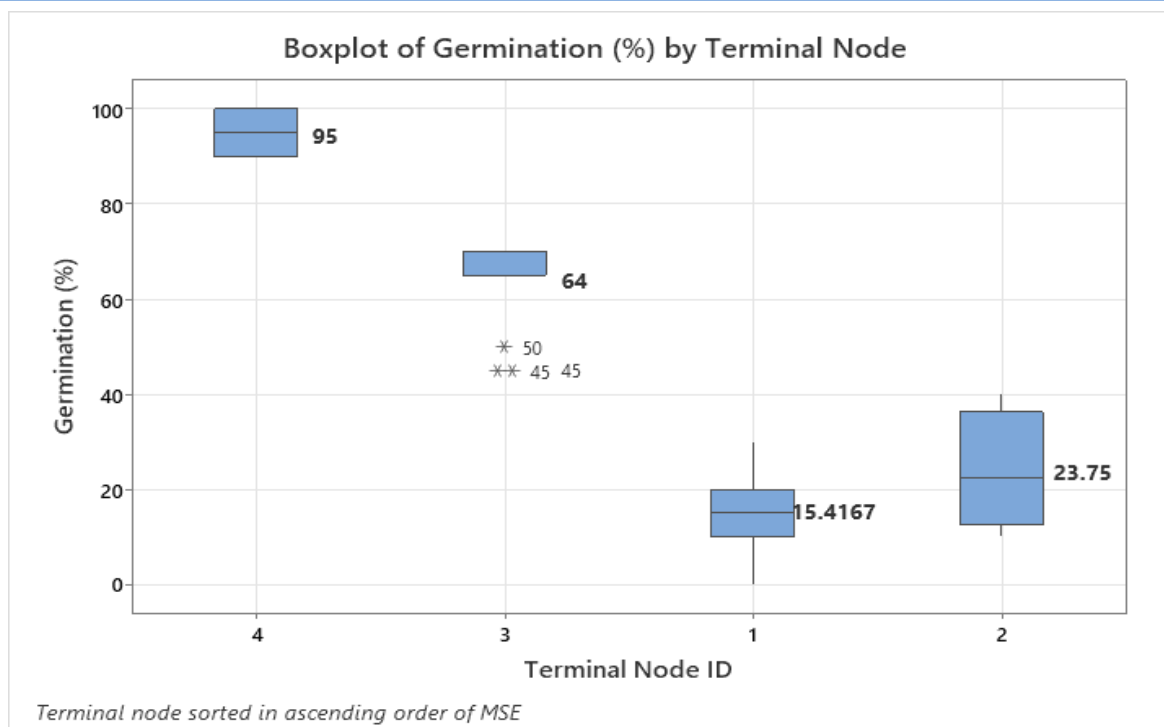Figure 8 Scatter Plots for Testing and Training

Figure 9 Boxplot for Percentage Germination w.r.t. Nodes

pointed out the relationship between the predicted response (% age germination) values and the actual response values, while model building (testing) and actual execution (training), respectively. In a scatter plot, the predicted response values are plotted on the x-axis, and the actual response values are plotted on the y-axis. In the present scenario, the points on the scatter plot fall on or around the diagonal line, which indicates a sufficient match between the predicted and actual response values.

The scatter plot allows us to visually examine the pattern of errors and identify any systematic deviations or outliers. These scatter plots are a valuable tool for evaluating the accuracy of the CART model and identifying areas for further improvement.

The box plot in Figure 9 illustrates the mean germination percentage and the maximum and minimum feasible germination percentages for four different nodes. The nodes represent various combinations of the independent variables, essential germination predictors (Figure 6). Node-1 has a mean germination percentage of 15.42%, less than the minimum feasible germination percentage of 30%. This suggests that the conditions represented by Node-1 are not favorable for germination. Similarly, Node-2 has a mean germination percentage of 23.75%, within the feasible range of 10-40%. This suggests that the conditions represented by Node-2 are favorable for germination but not optimal. Similarly, Node-3 has a mean germination percentage of 64%, within the feasible range of 45-70%. This suggests that the conditions represented by Node-3 are quite favorable for germination. Lastly, Node-4 has a mean

germination percentage of 95%, close to the maximum possible germination percentage of 100%. This suggests that the conditions represented by Node-4 are optimal for germination.

In concisely, the analysis of these nodes suggests that the independent variables used in this study significantly impact germination and that specific combinations of these variables are more favorable for germination than others.

Finally, the study results provide predictive data on the germination of Brinjal and Cowpea plants under different pH values, time intervals, node numbers and actual germination percentages. For Brinjal plants, the pH values range from 2.5 to 5.6, the time intervals range from 24 to 144 hours, and the node number is constant at 1. The actual germination percentages range from 0.0% to 30.0%, while the predicted percentage is constant at 15.4%. Cowpea plants' pH values also range from 2.5 to 5.6, the time intervals range from 24 to 144 hours, and the node number ranges from 2 to 4. The actual germination percentages range from 10.0% to 100.0%, while the predicted germination percentage is constant at 95.0% for node number 4 and 64.0% for node numbers 2 and 3. Overall, the table suggests that pH values and time intervals substantially impact the germination of Brinjal and Cowpea plants. However, the predicted germination percentage is constant across different pH values, time intervals, and node numbers, suggesting that other factors may play a role in determining the actual germination percentage.

4 Discussion

The present study aimed to investigate the effects of pH and time on the Brinjal and Cowpea plant's germination percentage. The study utilized both behavioral analyses by regression and predictive analysis by ML-based Decision Tree Algorithm to understand the relationship between the variables and their impact on germination. The behavioral analysis showed that pH and time significantly impacted the germination percentage of both Brinjal and Cowpea. The regression analysis showed that the R-squared values for both plants were significant, indicating that the model could explain considerable variation in the data. The results indicated that pH positively affected the germination percentage of both plants, with a pH range of 5-7 being the most favorable for germination (Smith et al. 2018). Moreover, the time variable also positively impacted the germination percentage of both plants. The results showed that the germination percentage increased with time up to a certain limit, after which it decreased. This was agreed with previous studies that reported time's effect on seed germination (Kaur et al. 2016).

In the present study, pH 5.6 was taken as the reference point. Differing viewpoints exist concerning the pH value selected as the reference (control) for investigating the impact of SAR on plants. While Sequeira (1982) and Charlson and Rhode (1982) express reservations about the suitability of pH 5.6 as the baseline reference, several researchers in previous studies have adopted pH 5.6 as the established control point. Like any other pollutant, SAR also may affect plants at any stage of development. Since seed germination is the first step in the life cycle of a seed plant, it was decided to study the effects of acid precipitation on the seed germination of Brinjal and Cowpea.

There are conflicting reports as far as the effect of simulated acid rain on the germination behavior of crop seeds is concerned. Various studies have reported a positive impact of acidity on the vigour and viability of crop seeds. In this concern, Baldwin (1934) reported that the seeds of *Picea rubra* germinate better in acidic conditions. Similarly, Verma and Prakash (1999) recorded stimulation in the germination of Cowpea seeds at pH 4.5 (though a decrease was observed at lower pH 3.5 and 2.5). Goubitz et al. (2003) and Perez-Fernandez et al. (2006) believed that acidic pH negatively affects seed germination in *Pinus alpensis*. The results of the present study revealed that the germination percentage of seeds of both the plants (Brinjal and Cowpea) was much lesser in trays treated with SAR pH 4.5 than those with SAR pH 5.6.

In the present study, rotting was observed in some Cowpea seeds germinating in solutions at pH 3.5 and 2.5. It is possible because tissue hardening does not occur much at the seedling stage. Yuan et al. (2011) observed that simulated acid rain of pH 2.5 seriously decreased the maize seed germination. The seedlings

with softer tissues are more prone to adverse effects of acidic solutions. However, this issue requires further analysis and intensive investigation. The inhibitory action of SAR on the seed germination process has been attributed to the presence of bio-toxic radicals, i.e. sulfite and bisulfate, which alter the seed water interaction necessary for ongoing enzyme activity. Acid rain is an abiotic hazard that affects the growth and development of endogenous hormones, photosynthesis, antioxidant defence and molecular mechanisms under elevated acid rain (Debnath et al. 2023).

The impact of simulated acid precipitation on seed germination of Brinjal and Cowpea has sparked conflicting findings within the scientific community. While some studies indicate detrimental effects on germination behavior, others suggest limited or positive effects. This disparity can be attributed to factors like Acid Rain Composition, Soil characteristics and Crop variability. Acid rain is a complex mixture of acidic components. The specific chemical composition, including sulfur dioxide (SO_2) and nitrogen oxides (NOx), along with other pollutants, can vary widely based on geographical location and industrial activities (Wang et al., 2020). This variability can lead to different effects on seed germination. Similarly, other crops respond differently to environmental stressors. Brinjal and cowpeas may exhibit varying sensitivities to acid rain due to differences in genetics, physiological traits, and inherent tolerance levels (Bhattacharya 2022). Soil pH, composition, and nutrient levels can mediate the effects of acid rain on seeds. Altered soil conditions can either amplify or mitigate the impact of acidity on germination (Yadav et al. 2020). The predictive analysis was conducted using an ML-based Decision Tree Algorithm to predict the germination percentage of Brinjal and Cowpea plants based on pH and time variables. The results showed that the Decision Tree Algorithm could predict the germination percentage of both plants with a high degree of accuracy. These findings align with previous studies that have reported the effectiveness of Decision Tree Algorithms in predicting plant growth (Zhang et al. 2019). Like any other pollutant, SAR may also affect plants at any stage of plant development; it was decided to study the effects of acid precipitation on seed germination development. The seed germination is the first step in the life cycle of a seed of Brinjal and Cowpea. The germination percentage of seeds of both the plants (Brinjal and Cowpea) was much lesser in trays treated with SAR pH 4.5 than those with SAR pH 5.6. The inhibitory effect was quite marked. The lower the SAR pH, the more seed germination inhibition. It can be concluded that all the plants do not respond to SAR uniformly. The present study observed rotting in some Cowpea seeds germinating in pH 3.5 and 4.5 solutions. The seedling also suffered rotting at pH 3.5 and 2.5. It is possible because tissue hardening does not occur much at the seedling stage. The seedlings with softer tissues are more prone to adverse

effects of acidic solutions. However, these issues require further analysis and intensive investigation.

The present study explored the effect of pH and time on the germination of Brinjal and Cowpea plants. The results showed that both pH and time significantly impacted the germination of these plants. Specifically, a pH of 7 was optimal for Brinjal and Cowpea seeds germination, while the germination rate decreased at extreme pH values. Moreover, the germination rate increased with time, up to a certain point, and then plateaued. Furthermore, regression analysis was employed to determine the relationship between the dependent (percentage germination) and independent variables (pH and time). The analysis revealed a significant linear relationship between pH and percentage germination, indicating that the germination rate increased as pH approached the optimal value of 7. Additionally, the predictive analysis using the decision tree algorithm demonstrated that pH was the most important variable in predicting the germination rate of these plants.

Conclusions

These findings have important implications for agriculture in optimizing the germination of Brinjal and Cowpea plants. Farmers can maximize the yield and quality of these crops by controlling the pH and time of germination. Additionally, machine learning algorithms can help predict the germination rate of these plants under different conditions, thereby providing valuable insights for plant breeders and researchers. The present study has highlighted the significance of pH and time in the germination percentage of Brinjal and Cowpea plants. The study utilized behavioral and predictive analysis to understand the relationship between the variables and their impact on germination. Farmers and agricultural researchers can use the findings to optimize the growth conditions of these important vegetable and fodder crop plants. Further research could explore the effect of other variables, such as temperature and light, on the germination of these plants. Overall, the present study contributes to our understanding of the factors that affect the germination of Brinjal and Cowpea plants and provides a foundation for future research in this area.

Acknowledgements

Conflict of Interest

The authors declare no conflict of interest.

Data availability

The data can be supplied as a supplementary file.

Funding Information

References

Akinci, I. E., & Akinci, S. (2010). Effect of chromium toxicity on gormination and early seedling crowth in melon (*Cucumis melo* L.). *African Journal of Biotechnology*, *9*, 4589- 4594.

Altae, M. (2022). Study of the effect of acid rain prepared in the laboratory on building materials in Salah Al-Din/Iraq. *British Journal of Global Ecology and Sustainable Development*, *3*, 18-31.

Anitha, P. C., & Ramanujam, M. P. (1992). Impact of simulated acid rain on germination and seedling growth of groundnut. *Advances in Plant Sciences*, *5*, 180- 186.

Arora, V., Singh, B. J., Bithel, N., Malik, N., Upadhyay, S. K., & Singh, R. (2022). Effect of simulated acid rain on plant growth behaviour of *Solanum melongena* Linn. and *Vigna unguiculata* ssp *cylindrica* (L.) Walp. *Environment, Development and Sustainability*, 1-29. https://doi.org/10.1007/s10668-022-02726-4

Baldwin, H. I. (1934). Germination of red spruce. *Plant Physiololgy, 9,* 491-532.

Bhattacharya, A. (2022). Effect of low-temperature stress on germination, growth, and phenology of plants: A review. In A. Bhattacharya (eds) *Physiological processes in plants under low temperature stress*, (pp. 1-106), Singapore Springer. DOI: https://doi.org/10.1007/978-981-16-9037-2_1.

Bisht, D. S., Tiwari, S., Srivastava, A. K., Singh, J. V., Singh, B. P., & Srivastava, M. K. (2015). High concentration of acidic species in rainwater at Varanasi in the Indo-Gangetic Plains, India. *Natural Hazards*, *75*(3), 2985-3003.

Borner, K., & Chen, C. (2018). Visualization. In A. Pertti, B. Leonard, & B. Julia B (Eds), the SAGE handbook of social research methods (pp. 303-326). Sage Publications. DOI: https://doi.org/10.4135/9781446212165.

Burns, D. A., Aherne, J., Gay, D. A., & Lehmann, C. (2016). Acid rain and its environmental effects: Recent scientific advances. *Atmospheric Environment*, *146*, 1-4.

Charlson, R. J., & Rhode, H. (1982). Factors controlling the acidity of natural rainwater. *Nature*, *295*, 683-685.

Debnath, B., Akhi, M. Z., Rob, M. M., Sikder, A., Rahman, M. M., Islam, M. S., & Ahammed, G. J. (2023). Role of Phytohormones in

Plant Responses to Acid Rain. In *Plant Hormones and Climate Change* (pp. 95-124). Singapore: Springer Nature.

De Ste Croix, M., Armstrong, N., Welsman, J., & Sharpe, P. (2016). Longitudinal changes in physical activity levels in children and adolescents. *Sports Medicine*, *46*(11), 1493-1518.

Du, E., Dong, D., Zeng, X., Sun, Z., Jiang, X., & de Vries, W. (2017). Direct effect of acid rain on leaf chlorophyll content of terrestrial plants in China. *Science of the Total Environment*, *605*, 764-769.

Goubitz, S., Werger, M. J. A., & Neeman, G. (2003). Germination response to five related factors of Seeds from non-serotinous and serotinous cones. *Plant Ecology*, *169*, 196-204.

Hu, X. F., Wu, A. Q., Wang, F. C., & Chen, F. S. (2019). The effects of simulated acid rain on internal nutrient cycling and the ratios of Mg, Al, Ca, N, and P in tea plants of a subtropical plantation. *Environmental monitoring and assessment, 191*(2), 1-14.

Kaur, G., Asthir, B., & Bains, N. S. (2016). Influence of temperature and light on seed germination of wild marigold (*Tagetes minuta* L.). *International Journal of Applied and Pure Science and Agriculture*, *2*(8), 58-64.

Kumar, A., Singh, R. K., & Singh, P. (2014). Effect of pH and temperature on germination and growth of Brinjal (*Solanum melongena* L.) seedlings. *International Journal of Agriculture, Environment and Biotechnology*, *7*(3), 551-556.

Lee, J. (1988). Acid rain'. *Biological Sciences Review*, *1*, 15-18.

Lee, J. J., Neely, G. E., Perrigan, S. C., & Grothaus, L. C. (1980). Effects of simulated sulfuric acid rain on yield, growth, and foliar injury of several crops. United States. https://doi.org/10.2172/6560198.

Li, Y., Li, T., Zhao, D., Wang, Z., & Liao, Y. (2021). Different tillage practices change assembly, composition, and co-occurrence patterns of wheat rhizosphere diazotrophs. *Science of the Total Environment*, *767*, 144252.

Majumdar, A., Samanta, D., & Das, R. (2022). Chemical Characteristics and Trends of Indian Summer Monsoon Rainfall: A Review. *Aerosoland Air Quality Research*, *22*, 220019. https://doi.org/10.4209/aaqr.220019

McCormick, J. (2013). Acid Earth: the global threat of acid pollution. Routledge.

Park, S. M., Seo, B. K., Lee, G., Kahng, S. H., & Jang, Y. W. (2015). Chemical composition of water-soluble inorganic species in precipitation at Shihwa Basin, Korea. *Atmosphere*, *6*(6), 732-750.

Perez Fernandez, M. A., Calvo-Magro, E., Montanero Fernandez, J. & Oyala-velasco, J. A. (2006). Seed germination in response to chemicals: effect of nitrogen and pH in the media. *Journal of Environmental Biology, 27*, 13-20.

Qian, G., Yang, N., Ma, A. H. Y., Wang, L., Li, G., Chen, X., & Chen, X. (2020). COVID-19 transmission within a family cluster by presymptomatic carriers in China. *Clinical Infectious Disease, 71*(15), 861-862.

Schiffer, M., & Ha, U. H. (2017). Heat maps. Wiley Statsref: Statistics Reference Online. doi: 10.1002/ 9781118445112.stat06596

Sequeira, R. (1982). Acid rain: an assessment based on acid-base considerations. *JAPCA, 32*, 241-245.

Shi, Z., Zhang, J., Xiao, Z., Lu, T., Ren, X., & Wei, H. (2021). Effects of acid rain on plant growth: A meta-analysis. *Journal of Environmental Management, 297*, 113213.

Singh, S., & Sodhi, Y. S. (2015). Predictive models for germination and emergence of cowpea. *Journal of Agricultural Science*, *7*(9), 105-117.

Singh, S., Singh, R. K., & Singh, P. (2018). Predictive model for germination of Brinjal (*Solanum melongena* L.) seeds. *International Journal of Agriculture, Environment and Biotechnology*, *11*(3), 547-551.

Smith, S. E., Fretz, T. A., & Gugino, B. K. (2018). Effects of soil pH on the germination and emergence of vegetable crops. *Journal of Horticulture, Environment, and Biotechnology*, *59*(2), 215-223.

Sodhi, Y. S., & Singh, S. (2013). Germination and emergence of cowpea as influenced by temperature and time of incubation. *International Journal of Seed Spices*, *3*(1), 67-71.

Tyagi, K. (2006). Acid rain pollution studies on some leguminous plante. Ph.D. thesis submitted to the CCS University, Meerut, UP, India.

Ulrich, B., Mayer, R., & Khanna, P. K. (1980). Chemical changes due to acid precipitation in a loess derived soil in Central Europe. *Soil Science*, *130*, 193-199.

Verma, A., Tewari, A., & Azami, A. (2010). An impact of simulated acid rain of different pH levels on some major vegetable plants in India. *Report and Opinion*, *2*, 38-40.

Verma, S.P., & Prakash, G. (1999). Simulated acid rain injury to germination and seedling growth of *Vigna unguiculata* L. Walpers. *Acta Botanica Indica*, *27*, 53-59.

Wang, M. H. S., Wang, L. K., & Shammas, N. K. (2020). Glossary of acid rain management and environmental protection. In Y.S., Hung, L.K., Wang, N.K., Shammas (eds.) *Handbook of environment and waste management: Acid rain and greenhouse gas pollution control* (pp. 719-749), World Scientific.

Yadav, D. S., Jaiswal, B., Gautam, M., & Agrawal, M. (2020). Soil acidification and its impact on plants. In P. Singh, S.K. Singh, S.M. Prasad (eds) *Plant responses to soil pollution* (pp. 1-26), Singapore Springer. https://doi.org/10.1007/978-981-15-4964-9_1.

Yin, M., Malkhi, D., Reiter, M. K., Gueta, G. G., & Abraham, I. (2019, July). HotStuff: BFT consensus with linearity and responsiveness. In *Proceedings of the 2019 ACM Symposium on Principles of Distributed Computing* (pp. 347-356).

Yuan, Z. Z., Zeng, S. & Zhou, Y. Y. (2011). Effects of simulated acid rain to seed germination and seedling growth in maize. *Journal of Shanxi Agricultural Sciences*, *39*(11), 1161-1164.

Zhang, W., Liu, X., Cai, D., & Zhang, Y. (2019). A decision tree algorithm for predicting plant growth in a complex environment. *Journal of Intelligent & Fuzzy Systems*, *37*(3), 3575-3582.

Zhang, Y., Li, J., Tan, J., Li, W., Singh, B.P., Yang, X., Bolan, N., Chen, X., Xu, S., Bao, Y. & Lv, D. (2023). An overview of the direct and indirect effects of acid rain on plants: Relationships among acid rain, soil, microorganisms, and plants. *Science of The Total Environment*, *873*, 162388.

Journal of Experimental Biology and Agricultural Sciences

Effect of nutrient management on physio morphological and yield attributes of field pea (*Pisum sativum* L.)

Reguri Harsha Vardhan Reddy[1], Arshdeep Singh[1*], Anita Jaswal[2], Shimpy Sarkar[3], Iza Fatima[4]

[1,2]Department of Agronomy, School of Agriculture, Lovely Professional University, Phagwara-144411 (Punjab), India
[3]Department of Entomology, School of Agriculture, Lovely Professional University, Phagwara-144411 (Punjab), India
[4]College of Agronomy & Biotechnology, China Agricultural University, Beijing, China

ABSTRACT

A field experiment was conducted to investigate the impact of nitrogen management on the growth and yield of field peas. The experiment took place during the rabi season (October–March of 2022–2023) at Lovely Professional University's Agriculture Research Farm in Phagwara, Punjab, India. Fifteen different treatment combinations were utilized, involving the application of chemical fertilizers (NPK) and micronutrients (boron and zinc). The experimental design followed a randomized complete block approach with three replications. Among the treatment combinations, the application of foliar spray with B at a rate of 0.2%, Zn at a rate of 0.5%, along with 100% recommended dose of fertilizer (RDF), resulted in the highest measurements for plant height (70.44 cm), leaf count (70.60), branch count (18.86), leaf area (32.24 cm²), dry matter accumulation (6.12 g), crop growth rate (0.299 g m^{-2} day^{-1}), and relative growth rate (0.05933 g g^{-1} day^{-1}). Furthermore, treatments involving 100% RDF, 0.2% B, and 0.5% Zn exhibited enhanced yield characteristics, including the number of seeds per pod (10.26), pods per plant (12.33), test weight of seeds (15.06 g), seed yield (3537 kg ha^{-1}), and harvest index (47.49%). Furthermore, 100% RDF and the inclusion of 0.2% B and 0.5% Zn outperformed the control. Applying 100% RDF along with the micronutrients B and Zn is recommended to maximize production and net profit in field pea cultivation.

* Corresponding author

E-mail: arshdeep.27269@lpu.co.in (Arshdeep Singh)

1 Introduction

Field pea, a grain legume classified under the Leguminosae family, is a major pulse crop. Its substantial content of carbohydrates, proteins, vitamins A and C, calcium, and phosphorus positions it as a widely consumed staple across the globe (Divéky-Ertsey et al. 2022). Notably, lysine and tryptophan are also abundant in field peas (Sharma et al. 2023). This legume crop ranks second internationally. Symbiotic rhizobium bacteria within its root nodules enable nitrogen fixation, a process critical to soil fertility preservation (Zhong et al. 2023). Thus, this plant species is vital for sustainable agriculture. Given the prevailing trend of declining soil fertility, the inherent ability of this crop to restore soil nutrients has rendered it an invaluable component of the cropping system (Haque et al. 2022; Gao et al. 2023). The synergy between nutrient management strategies and cultivar genetics is pivotal in enhancing field pea productivity. Fertilizers play a crucial role in bolstering the growth of field peas. Nitrogen is indispensable for the synthesis of chlorophyll, enzymes, and proteins. Phosphorus, on the other hand, is vital for root development, nodulation, energy storage, transport, and a multitude of metabolic activities. Potassium greatly enhances enzyme functionality, assimilate translocation, and protein synthesis (Uddin et al. 2023). However, the indiscriminate and excessive use of chemical fertilizers seriously threatens soil health, leading to reduced crop yields and long-term unsustainability of agricultural practices and contributing to environmental contamination. Thus, judicious and informed application of fertilizers is imperative to safeguard agrarian production and enhance soil health. The research conducted by Janusauskaite (2023) suggests that this approach can augment crop yields while strengthening the soil's physical, chemical, and biological properties and optimizing fertilizer utilization. Micronutrients have also been shown to positively impact field pea crop yield, as evidenced by the findings of Roy et al. (2022). In particular, boron is crucial in promoting the field pea plant's growth, yield, and nodulation. Similarly, zinc's physiological and enzymatic functions make it an essential element for crop nutrition. Processes such as protein and auxin synthesis, glucose metabolism, membrane maintenance, and pollen production heavily rely on these functions and activities. The application of micronutrients such as zinc through foliar fertilization, as studied by Sümer and Yaraşir (2022), has gained prominence owing to its precision, cost-effectiveness, and speed compared to traditional soil fertilization methods. However, comprehensive research on the nutritional composition of field peas, especially in the context of inorganic fertilizers and micronutrients, remains limited. In this regard, the integration of various nutrients, including the recommended dose of fertilizer (RDF) combined with foliar applications of boron and zinc, was investigated for its impact on the growth and yield of field peas (*Pisum sativum* L.).

2 Materials and Methods

2.1 Preliminary information

The experimentation took place within the agricultural premises of Lovely Professional University's School of Agriculture, located in Phagwara, India. The study employed a randomized block design, encompassing a series of 15 treatment combinations, and each replicated thrice during the rabi season in 2022. The geographic coordinates of the experimental site are 31.25°N latitude and 75.7°E longitude, positioned at an elevation of 232 m above mean sea level (MSL). A subtropical climate with moderate winters and hot summers characterizes the geographical region. Annual mean precipitation ranges from 400 to 500 mm, with approximately 80% of this rainfall concentrated between July and September 2022. The soil type identified at the experimental site is classified as sandy loam. Initial soil nutritional status was evaluated through a pre-experimental soil study. The combined content of nitrogen, phosphorus, and potassium (NPK) accessible at the experimental farm amounted to 149 kilograms per hectare (kg ha^{-1}), along with specific quantities of 17.62 kg ha^{-1}, 179 kg ha^{-1}, and 0.49% for organic carbon. Analysis indicated deficiencies in organic carbon, nitrogen, and potassium, while phosphorus content was sufficient. Additionally, the soil's pH ranges from mildly acidic to alkaline. The treatment plan is delineated as follows. The experimental treatments encompass the following nutrient ratios applied at a rate of kg ha^{-1}: control (0:0:0 N: P_2O_5:K_2O), 100% of the recommended dose of fertilizer (20:60:40 N: P_2O_5:K_2O), absence of nitrogen with 0:60:40 N: P_2O_5:K_2O, absence of phosphorus with 20:0:40 N: P_2O_5:K_2O, absence of potassium with 20:60:0 N: P_2O_5:K_2O, 60:40 N: P_2O_5:K_2O with foliar spray of boron at 0.2%, 20:0:40 N: P_2O_5:K_2O with foliar spray of boron at 0.2%, 20:60:0 N: P_2O_5:K_2O with foliar spray of boron at 0.2%, 60:40 N: P_2O_5:K_2O with foliar spray of zinc at 0.5%, 20:0:40 N: P_2O_5:K_2O with foliar spray of zinc at 0.5%, 20:60:0 N: P_2O_5:K_2O with foliar spray of zinc at 0.5%, foliar spray of boron at 0.2%, foliar spray of zinc at 0.5%, and foliar spray of boron at 0.2% combined with zinc at 0.5%, along with 100% RDF as illustrated in Figure 1.

The fertilizer formulation adhered to predetermined concentration levels for various fertilizer types. On November 1st, 2022, the field pea variety PU-89 sowing commenced, utilizing individual plots measuring 4m×3m. The spacing between rows and plants within each plot was 45 cm ×20cm. The recommended fertilizer composition for field pea, calculated per hectare basis, included 20 kg of N, 60 kg of P, and 40 kg of K. This composition represented 100% of the RDF. Fertilizer application involving Single Super Phosphate (SSP) and Muriate of Potash (MOP) was carried out during the ploughing phase before crop cultivation. Urea, the primary fertilizer used, was applied in two separate doses, i.e., during the blooming and pod formation phases. Prescribed interventions encompassed the foliar application of boron and zinc
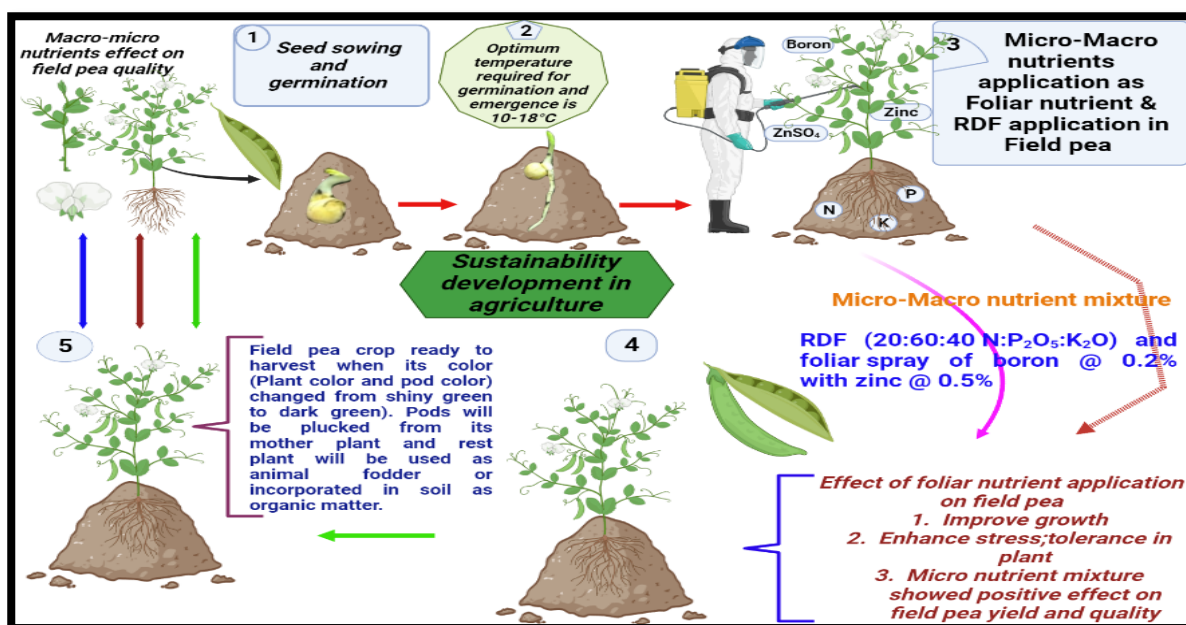
Figure 1 Experimental setup and key results

micronutrients. The cultivation practices adhered to the recommended guidelines. The evaluation of treatment effectiveness encompassed an assessment of its impact on growth, flowering, and yield parameters.

2.2 Morphophysiological and Yield Attributes

Morphophysiological and yield attributes were assessed using standardized methods. Plant height, branch count, plant dry matter, and leaf area were among the morphological and physiological traits measured. Morphological features were evaluated by randomly selecting five plants from each plot, and the mean values were used for analysis. The Chlorophyll index is a quantitative measure employed to assess the chlorophyll concentration inside a specific sample. The chlorophyll index was quantified using the Soil Plant Analysis Development (SPAD) meter, which measures green pigmentation in leaves. Mature leaves were chosen for chlorophyll index assessment, involving three SPAD meter measurements per leaf. Crop growth rate (CGR) signifies the rate of dry weight increase in a defined area over a specific timeframe; CGR is calculated using equations introduced by Watson (1952). Relative growth rate (RGR), expressed as grams per gram per day ($gg^{-1}day^{-1}$), quantifies an organism's mass or size increase within a given time, a concept first coined by Williams in 1946. Plant biomass accumulation represents the overall increase in dehydrated plant mass within a defined period, quantified as the ratio of dry weight to dry weight per unit of time ($g\ g^{-1}\ day^{-1}$). The analyzed parameters encompassed yield-related characteristics, including pods per plant, seeds per pod, test weight, seed yield, and harvest

index expressed as a percentage. These attributes were assessed at the maturity stage using well-established techniques.

2.3 Data analysis

The collected data in this study were subjected to statistical analysis using established methodologies. The analytical approach involved utilizing SPSS 22 software, employing the generalized linear model in univariate analysis. This model was specifically chosen to investigate mean variances while considering two parameters. A mean separation technique was applied to identify the most effective treatment, adopting a significance level of $p < 0.05$, alongside the Duncan multiple range test (DMRT). Additionally, Fisher's Least Significant Difference (LSD) test was employed as a posthoc analysis to assess potential statistically significant differences among the means. These calculations were performed utilizing the least significant difference (LSD) at a significance level of 5%.

3 Results and Discussion

3.1 Growth attributes

The findings presented in Tables 1 and 2 underscore the significant impact of the treatments on the plant's growth across various dimensions. Applying a foliar spray with 0.2% B and 0.5% Zn, combined with 100% RDF, led to plants reaching a height of 70.44 cm. In contrast, plants treated only with 100% RDF exhibited a height of 64.5 cm, while the control group displayed the lowest height of 48.30 cm. The observed increase in plant height can be attributed to the prescribed fertilizer quantity administered as a basal

Table 1 Effect of nutrient management on growth parameters of field pea

Treatments	Plant height (cm)	Branch count per plant	Leaf count per plant	Dry matter accumulation (g)
Control	$48.30^h \pm 0.83$	$12.83^e \pm 0.41$	$54.36^g \pm 0.79$	$1.33^f \pm 0.124$
100% RDF	$64.50^b \pm 0.521$	$17.14^b \pm 0.42$	$69.08^{ab} \pm 0.30$	$4.16^c \pm 0.124$
0:60:40 N:P$_2$O$_5$:K$_2$Okg ha^{-1}	$53.55^g \pm 0.95$	$15.07^d \pm 0.23$	$57.26^f \pm 0.86$	$2.23^e \pm 0.094$
20:0:40 N:P$_2$O$_5$:K$_2$Okg ha^{-1}	$58.83^d \pm 1.35$	$16.59^{bc} \pm 0.17$	$63.05^{cd} \pm 0.84$	$3.50^d \pm 0.163$
20:60:0 N:P$_2$O$_5$:K$_2$Okg ha^{-1}	$61.26^c \pm 0.86$	$17.04^b \pm 0.14$	$65.20^c \pm 0.90$	$3.60^d \pm 0.216$
0:60:40 N:P$_2$O$_5$:K$_2$Okg ha^{-1} + Foliar spray of 0.2% B	$55.44^{fg} \pm 0.69$	$16.17^{bcd} \pm 0.12$	$57.47^f \pm 2.35$	$2.46^e \pm 0.249$
20:0:40 N:P$_2$O$_5$:K$_2$Okg ha^{-1} + Foliar spray of 0.2% B	$57.40^{de} \pm 0.91$	$17.24^b \pm 0.20$	$59.50^e \pm 0.65$	$3.43^d \pm 0.169$
20:60:0 N:P$_2$O$_5$:K$_2$Okg ha^{-1} + Foliar spray of 0.2% B	$63.42^b \pm 0.70$	$17.33^b \pm 0.85$	$64.56^{cd} \pm 0.52$	$4.43b^c \pm 0.339$
0:60:40 N:P$_2$O$_5$:K$_2$Okg ha^{-1} + Foliar spray of 0.5% Zn	$57.46^{de} \pm 0.72$	$16.63^{bc} \pm 0.42$	$60.56^e \pm 0.45$	$3.40^d \pm 0.294$
20:0:40 N:P$_2$O$_5$:K$_2$Okg ha^{-1} + Foliar spray of 0.5% Zn	$60.83^c \pm 0.53$	$16.97^b \pm 0.20$	$67.81^b \pm 1.78$	$4.63^b \pm 0.205$
20:60:0 N:P$_2$O$_5$:K$_2$Okg ha^{-1} + Foliar spray of 0.5% Zn	$59.40^{cd} \pm 0.75$	$16.900^b \pm 0.29$	$65.30^c \pm 0.82$	$4.41^{bc} \pm 0.127$
Foliar spray of 0.2% B	$56.44^{ef} \pm 0.95$	$15.55^{cd} \pm 0.15$	$62.73^d \pm 0.56$	$3.16^d \pm 0.124$
Foliar spray of 0.5% Zn	$54.44^g \pm 1.64$	$16.63^{bc} \pm 0.21$	$63.60^{cd} \pm 0.49$	$3.30^d \pm 0.216$
Foliar spray of 0.2% B and 0.5% Zn	$58.34^{de} \pm 0.73$	$16.33^{bc} \pm 0.77$	$64.36^{cd} \pm 0.83$	$3.40^d \pm 0.326$
Foliar spray of 0.2% B and 0.5% Zn+ 100% RDF	$70.44^a \pm 0.69$	$18.86^a \pm 0.20$	$70.60^a \pm 0.44$	$6.12^a \pm 0.131$

*The mean values followed by letters were significantly different at p < 0.05 based on Duncan's multiple range test (DMRT).

Table 2 Effect of nutrient management on phenological parameters of field pea

Treatments	Chlorophyll index (SPAD)	Leaf area (cm^2)	Crop growth rate (gm^{-2}day^{-1})	Relative growth rate (g g^{-1} day^{-1})
Control	$36.43^h \pm 0.79$	$12.23^h \pm 0.82$	$0.060^i \pm 0.0014$	$0.03233^f \pm 0.00073$
100% RDF	$42.20^{de} \pm 0.82$	$19.23d^e \pm 0.33$	$0.236^b \pm 0.0041$	$0.05333^{ab} \pm 0.0016$
0:60:40 N:P$_2$O$_5$:K$_2$Okg ha^{-1}	$37.56^{gh} \pm 1.06$	$15.53^g \pm 0.40$	$0.085^h \pm 0.0063$	$0.03367^f \pm 0.00328$
20:0:40 N:P$_2$O$_5$:K$_2$Okg ha^{-1}	$42.20^{de} \pm 0.82$	$17.60^f \pm 0.29$	$0.123^g \pm 0.014$	$0.03967^e \pm 0.0052$
20:60:0 N:P$_2$O$_5$:K$_2$Okg ha^{-1}	$43.20^{cd} \pm 0.82$	$19.43^e \pm 0.74$	$0.136^{fg} \pm 0.0027$	$0.04000^e \pm 0.00112$
0:60:40 N:P$_2$O$_5$:K$_2$Okg ha^{-1} + Foliar spray of 0.2% B	$38.43^g \pm 0.87$	$19.43^{de} \pm 0.29$	$0.123^g \pm 0.0101$	$0.04467^{de} \pm 0.00274$
20:0:40 N:P$_2$O$_5$:K$_2$Okg ha^{-1} + Foliar spray of 0.2% B	$40.33^{ef} \pm 0.66$	$18.66^{ef} \pm 0.49$	$0.134^{fg} \pm 0.0009$	$0.04033^e \pm 0.00024$
20:60:0 N:P$_2$O$_5$:K$_2$Okg ha^{-1} + Foliar spray of 0.2% B	$42.20^{de} \pm 0.82$	$18.90^{ef} \pm 0.37$	$0.173^{de} \pm 0.0006$	$0.04533^{de} \pm 0.00124$
0:60:40 N:P$_2$O$_5$:K$_2$Okg ha^{-1} + Foliar spray of 0.5% Zn	$39.40^{fg} \pm 0.70$	$16.33^g \pm 0.37$	$0.194^{cd} \pm 0.0006$	$0.05467^{ab} \pm 0.00106$
20:0:40 N:P$_2$O$_5$:K$_2$Okg ha^{-1} + Foliar spray of 0.5% Zn	$44.46^{bc} \pm 0.70$	$17.66^f \pm 0.49$	$0.200^c \pm 0.0285$	$0.5567^{ab} \pm 0.00273$
20:60:0 N:P$_2$O$_5$:K$_2$Okg ha^{-1} + Foliar spray of 0.5% Zn	$45.20^{ab} \pm 0.82$	$20.33^d \pm 0.78$	$0.191^{cd} \pm 0.0063$	$0.05267^{bc} \pm 0.00168$
Foliar spray of 0.2% B	$40.43^{ef} \pm 0.79$	$25.46^b \pm 0.59$	$0.160^{ef} \pm 0.0097$	$0.05533^{ab} \pm 0.00131$
Foliar spray of 0.5% Zn	$38.46^g \pm 0.97$	$25.47^b \pm 0.69$	$0.152^{ef} \pm 0.0101$	$0.05367^{ab} \pm 0.00346$
Foliar spray of 0.2% B and 0.5% Zn	$38.63^{fg} \pm 0.74$	$23.71^c \pm 0.61$	$0.199^c \pm 0.0124$	$0.04767^{cd} \pm 0.00365$
Foliar spray of 0.2% B and 0.5% Zn+ 100% RDF	$46.40^a \pm 0.94$	$32.24^a \pm 0.73$	$0.299^a \pm 0.0240$	$0.05933^a \pm 0.0037$

* The mean values followed by letters were significantly different at p < 0.05 based on Duncan's multiple range test (DMRT)

dose alongside the foliar application of boron and zinc. These treatments likely facilitated enhanced cell division, metabolic and enzymatic activities, and cell size expansion. These physiological changes collectively contributed to the overall elevation in plant stature. This aligns with the findings reported by Kumar et al. (2022). Further, the foliar application of 0.2% B and 0.5% Zn + 100% RDF treatment yielded the highest branch (18.86) and leaf (70.60) counts per plant. Subsequently, applying 100% RDF alone resulted in 17.14 branches and 69.08 leaves. In comparison, the control group had the fewest branches (12.83). Incorporating boron and zinc through foliar and basal fertilizer applications contributed to elevated photosynthetic activity per plant, as evidenced by the increased leaf count and branch development. Additionally, zinc has been known to stimulate enzymes and photosynthetic pigments, thus promoting vegetative growth. Modifying key enzymes significantly influences protein synthesis, energy transmission, and essential nitrogen metabolism (Rahman and Schoenau 2022). The foliar spray treatment with B at 0.2% and Zn at 0.5% + 100% RDF achieved the highest dry matter accumulation, followed by the 100% RDF treatment with a dry matter accumulation of 4.43g. Conversely, the control treatment showed the lowest dry matter accumulation of 1.33g. The observed increase in dry matter within the treatment can be attributed to the increased application of NPK fertilizer, which enhances vegetative growth by stimulating various plant enzymes that play a crucial role in macromolecule synthesis, including proteins and carbohydrates. Furthermore, the essential roles of zinc and boron encompass crucial physiological activities, including photosynthesis, osmoregulation, cellular proliferation, stomatal regulation, water movement within plants, and hydrocarbon integration. While macronutrients are commonly emphasized, this study underscores the significance of micronutrients such as vitamin B and zinc in bolstering crop growth and biomass accumulation. Employing foliar sprays to deliver micronutrients has proven effective in addressing nutrient deficiencies and maintaining optimal nutrient levels in plants (Sharma et al. 2022; Dhaliwal et al. 2022). Quantifying chlorophyll content in plants is important owing to its pivotal role in photosynthesis. Findings indicate that applying a foliar spray containing 0.2% B and 0.5% Zn, coupled with 100% RDF, resulted in a notably higher chlorophyll index (measured at 46.4 SPAD) compared to those in both the control (measured at 36.43 SPAD) and other treatment groups. The chlorophyll content increased when employing a foliar spray containing 0.5% Zn and 0.2% B alongside a recommended dose of fertilizer. This effect was most pronounced in the treatment group receiving a foliar spray of 0.2% B and 0.5% Zn, along with 100% RDF. This phenomenon can be attributed to the enhanced assimilation of both macronutrients and micronutrients, facilitating chlorophyll biosynthesis. This finding aligns with the study conducted by Meena et al. (2022), which established the positive influence of increased nutrient levels on chlorophyll concentration

in plants. Leaf area is the leaves' total surface area ratio to the ground's corresponding area. Leaf area, a measure of a plant's efficiency in utilizing sunlight for photosynthesis, indicates the plant's photosynthetic activity. The findings indicate that foliar spray containing 0.2% B and 0.5% Zn, and 100% RDF yielded the largest leaf area (32.24 cm²). This was followed by applying foliar sprays containing 0.2% B, 0.5% Zn, and 100% RDF. The effect of the foliar application of 0.2% B and 0.5% Zn alongside 100% RDF can be attributed to their contribution to the uptake of critical macronutrients and micronutrients involved in photosynthesis and various plant metabolic processes. This, in turn, led to increased foliage production and future growth, consequently enhancing the overall leaf surface area. CGR is a metric to quantify the crop growth rate, reflecting biomass increase over a specific period. Results of the study revealed that applying a foliar spray containing 0.2% B and 0.5% Zn, along with 100% RDF, yielded the highest CGR ($0.299 \ g^{-1}m^{-2}day^{-1}$) among all treatments. This was followed by applying 100% RDF alone (CGR of $0.236 \ g^{-1} m^{-2} day^{-1}$). The control group exhibited the lowest CGR ($0.06 \ g^{-1} m^{-2} day^{-1}$). The observed effects can be attributed to the foliar application of zinc and boron, which likely impacted the uptake of crucial macro and micronutrients, thus enhancing photosynthesis and various plant metabolic processes. This led to new leaf production and subsequent growth, ultimately increasing the leaf area index (Kumar et al. 2022). The relative growth rate (RGR), measuring the pace of plant growth with size, is an effective growth assessment tool. Findings indicate that applying a foliar spray containing 0.2% B and 0.5% Zn and 100% RDF yielded the highest RGR ($0.059 \ g \ g^{-1} \ day^{-1}$) among all treatments. Conversely, the control group exhibited the lowest RGR ($0.053 \ g \ g^{-1} \ day^{-1}$). This increase in RGR after the foliar application of 0.2% B and 0.5% Zn, along with 100% RDF, can be attributed to various factors. Vishvakarma et al. (2022) noted that B contributes to cell wall synthesis, pollen tube elongation, and carbohydrate metabolism. Zn activates enzymes and supports photosynthesis and hormone regulation. Direct foliar application of these micronutrients likely supplied them to the plant's photosynthetic tissues, improving metabolic processes and nutrient utilization (Pandey and Parmar 2022). Considering the potential synergistic effects on plant growth resulting from combining B and Zn elements at the recommended 100% RDF is important. The balanced combination of macronutrients (nitrogen, phosphorus, and potassium) and micronutrients (boron and zinc) is pivotal in enhancing nutrient absorption and utilization, resulting in noticeable growth improvements. This aligns with conclusions made by Pathak and Sharma (2023).

3.2 Yield attributes

The results presented in Table 3 illustrate the impact of various treatments on field pea yield parameters, including the number of

Table 3 Effect of nutrient management on yield and yield attributes of field pea

Treatments	Number of seeds per pod	Number of pods per plant	Harvest index (%)	Seed yield (kg ha^{-1})	Test weight (g)
Control	6.700^f ± 0.0	5.66^h ± 0.47	39.82^d ± 2.48	906.67^j ± 66.00	7.66^h ± 0.41
100% RDF	9.367^b ± 0.0	10.66^b ± 0.47	45.15^{abc} ± 0.63	3324.67^b ± 43.86	15.03^a ± 0.31
0:60:40 N:P$_2$O$_5$:K$_2$Okg ha^{-1}	7.333^{ef} ± 0.5	8.00^{de} ± 0.00	44.94^{abc} ± 1.10	1931.33^h ± 41.35	9.40^{fg} ± 0.33
20:0:40 N:P$_2$O$_5$:K$_2$Okg ha^{-1}	8.300^{cd} ± 0.2	6.33^{gh} ± 0.47	45.23^{abc} ± 0.52	2274.00^f ± 36.36	10.33^{de} ± 0.47
20:60:0 N:P$_2$O$_5$:K$_2$Okg ha^{-1}	8.667^{bc} ± 0.5	7.33^{efg} ± 0.47	46.33^a ± 0.55	2694.33^d ± 36.12	11.00^{cd} ± 0.29
0:60:40 N:P$_2$O$_5$:K$_2$Okg ha^{-1} + Foliar spray of 0.2% B	7.633^{de} ± 0.0	7.66^{ef} ± 0.47	43.49^c ± 0.70	1892.00^{hi} ± 49.67	9.66e^{fg} ± 0.34
20:0:40 N:P$_2$O$_5$:K$_2$Okg ha^{-1} + Foliar spray of 0.2% B	8.333^{cd} ± 0.5	7.33^{efg} ± 0.47	45.86^a ± 0.59	2428.33^e ± 42.29	10.13^{def} ± 0.34
20:60:0 N:P$_2$O$_5$:K$_2$Okg ha^{-1} + Foliar spray of 0.2% B	9.000^{bc} ± 0.0	8.66^{cd} ± 0.47	46.57^a ± 0.56	3113.67^c ± 72.50	11.80^{bc} ± 0.45
0:60:40 N:P$_2$O$_5$:K$_2$Okg ha^{-1} + Foliar spray of 0.5% Zn	7.667^{de} ± 0.5	7.00^{efg} ± 0.00	44.55^{abc} ± 0.62	2051.32^g ± 66.68	10.53^{de} ± 0.41
20:0:40 N:P$_2$O$_5$:K$_2$Okg ha^{-1} + Foliar spray of 0.5% Zn	8.367^{cd} ± 0.1	9.33^c ± 0.47	45.91^a ± 0.36	3110.00^c ± 40.10	11.00^{cd} ± 0.33
20:60:0 N:P$_2$O$_5$:K$_2$Okg ha^{-1} + Foliar spray of 0.5% Zn	8.667^{bc} ± 0.5	10.33^b ± 0.47	45.69^{ab} ± 0.79	3075.00^c ± 37.48	12.33^b ± 0.25
Foliar spray of 0.2% B	7.667^{de} ± 0.0	7.33e^{fg} ± 0.47	45.86^a ± 0.41	2383.67^e ± 27.13	8.83^g ± 0.21
Foliar spray of 0.5% Zn	6.667^f ± 0.5	6.66^{fg} ± 0.47	43.64^{bc} ± 0.69	1798.00^i ± 67.49	9.00^g ± 0.65
Foliar spray of 0.2% B and 0.5% Zn	7.333^{ef} ± 0.5	7.33^{efg} ± 0.47	45.23^{abc} ± 0.61	2416.00^e ± 50.99	8.83^g ± 0.68
Foliar spray of 0.2% B and 0.5% Zn+ 100% RDF	10.267^a ± 0.0	12.33^a ± 0.47	47.49^a ± 0.47	3537.33^a ± 80.30	15.06^a ± 0.25

*The mean values followed by letters were significantly different at p < 0.05 based on Duncan's multiple range test (DMRT).

seeds per pod, pods per plant, test weight of seeds, seed yield, and harvest index. Among the diverse treatment combinations, applying a foliar spray containing 0.2% B and 0.5% Zn alongside 100% RDF yielded a notably higher seed count (10.26). The treatment using 100% RDF alone produced a seed count of 9.367. In contrast, the control group exhibited the lowest seed count (6.700). The treatment involving a foliar spray of 0.2% B and 0.5% Zn, and 100% RDF displayed the highest pod count (12.33). This was closely followed by the 100% RDF treatment with a pod count 10.66. Conversely, the control treatment had the lowest pod count (5.66), while the remaining treatments yielded pod counts ranging from 6.33 to 8.66. The synergistic effects of boron and zinc foliar spray application can be attributed to their crucial roles in promoting reproductive growth and development. Using 100% RDF has enhanced access to essential micronutrients and macronutrients, supporting robust plant growth and pod formation (Noori et al. 2023). In terms of the seed yield, employing a foliar spray containing 0.2% B and 0.5% Zn along with 100% RDF led to significantly higher seed yield (3324.67 kg ha^{-1}) compared to those for the control (906.67 kg ha^{-1}) and other treatments (ranging from 1798.00 to 3113.67 kg ha^{-1}). This result can be attributed to the combined effect of foliar sprays containing B and Zn, in addition to the appropriate dosage of fertilizer. The interventions

successfully addressed nutritional inadequacies, thus promoting strong plant growth and maximizing seed production. These findings underscore the importance of integrating micronutrient supplementation and adopting optimal fertilization practices to enhance crop productivity. This conclusion aligns with the results reported by Kohli et al. (2023) and Stanton et al. (2022). Moreover, a foliar spray containing 0.2% B and 0.5% Zn along with 100% RDF resulted in the highest seed index (15.03g). This was followed by applying 100% RDF, yielding a seed index of 15.03g. The control group exhibited the lowest seed index of 7.66g. This comprehensive approach produced significant seed index values, showcasing the positive outcomes of combined nutrient supplementation and proper fertilization practices. The simultaneous application of B and Zn through foliar sprays and adequate essential nutrient availability from RDF The developed combination is anticipated to yield favourable results regarding nutrient absorption, enzymatic responses, physiological functions, enhanced seed quality, and amplified production. Furthermore, the treatment utilizing a foliar spray containing 0.2% B and 0.5% Zn and 100% RDF achieved the highest harvest index of 47.49%. Following closely, the 20:60:0 N: P$_2$O$_5$:K$_2$O kg ha^{-1} treatment exhibited a harvest index of 46.33%. Additionally, the 20:60:0 N: P$_2$O$_5$:K$_2$Okg ha^{-1} treatment, combined with a foliar spray of 0.2%

B, demonstrated a harvest index of 46.57%. In contrast, the control treatment reported the lowest harvest index of 39.82%. A higher harvest index signifies efficient resource utilization. The observed phenomenon can be attributed to enhanced nutrient provision through fertilization and foliar spray applications, increasing plant growth and production (Kumar et al. 2022). The efficacy of foliar spray depends on various parameters, including crop type, nutrient form and concentration, application timing, and prevailing environmental conditions (Sumer and Yaraşir 2022).

3.3 Regression analysis

The effect of various parameters (such as the number of nodules per plant, number of pods per plant, and seeds per pod) on the chlorophyll index was predicted using quadratic response regression analysis. The results demonstrated a significant enhancement in field pea seed yield as these parameters increased. This trend is visually depicted in Figures 2, 3, 4, and 5, along with their corresponding R^2 values and polynomial equations. The observed trend shows that robust plant growth facilitates efficient nutrient utilization, resulting in higher chlorophyll indices and greater nodule formation per plant. The higher chlorophyll index leads to an increased accumulation of photosynthates, translating into a higher count of pods per plant and more seeds per pod. The cumulative effect of these growth factors profoundly influences the overall seed yield, and the developed treatments significantly affect this outcome. Therefore, it is clear that there is a positive correlation between the growth factors and the enhancement of yield.
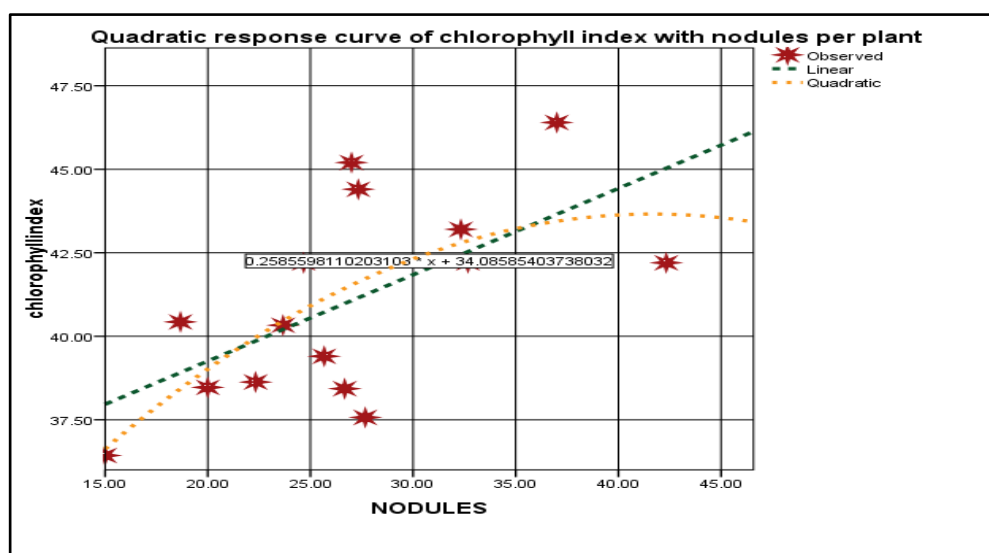

Figure 2 Regression analysis of chlorophyll index vs. number of nodules per plant
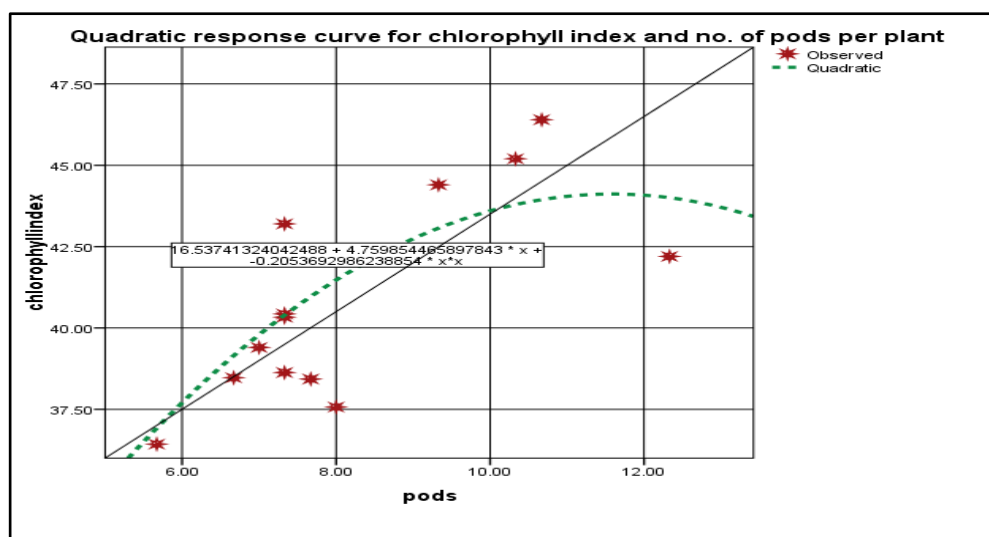

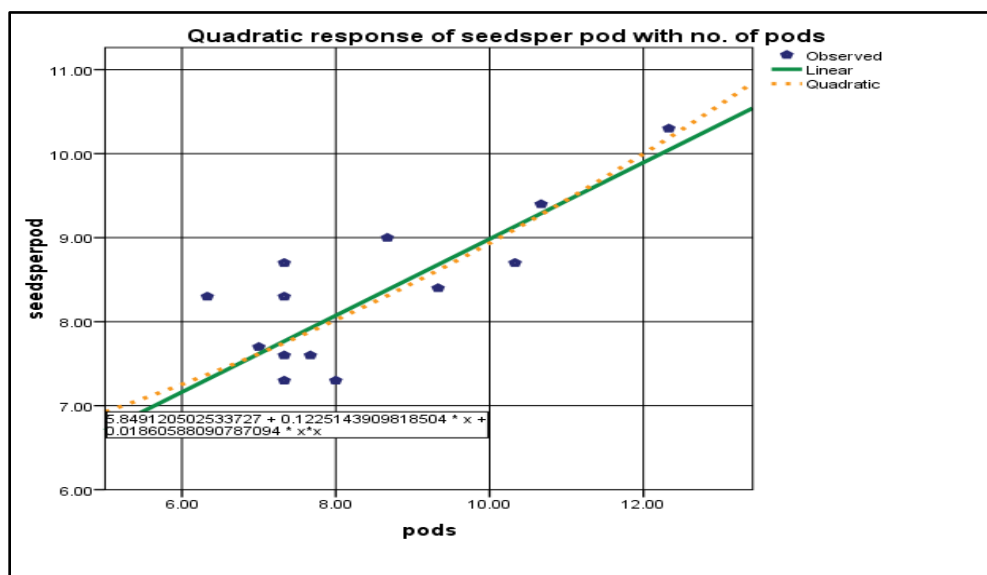Figure 3 Regression analysis of chlorophyll index vs. number of pods per plant

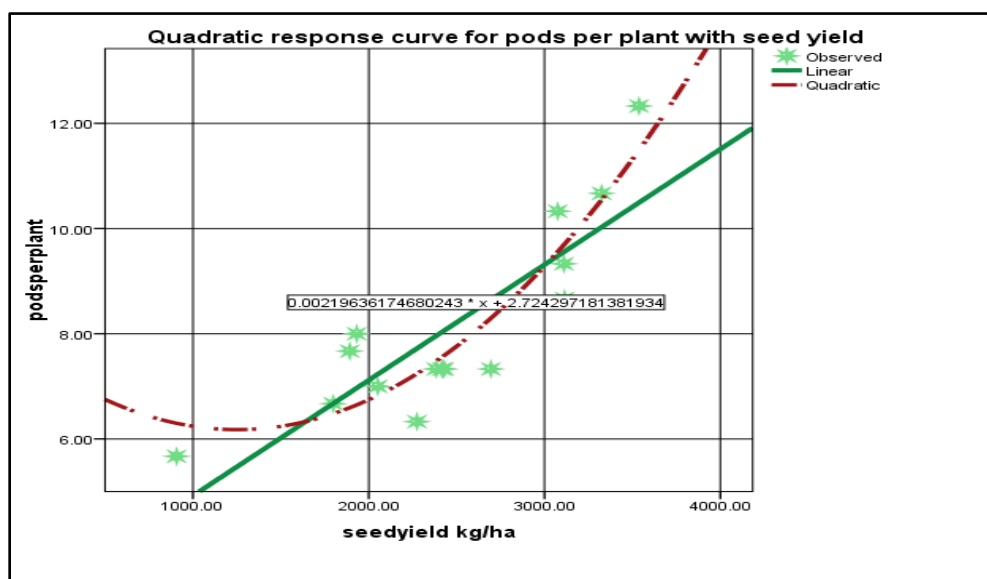Figure 4 Regression analysis of seeds per pod vs. number of pods per plant

Figure 5 Regression analysis of number of pods per plant vs. seed yield

Conclusion

This study showed that employing 100% RDF, along with 0.2% B and 0.5% Zn, led to notable increases in plant height, branch count, leaf count, dry matter accumulation, chlorophyll index, leaf area, crop growth rate, and relative growth rate. Similarly, using 100% RDF, along with boron and zinc, improved yield-related characteristics. Thus, it can be inferred that applying 100% RDF, 0.2% B, and 0.5% Zn is a promising alternative to the recommended dose of inorganic fertilizers for field pea cultivation within the experimental conditions. This approach enhances crop productivity and contributes to the sustainability of production practices.

Conflict of interest

The authors declare that they have no conflicts of interest.

References

Dhaliwal, S. S., Sharma, V., Shukla, A. K., Kaur, J., Verma, V., Kaur, M., & Hossain, A. (2022). Zinc-Based Mineral (ZnSO$_4$·7H$_2$O) and Chelated (Zn-EDTA) Fertilizers improve the Productivity, Quality and Efficiency Indices of Field Pea (*Pisum sativum L.*) through Biofortification. *Journal of Trace Elements and Minerals*, *2*, 100033. https://doi.org/10.1016/j.jtemin.2022.100033

Divéky-Ertsey, A., Gál, I., Madaras, K., Pusztai, P., & Csambalik, L. (2022). Contribution of pulses to agrobiodiversity in the view of EU protein strategy. *Stresses*, *2*(1), 90-112. https://doi.org/10.3390/stresses2010008

Gao, J., Zhang, X., Luo, J., Zhu, P., Lindsey, S., Gao, H., Li, Q., Peng, C., Zhang, L., Xu, L., Qiu, W., & Jiao, Y. (2023). Changes in soil fertility under partial organic substitution of chemical fertilizer: a 33-year trial. *Journal of the science of food and agriculture*, 10.1002/jsfa.12819. DOI: https://doi.org/10.1002/jsfa.12819

Haque, M. A., Moniruzzaman, S. M., Hossain, M. F., & Alam, M. A. (2022). Effects of organic mjavascript:void(0)anure and chemical fertilizers on growth and yield of garden pea. *Bangladesh Journal of Agriculture*, *47*(1), 121-129.

Janusauskaite, D. (2023). Productivity of Three Pea (*Pisum sativum L.*) Varieties as Influenced by Nutrient Supply and Meteorological Conditions in Boreal Environmental Zone. *Plants*, *12*(10), 1938. https://doi.org/10.3390/plants12101938

Kohli, S. K., Kaur, H., Khanna, K., Handa, N., Bhardwaj, R., Rinklebe, J., & Ahmad, P. (2023). Boron in plants: Uptake, deficiency and biological potential. *Plant Growth Regulation*, *100*(2), 267-282. https://doi.org/10.1007/s10725-022-00844-7

Kumar, P., David, A. A., Thomas, T., & Reddy, I. S. (2022). Impact of Integrated Nutrient Management on Physico-chemical properties of soil in Pea (*Pisum sativum L.*) var. GS 10. *International Journal of Plant & Soil Science*, *34*(20), 521-526. http://dx.doi.org/10.9734/ijpss/2022/v34i2031183

Meena, S., Gupta, V., Ram, B., Yadav, V. K., Koli, N. R., & Dhakad, U. (2022). Response of field pea (*Pisum sativum var. arvense* (L.) to phosphorus and zinc fertilizers and their solubilizers on growth, yield and economics. *The Pharma Innovation Journal, 11*(10), 292-294

Noori, R., Sharma, A., Rana, S. S., Lata, H., Sharma, P., & Rana, R. S. (2023). Differential response of nutrient management practices on different varieties in chilli-garden pea cropping system. *Himachal Journal of Agricultural Research*, *49*(1), 84-92.

Pandey, V., & Parmar, K. (2022). Impact of Integrated Nutrient Management on Seed Quality of Field Pea During Ambient Storage. *Indian Journal of Ecology*, *49*(5), 2020-2025. https://doi.org/10.55362/IJE/2022/3779

Pathak, S., & Sharma, H. R. (2023). Economics of zinc biofortification and nutrient management in garden pea. *Progressive Agriculture*, *23*(1), 133-138.

Rahman, N., & Schoenau, J. (2022). Bioavailability, Speciation, and crop responses to copper, zinc, and boron fertilization in South-Central saskatchewan soil. *Agronomy*, *12*(8), 1837. https://doi.org/10.3390/agronomy12081837

Roy, S., Das, S., Saha, K. K., Rahman, M. R., Sarkar, S. K., Rashid, M. H., & Paul, S. K. (2022). Growth and seed yield of faba bean (*Vicia faba L.*) as influenced by zinc and boron micronutrients. *Fundamental and Applied Agriculture*, *7*(2), 139-149. https://doi.org/10.5455/faa.106842

Sharma, R., Bharat, N. K., Thakur, K. S., & Kumar, P. (2022). Effect of Seed Coating and Foliar Spray Treatments on Plant Growth, Seed Yield and Economics of Seed Production in Garden Pea (*Pisum sativum* L.). *Indian Journal of Ecology*, *49*(2), 378-382. https://doi.org/10.55362/IJE/2022/3532

Sharma, V., Singh, C. M., Chugh, V., Prajapati, P. K., Mishra, A., Kaushik, P., & Yadav, A. (2023). Morpho-Physiological and Biochemical Responses of Field Pea Genotypes under Terminal Heat Stress. *Plants*, *12*(2), 256. https://doi.org/10.3390/plants12020256

Stanton, C., Sanders, D., Krämer, U., & Podar, D. (2022). Zinc in plants: Integrating homeostasis and biofortification. *Molecular Plant*, *15*(1), 65-85.https://doi.org/10.1016/j.molp.2021.12.008

Sümer, F. Ö., & Yaraşir, N. (2022). The Effects of Foliar Zinc Application on Yield and Quality Components of Pea (*Pisum sativum L.*) in Mediterranean Climate Conditions. *Journal of the Institute of Science and Technology*, *12*(3), 1820-1830. https://doi.org/10.21597/jist.1121560

Uddin, S. N., Zakaria, M., Hossain, M. M., Hossain, T., & Sirajul, A. J. M. (2023). Effect of NPK Fertilizers on Growth, Yield and Nutritional Quality of Garden Pea. *International Journal*, *3*(1), 1-6.

Vishvkarma, B., SinghTiwari, A., & Patle, T. (2022). Integrated nutrient management in pea (*Pisum sativum L.*). *The Pharma Innovation Journal*, *11*(10), 1348-1351

Watson, D. J. (1952). The physiological basis of variation in yield. *Advances in agronomy*, *4*, 101-145.

Williams, R. F. (1946). The physiology of plant growth with special reference to the concept of net assimilation rate. *Annals of Botany*, *10*(37), 41-72.

Zhong, Y., Tian, J., Li, X., & Liao, H. (2023). Cooperative interactions between nitrogen fixation and phosphorus nutrition in legumes. *New Phytologist*, *237*(3), 734-745. https://doi.org/10.1111/nph.18593

Journal of Experimental Biology and Agricultural Sciences

Halotolerant Plant Growth Promoting Bacilli from Sundarban Mangrove Mitigate the Effects of Salinity Stress on Pearl Millet (*Pennisetum glaucum* L.) Growth

Pallavi[1,3], Rohit Kumar Mishra[2], Ajit Varma[1], Neeraj Shrivastava[1], Swati Tripathi[1*]

[1]Amity Institute of Microbial Technology, Amity University Uttar Pradesh, Noida201301, India
[2]Centre of Science and Society, University of Allahabad, Prayagraj, Uttar Pradesh- 211002, India
[3]ICAR- National Bureau of Agriculturally Important Microorganism, Kushmaur, Mau, Uttar Pradesh- 275103, India

ABSTRACT

Pearl millet (*Pennisetum glaucum* L.) is one of the major crops in dry and saline areas across the globe. During salinity stress, plants encounter significant changes in their physio and biochemical activities, leading to decreased growth and yield. *Bacillus* species are used as biofertilizers and biopesticides for pearl millet and other crops to promote growth and yield. The use of *Bacillus* in saline soils has been beneficial to combat the negative effect of salinity on plant growth and yield. In this context, the present study emphasizes the use of two *Bacillus* species, i.e. *Bacillus megaterium* JR-12 and *B. pumilus* GN-5, which helped in alleviating the impact of salinity stress on the growth activities in salt-stressed pearl millet. Pearl millet seeds were treated with two strains, *B. megaterium* JR-12 and *B.pumilus* GN-5, individually and in combination under 50, 100 and 150 mM of sodium chloride stress. The treated plants showed higher plant height, biomass accumulation, and photosynthetic apparatus than the non-treated plants. Additionally, the treated plants showed increased osmoprotectant levels under salinity stress compared to control plants. The antioxidant enzyme content was improved post-inoculation, indicating the efficient stress-alleviating potential of both strains of *Bacillus* species. Moreover, inoculation of these microbes significantly increased plant growth attributes in plants treated with a combination of Bp-GN-5 + Bm-JR-12 and the reduction rates of plant growth were found to be alleviated to 9.12%, 20.30% and 33%, respectively. Overall, the results of the present study suggested that these microbes could have a higher potential to improve the productivity of pearl millet under salinity stress.

* Corresponding author

E-mail: swatitri@gmail.com; stripathi2@amity.edu (Swati Tripathi)

1 Introduction

Pearl millet (*Pennisetum glaucum*) is an important crop contributing to global nutritional security. It belongs to the family Gramineae and serves as a staple source of food and fodder in millions of poor households under low rainfall conditions. With rising concerns over widespread deficiency of nutrients in most of the world population, millet crops are a viable option to replace major cereals. Conversely, the ability of pearl millet to grow in poor, infertile soils makes it the best choice to grow in soils that cannot be used for other cereal crops (Kumar et al. 2010).

Salt stress is among the prominent abiotic factors limiting global agricultural productivity (Munns and Tester 2008; Shahbaz and Ashraf 2013). High sodium and chloride content interferes with the activities of various vital enzymes and thus affects plant physiology (Munns and Tester 2008). This leads to a reduction in overall productivity and yield of salt-sensitive crops and ultimately results in consumable diets low in nutrients. Millet crops generally tolerate up to 6 dS m^{-1} of salinity levels in the soil (ECe) without substantially losing dry matter. However, higher salinity levels have been reported to cause damage to the soil, especially by organic matter decomposition, nitrification, denitrification, microbial activity, and biodiversity (Schirawski and Perlin 2017; Upadhyay et al. 2019). Removing excessive sodium from the soil by conventional physical and chemical methods is an unsustainable and time-consuming process that is unsustainable and stands ineffective with higher salt concentrations (Ayyam et al. 2019). Salt stress can significantly reduce the productivity of various crops (Toro et al. 2021). However, a salinity level above ECe of 9 dS m^{-1} is reported to reduce plant productivity significantly (Evans 2006). The effect of salinity on the morphology, anatomy and physiology of pearl millet is well documented (Hussain et al. 2008, 2010). Thus, it is important to consider strategies to enhance salinity tolerance in pearl millet to maintain or increase its production under saline infertile soils.

The term "plant-growth-promoting rhizospheric bacteria" (PGPR) refers to a class of microorganisms that colonize the roots of plants or exist in the rhizosphere as free-living organisms and promote the plant growth by direct and indirect methods (Dodd and Perez-Alfocea 2012; Orhan 2016; Bhat et al. 2020). Some processes by PGPRs, such as organic acids production, which can solubilize minerals and break organic matter, P-solubilization, K-solubilization, Zn-solubilization, siderophore production for iron chelation, indole acetic acid (IAA) production for cell elongation, HCN production as a defensive compound help in the overall growth and productivity of plants (Kumar and Gera 2014). This study hypothesized that the application of halotolerant bacteria could enhance growth under high levels of salt stress conditions and focused on exploring the PGPR properties of potential halophile bacteria isolated from the natural salt-affected soils of the Sundarbans mangrove region of West Bengal, India, and to evaluate the potential of PGPR strains to alleviate effect of salinity stress on pearl millet cultivar.

2 Materials and Methods

2.1 Source of inoculum

Potential PGPR strains (*B. megaterium* JR-12 and *B. pumilus* GN-5) were obtained from the rhizospheric soil of mangrove plants thriving in saline circumstances in Sundarbans, West Bengal, India (Pallavi et al. 2023).

2.2 Plant Growth Promoting Assays

2.2.1 Screening for phosphate solubilization

The test colonies of the isolates were spot inoculated on Pikovskaya's agar medium (Pikovskaya 1948), followed by incubation at 28 ±2°C for 48 hours. Clear solubilization zones surrounding the colonies were considered positive for P-solubilization. The formula presented in Edi-Premono et al. (1996) was used to compute the solubilization index by considering the colony diameter and the diameter of the halo zone.

Phosphate Solubilization Index (PSI) = Colony diameter + Halo zone diameter /Colony diameter

2.2.2 Quantitative phosphate solubilization

By measuring the total amount of soluble phosphate in the cell-free supernatant of Pikovskaya's broth supplemented with 0.5% TCP, the quantitative measurement of phosphate solubilization efficiency of chosen PGPRs was evaluated. The amount of accessible phosphate in the culture supernatant was assessed using the phosphomolybdate technique (Watanabe and Olsen 1965).

2.2.3 IAA production potential

The IAA production potential of the selected PGPR strains was determined by the method described by Brick et al. (1991). Two sets of 25 mL nutrient broth were inoculated with 24h old culture (with and without tryptophan) and incubated at 37±2°C for 36h at 120 rpm in an incubator shaker. The IAA production (µg/mL) was determined using the standard plot of IAA.

2.2.4 Siderophore production

The qualitative analysis of siderophore production was done by the Chrome Azurol Sulfonate (CAS) method (Pérez-Miranda et al. 2007). Schwyn and Neilands (1987) method was followed to prepare CAS agar plates, which were spot inoculated by the potential PGPR isolates and incubated for 48 h (37 ± 2°C) to observe the yellow-orange halo around the colonies.

2.2.5 Zinc Solubilization Potential

The zinc solubilization efficiency of the isolates was assessed using Zinc oxide (ZnO). The 24 h old colonies were aseptically spot inoculated on respective zinc-supplemented plates (amended with 1% ZnO). The plates were incubated at $37 \pm 2°C$ in the dark for seven days, and clear zones surrounding the colonies of zinc solubilizing isolates were observed. The zone diameters were recorded (Sharma et al. 2012).

2.2.6 Ammonia Production

The ammonia production was assessed in peptone broth following the protocol of Cappuccino and Sherman (1992). Bacterial isolates were inoculated for culture in 10 mL of peptone broth. They were further incubated at $37 \pm 2°C$ (for 48 h), to which 0.5 mL of Nessler's reagent was added and observed for the colour change from brown to yellow, indicating positive for ammonia production.

2.3 *In planta* testing of plant growth promotion

The plant growth-promoting potential of the PGPR isolates *B. pumilus* GN-5 and *B. megaterium* JR-12 individually and in combination was tested in pearl millet (*Pennisetum glaucum* L.) cultivar Pusa composite 443.

2.3.1 Inoculation of seeds

Seeds were surface sterilized for 3 minutes with 1.2% sodium hypochlorite, rinsed thrice with sterile water and dried at room temperature (Sahu et al. 2022). Bacterial isolates were cultured in 500 mL of nutrient broth at 37°C for 48 h and centrifuged at 10,000 rpm for 10 minutes at 4°C. The pellets were rinsed and suspended in sterilized water. The final OD was adjusted to 0.8 at 600 nm (approx. 2×10^8 CFU/mL). The inoculum was applied to the seeds @ 2mL per kg seed, while in control treatments, seeds were treated with sterile nutrient broth in place of the bacterial suspension.

2.3.2 Effects of NaCl and bacterial Inoculation on pearl millet growth

The effects of salt stress and PGPR treatment on the pearl millet variety (Pusa Composite 443) were assessed in pot experiments under random block design in triplicates. Three kgs of soil with an initial pH of 7.2 and EC of 0.92 were supplemented with 0, 8.79, 17.55 and 26.46 g of sodium chloride dissolved in 300 mL of water to achieve salt concentrations of 0, 2.93, 5.85 and 8.82 g/kg soil, respectively. The treated seeds were planted in salt-amended pots in the greenhouse at $25 \pm 2°C$ with RH maintained at 50% and 12:12 hour light: dark cycle. The electrical conductivity of the soil extract (obtained by dissolving 30g of dry soil in 20 mL of deionized water and agitated for an hour) was measured by a conductivity meter. The moisture content of the soil was maintained at 25% by watering the pots twice with deionized water. The plants were thinned to 5 per pot after 10 days and harvested at 45 days to observe phenotypic parameters.

2.4 Plant growth parameters

The plants were harvested after 45 days to assess growth parameters in control and PGPR-treated plants under salt stress. The total biomass accumulation was evaluated by plant dry weight by oven-dried samples at 65±5 °C for 5 days to reach constant weight. The relative water content of the leaf was measured as per the protocol given by Sairam et al. (2002) and was calculated by the following equation used to determine the relative water content of the leaf.

$$RWC\ (\%) = [(FW - DW)/(TW - DW)] \times 100$$

Here FW - fresh weight, TW - turgid fresh weight after 24 h, DW - dry weight

The chlorophyll content (Chl a and Chl b) in leaves was determined using acetone extraction followed by spectrophotometry described by Arnon (1949). The contents of Chl a, Chl b, and total chlorophyll were determined by using the formula given in Sadasivam and Manickam (1996).

2.5 Determination of proline, total reducing sugar contents, carbohydrate content and total soluble protein content

To determine the proline content in pearl millet leaves, 0.5 g of fresh leaves were crushed in liquid nitrogen and homogenized using 10 mL of 3% sulfosalicylic acid. The amount of proline (μmol/g FW) was determined by taking absorbance at 520 nm using a standard curve (Bates et al. 1973). For total reducing sugar estimation, the DNSA method was followed (Miller1959). Absorbance was taken at 540nm. The carbohydrate content determination was carried out by the method of Yemm and Wills (1954). The Bradford (1976) method was used to estimate the total protein concentration in plant leaves. The absorbance was recorded at 595nm.

2.6 Antioxidant Enzyme Assays: Superoxide dismutase (SOD) and Catalase (CAT)

To determine the antioxidant enzyme superoxide dismutase, 0.5 g fresh leaves were homogenized in 2 mL of 50 mM SOD extraction buffer and assessed activity (Dhindsa and Thorpe 1981).

The reaction mixtures of 50 mM phosphate buffer and individual enzyme extracts were prepared for the catalase activity. The enzyme activity was determined by measuring the decrease in absorbance (ΔE, min-1·g-1·FW) 240 nm (Aebi 1984).

Table 1 Plant growth promotion traits of salt tolerant *Bacillus* species

| S. No | Strain | NCBI Accession | IAA Production | Zinc Solubilization | Phosphate Solubilization | | Siderophore Production | Ammonia Production |
					MgP$_2$O$_5$/ 100ml (8th Day)	MgP$_2$O$_5$/ 100ml (15th Day)		
1.	*B. pumilus GN-5*	MK 559616	38.34±0.76	+	25.54±0.79	35.67±0.78	+	++
2.	*B. megaterium JR-12*	MK 559615	42.34±0.56	+	27.89±1.11	37.67±1.16	+	+

2.7 Statistical analysis

All the data were taken in replicates and presented as average means with standard error. The data were analyzed using the PRISM 7.0 programme. ANOVA was used for the significance of treatments, and the significant treatments were determined at p 0.001 probability level.

3 Results

3.1 PGP activity of salt-tolerant isolates

The bacterial strains Bp-GN-5 and Bm-JR-12 isolated from the rhizosphere of mangrove soil were investigated for PGP activities such as IAA production, zinc solubilization, P$_i$ solubilization, siderophore production and ammonia production. Results of the study revealed that Bp-GN-5 solubilized 35.67 μg/ml phosphate and produce 38.34 μg/ml indole acetic acid, while Bm-JR-12 solubilized 37.67 μg/ml phosphate and produced 42.34 μg/ml IAA. Both the isolates were zinc solubilizers, ammonia producers and siderophore producers (Table 1).

3.2 Effect of salinity on growth traits

The present study investigated two PGPR strains, Bp-GN-5 and Bm-JR-12, for their role in alleviating salinity stress on plant growth promotion in pearl millet. An increase in salt concentration from 0 to 150 mM in soil was found to reduce the growth

parameters in pearl millet in untreated control, but the treatment of the two PGPR strains under salt stress was found to significantly alleviate the negative effect of salt stress on plant growth parameters. It could also help to reduce the adverse effects of ion toxicity.

The plants treated with salt-tolerant PGPR strains performed better in terms of plant growth under both salinized and non-salinized conditions. The reduction of plant height in 50, 100, 150 mM salt and PGPR-treated plants compared to untreated respective control plants were 7.46%, 29.03% and 47.93%, respectively, whereas in plants treated with a combination of Bp-GN-5 + Bm-JR-12 the reduction of plant height was found to be 9.12%, 20.30% and 33% respectively (Figure 1). Similarly, the results obtained for other plant growth parameters such as shoot dry weight were also found to be reduced in control plants by 0.56%, 8.93% and 40.73% respectively, at all salt concentration treatments whereas in plants treated with combination of Bp-GN-5 + Bm-JR-12the reduction was found to be alleviated to 38.72% in 150 mM respectively (Figure 2). Whereas, in addition of PGPR individually or in combination the growth parameters were alleviated during NaCl stress (Figure 1 and 2). The effect of salinity was reflected in the loss of relative water content as indicated by the reduction in relative water content with an increase in salt concentration (Figure 3). The individual application of Bp-GN-5 and Bm-JR-12 resulted in a non-significant difference in the growth parameters. The level of both Chl a and b content in PGPR treated plants was increased
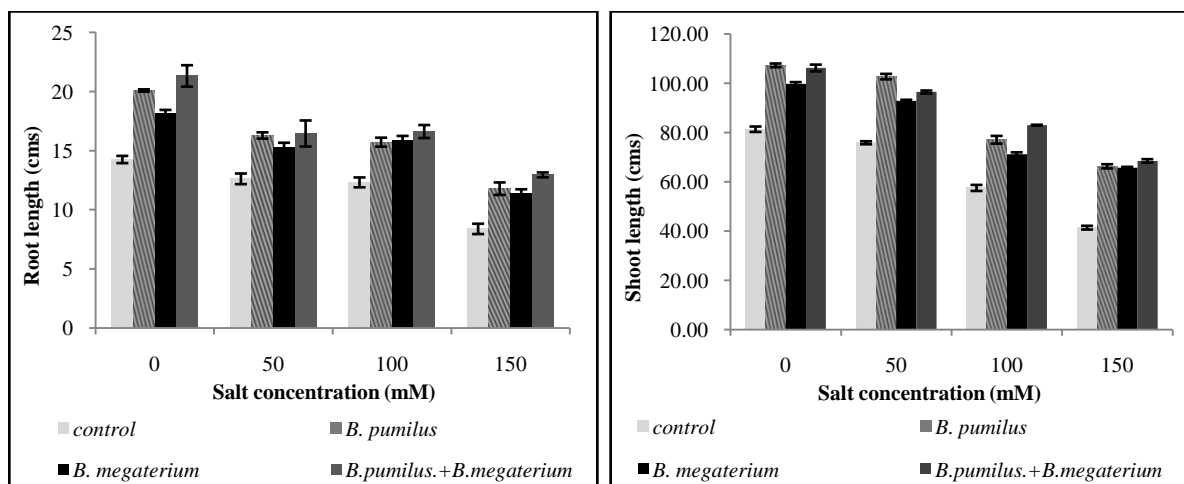

Figure 1 Effect of PGPR on shoot and root length of Pearl millet under NaCl stress
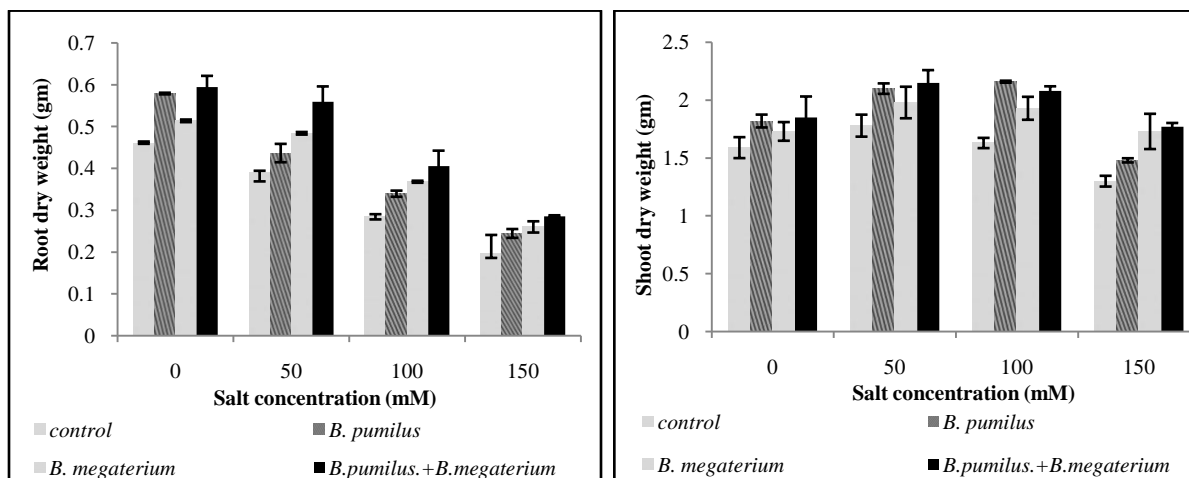
Figure 2 Effect of PGPR on shoot and root dry weight of Pearl millet under NaCl stress
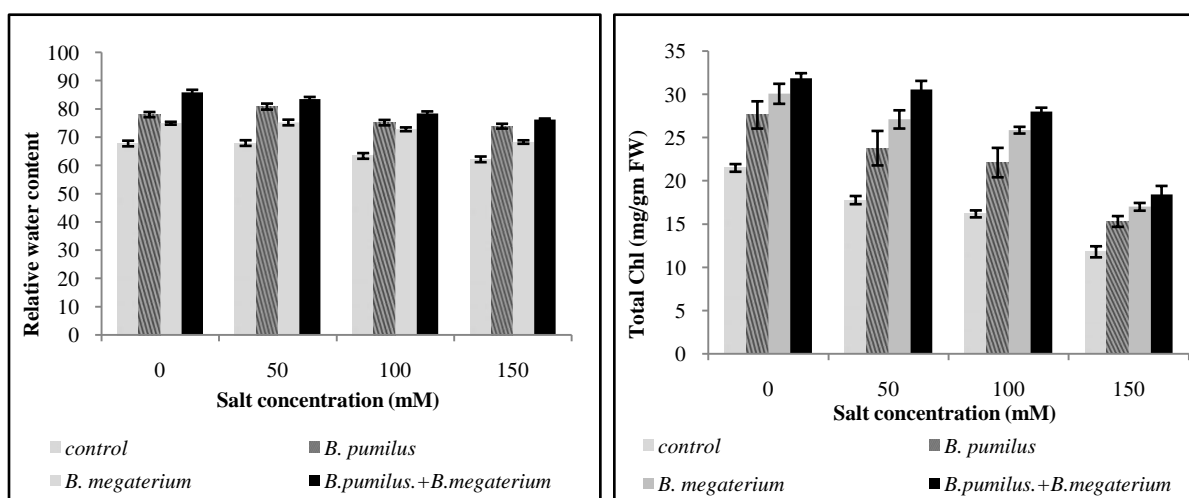

Figure 3 Effect of PGPR on leaf relative water content and total chlorophyll content of Pearl millet under NaCl stress

compared to the untreated control. The total chlorophyll content in pearl millet plants treated with Bp-GN-5 + Bm-JR-12 was found to be increased to 17.3, 24.69, and 45.09 % in comparison to 4.13%, 12.13% and 42.13% in control (only salt) stress treatments respectively (Figure 3).

3.3 Osmolyte Production as Defense Mechanism against Osmotic Stress

An increase in plant biochemical activities was observed under salt stress in pearl millet compared to negative control, i.e., no salt and no PGPR. The treatment of PGPR strains in the salt-amended soil helped increase the biochemical activities more than untreated plants, which in turn helped in plant growth promotion. All the biochemical activities, like the production of phenol content, reducing sugar, amino acid, protein, and proline, were increased in the presence of PGPR strains individually and in combination. However, no significant difference was observed in treated and

untreated plants' flavonoid and carbohydrate content production under salt stress (Table 2). Among the treatments, combining two PGPRs, i.e., Bp-GN-5 + Bm-JR-12, showed a significant increase in biochemical activities compared to individual PGPR strain treatment and untreated plants in NaCl stress.

The phenol content in control 0, 50, 100 and 150 mM salt stress plants was found to be 109.43, 124, 97.10 and 169.48 mg/gm DW, respectively, and this improvement was recorded 186.53, 210.60, 237.85 and 323.69mg/gm DW in the salt stress and Bp-GN-5 + Bm-JR-12 combination treated plants, respectively. Similarly, the reducing sugar content in untreated plants was increased in PGPR combination treated plants from 3.17, 7.23, 11.62 and 13.89 mg/gm FW to 6.24, 8.83, 14.8 and 16.7, respectively. Similarly, the amino acid content was 277.71, 316.06, 357.01 and 343.72ug/gm FW in untreated pearl millet plant during salt stress, which was found to be enhanced to 377.64, 404.51, 454.81 and 466.95ug/gm FW in Bp-GN-5 + Bm-JR-12 treated plants. The

Table 2 Effect of PGPR on biochemical activity of Pearl millet under salt stress in pot study

| Salt concentration	Treatments	Reducing sugar (mg/gmFW)	Carbohydrate (mg/gm FW)	Protein (mg/gm FW)	Proline (umol/min mg FW)
0 mM	Control	3.17±0.98[b]	16.37±0.17[c]	31.47±0.75[d]	112.33±0.17[d]
	Bp-Gn-5	5.16±0.88[a]	18.08±0.38[b]	38.473±0.63[c]	123.23±0.27[b]
	Bm-Jr-12	5.97±0.53[a]	17.54±0.67[b]	41.41±0.75[b]	121.60±0.06[c]
	Bp-Gn-5 + Bm-Jr-12	6.24±0.45[a]	19.29±0.31[a]	48.89±0.51[a]	130.54±0.07[a]
50 mM	Control	7.22±0.37[b]	19.77±0.06[c]	34.60±0.49[d]	123.43±0.10[d]
	Bp-Gn-5	7.52±0.11[b]	21.29±0.42[ab]	44.39±0.66[c]	132.10±0.25[b]
	Bm-Jr-12	7.84±0.04[ab]	20.51±0.10[bc]	49.93±0.59[b]	129.45±0.25[c]
	Bp-Gn-5 + Bm-Jr-12	8.82±0.57[a]	22.33±0.33[a]	53.44±0.38[a]	133.36±0.37[a]
100 mM	Control	11.62±0.40[a]	21.39±0.09[d]	35.41±0.28[d]	140.96±0.44[d]
	Bp-Gn-5	13.95±1.50[a]	23.49±0.17[b]	46.93±0.35[c]	156.86±1.15[b]
	Bm-Jr-12	13.70±0.28[a]	22.58±0.12[c]	51.21±0.18[b]	151.96±0.24[c]
	Bp-Gn-5 + Bm-Jr-12	14.79±0.75[a]	24.57±0.24[a]	53.58±0.65[a]	160.93±0.46[a]
150 mM	Control	13.89±0.57[a]	23.54±0.07[c]	28.50±0.20[d]	157.99±0.35[d]
	Bp-Gn-5	15.41±1.44[a]	25.36±0.34[b]	48.65±0.61[c]	171.61±0.59[b]
	Bm-Jr-12	14.83±0.85[a]	24.27±0.12[c]	53.04±0.32[b]	165.66±0.37[c]
	Bp-Gn-5 + Bm-Jr-12	16.69±0.29[a]	26.55±0.12[a]	58.46±0.13[a]	187.50±1.16[a]
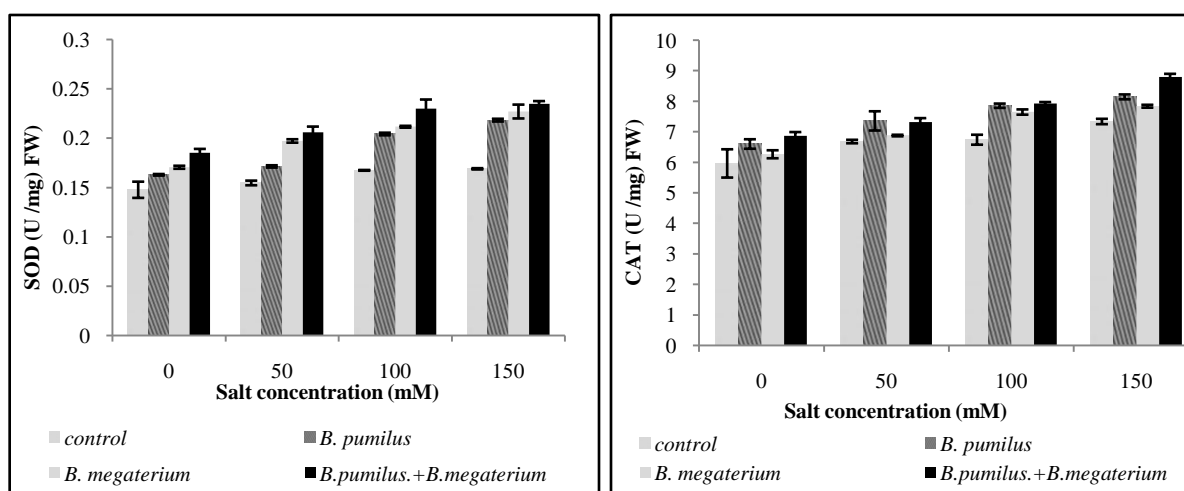
Figure 4 Effect of PGPR on SOD and CAT content of Pearl millet under NaCl stress

protein content in Bp-GN-5 + Bm-JR-12 treated plants were found to be increased to 48.90, 53.45, 53.58 and 58.47 mg/gm FW from 31.50, 34.60, 35.41 and 28.50 in 0, 50, 100 and 150mM salt stress, respectively. Similarly, the proline content in Bp-GN-5 + Bm-JR-12 treated plants were found to be 130.54, 133.36, 160.94 and 187.50 µmol/min mg FW from 112.33, 123.43, 140.96 and 157.99 respectively during salt stress (Table 2). Combining two PGPR strains increased tissue sugar levels and osmolytes to enhance tolerance to short-term salinity stress.

3.4 ROS Scavenging Activity as a Defense Mechanism against Oxidative Stress

The enzymes are responsible for salt tolerance in plants, i.e., superoxide dismutase (SOD) and catalase, were also investigated in the present study and were observed to be enhanced in the PGPR treated pearl millet plants compared to untreated plants under salinity stress. The results obtained for PGR supplementation individually and in combination showed similar

effects on SOD and CAT enzyme production with an increase up to 10-25% and 10-21%, respectively. Similarly, the results obtained for biochemical activities showed the increase in salt concentration induced the plant to produce more phenol, flavonoid, reducing sugar, carbohydrate, amino acid, protein, and proline, which helped the plant to sustain the salt stress.

4 Discussion

The investigated bacterial strains Bp-GN-5 and Bm-JR-12 were isolated from the rhizosphere of mangrove soil. For various microorganisms, mainly bacteria, the rhizosphere region of plants acts as a natural hotspot (reservoir) (Auta et al. 2017; Ling et al. 2022). Saline soils and deep-sea hypersaline sediments, among other environments, have previously been shown to contain Bacillus-like halophilic bacteria. This study was observed to agree with the findings of former studies reported by Sharma et al. 2021, Patel et al. 2023. These strains were investigated for PGP activities viz., IAA production, zinc solubilization, P- solubilization, siderophore and ammonia production. Bp-GN-5 was able to solubilize 35.67 µg/ml phosphate and produce 38.34 µg/ml indole acetic acid, while Bm-JR-12 was able to solubilize 37.67 µg/ml and produce 42.34 µg/ml IAA. Both the isolates were zinc solubilizers, ammonia producers and siderophore producers (Table 1). Exopolysaccharides, siderophores, volatile organic compounds (VOCs), compatible osmolytes, and phytohormones are just a few of the beneficial metabolites produced by ST-PGPR that help the saline-agro ecosystem become more productive (Ullah and Bano 2015; Pallavi et al. 2023). Phosphate solubilizing bacteria have been isolated from soils that have been subjected to environmental extremes, such as saline-alkaline soils, with a high level of nutrient deficit; PSB can solubilize phosphate under moderate saline conditions (Thant et al. 2018; Alotaibi et al. 2022). This increased P content in crops helps mitigate the growth-inhibiting effect of salt stress. PGP bacteria produce IAA, which leads to initiation of rooting, cell division, and expanded root surface range, where root surface region and root engineering play the foremost vital part (Ayaz et al. 2022; Tripathi et al. 2022) on plant development under saline soil conditions. Earlier, Singh et al. (2020) have also reported that multi-trait PGP isolates have shown phosphate solubilization, siderophore, IAA, ammonia and H_2S production, respectively and can be considered as great bioinoculants to alleviate adverse effects of abiotic stresses on plants.

The halotolerant PGPR has been reported to significantly reduce salt stress in agricultural crops. These two Bacilli used in the present study were also investigated for their role in alleviating salinity stress effect on plant growth promotion activities in pearl millet under salt stress. An increase in salt concentration from 0 to 150 mM in soil was found to reduce the growth parameters in pearl millet in the untreated control. Still, the supplementation of the two PGPR strains

under salt stress alleviated the negative effect of salinity stress on growth parameters significantly and performed better in plant growth under salinized and non-salinized conditions. The observations made during the study regarding the impact of salt stress, individual PGPR and combinatorial inoculation of both the PGPR, as presented in figures 1, 2, 3 and 4, are in accordance with other previous studies where it has been reported that multi-trait *B. safensis* (BS) and rhizospheric *B. haynesii* (BH) strains showed significant PGP properties under *in vitro* conditions for the growth promotion of the *Amaranthus viridis* plant under salinity (4 dS m^{-1} and 6 dS m^{-1}) conditions. Both strains were effective under abiotic stress conditions such as pH, temperature, salt, and drought (Patel et al. 2023). In the present study, both the bacterial isolates were able to enhance the plant growth under salt stress conditions in comparison to the PGPR untreated control plants, and both *B. megaterium* and *B. pumilus* strains were observed to improve various parameters such as germination percentage, shoot length, root length, FW, DW of pearl millet plant. In another study, *Bacillus* spp. strains, i.e., NMCN1 and LLCG23 isolated from the extreme environments of the Qinghai–Tibetan region of China, showed high salinity stress tolerance and could grow at up to 16% and 18% NaCl concentrations (Venieraki et al. 2021; Ayaz et al. 2022). The variations in germination percentage and all growth parameters could be attributed to the deposition of Na$^+$ and Cl$^-$ ions in the tissues, eventually compromising the germination metabolism. In another study, Khan et al. (2022) reported that the *Bacillus* strain could improve all growth parameters in wheat plants under 200 mM salt stress conditions.

The PGPR treated plants produce certain osmolytes such as proline, trehalose, and add up to dissolvable sugars that are biosynthesized and accumulate in cytoplasm as consistent solutes in response to osmotic stress under saline conditions. All these are effortlessly retained by plants to control water potential, regulate stomatal openings and transpiration rate, adjust osmosis, and avoid cellular oxidative damage. Several other physiological and biological responses are also controlled, including activating the antioxidant enzyme system, a defence mechanism triggered to eliminate free radicals created under stress and keep their levels low (Habib et al. 2016). This system contains several ROS-scavenging enzymes, including POD, SOD, APX, and CAT, which can reduce abiotic stress, such as salt stress, eliminate free radicals, and prevent the toxicity of ROS produced in stressed cells (Santos et al. 2018). In this work, pearl millet plants inoculated with the isolates Bm JR-12 and Bp GN-5 underwent salinity stress and showed elevated SOD and CAT activity, whereas H_2O_2 and lipid peroxidation decreased. This finding supports that microorganisms positively impact the equilibrium of antioxidant enzymes detoxifying ROS metabolism (Santos et al. 2018). Under conditions of salt stress, ROS, such as SOAs and hydrogen peroxide, are typically formed at high rates and lead to oxidative damage to the cell structure (Sahu et al. 2021).

In this study, it was also observed that the two halotolerant strains *B. megaterium* JR-12 and *B.pumillus* GN-5 consortium treated plant significantly increased protein content in comparison to the uninoculated control in pearl millet under salt stress (150 mM NaCl). The results were consistent with the findings of Ullah and Bano (2015), who discovered that PGPR inoculation to crops enhanced the levels of osmolytes such as proline, sugars, and amino acids compared to un-inoculated controls.

Conclusion

This study's results indicate that PGPR positively impacts the physicochemical properties of inoculated plants, resulting in improved water conditions and increased accumulation of compatible solutes and antioxidant properties. These changes in cellular metabolism ultimately led to improved growth and yield of salt-tolerant and sensitive strains under salt stress. However, salt-tolerant cultivars showed much better growth and yield than susceptible ones. Individual and co-inoculation showed more pronounced effects on pearl millet by playing an essential role in improving growth and yield. The study shall enable these microorganisms to be utilized as biofertilizers for improved pearl millet crop production in saline soils. It can be concluded that the two PGPR strains, *B. pumilus* isolate GN-5 and *B. megaterium* isolate JR-12, can further be used in agricultural practice for alleviating the adverse salinity stress effects on plant growth promotion activities in different crops under salt stress conditions.

Author Contributions

P. and ST conceptualized and designed the experiments. P., ST collected and analyzed the data. P., RKM, NS and ST contributed to the manuscript. AV and ST supervised the work.

Declaration

There are no conflicts of interest among the authors.

Acknowledgments

References

Aebi, H. (1984). Catalase in vitro. *Methods in Enzymology,105,*121-126

Alotaibi, N.M., Kenyon, E.J, Bertelli, C.M., Al-Qthanin, R.N., Mead, J., Parry, M., & Bull, J.C. (2022). Environment predicts seagrass genotype, phenotype, and associated biodiversity in a temperate ecosystem. *Frontiers in Plant Science, 13*, 887474. doi: 10.3389/fpls.2022.887474

Arnon, D. I. (1949). Copper Enzymes in Isolated Chloroplasts. Polyphenoloxidasein *Beta vulgaris*. *Plant physiology*, *24*(1), 1–15. https://doi.org/10.1104/pp.24.1.1

Auta, H. S., Emenike, C. U., & Fauziah, S. H. (2017). Screening of Bacillus strains isolated from mangrove ecosystems in Peninsular Malaysia for microplastic degradation. *Environmental pollution (Barking, Essex : 1987)*, *231*(Pt 2), 1552–1559. https://doi.org/10.1016/j.envpol.2017.09.043

Ayaz, M., Ali, Q., Jiang, Q., Wang, R., Wang, Z., et al. (2022). Salt tolerant *Bacillus* strains improve plant growth traits and regulation of phytohormones in wheat under salinity stress. *Plants*, *11*(20), 2769. https://doi.org/10.3390/plants11202769

Ayyam, V., Palanivel, S., & Chandrakasan, S. (2019). Approaches in land degradation management for productivity enhancement. In V. Ayyam, S. Palanivel, & S. Chandrakasan (Eds.), *Coastal Ecosystems of the Tropics—Adaptive Management* (pp. 463–491); Singapore Springer.

Bates, L.S., Waldren, R.P., & Teare, I.D. (1973).Rapid determination of free proline for water stress studies. *Plant and Soil, 39,* 205-207

Bhat, M.A., Kumar, V., Bhat, M.A., Wani, I.A., Dar, F.L., Farooq, I., Bhatti, F., Koser, R., Rahman, S., & Jan, A.T. (2020). Mechanistic insights of the interaction of plant growth-promoting rhizobacteria (PGPR) with plant roots toward enhancing plant productivity by alleviating salinity stress. *Frontiers in Microbiology*, *11*, 1952. doi: 10.3389/fmicb.2020.01952

Bradford, M.M. (1976). A rapid and sensitive method for the quantification of microgram quantities of protein utilizing the principle of protein-dye binding. *Analytical Biochemistry, 72*, 248-254

Brick, J.M., Bostock, R.M., & Silverstones, S.E. (1991). Rapid in situ assay for indole acetic acid production by bacteria immobilized on nitrocellulose membrane. *Applied Environment Microbiology, 57*(2), 535-538

Cappuccino, J.C., & Sherman, N. (1992). Microbiology "A Laboratory Manual", Benjamin/Cummings, New Yorkpp. Pp. 125–179

Dhindsa, R.H., & Thorpe, T.A. (1981). Leaf senescence correlated with increased level of membrane permeability, lipid peroxidation and decreased level of SOD and CAT. *Journal of Experimental Botany, 32*, 93-101

Dodd, I.C., & Pérez-Alfocea, F. (2012). Microbial amelioration of crop salinity stress. *Journal of Experimental Botany, 63*, 3415-28

Edi-Premono, M., Moawad, A.M., & Vleck, P.L.G. (1996). Effect of phosphate solubilizing *Pseudomonas putida* on the growth of maize and its survival in the rhizosphere. *Indonesian Journal of Crop Science,11* (1), 13-23.

Evans, L. (2006). *Millet for reclaiming irrigated saline soils*. Prime facts, Profitable and sustainable primary industries www.dpi.nsw.gov.au

Habib, S. H., Kausar, H., & Saud, H. M. (2016). Plant growth-promoting rhizobacteria enhance salinity stress tolerance in okra through ROS-scavenging enzymes. *Biomed Research International, 2016*, 6284547.doi: 10.1155/2016/6284547

Hussain, K., Ashraf, M., & Ashraf, M.Y. (2008). Relationship between growth and ion relation in pearl millet (*Pennisetum glaucum* (L.) R. Br.) at different growth stages under salt stress. *African Journal of Plant Science, 3*(2), 23- 27

Hussain, K., Nawaz, K., Majeed, A., Khan, F., Lin, F., et al. (2010). Alleviation of salinity effects by exogenous applications of salicylic acid in pearl millet (*Pennisetum glaucum* (L.) R. Br.) Seeding. *African Journal of Biotechnology, 9*(50), 8602-8607

Khan, M. Y., Nadeem, S. M., Sohaib, M., Waqas, M. R., Alotaibi, F., Ali, L., Zahir, Z. A., & Al-Barakah, F. N. I. (2022). Potential of plant growth promoting bacterial consortium for improving the growth and yield of wheat under saline conditions. Frontiers in microbiology, 13, 958522. https://doi.org/10.3389/fmicb.2022.958522

Kumar, A., Kumar, R., Yadav, V.P.S., & Kumar, R. (2010). Impact assessment of frontline demonstrations of Bajra in Haryana state. *Indian Research Journal of Extension Education, 10*(1), 105–108.

Kumar, V. & Gera, R. (2014). Isolation of a multi-trait plant growth promoting *Brevundimonas sp*. and its effect on the growth of Bt-cotton. *3 Biotech, 4*, 97-101

Ling, N., Wang, T., & Kuzyakov, Y. (2022). Rhizosphere bacteriome structure and functions. *Nature Communications, 13,* 836 https://doi.org/10.1038/s41467-022-28448-9

Miller, G.L. (1959). Use of dinitrosalicylic acid reagent for determination of reducing sugar. *Analytical Chemistry, 31*(3), 426-428

Munns, R., & Tester, M. (2008). Mechanisms of salinity tolerance. *The Annual Review of Plant Biology, 59*, 651–681

Orhan, F. (2016). Alleviation of salt stress by halotolerant and halophilic plant growth-promoting bacteria in wheat (*Triticum aestivum*). *Brazilian Journal of Microbiology, 47*(3), 621–627. https://doi.org/10.1016/j.bjm.2016.04.001.

Pallavi, Mishra, R. K., Sahu, P. K., Mishra, V., Jamal, H., Varma, A., & Tripathi, S. (2023). Isolation and characterization of halotolerant plant growth promoting rhizobacteria from mangrove region of Sundarbans, India for enhanced crop productivity. Frontiers in Plant Science, 14, 1122347. https://doi.org/10.3389/fpls.2023.1122347

Patel, M., Vurukonda, S.S.K.P., & Patel, A. (2023). Multi-trait halotolerant plant growth-promoting bacteria mitigate induced salt stress and enhance growth of *Amaranthus viridis*. *Journal of Soil Science and Plant Nutrition, 23* (2), 1860-1883. doi: 10.1007/s42729-023-01143-4

Pérez-Miranda, S., Cabirol, N., & George-Téllez, R. (2007). O-CAS, a fast and universal method for siderophore detection. *Journal of Microbiological Methods, 70* (1), 127–131

Pikovskaya, R.I. (1948). Mobilization of phosphorus in soil in connection with the vital activity of some microbial species. *Mikrobiologiya,*17, 362-370

Sadasivam, S., & Manickam, A. (1996). *Biochemical Methods for Agricultural Sciences*. New Delhi: New Age International (P) Ltd. pp. 1–97

Sahu, P.K., Singh, S., Singh, U.B., Chakdar, H., Sharma, P.K., et al. (2021). Inter-Genera colonization of *Ocimum tenuiflorum* endophytes in tomato and their complementary effects on Na+/K+ Balance, Oxidative Stress Regulation, and Root Architecture Under Elevated Soil Salinity. *Frontiers in Microbiology, 18*(12), 744733. doi: 10.3389/fmicb.2021.744733.

Sahu, P.K., Tilgam, J., Mishra, S., Hamid, S., Gupta, A., Verma, S.K., & Kharwar, R.N. (2022). Surface sterilization for isolation of endophytes: Ensuring what (not) to grow. *Journal of Basic Microbiology, 62*(6), 647-668. doi: 10.1002/jobm.202100462

Sairam, R.K., Rao, K.V., & Srivastava, G.C. (2002). Differential response of wheat genotypes to long term salinity stress relation to oxidative stress, antioxidant activity and osmolyte concentration. *Plant Sciences, 163*, 1037– 1046

Santos, A. D. A., Silveira, J. A. G. D., Bonifacio, A., Rodrigues, A. C., & Figueiredo, M. D. V. B. (2018). Antioxidant response of cowpea co-inoculated with plant growth-promoting bacteria under salt stress. *Brazilian Journal of. Microbiology*, 49, 513–521. doi: 10.1016/j.bjm.2017.12.003

Schirawski, J., & Perlin, M. H. (2017). Plant-microbe interaction. The good, the bad and the diverse. *International Journal of Molecular Sciences, 19,* 1374.

Schwyn, B., & Neilands, J.B. (1987). Universal chemical assay for the detection and determination of siderophores. *Analytical Biochemistry, 160*, 47–56

Shahbaz, M., & Ashraf, M. (2013). Improving salinity tolerance in cereals. *Critical Review in Plant Sciences*, *32*, 237–249

Sharma, A., Dev, K., Sourirajan, A., & Choudhary, M. (2021). Isolation and characterization of salt-tolerant bacteria with plant growth-promoting activities from saline agricultural fields of Haryana, India. *Journal of Genetic Engineering and Biotechnology, 19*, 99 (2021). https://doi.org/10.1186/s43141-021-00186-3.

Sharma, P., Jha, A. B., Dubey, R. S., & Pessarakli, M. (2012). Reactive oxygen species, oxidative damage, and antioxidative defense mechanism in plants under stressful conditions. *Journal of Botany, 2012*, 217037. doi: 10.1155/2012/217037

Singh, T.B., Sahai, V., Ali A., Prasad, M., Yadav, A., Shrivastav, P., Goyal, D., & Dantu, P.K. (2020). Screening and evaluation of PGPR strains having multiple PGP traits from the hilly terrain.*Journal of Applied Biology & Biotechnology, 8*(04), 38-44.

Thant, S., Aung, N.N., Aye, O.M., Oo, N.N., et al. (2018). Phosphate solubilization of *Bacillus megaterium* isolated from non-saline soils under salt stressed conditions. *Bacteriol Mycology, 6*(6), 335–341.

Toro, G., Pimentel, P., & Salvatierra, A. (2021). Effective categorization of tolerance to salt stress through clustering Prunus rootstocks according to their physiological performances. *Horticulturae,7,* 542. doi: 10.3390/horticulturae7120542

Tripathi, S., Bahuguna, R., Shrivastava, N., Singh, S., Chatterjee, A., Varma, A., & Jagadish, K. (2022). Microbial biofortification: A sustainable route to grow nutrient-rich crops under changing climate. *Field Crops Research*, 287. 10.1016/j.fcr.2022.108662.

Ullah, S., & Bano, A. (2015). Isolation of plant-growth-promoting rhizobacteria from rhizospheric soil of halophytes and their impact on maize (*Zea mays* L.) under induced soil salinity. *Canadian Journal of Microbiology, 61*(4), 307-13.

Upadhyay, S.K., Singh, D.P., & Saikia, R. (2009). Genetic diversity of plant growth promoting rhizobacteria isolated from rhizospheric soil of wheat under saline condition. *Current Microbiology, 59*(5), 489-96.doi: 10.1007/s00284-009-9464-1

Venieraki, A., Chorianopoulou, S. N., Katinakis, P., & Bouranis, D. L. (2021). Multi-trait wheat rhizobacteria from calcareous soil with biocontrol activity promote plant growth and mitigate salinity stress. *Microorganisms*, *9*(8), 1588. https://doi.org/10.3390/microorganisms9081588

Watanabe, F.S., & Olsen, S.R. (1965). Test of an ascorbic acid method for determining phosphorous in water and NaHCO$_3$ extracts from soil. *Soil Science Society of American Journal, 29*, 677-678

Yemm, E., & Willis, A.J. (1954). The estimation of carbohydrate in plant extracts by Anthrone. *Journal of Biochemistry, 57*, 508-514

CrossMark
click for updates

Journal of Experimental Biology and Agricultural Sciences

An Insight into Application of Land Use Land Cover Analysis towards Sustainable Agriculture within Jhajjar District, Haryana

Jyoti Singh[1] iD, Mansi[1] iD, Pooja Baweja[1*] iD, Neha[1] iD, Isha Arya[1], Haritma Chopra[1] iD, Sandhya Gupta[1] iD, Pinkey B. Gandhi[1] iD, Priyadarshini Singh[1, 2*] iD, Vikas Rena[2*] iD

[1]Maitreyi College, University of Delhi, New Delhi, India
[2]School of Environmental Sciences, Jawaharlal Nehru University, New Delhi, India

ABSTRACT

The increasing population, depletion of natural resources, semi-arid climatic and poor soil health conditions in Jhajjar district of Haryana have drawn major attention towards the changes in Land Use/Land Cover (LULC). The region's increasing population is mainly dependent upon the agrarian economy; thus, sustainable agricultural production is a major thrust area of research. The present study analyses the LULC changes in the area during two decades 2000 – 2020, using remote sensing and Geographic Information System (GIS). Landsat satellite images (Landsat-7 and Landsat-8 satellites) for 2000 and 2020 were analyzed for mixed classification based on unsupervised classification followed by supervised classification. The study area has experienced an increase in agricultural land, surface water bodies and built-up land by 16.89%, 79.73% and 56.41%, respectively. There is a decrease in barren land and fallow land by 48.53% and 36.97%, respectively, as per the five major LULC classes. The LULC analysis indicates an increase in built-up land, which is responsible for controlling agricultural productivity and unsustainable agricultural activities. The study provides a comprehensive understanding of the land use trajectory in a specific region in two decades and associated unsustainable changes in the agrarian economy through pressure on the increase in agricultural production and conversion of land mass into croplands. It also signifies climate-resilient agriculture and the management of sustainable agriculture.

* Corresponding author

E-mail: vikasrena.sesjnu@gmail.com (Vikas Rena); pbaweja@maitreyi.du.ac.in (Pooja Baweja); psingh1@maitreyi.du.ac.in (Priyadarshini Singh);

1 Introduction

The dynamics of the earth's surface are attributed to the utilization of land by living and non-living components. In contrast, the land cover denotes what covers the earth's surface (Suzanchi and Kaur 2011), which can be associated with various natural and anthropogenic factors (MohanRajan et al. 2020). Land Use Land Cover (LULC) changes can be accessed by analyzing earth observation datasets using Geographic Information System (GIS). The change detection in LULC is of utmost scientific importance for a comprehensive understanding of the relationship between nature and human beings. The various satellite images as primary data sources provide vast opportunities with different algorithms using GIS tools (Chughtai et al. 2021).

India is a developing country where the agricultural sector plays a pivotal role in establishing a stable economy, providing the main source of livelihood, particularly in the rural sector. An agricultural field is sustainably cultivated when it protects the environment and produces a sufficient quantity of superior-quality food while conserving environmental components (Reganold et al. 1990). However, the burgeoning population pressure in many countries, such as India, has compelled them to use unsustainable methods to increase the farm yield to meet the ever-increasing demand, resulting in continuous depletion in natural resources required for agriculture, such as inadequate availability of cultivable land and water resources (Yadav et al. 2013). This has increased the cost of crop inputs, all indicative of the ongoing unsustainable agriculture practices that are putting the agrarian population of India at risk.

Land and water are the crucial natural resources that directly impact agriculture. In particular, the unethical management and overexploitation of land resources can transform productive land into impervious land (Rahman et al. 2012). Further, continuous overexploitation of the available cultivable land renders the soil infertile (Murungweni et al. 2016). There is supportive evidence proving the rapid change in LULC may make the land unsuitable for agriculture in future. Along with fertile land in arid and semi-arid regions of the world, water is another major limiting factor in crop production. In India's arid to semi-arid areas, climate change has a declining trend in the average rainfall, forcing farmers to use groundwater for irrigation (CGWB, Haryana 2015-16). The increasing number of tube wells, inappropriate cropping patterns, irrigation techniques, and lack of proper planning of systematic groundwater extraction have resulted in excessive exploitation of the available surface and groundwater resources (Kumar 2019). As per WHO estimation, 97 million ha of Indian land is facing freshwater scarcity today (Kumar 2019). Additionally, the adverse effects of the green revolution, extensively practised during the 1970s, are now seen in terms of seasonal mono-cropping of wheat and paddy in rabi and kharif seasons. There is also supportive evidence regarding water logging conditions in fields, increased

water and soil salinity, and decreased farmers' income (Rena et al. 2021, Singh et al. 2012). Maintaining land fertility with high water retention capacity, ensuring high crop productivity for extended periods, and utilizing the resources must be scientifically planned and managed without compromising future needs (Singh and Amrita 2017).

Tracking the changes in LULC through Remote Sensing (RS) and Geographic Information Systems (GIS) can help manage sustainable agriculture practices and aid in adopting planning strategies. LULC classification is crucial for understanding the interactions between human activities and the environment. This enables convenient monitoring and detection of changes bringing negative and positive environmental impacts (Ali 2006; Güler et al. 2007; Anil et al. 2011; Arowolo and Deng 2018). The observed changes can further help to monitor and maintain suitable land use practices for achieving the goal of sustainable farming practices within agricultural-dominated regions (Suzanchi and Kaur 2011; Pawar and Singh 2021; Szarek-Iwaniuk 2021).

Presently, more focus is laid on satisfying the short-term supply needed for a growing population without considering the harm caused to the ecosystem services and environmental components (Duraisamy et al. 2018). This negligence can lead to long-term damage and permanent resource loss. Therefore, regular monitoring of LULC change over time can help to effectively apply methods for reduction in degradation of land and water resources and allow sustainable resource maintenance.

The present work is focused on the study of LULC change dynamics within the Jhajjar district in Haryana to monitor and assess possible degradation by the current methods of practising agriculture and the probable remedial measures that can be taken to promote sustainable agriculture in future. To analyze the dynamics of LULC for agricultural sustainability in the Jhajjar district, the important objectives undertaken in this study are (i) Study of the proportion of areas under major LULC classes in different time scales, (ii) the analysis of LULC change to assess the possible drivers of land-use change and (iii) dynamics of LULC change to evaluate the impact on agriculture.

2 Materials and Methods

2.1 Study Area

Haryana (Figure 1) is an arid to semi-arid landlocked state in the North Western region of India with an area of 44,212 sq. Km. It lies between 27°39' - 30°35' N latitude and 74°28' - 77°36' E longitude (Malik 2012). Haryana serves as India's frontline state regarding food grain production. Jhajjar district's economy heavily depends on agriculture (Kumar and Gaur 2015). The district covers the state's southeast region with a total area of 1,834 sq. Km lying
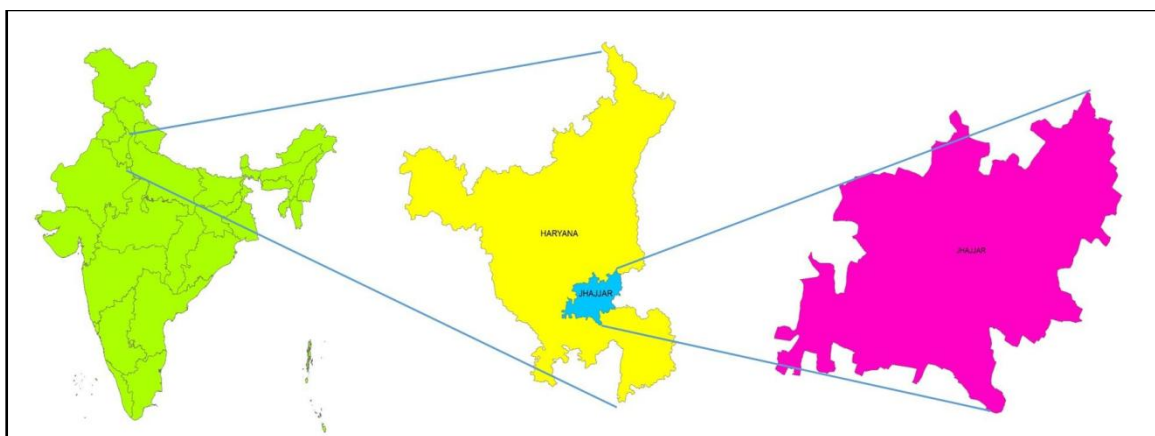
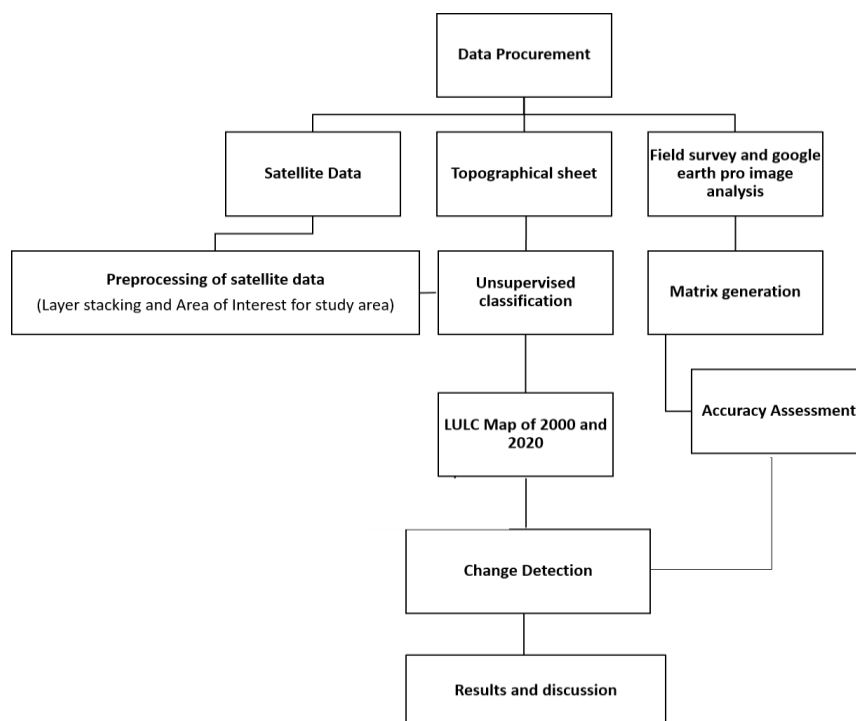Figure 1 Map showing the location of the study area (map not to scale)

Figure 2 Methodological framework for LULC analysis

between 28°22': 28°49' north latitudes and 76°18': 76°59' east longitudes (Yadav et al. 2009). The topography of the eastern part of the district is considerably even, but some areas are uneven, making it prone to inundation and water logging during the monsoon season. The elevation lies about 222 meters above sea level with a gentle slope from North to South (Arya et al. 2015). The district is classified as an arid to semi-arid area, with the main climatic regime showing a hot and dry summer, cold winter and sparse rainfall during the monsoon (Krishnan 2013). The average annual rainfall received within the district is 532 mm. The maximum and minimum temperatures range from 45°C and 4°C during June and January, respectively (Krishnan 2013). The major crops in the study area are wheat and mustard in winter (Rabi), sugarcane and vegetables in summer (Kharif). The chemical-based fertilizers to augment crop yield and pesticides to protect the crop from harmful pests and diseases are quite common in the study area. With the limited water resources in the region, the primary irrigation methods are tube wells, bore wells and canals to irrigate the crops in the dry season.

2.2 Methodology

For the analysis, both primary and secondary data sources were used (Figure 2).

Table 1 Metadata of Landsat series

Year	Date of Acquisition	Satellite (sensor)	Path / Row	Spatial Resolution
2000	18/2/2000	Landsat 7 (ETM +)	147/40	30 m/ pixel
2020	1/2/2020	Landsat 8 (OLI)	147/40	30 m/ pixel

2.3 Primary Data

The Landsat satellite data of February month were used for the years 2000 and 2020 for LULC change analysis (Table 1). Satellite images were downloaded from USGS Earth Explorer – GLOVIS (https://earthexplorer.usgs.gov/).

To start with the analysis of satellite images, the satellite images of no cloud cover and terrain-corrected images were downloaded from the open data source interface of NASA. The images consisted of different spectral bands with specific spectral information in each band. Layer stacking was carried out in ERDAS Imagine software to utilize the data from the spectral bands. After the layer stacking, the Area of Interest (AOI) corresponding to the study area was clipped from the composite satellite image. Further, image corrections (radiometric correction) were done for Landsat 7 and Landsat 8 images for the years 2000 and 2020 respectively, using ERDAS Imagine software.

2.4 Secondary Data

Secondary data were collected from two methods viz., Google Earth Images and Survey of India topographical sheets of Jhajjar district Toposheet number 53 D/6, 53 D/7, 53D/9, 53D/10, 53 D/11, 53 D/13, 53D/14, 53 D/15 (Map-Scale: 1:25,000)

2.5 Software Used

The software used in this study are (i) ERDAS IMAGINE 2015 for classification, (ii) ArcGIS 10.2 software was used for final map creation, and (iii) ENVI 5.2 software for thematic change detection analysis

2.6 Land Use/Cover Classification Scheme

Based on literature studies and field-based surveys, the LULC analysis for five major classes was carried out for agricultural land, barren land, built-up land, fallow land and water bodies. Unsupervised classification was done through ERDAS Imagine software on satellite images of the years 2000 and 2020 using the K-means classifier method. The supervised classification followed by unsupervised classification has provided the hybrid classification images.

2.7 Field survey and accuracy assessment

Field verification was carried out in different parts of Jhajjar, covering all the LULC classes. Photographs taken during the field survey are shown in Figure 3. The accuracy assessment for LULC classification was done using the quantitative confusion matrix method (Table 2).

2.8 Statistical Analysis

The statistical analysis based on ArcGIS and ERDAS imagines GIS software tools have resulted in significant accuracy in creating thematic maps for LULC classes for 2000 and 2020 satellite images. The accuracy assessment used the quantitative confusion matrix method (Asthana et al. 2020). The statistical comparison for the satellite images has suggested a significant change in various LULC classes, revealing the increasing population and the associated anthropogenic implications creating unsustainability in agricultural practices. The results related to the statistical analysis have been discussed in detail in the Results and Discussion section.

Table 2 Confusion Matrix for accuracy assessment of LULC classification

| Sum of Area (Hectares)	Column Labels					
Classes	Water Body	Agricultural Field	Fallow land	Settlements	Bare land	Grand Total 2020
Water Body	1114.96	2720.3	1748.47	862.357	236.542	6682.629
Agricultural land	456.142	63455.4	39868.9	2124.25	3482.53	109387.222
Fallow land	1260.97	16319.2	16496	5821.74	2756.34	42654.25
Settlements	815.985	8645.02	8219.86	8961.28	1332.79	27974.935
Bare land	69.93	2434.66	1347.1	115.177	105.818	4072.685
Grand Total 2000	3717.987	93574.58	67680.33	17884.804	7914.02	190771.721
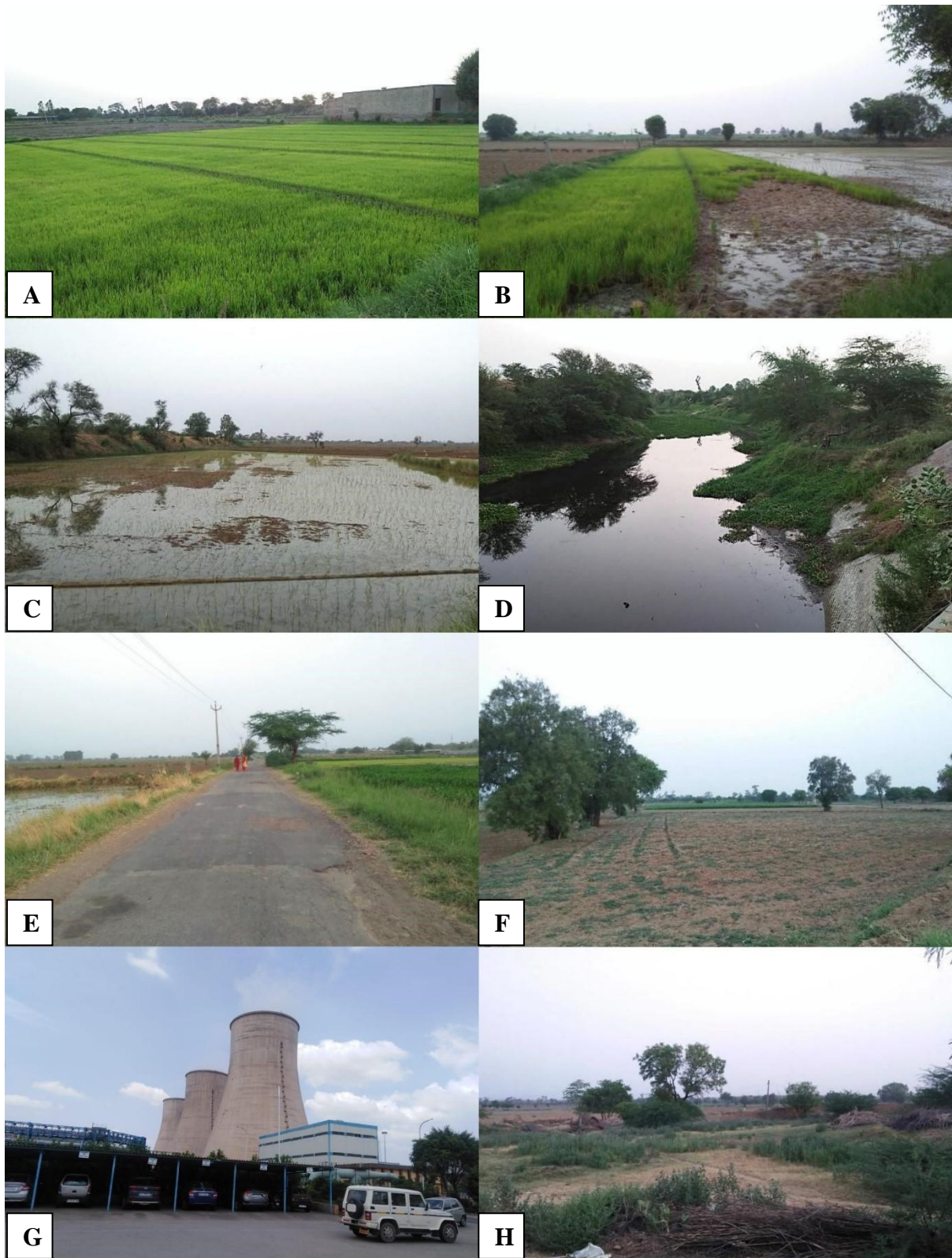
Figure 3 Field photographs of different sites of the study areas A, B & C; Paddy fields, D; Drain No. 8, E; Road passing through the district, F; Fallow lands, G; Jharli Power Plant, H; Barren land.

Table 3 Summary of land use/ land cover classification statics for 2000 and 2020

LAND USE	2000 AREA (HA)	(%)	2020 AREA (HA)	(%)	Change	Relative change (%)
WATER BODY	3717.987	1.94	6682.629	3.50	2964.642	79.73
AGRICULTURAL LAND	93574.58	49.05	109387.222	57.33	15812.642	16.89
FALLOW LAND	67680.33	35.47	42654.25	22.35	−25026.08	-36.97
BUILT-UP LAND	17884.804	9.37	27974.935	14.66	10090.131	56.41
BARREN LAND	7914.02	4.14	4072.685	2.13	−3841.335	-48.53

3 Results and Discussions

The data analysis for LULC change detection (Table 3) depicts that the area covered by water bodies in Jhajjar district has increased from 3717.987 ha (1.94%) in 2000 to 6682.629 ha (3.50%) in 2020, from close observation of the spatial distribution of the water bodies in the maps (Figure 4, 5) it can be inferred that the increase in the area is primarily due to the construction of the reserve pond close to the Mahatma Gandhi and Indira Gandhi thermal power plant in the southeastern part (Figure 3G). Further waterlogged areas and paddy cultivation having inundated fields with water are also inferred to have contributed to the increase in the area of water bodies (Figure 3, B & C). Surface water bodies in the Jhajjar district include ponds, lakes, reservoirs, water canals, waterlogged agricultural fields, etc., covering the second largest land use (Figures 4 and 5).

During the last 50 years, large investments have been made worldwide in arid and semi-arid regions to increase agricultural production, particularly for its diversification (Ram et al. 2008). Jhajjar also lies in the arid to semi-arid belt, where the water requirement for irrigation is fulfilled through groundwater extraction or canal irrigation to improve and stabilize yields. Major canals in the district are the Western Yamuna Canal and the Jawaharlal Nehru Lift Canal. Water from the Western Yamuna Canal is used for drinking, irrigation, industrial sector, domestic purposes, etc.

The groundwater level increased due to the arrival of the Jawaharlal Nehru Canal in the 1970s, and people saw a golden opportunity to grow water-intensive paddy crops. Increased cultivation of paddy and wheat leads to the problem of water logging in several parts of the district (Figure 3, B & C), further
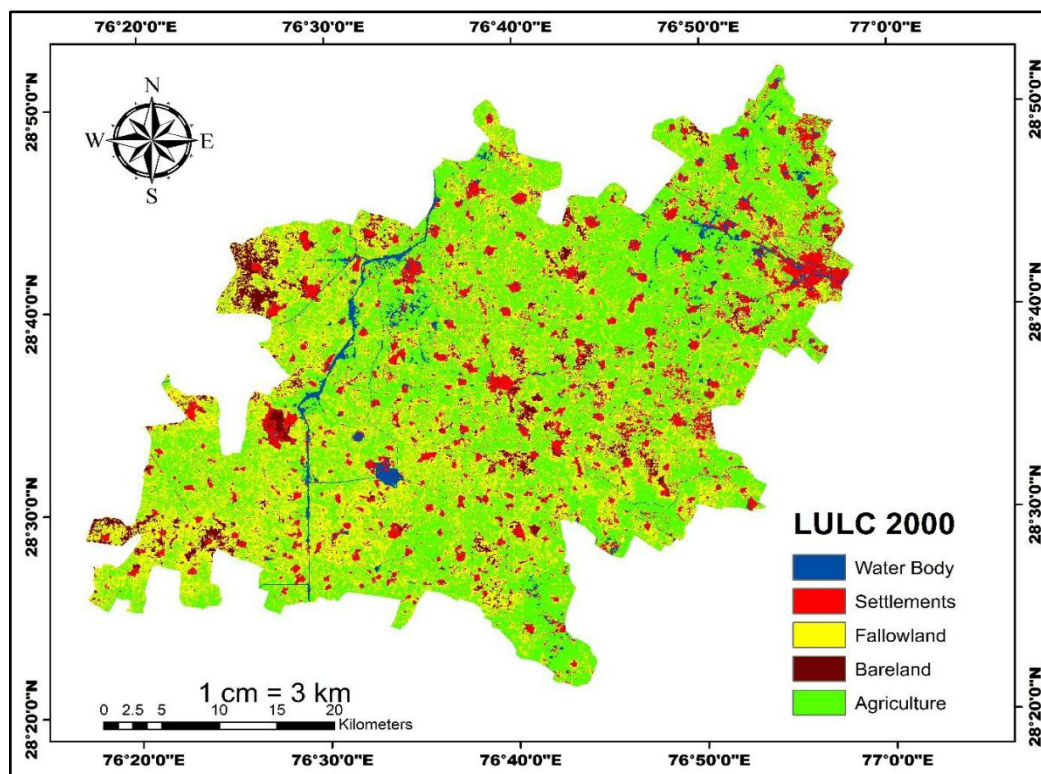

Figure 4 Land use/ land cover of Jhajjar district in different categories during the year 2000
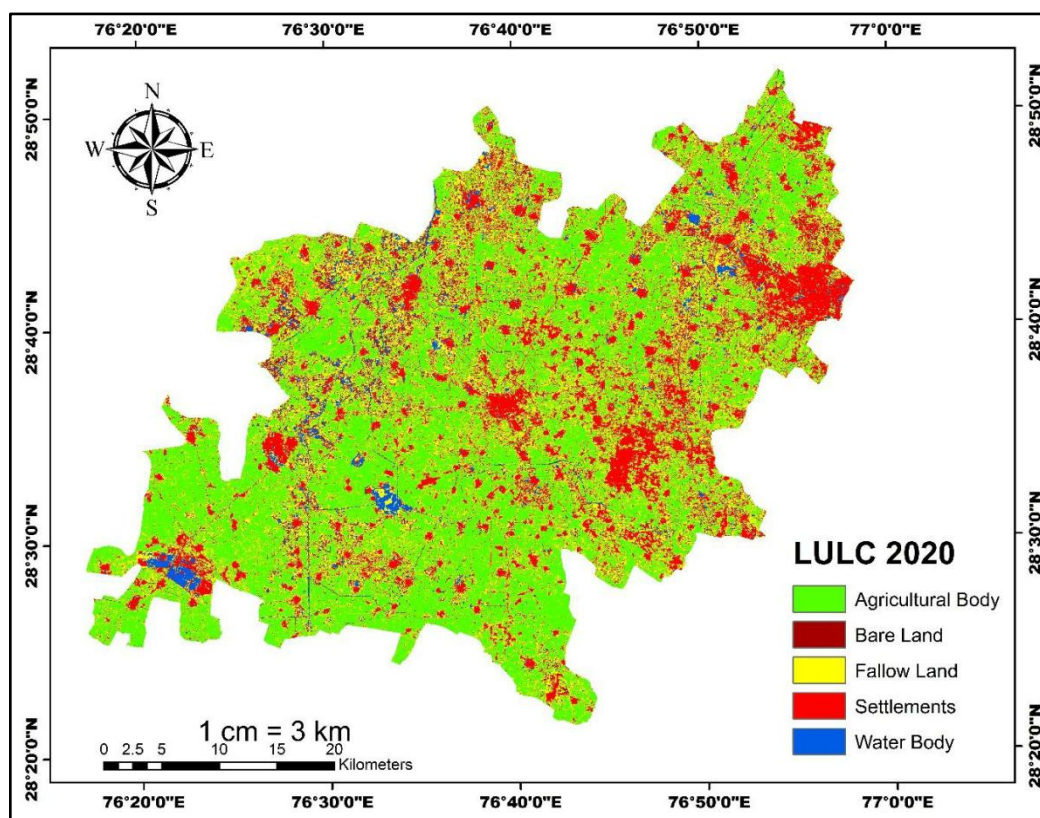
Figure 5 Land use/ land cover of Jhajjar district in different categories during the year 2020

leading to groundwater and soil salinity. Stagnant water in the rice fields decreases the porosity of the soil, affecting the infiltration rate and consequently leading to water logging conditions (Chaudhary and Aneja 1991).

Additionally, the district and the neighbouring areas in the South-West and North-West directions were profoundly exposed to floods due to saucer-like depressions. These parts are situated in low-lying areas and are inappropriate for agriculture. During monsoon season, drain congestion further leads to floods affecting the crops in the villages within the nearby areas. Jawaharlal Nehru Canal flows through the areas of the district where the groundwater table is high, causing severe water logging problems. The rainwater further amplifies this problem, leading to crop damage (Komal 2019).

It has been understood that the characteristic features of an area's soil play a significant role in increasing the water table. The sandy soil in most parts of the Jhajjar district allows water percolation in the deeper subsurface layers. Further, surface runoff is received from Rajasthan through the Sahibi River and other rivers from the South (Rathore et al. 2001). Along with that, runoff from other districts of Haryana, like Rewari and Gurugram, also flows towards Jhajjar (Komal 2019). This increases the water table, causing further soil saturation within the paddy fields. Stagnant

water in these fields affects the soil's physical condition, leading to compactness, consequently decreasing the infiltration rate and increasing water logging and soil salinity (Chaudhary and Aneja 1991).

Over the past two decades, groundwater has emerged as one of the principal sources of irrigation (Shah et al. 2006). Development in agriculture and irrigation facilities has led to several complex problems, such as the rise and fall in the groundwater table and its quality deterioration. These problems have threatened the sustainability of agriculture within several regions of the world (Singh and Amrita 2017).

Paddy cultivation should be reduced in the area to rectify the problem of decreasing groundwater levels and address the issue of salinization. Farmers should also be encouraged to plant water-transpiring *Eucalyptus* trees and saline fisheries in some parts of the district for bio-drainage to tackle the problem of increased soil salinity.

From the data obtained, maps (Figures 4 and 5) and a graph (Figure 6) were made to interpret the changes in LULC classes within the Jhajjar district. The LULC analysis also shows an increase in the area covered by agricultural land from 93574.58 ha (49.05%) in 2000 to 109387.222 ha (57.33%) in 2020. This is
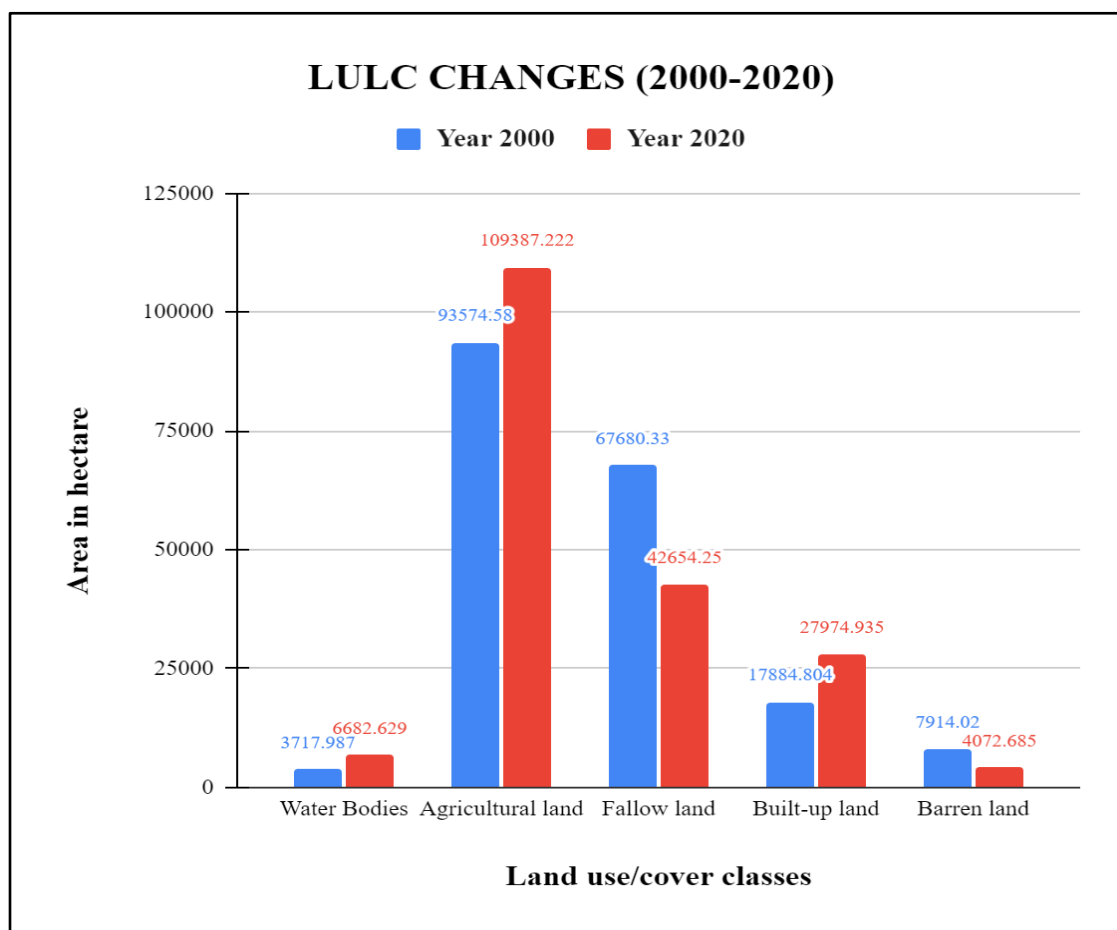
Figure 6 Comparison of Land Use/ Land Cover pattern in Jhajjar district in the years 2000 and 2020

mainly because uncultivable and fallow lands are transformed into agricultural lands (Figure 6). Rather than following traditional cropping methods involving mixed cropping patterns, farmers have shifted to market-oriented approaches by which they can earn more and more profit. There have been perceptible shifts in the type of crop grown from cereals, pulses and oilseeds to rice and wheat to generate high revenue over the past years (Chaudhary and Aneja 1991). The extensive cropping or over-exploitation of the land resource has led to land quality degradation and increasing compactness, soil salinity, water logging, and multiple nutrient deficiencies with low organic carbon content (Deen and Bala 2021). Using fertilizers and pesticides has also increased artificial productivity to make more money and reach the required food production. Furthermore, a steady increase is observed in the net sown area, the yield of wheat and rice after the green revolution. However, despite claims, the suitable land area for crop production is minimal in most developing countries with growing food demand (Young 1999).

As the groundwater of Jhajjar district is highly saline in some parts, it is unfit to be applied in the fields. The saline regions in Haryana have increased by 35% to 80,000 hectares in the last 20 years (CSSRI 2016). During the rainy season, the saline groundwater spills over the waterlogged agricultural fields, further worsening the condition. The farmers must leave the field uncultivated for a few seasons until the soil is functional and fertile again. Also, mono-cropping over the years has led to a problem of weed infestation, which has become so deleterious that without chemical control measures, it is difficult to harvest any yield (Chaudhary and Aneja 1991).

Although there is an increase in the net sowing area in the district, soil fertility is lost. Judicious use of agricultural land is necessary, along with crop diversification, to maintain the fertile land. The soil may be left unsuitable for cropping in the coming years if remedial measures are not undertaken soon. Fallow land is agricultural land left uncultivated for a certain period, especially during the growing season. The main reasons for land fallowing are low soil fertility, poor or low irrigation facilities, uncertainty of rainfall, and limited economic means of farmers (Malik 2012). The temporary rest for a while compensates for the low nitrogen content and other deficient nutrients, low moisture of the soil and

weeds in the field. However, prolonged soil exposure can lead to water and wind erosion.

During the last two decades, the fallow land has decreased from 67680.33 ha (35.47%) in 2000 to 42654.25 ha (22.35%) in 2020 (Table 2). The field survey shows that fallow land is now utilized for agricultural and other developmental activities to house and expand built-up areas (Pawar and Singh 2021). From the data obtained, there has been an increase in agricultural land, built-up land and water bodies. Consequently, there has been a decrease in the fallow and barren land. From this, it can be inferred that the farmers have intensively utilized the fallow land for agricultural purposes. There is an ever-increasing food demand, compelling farmers to overutilize land resources. They are adopting unsustainable methods like chemical fertilizers to convert fallow land into fertile land. Although there is a visible positive impact on overall net production, the loss of soil fertility, erosion, and toxicity can't be neglected simultaneously.

A significant decrease in barren land has also been observed in the district during the twenty-year duration, i.e. 2000-2020 (Figure 5). The area under this category in 2000 was 7914.02 ha, constituting about 4.14% of the geographical area, which decreased to 2.13 ha in 2020, including 2.13% of the geographical area. As the urban population in the area has exceeded the rural population (Suzanchi and Kaur 2011), the barren land has been mainly utilized for urban developmental activities that have ultimately led to the expansion of built-up areas.

Scrubland is present in the central region of the district. Due to excessive salinity or excess availability of salt and sodium, these are prominent in the district's western part (Arya et al. 2015). Mine dumps of brick kilns also contribute to the formation of barren lands. Although these lands can be reclaimed for agricultural use after regular inputs, they lack proper soil conservation and drainage for long-term agricultural use.

The LULC analysis also shows an increase in urbanization since Jhajjar lies in Haryana, which is close to Delhi, the country's capital. According to the population census data, the difference between 2001 and 2021 shows an increase in population in Jhajjar district from 42,305 in 2001 to 1,33,261 in 2021. The land use analysis indicates that during the period 2000-2020, the built-up area has significantly increased by >56%, i.e. from 17884.804 ha (9.37%) to 27974.935 ha (14.66%), adding 10090.131 ha more to the built-up category. The increasing trend shows the impact of rapid urbanization. The commercial use of land has been increased. Since the inclusion of the district in the National Capital Region in 1997, various industries have been relocated from the non-conforming areas of Delhi to the parts of the National Capital Region (NCR), including Jhajjar. Further, a significant rise in industrial development has been reported due to the establishing of

an extended railway network within the district, allowing for better transportation and connectivity that has developed Jhajjar as a hub for bigger industrial settlements and projects. On the one hand, the built-up area has increased, but on the other hand, it has affected natural vegetation in the study area. Jhajjar has experienced fluctuating average rainfall, creating problems for the rain-dependent regions. It is also inferred that the haphazard and rapid unplanned infrastructure development may complicate the situation soon.

Conclusion

The present study suggests that the major land-use change factors are rapid urbanization, climate change and agricultural expansion. The agricultural-dominated region of Jhajjar district in Haryana shows that urbanization accompanied by unplanned agricultural development and inappropriate agricultural techniques have severely threatened sustainability. These changes are estimated to enhance further water logging problems, soil salinity, loss of cultivable land and lack of suitable water for irrigation within this semi-arid region. The changes observed using LULC analysis between 2000 and 2020 suggest that major improvements such as crop diversification, sustainable use of groundwater for irrigation, and drainage of waterlogged areas must be introduced broadly to restore the degraded cultivable land.

Conflict of Interest

There is no conflict of interest.

References

Ali, A. M. S. (2006). Rice to shrimp: Land use/land cover changes and soil degradation in Southwestern Bangladesh. *Land Use Policy*, *23*, 421-435.

Anil, N. C., Sankar, G. S., Rao, M. J., Prasad, I. V. R. K. V., & Sailaja, U. (2011). Studies on Land Use/Land Cover and change detection from parts of South West Godavari District, AP- Using Remote Sensing and GIS techniques. *The Journal of Indian Geophysical Union*, *15*, 187-195.

Arowolo, A.O., & Deng, X. (2018). Land use/land cover change and statistical modelling of cultivated land change drivers in Nigeria. *Regional Environmental Change, 18*, 247–259. https://doi.org/10.1007/s10113-017-1186-5.

Arya, V. S., Arya, S., Kumar, S., & Hooda, R. S. (2015). Change detection of Wastelands of Jhajjar District, Haryana using

Geoinformatics. *International Research Journal of Environmental Sciences*, *4*, 42-26.

Asthana, H., Vishwakarma, C. A., Singh, P., Kumar, P., Rena, V., & Mukherjee, S. (2020). Comparative analysis of pixel and object based classification approach for rapid landslide delineation with the aid of open source tools in Garhwal Himalaya. *Journal of the Geological Society of India*, *96*, 65-72.

CGWB, Haryana. (2015-16). Ground Water Year Book of Haryana State 2015-16, Ministry of Water Resources, River Development and Ganga Rejuvenation, Government of India. http://cgwb.gov.in/Regions/GW-year-Books/GWYB-2015-16/GWYB%20NWR%20%20Haryana%202015-16.pdf.

Chaudhary, M. K., & Aneja, D. R. (1991). Impact of green revolution in long term sustainability of land and water resources in Haryana. *Indian Journal of Agricultural Economics*, *46*, 427-432.

Chughtai, A. H., Abbasi, H., & Karas, I. R. (2021). A review on change detection method and accuracy assessment for land use land cover. *Remote Sensing Applications: Society and Environment*, *22*, 100482.

CSSRI. (2016). Annual Report. In P.C. Sharma, & A. Singh (Eds.) ICAR – Central Soil Salinity Reseach Institute, India..Government of India.

Deen, S., & Bala, S. (2021). Changing Cropping Pattern in Haryana: A Spatio-Temporal Analysis of Major Food Crops. *International Journal of All Research Education and Scientific Methods*, *9*, 212-225.

Duraisamy, V., Bendapudi, R., & Jadhav, A. (2018). Identifying hotspots in land use land cover change and the drivers in a semi-arid region of India. *Environmental Monitoring and Assessment*, *190*, 1-21.

Güler, M., Yomralıoğlu, T., & Reis, S. (2007). Using landsat data to determine land use/land cover changes in Samsun, Turkey. *Environmental Monitoring and Assessment, 127*, 155–167. https://doi.org/10.1007/s10661-006-9270-1.

Komal. (2019). Causes of water logging in Jhajjar District. *Journal of Advances and Scholarly Researches in Allied Education*, *16*, 359-361.

Krishnan, G. P. (2013). Groundwater information booklet, Jhajjar district, Haryana. Central Ground Water Board, Ministry of water resources, Government of India, Retrieved from http://cgwb.gov.in/District_Profile/Haryana/Jhajjar.pdf.

Kumar, P., & Gaur, S. (2015). Remote Sensing and GIS Enabled Mapping of Urban Outgrowth and Changing Land Use Pattern of

Jhajjar City. *International Journal of Research in Humanities and Social Sciences*, *3*(6), 1-12.

Kumar, R. (2019). Emerging challenges of water scarcity in India: the way ahead. *International Journal of Innovative Studies in Sociology and Humanities*, *4*(4), 6-28.

Malik, J. (2012). Changing land use pattern in Haryana. *International Journal of Computing and Corporate Research*, *2*(6), 1-20.

MohanRajan, S. N., Loganathan, A., & Manoharan, P. (2020). Survey on Land Use/Land Cover (LU/LC) change analysis in remote sensing and GIS environment: Techniques and Challenges. *Environmental Science and Pollution Research*, *27*, 29900-29926.

Murungweni, C., Wijk, M. T. V., Smaling, E. M. A., & Giller, K. E. (2016). Climate-smart crop production in semi-arid areas through increased knowledge of varieties, environment and management factors. *Nutrient cycling in Agroeconomics*, *105*, 183-197.

Pawar, S., & Singh, R. (2021). Geospatial Applications in Land Use/Land Cover Change Detection for Sustainable Regional Development: The Case of Central Haryana, India. *Geomatics and Environmental Engineering*, *15*, 81–98.

Rahman, A., Kumar, S., Shahab, F., & Siddiqui, M. A. (2012). Assessment of Land use/land cover Change in the North-West District of Delhi Using Remote Sensing and GIS Techniques. *Journal of the Indian Society of Remote Sensing*, *40*, 689-697.

Ram, J., Dagar, J., Singh, G., Lal, K., Tanwar, V. S., Shoeran, S. S., Kaledhonkar, M. J., Dar, S. R., & Kumar, M. (2008). Biodrainage: Eco-Friendly Technique for Combating Waterlogging & Salinity. Technical Bulletin 9: Central Soil Salinity Research Institute, Karnal and Haryana Forest Department, Panchkula, India.

Rathore, D. S., Jain, S. K., & Chaudhry, A. (2001). Remote Sensing and GIS Application in Zonations of Waterlogging in Irrigation Command.National Institute of Hydrology. Retrieved from https://www.indiawaterportal.org/sites/default/files/iwp2/Remote_Sensing_and_GIS_Applications_in_Zonation_of_Water_Logging_in_Irrigation_Command.pdf.

Reganold, P. J., Papendick, R. I., & Parr, J.F. (1990). Sustainable Agriculture. *Scientific American*, *262*, 112-121.

Rena, V., Kamal, V., Singh, D., Roy, N., Shikha, A., & Mukherjee, S. (2021). Hydrogeological assessment of high salinity in groundwater in parts of Bharatpur district, Rajasthan, India. *Ecology Environment and Conservation*, *27*, S372-S380.

Shah, T., Singh, O. P., & Mukherjee, A. (2006). Some aspects of South Asia's groundwater irrigation economy: analysis from a survey in India, Pakistan, Nepal Terai and Bangladesh. *Hydrogeology Journal*, *14*, 286-309.

Singh, A., Nath Panda, S., Flugel, W. A., & Krause, P. (2012). Waterlogging and farmland salinization: causes and remedial measures in an irrigated semi-arid region of India. *Irrigation and Drainage*, *61*(3), 357-365.

Singh, O., & Amrita. (2017). Management of Groundwater Resources for Sustainable Agriculture in Haryana. *Transactions of the Institute of Indian Geographers*, *39*, 133-150.

Suzanchi, K., & Kaur, R. (2011). Land use land cover change in the National Capital Region of India: A remote sensing & GIS based two decadal spatial- temporal analysis. *Procedia - Social and Behavioral Sciences*, *21*, 212–221.

Szarek-Iwaniuk, P. (2021). A Comparative Analysis of Spatial Data and Land Use/Land Cover classification in Urbanized Areas and Areas Subjected to Anthropogenic Pressure for the Example of Poland. *Sustainability*, *13*, 1-24.

Yadav, J. P., Lata, S., & Kataria, S.K. (2009). Fluoride distribution in groundwater and survey of dental fluorosis among school children in the villages of the Jhajjar District of Haryana, India. *Environmental Geochemistry Health*, *31*, 431-438.

Yadav, S. K., Babu, S., Yadav, M. K., Singh, K., Yadav, G. S., & Pal, S. (2013). A review for Organic Farming for Sustainable Agriculture in Northern India. *International Journal of Agronomy*, *13*, 1-8.

Young A. (1999). Is there really spare land? A critique of estimates of available cultivable land in developing countries. *Environment Development and Sustainability*, *1*, 3–18.

Journal of Experimental Biology and Agricultural Sciences

Effects of forest conversion to oil palm plantation on soil erosion and surface runoff

Adi Jaya[*], Salampak, Nyahu Rumbang, Mofit Saptono, Lusia Widiastuti,
Sri Endang Agustina Rahayuningsih, Shella Winerungan

Faculty of Agriculture, University of Palangka Raya, Indonesia

ABSTRACT

The vegetation type and its coverage in forest ecosystems are crucial in soil erosion and surface runoff. Cover crops provide significant protection to the soil aggregates, preventing damage caused by rainfall and runoff that might occur in the absence of these crops. However, changes in land use, such as converting forests into oil palm plantations, have resulted in changes to the land cover, which affect erosion, surface runoff, and, ultimately, the forest ecology of the watershed. This study aimed to provide an overview of erosion and runoff in forest areas and oil palm plantations. This field research was conducted to study erosion, runoff, and nutrient loss using plots measuring 15m x 25m, including oil palm plantation areas and forest areas. After each rain, sediment weighing and runoff volume measurements were carried out. Laboratory analysis was conducted for sediment and surface runoff water samples' N, P, and K elements. The study results showed that five-year-old oil palm plantation areas experience the highest levels of erosion and runoff, followed by three-year-old oil palm plantation and forest areas. Nutrients were found to be lost in sediment across all land cover types, with a minimal amount recorded in surface runoff.

* Corresponding author

E-mail: adijaya@agr.upr.ac.id (Adi Jaya)

1 Introduction

Over the past decade, Indonesia has experienced notable growth in palm oil production, which has become the fastest-growing industry in the country. According to the Indonesian Ministry of Agriculture's 2010 report, the government had targeted increasing crude palm oil production to 40 million tonnes by 2020 from regions such as Sumatra, Kalimantan, and West Papua. However, the country exceeded its intended palm oil production target, producing over 44.67 million tonnes. The Riau Province in Sumatra is Indonesia's largest palm oil producer, accounting for approximately 19.62% of the total national production, followed by Central Kalimantan, which contributes around 12.89% of the national output. Additionally, between 2016 and 2020, Indonesia's palm oil cultivation area expanded by 30.3%, growing from 11.20 million hectares to 14.59 million hectares. The largest palm oil cultivation area is in Riau Province, followed by West Kalimantan and Central Kalimantan (Kurniawan et al. 2018; BPS 2020).

The palm oil industry plays a crucial role in Indonesia's economy, contributing 3.5% to the country's GDP as per GAPKI (2022). According to UNcomtrade (2022), Indonesia exported 25.94 million tons of palm oil, with a total value of USD 17.37 million, accounting for 55.48% of the global market share in 2020. Notably, Indonesia and Malaysia are the leading countries in palm oil exports (Tandra et al. 2022). Furthermore, palm oil cultivation can benefit smallholders without increasing economic risk (Suroso and Ramadhan 2014; Acosta and Curt 2019; Mehraban et al. 2021). The industry also contributes significantly to Indonesia's non-oil and gas exports.

Indonesia has seen a significant shift in land usage, particularly with the rapid expansion of the oil palm industry, which has negatively affected the environment and human health. Although the growth of the oil palm (OP) plantations has positively impacted the country's economy, it has also brought some unintended ecological and societal issues. Several previous studies (Oyarzun et al. 2007; Setiawan et al. 2016; Vijay et al. 2016; Austin et al. 2017) suggest that the spread of OP plantations has led to forest removal, resulting in reduced carbon stocks, deforestation, forest fires (Dadi 2021), and the destruction of biodiversity (Koh and Wilcove 2009; Lees et al. 2015; Linder and Palkovitz 2016; Dadi 2021), as well as water scarcity and the exploitation of soil and water resources (Safitri et al., 2018). Additionally, the development of OP has resulted in negative social impacts, including land grabbing, subpar working conditions on plantations (Dhiaulhaq et al. 2015; Gellert 2015), and disputes between migrants and locals due to social jealousy and ethnic migrants' dominance (Dadi 2021).

Compared to natural forests, oil palm (OP) plantations have a less dense, more uniform canopy, significantly affecting the local climate by raising air temperature, soil temperature, and humidity (Hardwick et al. 2015; Meijide et al. 2018). This change in canopy cover also affects hydrological aspects such as flooding, soil erosion, nutrient leaching (Dislich et al. 2017), and groundwater availability and levels. Water storage can also be reduced, annual water yield can increase, and water quality can decrease when forests are converted to OP plantations. However, the adverse effects tend to fall as plantations age (Comte et al., 2012) and can be mitigated by effective management practices (Yusop et al. 2007). Nonetheless, there is a lack of reliable data on the water problem in various locations. Some small-scale studies suggest that well-managed oil palm can regulate the essential hydrological characteristics of the catchments reasonably well.

Developing and managing plantations, such as forest clearing, building roads and drainage systems, using agricultural pesticides, and discharging wastewater, can cause soil erosion and affect groundwater quality (Environment Conservation Department, 2000; Goh et al. 2003). The water quality in aquatic ecosystems near plantations can also be affected by erosion and surface runoff. These effects cause the nutrients from water sources to dissolve in sediments. Applying fertilizers at high dosages to plantations can lead to declining water quality in nearby aquatic ecosystems and hydrological conditions (Sheil et al. 2009).

To control the surface runoff and drainage water from OP plantations, cover crops plantation or vegetation cover can retain excess water and nutrient-rich sediment. However, the decomposition of legume cover crops under a mature canopy releases nitrogen that previously occurred through nitrogen fixation (Goh et al. 2003; Breure 2003; Campiglia et al. 2011). Sandy soils see higher nitrate losses by leaching from legumes (Goh and Chew, 1995). The OP plantations have a closed canopy, which causes the understorey to vanish as the plantations age. As a result, changes in land use, especially when switching from forests to agricultural or grasslands, significantly impact the flow of nutrients in the watershed (Vitousek et al. 1997).

It's unclear how converting forests to plantations will impact nitrogen and phosphorus levels in Indonesian conditions. Generally, tropical forests are rich in available nitrogen, retain high levels of N and exhibit high rates of soil N cycling (Hedin et al. 2009). However, systems with high available N are prone to significant N losses (Veldkamp et al. 2008). When forests are converted to crops, there is an initial increase in the rate of N mineralization, which results in a rise in soil NO flux, N2O emissions and N leaching (Veldkamp et al. 2008). Over time, cultivated systems may experience a decrease in available N, alkaline cations and overall soil fertility. However, systems utilizing N-fixing tree species or N fertilizers do not undergo the same reduction in soil N availability (Corre et al. 2006). Conversely, they can experience N loss through leaching or

emissions (Veldkamp et al. 2008). Vegetation substitution, such as logging, affects the forest floor and accelerates soil erosion and N mineralization (Nykvist et al. 1994).

This research aims to investigate the extent of erosion and surface runoff on forest and oil palm plantations of varying ages. The study will provide insights into the impact of forest-to-oil-palm conversion on a watershed, primarily due to soil erosion, surface runoff, and nutrient loss. The research will examine the relationship between land use, the amount of erosion and surface runoff, and the nutrients N, P, and K carried in sediments and surface runoff.

2 Materials and Methods

The research was carried out on forest land and OP plantations owned by PT. KHS is located in the Jalemu Watershed, Manuhing Subdistrict, Gunung Mas Regency, as shown in Figure 1. The study was conducted for six months, from May to October 2017. Erosion and runoff measurements were taken under field conditions, while sediment and water analysis was carried out at the Analytical Laboratory of the University of Palangka Raya in Indonesia.

During this research, field conditions were used to study the effects of different land use factors on erosion. The study involved three factors, i.e., forest, 3-year-old oil palm plantations, and 5-year-old oil palm plantations, with two replications. To achieve this, erosion plots were established, each with a width of 15m and length of 25m. Plates were planted on each side of the plot, 20cm above the soil surface, so all the water entering the erosion patch flows into the erosion reservoir and surface runoff. At the end of the plot, a

box was installed to collect erosion and surface runoff. This box was 5m long, 0.5m wide, and 0.5m high. It has seven holes on the side facing outward, each with a diameter of 2.5 inches. A 2.5-inch pipe connects the centre hole to box B (Figure 2). The amount of erosion and surface runoff was measured after each rainfall event. Soil and sediment samples were taken and weighed in the field to determine their weight. The moisture content of sediment samples was determined by drying in an oven at 105°C for 24 hours. The dry weight of soil/sediment in each erosion event was calculated as the moist weight of soil/sediment multiplied by (100-% water content). Sampling was also carried out to analyze the nutrient content in the surface runoff. The data collected were analyzed using descriptive analysis to compare each factor.

$$\text{Water content (\%)} = \frac{(\text{weight of moist soil sample}(M) - \text{weight of dry sample}(D))}{\text{weight of dry sample } (D)} \times 100\%$$

Water and sediment analysis was conducted at the Analytical Laboratory of Palangka Raya University. The estimation of Total N (using the Kjeldahl method), while the Total P, and Total K was done with the help of 25 percent Ekstraksi HCl and a spectrophotometer, as described in Sulaeman et al. (2009). The water analysis included the estimation of NH3 (Kjedhahl) and NO_2 (measured using the sulpanilamide method, APHA Standard method 4500 NO_2-B). In an acidic environment, NO_2 reacts with sulfanilamide (SA) and N-(1-naphthyl) ethylene diamine dihydrochloride (NED dihydrochloride) to form red-purplish azo compounds. The absorbance of the color formed was measured spectrophotometrically at a maximum wavelength of 543 nm, as per Clesceri et al. (1998). Nitrate (NO_3) was analyzed using the colorimetric method with Brusin dye reagent and measured with a
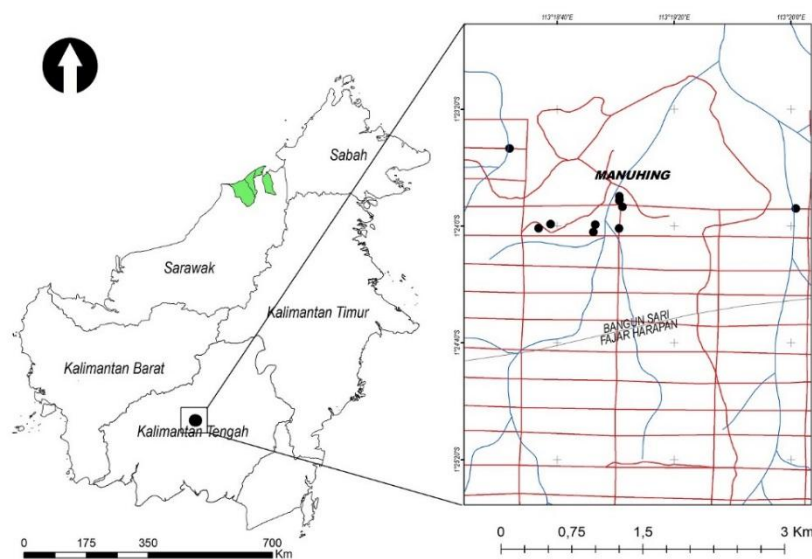

Figure 1 Map of research location in Jalemu Watershed which mainly dominated by OP plantation
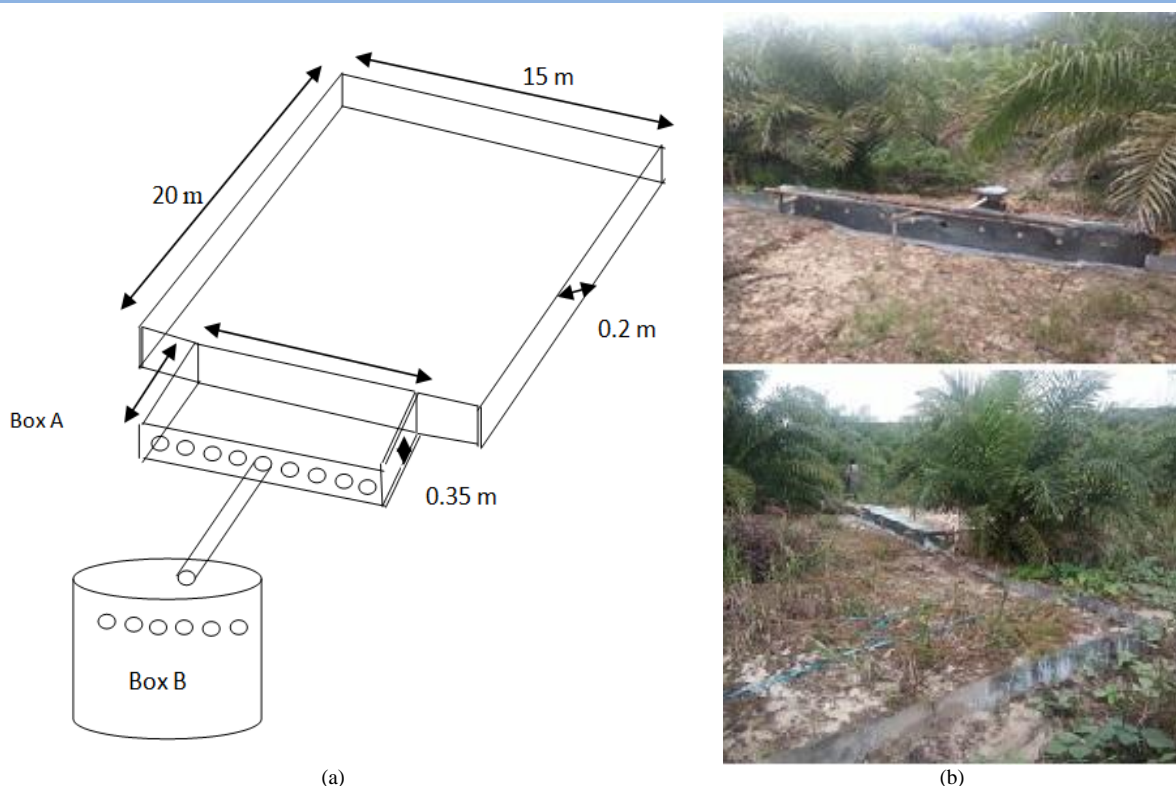
(a) (b)

Figure 2 (a) The collection box for erosion and runoff and (b) the condition of the erosion plots in the field

spectrophotometer at a wavelength of 432 nm. Phosphate (P) in water filtrate can be measured directly colorimetrically with a spectrophotometer at a wavelength of 889 nm, with the formation of a molybdate blue color. Potassium (K) concentration was determined using an Atomic Absorption Spectrophotometer (AAS). The results of the Total N, P, and K analysis through erosion or surface runoff can be calculated using the following equation:

$$X = Y \times E$$

where:

X = N, P and K losses due to erosion or surface runoff (kgha^{-1})

Y = Total N (%), P (ppm) and K (me100gr^{-1} soil) concentrations in sediment or surface runoff (mg L^{-1})

E = Total soil erosion (kgha^{-1}) or volume of surface runoff (L)

2.1 Data Analysis

In-depth data analysis was conducted by comparing erosion and sedimentation values. A one-way ANOVA test was performed at a 5% significance level with IBM Statistics SPSS version 24 software to determine the variance in nutrient content between sediments and runoff.

3 Results

3.1 Rainfall

Rainfall data collected using a tipping bucket ombrometer during research and processing monthly results are presented in Figure 3. The observations indicate 117 rainy days between May 2017 and February 2018.

Figure 3 shows a noticeable decrease in rainfall during the dry season in May and June. The month with the highest precipitation was October 2017 with 459.5mm, while the lowest was reported in June 2017, with 86.5mm. Regarding rainy days, November had the highest number with 24 days, while May 2017 had the lowest with only 7 days.

3.2 Erosion and Surface Runoff

Figure 4 compares erosion calculations between forest areas and 3 and 5-year-old OP plantations after various rainfall events. The results show that erosion values are higher during rainy seasons in three-year-old oil palm plantations (0.10 tonnes ha^{-1}) compared to those in the five-year-old plantations (0.09 tonnes ha^{-1}) and forest areas (0.002 tonnes ha^{-1}). The erosion during rainfall events is closely related to the volume and intensity of rain on that particular date. The density of crop canopy cover is a critical factor influencing
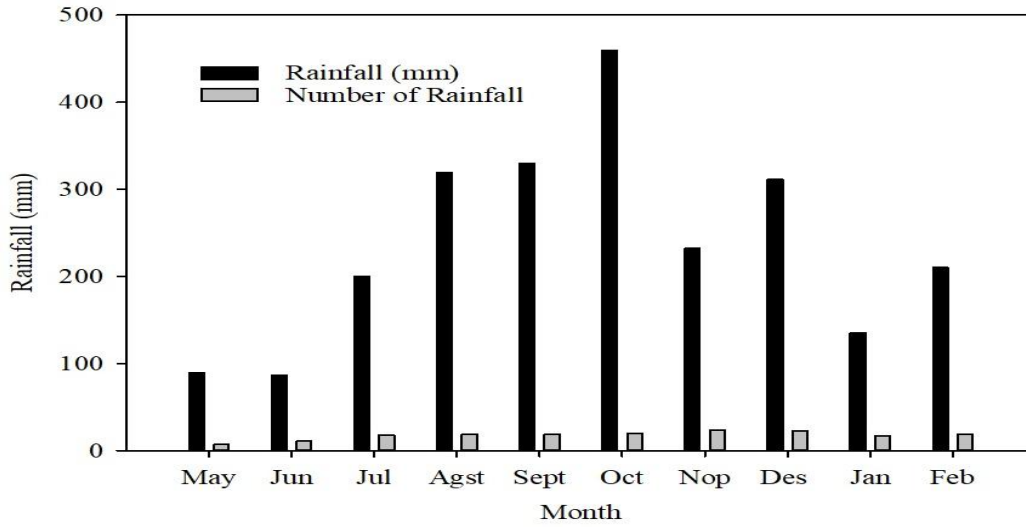
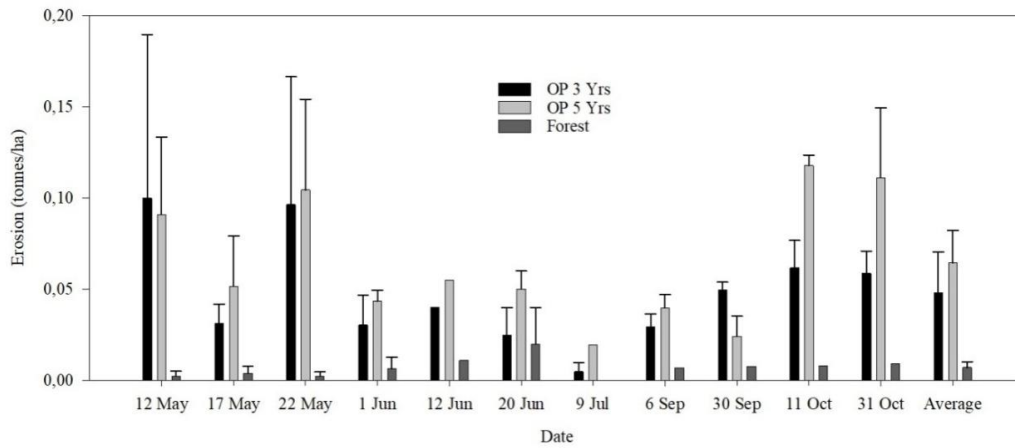Figure 3 Amount of rainfall and number of rainy days at the research location

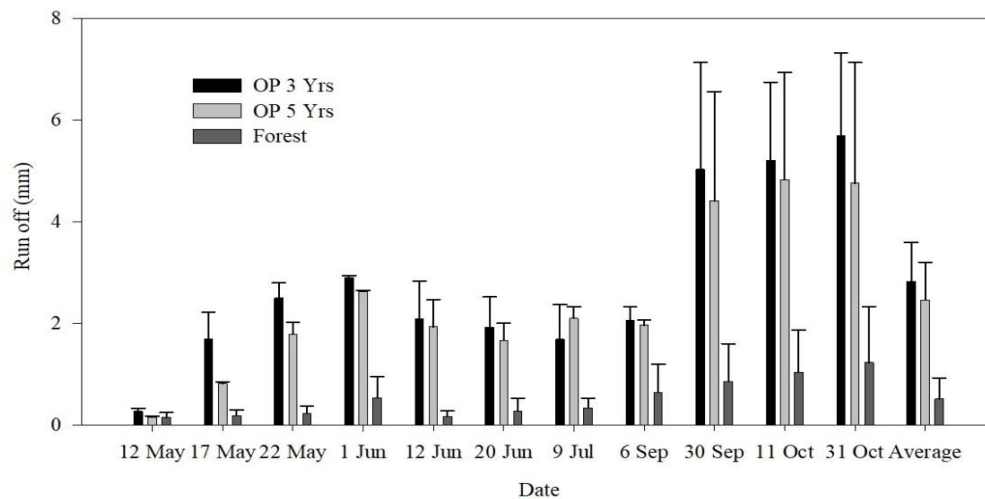Figure 4 Erosion that occurs in forest areas and OP plantations aged 3 years and 5 years

Figure 5 Surface runoff that occurs in forest areas and OP plantations

Table 1 Average results of laboratory analysis for N, P and K in eroded soils

Land use	N (%)	P (ppm)	K(me/100 g)
Oil Palm 3 yrs	0.19[a]	19.63[a]	0.09[a]
Oil Palm 5 yrs	0.21[a]	12.34[a]	0.08[a]
Forests	0.22[a]	60.01[a]	0.33[a]

Values without common letters differ significantly at LSD P<0.05

Table 2 Average results of laboratory analysis for N, P and K in surface runoff

Land use	NH_3 (mg L^{-1})	NO_2 (mg L^{-1})	NO_3 (mg L^{-1})	N-Total (mg L^{-1})	P total (mg L^{-1})	K Total (mg L^{-1})
Oil Palm 3 yrs	0.08	0.01	0.22	0.31[a]	3.71[a]	1.02[a]
Oil Palm 5 yrs	0.10	0.02	0.08	0.19[a]	0.04[a]	0.77[a]
Forests	0.05	0.02	0.11	0.17[a]	0.09[a]	2.36[a]

Values without common letters differ significantly at LSD P<0.05

erosion rates. The vegetation canopy in the 3 and 5-year-old OP plantation regions is less dense than the surrounding forest.

The results of the calculation of surface runoff during rainfall events for both forested areas and oil palm (OP) plantations aged 3 and 5 years are presented in Figure 5. Figure 5 shows that the surface runoff on a 3-year-old OP plantation is typically higher than that of a 5-year-old plantation and the forested area during most rain events. On average, the surface runoff in oil palm plantations that have been operating for three years is 2.83 mm; for those that are five years old, it is 2.46 mm, and in forest areas, it is 0.52 mm.

3.3 Nutrients losses in erosion and runoff

Tables 1 and 2 illustrate the average results of laboratory analyses for N, P, and K losses in erosion and surface runoff, respectively. Figure 6-11 displays the nutrients N, P, and K carried in erosion in each treatment plot. The table shows that the total N content in eroded soil for the three-year-old oil palm plantations was between 0.16 - 0.23% (average of 0.19%). In comparison, the five-year-old OP plantation reported between 0.15 - 0.30% (average of 0.21%), while the forest area ranged between 0.17 - 0.33% (average of 0.22%). Likewise, the highest total P content was reported in the three-year-old OP plantation, ranging between 10.09-29.39 ppm (average of 19.63 ppm). The five-year-old OP plantation reported 5.45-18.14 ppm (average of 12.34 ppm), while the forest area reported between 16.08-171.72 ppm (average of 60.01 ppm P). Total K in eroded sediments ranged from 0.03-0.19 me $100g^{-1}$ soil (averaged 0.09 me $100g^{-1}$) for three years of OP, from 0.05-0.14 me $100g^{-1}$ soil (averaged 0.08 me $100g^{-1}$ soil) for five years of OP, and 0.08-0.90 me $100g^{-1}$ soil (averaged 0.33 me $100g^{-1}$ soil) for the forest. The sediment or soil carried away by erosion from the forest areas appears to contain more N, P, K than the 3 and 5-year-old OP plantations.

The data presented in Table 2 shows that the total nitrogen in surface runoff from three-year-old OP ranges from 0.02-0.86 mg L^{-1}, with an average of 0.31 mg L^{-1}. In contrast, the total nitrogen in surface runoff from five-year-old OP ranges from 0.02-0.69 mg L^{-1}, with an average of 0.19 mg L^{-1}. Most of the nitrogen is found in ammonia (NH_3), which ranges from 0.02-0.29 mg L^{-1}, with an average of 0.17 mg L^{-1} for forests. After three years of observation, the total phosphorus levels range from 0.02 to 22.57 mg L^{-1}, with an average concentration of 0.04 mg L^{-1}. On the other hand, after five years, the total phosphorus levels range from 0.01-0.12 mg L^{-1}, with an average concentration of 0.04 mg L^{-1}. The total phosphorus levels in forest areas range from 0.02-0.24 mg L^{-1}, with an average concentration of 0.09 mg L^{-1}. The total potassium concentration in surface runoff ranges from 0.01-4.18 mg L^{-1}, with an average value of 1.02 mg L^{-1} for three-year-old OP. In contrast, for five-year-old OP, the total potassium concentration ranges from 0.59-4.55 mg L^{-1}, with an average value of 2.36 mg L^{-1}. In summary, the results suggest that the nitrogen, phosphorus, and potassium levels delivered by surface runoff from forest regions are frequently higher than those of OP plantations three and five years old.

Based on Figure 6, the sediment eroded from the plantation areas contained a total of nitrogen ranging from 1.16 to 35 kg per hectare (with an average of 12.90 kg/ha) for three years. Over the same period, the sediment eroded from the plantation areas contained a total of nitrogen ranging from 1.19 to 39.48 kg per hectare (with an average of 13.04 kg/ha), while the sediment eroded from the forested areas contained a total of nitrogen ranging from 0.42 to 6.80 kg per hectare (with an average of 1.93 kg/ha).

Furthermore, Figure 7 showed that erosion rates were highest in the 3-year-old plantation areas, with a range of 0.30 to 5.01 kg per hectare (with an average of 2.65 kg/ha), followed by the 5-year-old plantation areas, with a range of 0.43 to 4.51 kg per hectare (with
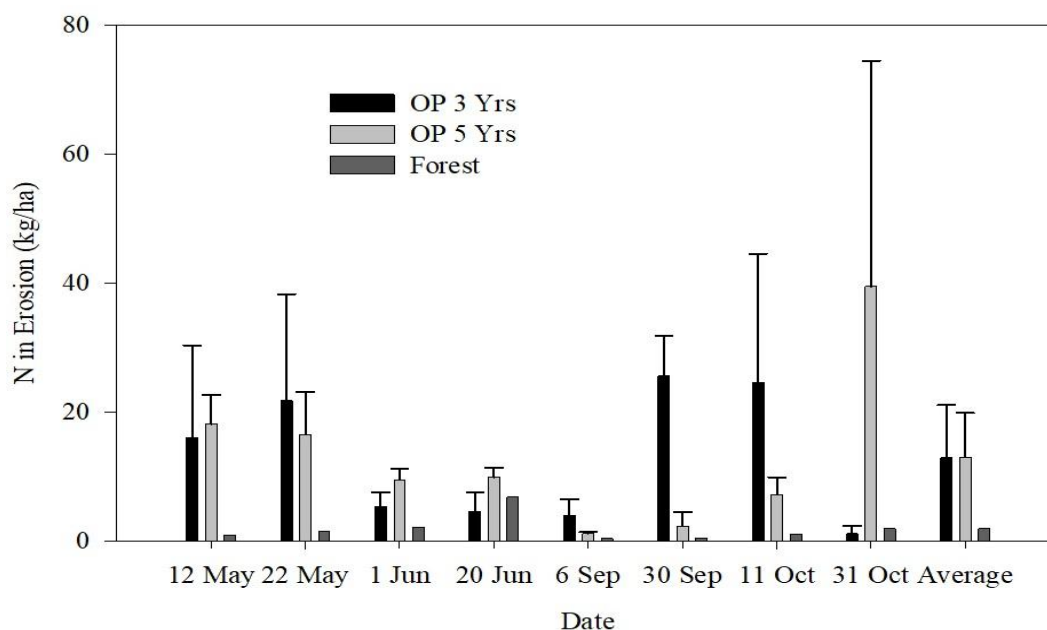
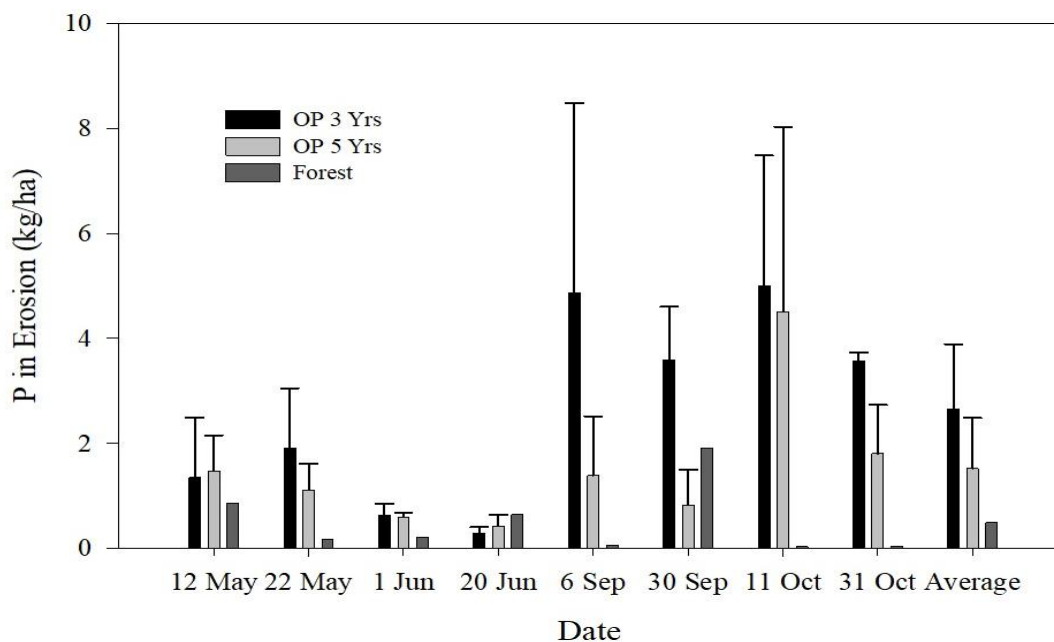Figure 6 N in Erosion on 3 and 5-year-old OP plots and forest areas

Figure 7 P in Erosion on 3 and 5-year old OP plots and forest areas

an average of 1.52 kg/ha), and the forested areas, with a range of 0.03 to 1.91 kg per hectare (with an average of 0.49 kg/ha).

Regarding the total potassium content in the eroded sediment, Figure 8 revealed that the highest loss of potassium was from the 5-year-old plantation areas, with a range of 0.92 to 62.82 kg per hectare (with an average of 15.17 kg/ha), followed by the 3-year old plantation areas, with a range of 0.45 to 32.38 kg per hectare

(with an average of 10.46 kg/ha), and the forested areas, with a range of 0.33 to 3.42 kg per hectare (with an average of 1.61 kg/ha).

In conclusion, the soil erosion caused by the OP plantations resulted in a more significant loss of nitrogen, phosphorus, and potassium compared to the forested areas. This was particularly evident in the 3 and 5-year-old plantations.
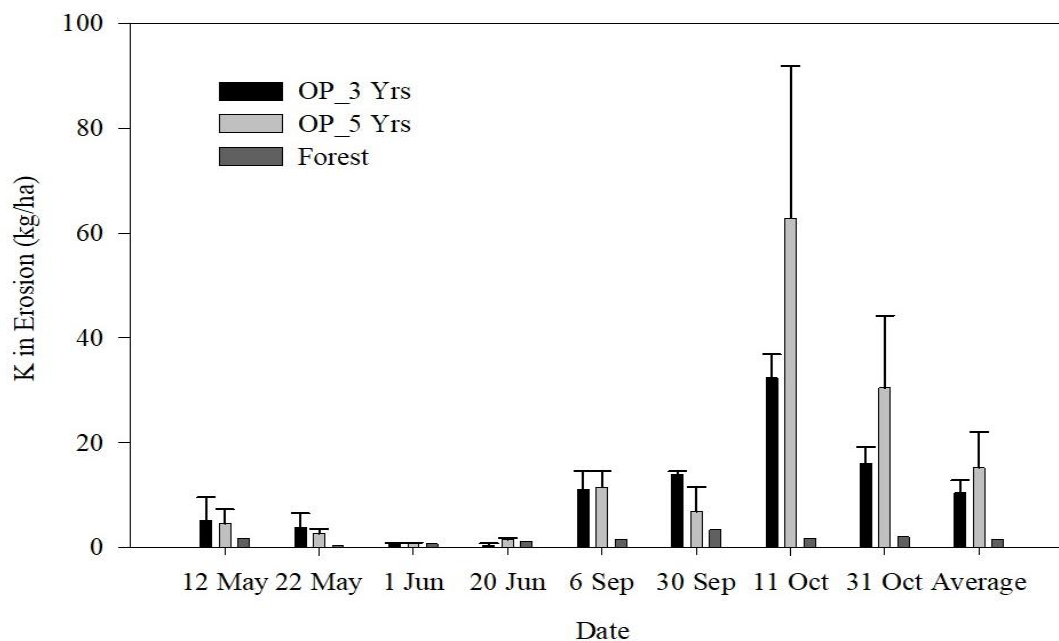
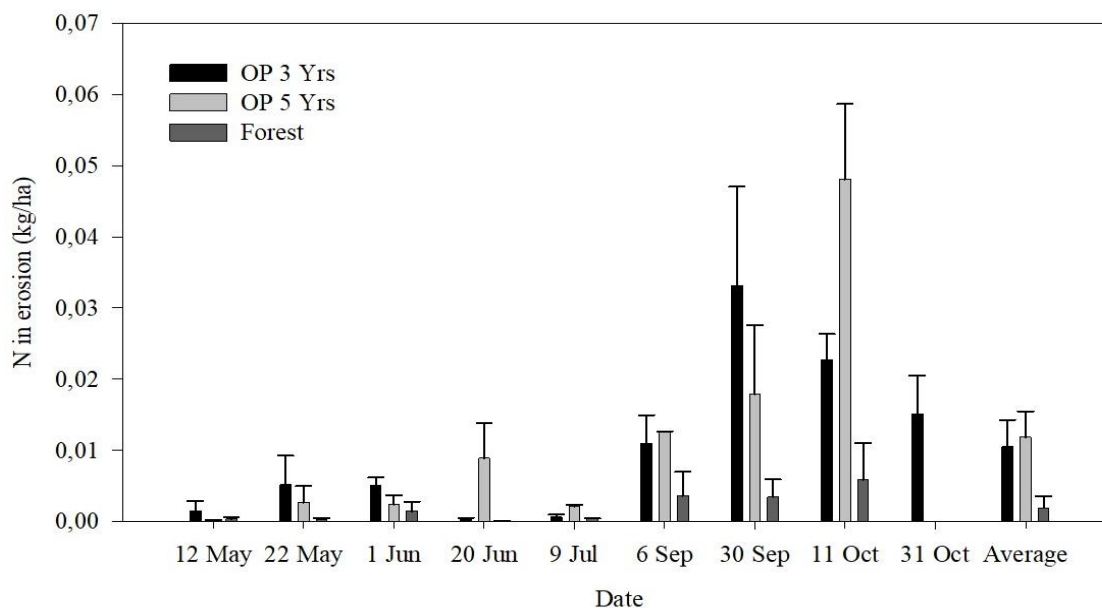Figure 8 K in Erosion on 3 and 5-year-old OP plots and forest areas

Figure 9 N in the surface runoff of 3 and 5-year-old OP plots and forest areas

When surface runoff occurs in a forest or an oil palm plantation, the nutrients N, P, and K are carried away with the water. The amount of nutrients lost through surface runoff is determined by the volume of the water and the nutrient content of N, P, and K in the water. Figure 9 shows that at 3 years OP, the total amount of nitrogen lost with surface runoff ranges from 0.004 to 0.0332 kg ha^{-1}, with an average of 0.0105 kg ha^{-1}. For 5-year OP, the range is from 0-0.481 kg ha^{-1}, with an average of 0.0105 kg ha^{-1}, while for forests, the range is from 0-0.0058 kg ha^{-1}, with an average of

0.0017 kg ha^{-1}. The majority of nitrogen losses occur in the form of ammonia (NH_3).

As for P-total, for an OP of 3 years, the amount lost ranges from 0 to 1.1105 kg ha^{-1}, with an average of 0.1691 kg ha^{-1}. For 5-year OP, the losses in surface runoff range from 0 to 0.5420 kg ha^{-1}, with an average of 0.1016 kg ha^{-1}. The losses in forests range from 0 to 0.017 kg ha^{-1}, with an average of 0.0058 kg ha^{-1}, as shown in Figure 10.
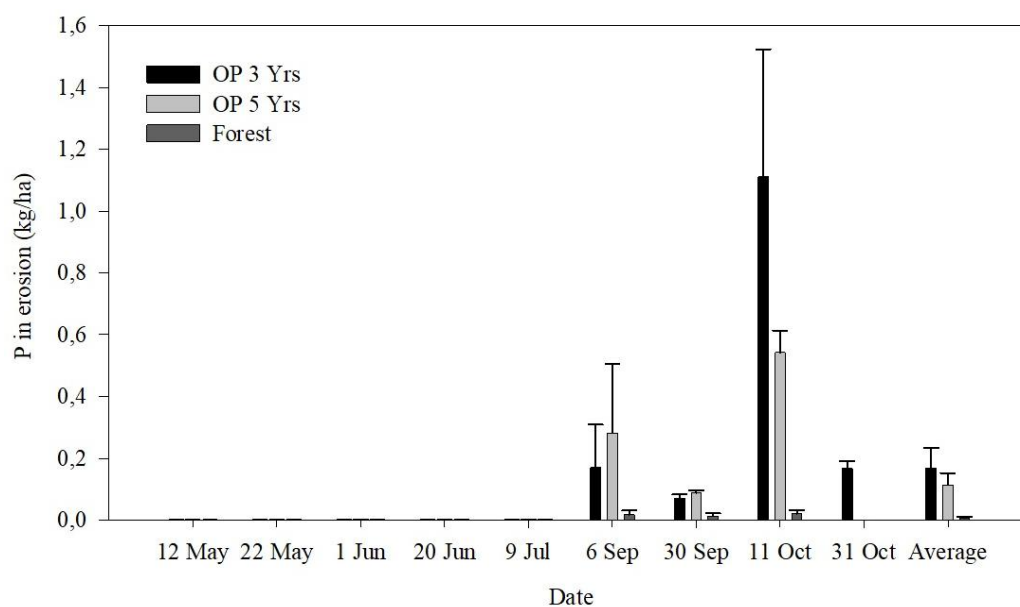
Figure 10 P in the surface runoff in 3 and 5-year-old OP plots and forest areas
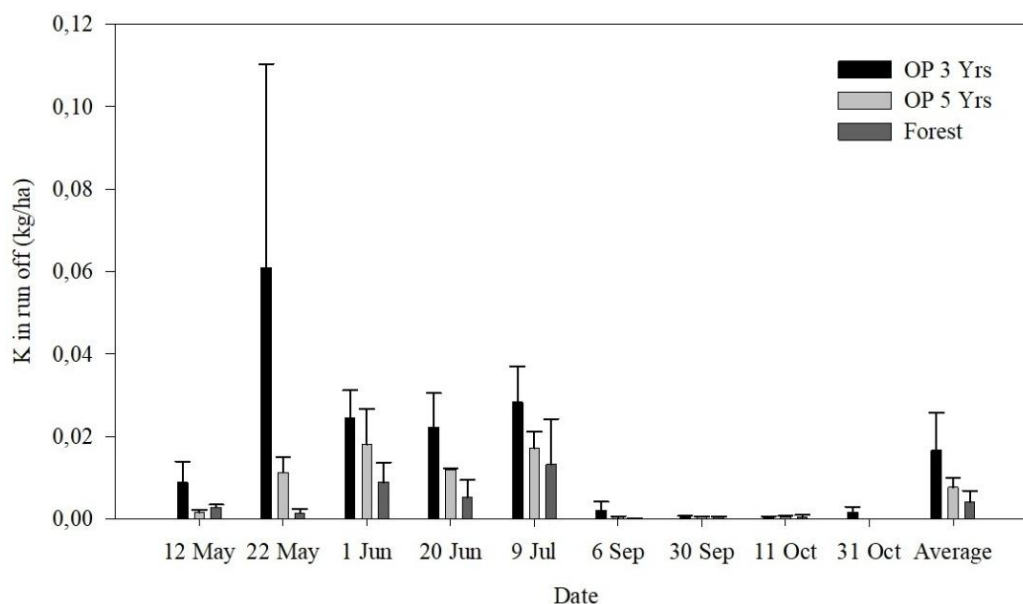

Figure 11 K in surface runoff in 3 and 5-year-old OP plots and forest areas

Figure 11 shows the total K content in the surface runoff for different studied parameters. The results showed that for a 3-year OP plantation, the total K content ranged from 0.0005 to 0.0610 kg ha^{-1}, with an average of 0.0167 kg ha^{-1}. For a 5-year OP plantation, the total K content ranged from 0 to 0.0181 kg ha^{-1}, with an average of 0.0068 kg ha^{-1}. Finally, the total K content for the forest area ranged from 0 to 0.0132 kg ha^{-1}, with an average of 0.0036 kg ha^{-1}. Overall, the 3-year OP plantation had a higher surface runoff in terms of N, P, and K content than the 5-year OP plantation and the forest area.

4 Discussion

Rainfall is a significant climate variable that impacts surface runoff and erosion. Various aspects of rainfall, such as its type, intensity, length, distribution, and direction, influence the amount of soil erosion and surface runoff (Haridjaja et al. 1990; Kee and Chew 1996). The volume and flow rate of surface runoff are directly proportional to rainfall intensity. Higher rainfall intensity generally increases surface runoff, but it depends on the soil's infiltration capacity. If the intensity of rainfall exceeds the soil's ability to

Table 3 Nutrient losses from erosion and runoff (kg ha^{-1}).

Nutrient	Sediment			Runoff			Total		
	3 yr-OP	5 yr-OP	Forest	3 yr-OP	5 yr-OP	Forest	3 yr-OP	5 yr-OP	Forest
N	12.900	13.000	1.900	0.011	0.011	0.002	12.911	13.011	1.902
P	2.650	1.520	0.490	0.169	0.102	0.006	2.819	1.622	0.496
K	10.460	15.170	1.610	0.017	0.007	0.004	10.477	15.177	1.614

absorb water, the surface runoff will increase proportionally. Moreover, the duration of rainfall also affects the amount of surface runoff (Sukartaatmadja 1998; Banabas et al. 2008). The longer the rainfall, the greater the surface runoff, depending on the strength and amount of rainfall.

According to the study results, the largest erosion and highest runoff occur in 3-year-old Oil Palm (OP) plantations, followed by 5-year-old OP plantations and forests. As many previous studies have reported, the amount of erosion is affected by vegetation coverage. Trees in forest areas can intercept falling rain and reduce the impact of raindrops on the soil, which can cause the dispersion of soil particles. Whereas in OP plantations, the percentage of canopy cover is lower, allowing more rain to fall through it.

Like OP plants, plants with fibrous roots are more effective in controlling erosion. This is because the fine threads on the fibre roots can bind soil particles into a solid soil aggregate. The growth phase or age of the plant also has a different effect on the erosion control process. Initially, the growth of canopy cover plants is still relatively open, causing rainwater to fall directly on the soil surface. This can accelerate the occurrence of surface flow because of the slow infiltration of water into the soil. Plant height also plays a key role in increasing the effectiveness of cover crops in reducing erosion. A lower and tighter plant canopy can change the energy of the rain that reaches the soil's surface (Arsyad 2006). In addition, vegetation can affect erosion due to (i) interception of rainfall by the canopy and absorption of rainwater energy, minimizing soil erosivity, (ii) influence on surface runoff, (iii) increase in soil biological activity, and (iv) increase in the speed of water loss through transpiration (Rahim 2003).

The level of erosion that occurs can be influenced by vegetation factors such as crop canopy cover and vegetation cover in the forest and oil palm (OP) plantations. In the studied OP plantations, which are 5-6 years old, the canopy cover levels are relatively close compared to younger OP but still more open than forests. This can be observed by the distance between canopies, which are close enough. The relatively close canopy cover levels enable plants to retain more falling rain. In addition to being intercepted by the plants, rainfall can flow through the stems and then be transferred to the soil surface, albeit with less force than at the point of origin. The reduced energy of rainfall that reaches the soil surface results in a lesser ability of raindrops to disperse the soil,

ultimately reducing the amount of erosion. In forest areas, canopy stratification also has a decreasing effect on raindrops and surface runoff, which can reduce erosion (Arsyad 2006).

Based on the results presented in Table 3, it can be observed that nitrogen, phosphorus, and potassium are lost due to erosion and surface runoff. Therefore, it is crucial to implement measures to control erosion. In addition to the loss of N, P, and K minerals, erosion can introduce other nutrients and organic materials and change the composition of soil particles in the area. Sediment movement is stronger in fine particles, which can cause clay and dust to leave more sand in the soil. Previous studies have reported that a catchment area with native forests has a lower loss of NO_3 per year compared to areas with plantations where the river discharge output exceeds the rainfall input. Loss of nutrients on OP plantations can be influenced by various factors such as soil type, rainfall intensity, age of plantations, agricultural practices, type of fertilizers, water management, and level of fertilizer applications. Generally, OP plantations that receive chemical fertilizers have lower nutrient losses through leaching and concentrations of nutrients in groundwater quality. However, larger nutrient losses are expected in mature plantations due to reduced nutrient absorption by palm roots and higher use of fertilizers. These factors can contribute to an overall increase in nutrient loss. This study found that the forest lost 1,050 g ha^{-1} of nitrogen, 21.69 g ha^{-1} of phosphorus, and 1,084 g ha^{-1} of potassium. Compared to Ariesca's (2004) findings, nitrogen loss was substantially more significant. Similarly, the total loss recorded in Papua New Guinea was between 0.3 and 2.2 kg Nha^{-1} year^{-1}, lower than the 15-22 kg Nha^{-1} year^{-1} reported in Malaysia. Smallholder OP plantations have experienced increased leaching losses of potassium and other nutrients such as sodium, calcium, magnesium, and total aluminium since applying inorganic fertilizers and liming.

Conclusion

The study showed that the highest rainfall occurred in October, with a total of 459.5mm, while the lowest rainfall was recorded in June. November had the most wet days, with 24, while May had the lowest, with only 7 days. Erosion and runoff were found to be higher in 3- and 5-year-old oil palm (OP) plantations compared to forest areas. The largest surface runoff was observed in 3-year-old oil palm plantations with a recorded value of 2.83mm, followed by 5-year-old oil palm plantations with 2.46mm, and forest areas with

0.52mm. The study also found that nutrients are lost due to erosion and runoff from 3- and 5-year-old OP plantations, which is higher than in forest areas. Nutrients are mostly lost along with sediment; only a small percentage is lost in water surface flow. The total nitrogen content in eroded sediments and surface runoff in OP plantations aged 3 years, 5 years and forests are 12.91 kgha[-1], 13.05 kgha[-1], and 1.94 kgha[-1], respectively. The total phosphorus content lost in erosion and runoff was 2.82 kgha[-1], 1.62 kgha[-1], and 0.50 kgha[-1], while the average potassium loss was 10.48 kgha[-1], 15.18 kgha[-1], and 1.61 kgha[-1] for 3 years, 5 years, and forests, respectively.

Acknowledgements

References

Acosta, P., & Curt, M. D. (2019). Understanding the expansion of oil palm cultivation: A case-study in Papua. *Journal of Cleaner Production*, *219*, 199-216. https://doi.org/10.1016/ j.jclepro.2019.02.029.

Ariesca, R. (2004). *Studi Tentang Terjadinya Erosi, Aliran Permukaan, dan Hilangnya Unsur Hara Dalam Aliran Permukaan Pada Lahan hutan Sekunder 1 Tahun Bekas Terbakar. Skripsi.* Bogor: Depertemen Manajemen Hutan Fakultas Kehutanan Institut Pertanian Bogor. Retrieved from http://repository.ipb.ac.id/ bitstream/handle/123456789/19012/E04RAR.pdf?sequence=2, diakses 11 Oktober 2012.

Arsyad, S. (2006). *Konservasi Tanah dan Air, Fakultas Pertanian IPB*. IPB Press, Cetakan Ke Tiga. Gedung Lembaga Sumberdaya Informasi Lt. 1 Kampus Darmaga, Bogor.

Austin, K.G., Mosnier, A., Pirker, J., McCallum, I., Fritz, S., & Kasibhatla, P.S. (2017). Shifting patterns of oil palm driven deforestation in Indonesia and implications for zero-deforestation commitment. *Land Use Policy, 69*, 41–48. https://doi.org/10.1016/j. landusepol.2017.08.036.

Banabas, M., Turner, M. A., Scotter, D. R., & Nelson, P. N. (2008). Losses of nitrogen fertilizer under oil palm in Papua New Guinea: 1. Water balance, and nitrogen in soil solution and runoff. *Australian Journal of Soil Research*, *46*(4), 332-339. https://doi.org/10.1071/SR07171.

BPS. (2020). *Statistik Kelapa Sawit Indonesia 2020*. Jakarta: Badan Pusat Statistik.

Breure, K. (2003). The search for yield in oil palm: Basic principles. In T. Fairhurst, & R. Hardter (Eds.) *Oil Palm: Management for Large and Sustainable Yields* (pp. 59–98), Potash & Phosphate Institute/Potash Institute of Canada and International Potash Institute, Singapore.

Campiglia, E., Mancinelli, R., Radicetti, E., & Marinari, S. (2011). Legume cover crops and mulches: effects on nitrate leaching and nitrogen input in a pepper crop (*Capsicum annuum* L.). *Nutrient Cycling in Agroecosystems*, *89*(3), 399-412. https://doi.org/ 10.1007/s10705-010-9404-2.

Clesceri, L. S., Greenberg, A. E., & Eaton, A. D. (1998). Method 4500-NO2-B. *Standard methods for the examination of water and wastewater. 20th ed. Washington (DC): American Public Health Association (DC)*.

Comte, I., Colin, F., Whalen, J. K., Grünberger, O., & Caliman, J. P. (2012). Agricultural practices in oil palm plantations and their impact on hydrological changes, nutrient fluxes and water quality in Indonesia: a review. *Advances in Agronomy*, *116*, 71-124. https://doi.org/10.1016/B978-0-12-394277-7.00003-8.

Corre, M. D., Dechert, G., & Veldkamp, E. (2006). Soil nitrogen cycling following montane forest conversion in central Sulawesi, Indonesia. *Soil Science Society of America Journal*, *70*(2), 359-366.

Dadi, D. (2021). Oil Palm Plantation Expansion: An Overview of Social and Ecological Impacts in Indonesia. *Budapest International Research and Critics Institute (BIRCI-Journal): Humanities and Social Sciences*, *4*(3), pp.6550-6562. https://doi.org/10.33258/birci.v4i3.2469.

Dhiaulhaq, A., De Bruyn, T., & Gritten, D. (2015). The use and effectiveness of mediation in forest and land conflict transformation in Southeast Asia: Case studies from Cambodia, Indonesia and Thailand. *Environmental Science & Policy*, *45*, 132-145. https://doi.org/10.1016/j.envsci.2014.10.009.

Dislich, C., Keyel, A. C., Salecker, J., Kisel, Y., Meyer, K. M., et al. (2017). A review of the ecosystem functions in oil palm plantations, using forests as a reference system. *Biological Reviews*, *92*(3), 1539-1569. https://doi.org/10.1111/brv.12295.

Environment Conservation Department. (2000). *Environmental impact assessment (EIA) guidelines on oil palm plantation development*. Environmental Conservation Department, Sabah, Malaysia. Retrieved from http://www.sabah.gov.my/jpas/programs/ecd-cab/technical/ OP211100.pdf access on Apr 13th, 2011).

GAPKI. (2022). *Despite Being Tough Palm Oil Continually Needs Synergy*. Retrieved from https://gapki.id/en/news/21030/despite-being-tough-palm-oil-continually-needs-synergy.

Gellert, P. K. (2015). Palm oil expansion in Indonesia: land grabbing as accumulation by dispossession. In *States and citizens: accommodation, facilitation and resistance to globalization* (Vol. 34, pp. 65-99). Emerald Group Publishing Limited.

Goh, K. J., & Chew, P. S. (1995). Managing soils for plantation tree crops. 1. General soil management. In S. Paramanathan (Ed.) *Course on Soil Survey and Managing Tropical Soils* (pp. 228–245), MSSS and PASS, Kuala Lampur.

Goh, K. J., Härdter, R. &Fairhurst, T. (2003). Fertilizing for maximum return. In: T. Fairhurst & R. Hardter (eds) *Oil Palm: Management for Large and Sustainable Yie* (pp 279–306). Potash & Phosphate Institute/Potash & Phosphate Institute of Canada and International Potash Institute (PPI/PPIC and IPI, Singapore, pp 279–306.

Hardwick, S. R., Toumi, R., Pfeifer, M., Turner, E. C., Nilus, R., & Ewers, R. M. (2015). The relationship between leaf area index and microclimate in tropical forest and oil palm plantation: Forest disturbance drives changes in microclimate. *Agricultural and Forest Meteorology*, *201*, 187-195. https://doi.org/10.1016/j.agrformet.2014.11.010.

Haridjaja, O., Kukuh, M., Sudarmo, & L. M. Rachman. (1990). *Hidrologi Pertanian*. Jurusan Tanah, Fakultas Pertanian, Institut Pertanian Bogor. Bogor.

Hedin, L. O., Brookshire, E. J., Menge, D. N., & Barron, A. R. (2009). The nitrogen paradox in tropical forest ecosystems. *Annual Review of Ecology, Evolution, and Systematics*, *40*, 613-635.

Indonesian Ministry of Agriculture. (2010). *Area and production by category of producers: palm oil*. Direktor at Jenderal Perkebunan. KementerianPertanian. Retrieved from http://ditjenbun.deptan.go.id/index.php/direktori/3-isi/4-kelapa-sawit.html access on April 13th, 2011)

Kee, K. K., & Chew, P. S. (1996). Nutrient losses through surface runoff and soil erosion—Implications for improved fertilizer efficiency in mature oil palms. In A. Ariffin, M. B. Wahid, N. Rajanaidu, D. Tayeb, K. Paranjothy, S. C. Cheah, K. C. Chang, & S. Ravigadevi (Eds.) *Proceedings of the PORIM Internation Palm Oil Congress* (pp. 153–169), Palm Oil Research Institute of Malaysia, Kuala Lampur.

Koh, L. P., & Wilcove, D. S. (2009). Oil palm: disinformation enables deforestation. *Trends in Ecology & Evolution*, *24*(2), 67-68. https://doi.org/10.1016/j.tree.2008.09.006.

Kurniawan, S., Corre, M. D., Utami, S. R., & Veldkamp, E. (2018). Soil biochemical properties and nutrient leaching from smallholder oil palm plantations, Sumatra-Indonesia. *AGRIVITA,*

Journal of Agricultural Science, *40*(2), 257-266. http://doi.org/10.17503/agrivita.v40i2.1723.

Lees, A. C., Moura, N. G., de Almeida, A. S., & Vieira, I. C. (2015). Poor prospects for avian biodiversity in Amazonian oil palm. *PloS one*, *10*(5), e0122432. https://doi.org/10.1371/journal.pone.0122432.

Linder, J. M., & Palkovitz, R. E. (2016). The threat of industrial oil palm expansion to primates and their habitats. *Ethnoprimatology: Primate conservation in the 21st century* (pp. 21-45). https://doi.org/10.1007/978-3-319-30469-4_2.

Mehraban, N., Kubitza, C., Alamsyah, Z., & Qaim, M. (2021). Oil palm cultivation, household welfare, and exposure to economic risk in the Indonesian small farm sector. *Journal of Agricultural Economics*, *72*(3), 901-915. https://doi.org/10.1111/1477-9552.12433.

Meijide, A., Badu, C. S., Moyano, F., Tiralla, N., Gunawan, D., & Knohl, A. (2018). Impact of forest conversion to oil palm and rubber plantations on microclimate and the role of the 2015 ENSO event. *Agricultural and Forest Meteorology*, *252*, 208-219. https://doi.org/10.1016/j.agrformet.2018.01.013.

Nykvist, N., Grip, H., Liang Sim, B., Malmers, A. & Khiong Wong, F. (1994). Nutrient Losses in Forest Plantations in Sabah, Malaysia. *Ambio*, *23* (3), 210-215.

Oyarzun, C., Aracena, C., Rutherford, P., Godoy, R., & Deschrijver, A. (2007). Effects of land use conversion from native forests to exotic plantations on nitrogen and phosphorus retention in catchments of southern Chile. *Water, air, and soil pollution*, *179*(1), 341-350. https://doi.org/10.1007/s11270-006-9237-4

Rahim, S. E. (2003). *Pengendalian Erosi Tanah dalam Rangka Pelestarian Lingkungan Hidup*. Edisi I. Bumi Aksara. Jakarta.

Safitri, L., Hermantoro, H., Purboseno, S., Kautsar, V., Saptomo, S.K. & Kurniawan, A. (2018). Water footprint and crop water usage of oil palm (*Eleasis guineensis*) in Central Kalimantan: Environmental sustainability indicators for different crop age and soil conditions. *Water*, *11*(1), 35. https://doi.org/10.3390/w11010035.

Setiawan, E.N., Maryudi, A., Purwanto, R.H. & Lele, G. (2016). Opposing interests in the legalization of non-procedural forest conversion to oil palm in Central Kalimantan, Indonesia. *Land Use Policy,* 58, 472–481. https://doi.org/10.1016/j.landusepol.2016.08.003

Sheil, D., Casson, A., Maijaard, E., van Noordwijk, M., Gaskell, J., Sunderland, G. J., Wertz, K., & Kanninen, M. (2009). *The impacts*

and opportunities of oil palm in Southeast Asia. Center for International Forestry Research, Bogor.

Sukartaatmadja, S. (1998). *Perlindungan Lereng dan Pengendalian Erosi Menggunakan Vegetasi Penutup*. Jurusan Teknik Pertanian, Fakultas Teknologi Pertanian. IPB.

Sulaeman, Suparto & Eviati(2009). Petunjuk teknis analisis kimia tanah, tanaman, air, dan pupuk.Balai Penelitian Tanah, Bogor, pp. 234. Retrieved from https://repository.pertanian.go.id/server/api/core/bitstreams/77f52e6b-6a13-48bc-96d1-d6a35025d793/content

Suroso, A. I., & Ramadhan, A. (2014). Structural path analysis of the influences from smallholder oil palm plantation toward household income: One aspect of e-Government initative. *Advanced Science Letters*, *20*(1), 352-356. https://doi.org/10.1166/asl.2014.5317.

Tandra, H., Suroso, A. I., Syaukat, Y., & Najib, M. (2022). The determinants of competitiveness in global palm oil trade. *Economies*, *10*(6), 132. https://doi.org/10.3390/economies10060132.

UNcomtrade. (2022). *UNcomtrade Database*. Retrieved from https://comtrade.un.org/data/

Veldkamp, E., Purbopuspito, J., Corre, M. D., Brumme, R., & Murdiyarso, D. (2008). Land use change effects on trace gas fluxes in the forest margins of Central Sulawesi, Indonesia. *Journal of Geophysical Research: Biogeosciences*, *113*(G2).

Vijay, V., Pimm, S.L., Jenkins, C.N., & Smith, S.J. (2016). The impacts of oil palm on recent deforestation and biodiversity loss. *PLoS One,11* (7), e0159668. https://doi.org/10.1371/journal.pone.0159668.

Vitousek, P. M., Aber, J.D., Howarth, R. W., Likens, G. E., Matson, P. A., & Schindler, D.W. (1997). Technical report: Human alteration of the global nitrogen cycle: Sources and consequences. *Ecological Applications*, *7*(3), 737–750.

Yusop, Z., Chan, C. H., & Katimon, A. (2007). Runoff characteristics and application of HEC-HMS for modelling stormflow hydrograph in an oil palm catchment. *Water Science and Technology*, *56*(8), 41-48.https://doi.org/10.2166/wst.2007.690.